Characterisation of a plastid DNA replicase in *Plasmodium falciparum*

Sze Inn Fiona Seow

Division of Infection and Immunity
Institute of Biomedical and Life Sciences

This thesis is submitted for the degree of Doctor of Philosophy
Faculty of Biomedical and Life Sciences
University of Glasgow

June 2004

ProQuest LLC.
789 East Eisenhower Parkway
P.O. Box 1346
Ann Arbor, MI 48106 – 1346

Abstract

Human malaria is caused by the parasite genus, *Plasmodium*, with *P. falciparum* being the most pathogenic species. The disease affects between 300 to 500 million worldwide. Currently, efforts to contain the disease are curbed by the limited range of antimalarials and the rise of resistance to these treatments. The race is now on to gain a thorough understanding of the biology of the parasite that can be use for the development of strategies to combat the wrath of this disease. Since the 22.8 Mb genome sequence of *P. falciparum* has been fully-sequenced, the data has provided new candidate genes that may be valid drug targets. One area that is of great interest is that of the apicoplast of *Plasmodium.* The evolutionary origin of the apicoplast is generally believed to reflect a secondary endosymbiotic event, in which a proto-eukaryote harbouring a photosynthetic cyanobacterium itself became an endosymbiont of a heterotrophic eukaryote. In *Plasmodium*, this organelle appears to be essential in these parasites and enzyme systems specific to apicoplast have been identified as targets for anti-protozoal chemotherapy.

Segments of a gene (*PfPREX*; formerly referred to as *PfPOM1*), encoding a large protein with a typical N-terminal bipartite plastid targeting sequence have been cloned from *Plasmodium falciparum* and expressed in bacteria. Domains with homology to prokaryotic DNA polymerase, DNA primase and DNA helicase, all were found specified in an opening reading frame (ORF). The putative polymerase domain possesses both DNA polymerase activity and 3'-5' exonuclease activity. The putative helicase-primase domain has also been expressed and both DNA primase and helicase activities were detected. RT-PCR indicates that the open reading frame is expressed as a single transcript whilst Western blot analysis

has shown that the protein is cleaved post-translationally. Localisation studies carried out by collaborators (Sato S, NIMR, Mill Hill) with a GFP-reporter revealed that the protein is targeted exclusively to the plastid.

In addition, the evolutionary history of *PfPREX* appears to be more complex and cannot be explained fully using the secondary endosymbiotic theory. The DNA polymerase domain has great homology to prokaryotic DNA polymerase I. The DNA primase and DNA helicase domain, on the other hand, shows striking similarity to proteins with these functions encoded in T-odd bacteriophages. T-odd bacteriophage related RNA polymerase proteins have previously been identified as playing roles in transcription of plastid genes. Now it seems that additional phage-like proteins also play a key role in the replication of the *Plasmodium* plastid genome. The presence of these T-odd genes in *Plasmodium* may be explained with different theories, mainly the non-orthologous gene displacement with the T-odd bacteriophage genes.

Nonetheless, the discovery of *PfPREX* has opened insights to many exciting possibilities and insight into *Plasmodium falciparum*. This gene can provide not only a valid drug target, due to its prokaryotic origin, but also an insight into the complex evolutionary history of *Plasmodium*.

Acknowledgements

Firstly, I would like to thank my supervisor, Dr Michael Barrett, for all his support and guidance and most important his confidence in me throughout the project.

I would also like to thank everyone in the North Labs, their company throughout my stay in the lab had been great. The lunches we took together, the chats we had, I am going to miss you all. I would like to especially thank Dorothy who had been tremendously help in the lab. All my good friends that I had made in the lab, thank you for your support.

Finally, I would like to thank my family, my parents who supported my decision to come to UK to do my postgraduate training. My husband, Frederic Waldteufel, who has been always by my side, for his support and most important, his love, which is the reason that I could have achieved so much.

Declaration

This thesis and the results presented in it are entirely my own work, except where indicated.

Sze Inn Fiona Seow

TABLE OF CONTENTS

List of Figures

Chapter I – Introduction

Chapter II - Materials and Methods

Chapter III - Identification of a novel gene, *PfPREX* from *Plasmodium falciparum*

Chapter IV - Functional analysis and subcellular localisation of the DNA polymerase (PfPREXpol) domain encoded by the *PfPREX* gene

Chapter VI - The Evolution of *PfPREX*

Chapter VII – General Discussion

Appendix C

Appendix D

List of Tables

Chapter VI - The Evolution of *PfPREX*

List of Abbreviations

ι - Iota

α - Alpha

β - Beta

δ - Delta

ε - Epsilon

η - Eta

γ - Gamma

κ - Kappa

λ - Lambda

μ - Mu

θ - Theta

ζ - Zeta

μg – Microgram

3D – Three-dimensional

A – Adenine

aa – amino acid

ACC – Acetyl CoA carboxylase

ACP – Acyl carrier protein

ADP – Adenosine-5'- diphosphate

ALAD - δ-aminolevulinate dehydratase

ALAS - δ-aminolevulinate synthetase

Amp – Ampicillin

APS – Ammonium persulphate

araATP – 1-β-D-arabinofuranosyladenine-5'-triphosphate

ATP – Adenosine-5'-triphosphate

ATPase – Adenosine triphosphatase

bp – Base pairs

BSA – Bovine serum albumin

C - Cytosine

cDNA – Complementary DNA

Ci – Curie

CO_2 – Carbon dioxide

CTP – Cytosine-5'-triphosphate

DAPI – 4,6-diamidino-2-phenylindole

dATP – Deoxyadenosine-5'triphosphate

dCTP – Deoxycytosine-5'-triphosphate

ddH_2O – Double-distilled water

ddTTP – Didoexy-thymidine-5'-triphosphate

dGTP – Deoxyguanosine-5'-triphosphate

DMSO – Dimethyl sulphoxide

DNA – Deoxyribonucleic acid

DNase – Deoxyribonuclease

dNMP – Deoxynucleoside monophosphate

DOXP – 1-deoxy-D-xylulose-5-phosphate

dsDNA – Double-stranded DNA

DTT – 1,4-dithio-DL-threitol

dTTP – Deoxythymidine-5'-triphosphate

DUE – DNA unwinding element

dUTP – Deoxyuridine-5'-triphosphate

E. coli – *Escherichia coli*

EDTA – Ethylenediamine tetraacetic acid

EtBr – Ethidium bromide

FabH - β-ketoacyl-ACP synthase III

FabI – Enoyl-ACP-reductase

SPA – Scintillation proximity assay

SSB – Single-stranded specific DNA binding protein

ssDNA – Single-stranded DNA

ssurRNA - Small subunit ribosomal RNA

T – Thymine

TAE – Tris-acetate-EDTA

TBS – TRIS-buffered saline

TCA – Trichloroacetic acid

TE – Tris-EDTA

TEMED - N,N,N',N'-tetraethylethylenediamine

T_m – Melting point temperature

TRIS – Tris(hydroxymethyl)aminomethane

tRNA – Transfer RNA

U – Unit

UPGMA – Unweighted pair group method with arithmetric mean

UTP – Uridine-5'-triphosphate

UV – Ultra-violet

V – Volts

v/v – concentration weight to volume

w/v – concentration volume to volume

WHO – World Health Organisation

µM – Micromolar

FITC – Fluorescein isothiocyanate

FSB – First strand buffer

g – Gram

G – Guanine

GFP – Green fluorescent protein

GO – Gene ontology

GPI – Glycosylphosphatidylinositol

GST – Glutathione-S-transferase

GTP – Guanosine-5'-triphosphate

H_2SO_4 – Sulphuric acid

HB – Hybridisation buffer

HEPES – 4-(2-hydroxyethyl)-piperazineethanesulphonic acid

HGT – Horizontal gene transfer

His – Histidine

HPMPA – S-9-(3-hydroxy-2-phosphoryl)-methoxy-propyladenine

IC_{50} - Inhibitory concentration 50%

IDF – Indirect immunofluroscence

Ig – Immunoglobulin

IR – Inverted repeat

kb – Kilobases

KCl – Potassium chloride

kDa – Kilodaltons

Km – Kanamycin

LB – Luria-Bertani

M – Molar

Mb – Megabases

mCi – Millicurie

ME – Minimum evolution

mg – Milligram

Mg^{2+} - Magnesium ions

$MgCl_2$ – Magnesium chloride

ml – Millilitre

mM – Millimolar

mmol – Millimole

MOPS - 3-(N-Morpholino) propanesulfonic acid

MP – Maximum parsimony

N_2 – Nitrogen

NaCl – Sodium chloride

NEM – N-ethylmaleimide

ng – Nanogram

NJ – Neighbour-joining

nm – Nanometer

NTP – Nucleoside-5'-triphosphate

O_2 – Oxygen

OD – Optical density

ORF – Open reading frame

PAGE – Polyacrylamide gel electrophoresis

PBS – Phosphate-buffered saline

PCR – Polymerase chain reaction

pol – Polymerase

Poly (dT) – Deoxyribothymidylate homopolymer chain of undefined length

rbc – Red blood cell

RNA – Ribonucleic acid

RNase – Ribonuclease

rp – Ribosomal protein

rRNA – Ribosomal RNA

RT-PCR – Reverse transcriptase PCR

SDS – Sodium dodecyl sulphate

Chapter I

Introduction

1.1. Malaria – an introduction

Over 40% of the world's population lives in tropical and subtropical areas (Figure 1.1) where malaria is endemic (WHO, 1998). In a poem written 102 years ago by Ronald Ross, malaria was described as the 'million murdering death'. This remains true today as it still affects about 300-500 million people and kills 1.5 to 2.7 million a year (WHO, 1998). Most of these deaths are children; every 40 seconds, a child dies of malaria (Bremen, 2001). Despite the efforts of different organisations, especially the World Health Organisation (WHO) and their control programmes, the disease remains a threat to public health and economic development of the endemic countries.

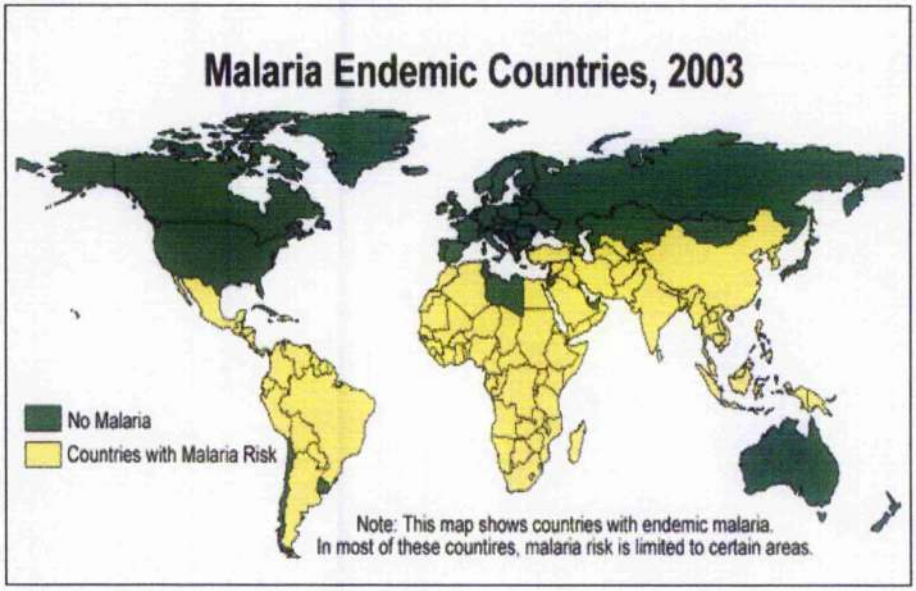

Figure 1.1. Geographical distribution of the incidence of malaria. The areas in yellow are transmission areas with malaria and green with no malaria. (Source: Parasite Image Library, http://www.dpd.cdc.gov/dpdx/HTML/Image_Library.htm)

The rapid spread of resistance of both the parasite and the mosquito vector to currently available anti-malarials and insecticides respectively is making the control of malaria difficult. In addition to this, other factors come into play, all of which contribute

to the ever-increasing disease burden. Population movements into malarious regions, deforestation and global warming are just a handful of factors that contribute to the resurgence of malaria. Therefore, there is an immediate need to find new innovative ways to combat this disease.

1.2. *Plasmodium* – the parasite

Malaria is caused by protozoan parasites of the genus *Plasmodium*. There are more than 50 species of *Plasmodium* known but only four, *P. vivax*, *P. falciparum*, *P. malariae* and *P. ovale*, cause malaria in humans. The most pathogenic species is *P. falciparum* as it causes the most severe form of malaria.

The life cycle of *P. falciparum* (and other *Plasmodium* species) involves several stages in both human and mosquito hosts (Figure 1.2a). The vector responsible for transmission of the disease is the female anopheline mosquito (Figure 1.2b). Following the bite of an infected mosquito, sporozoites injected from the insect's salivary glands enter the bloodstream. They disappear from the bloodstream and invade the liver. The hepatocytes are invaded and after an incubation period of 8 to 12 days, asexual replication of the parasite initiates, generating many daughter merozoites. Eventually these merozoites are released from infected ruptured hepatocytes into the blood circulation. This is where the erythrocytic cycle (blood stage) begins. The merozoites invade other uninfected erythrocytes.

During the erythrocytic cycle, the merozoite grows into a ring form within the erythrocyte. This is followed by the development of early trophozoites and onto

(A)

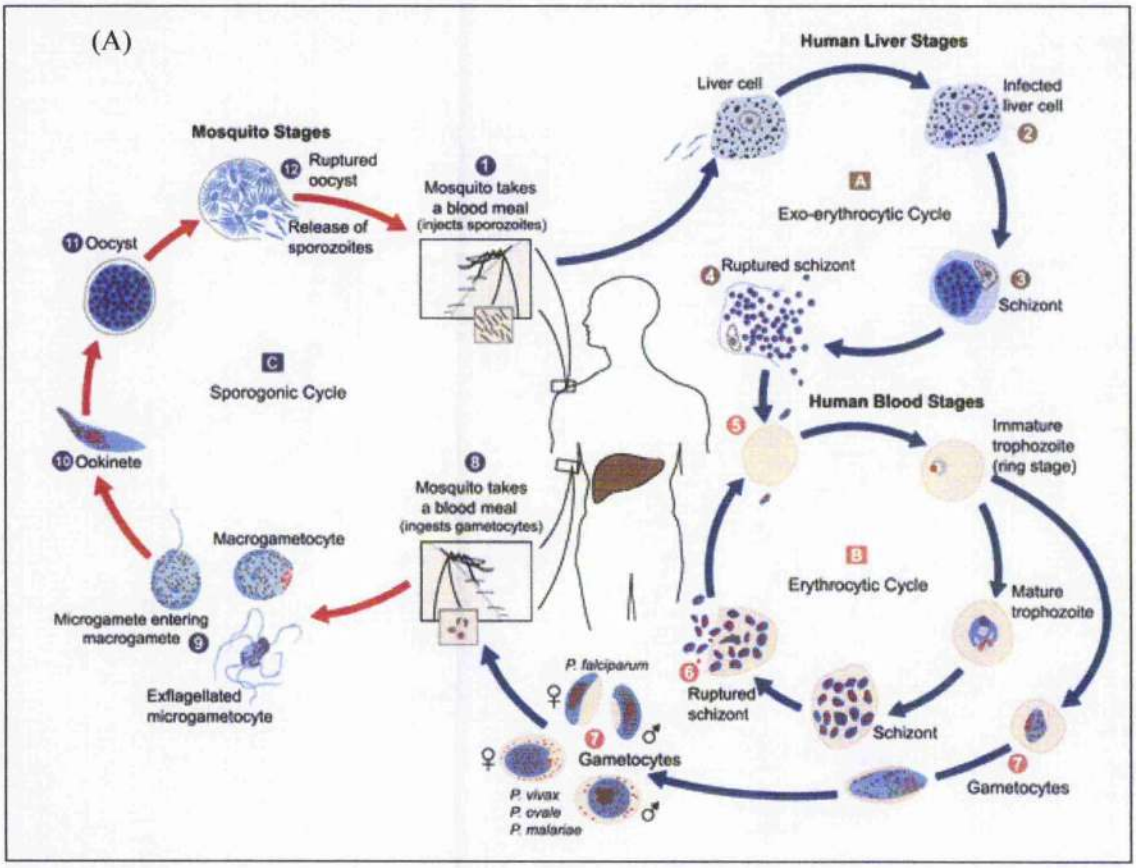

(B)

Figure 1.2. (A) Life cycle of *Plasmodium*. (B) Photograph of a female anopheline mosquito. (Source: Parasite Image Library, http://www.dpd.cdc.gov/dpdx/HTML/Image_Library.htm)

mature trophozoites. These undergo multiple nuclear fissions without cell division to become schizonts which in turn give rise to daughter merozoites. Rupture of the infected erythrocytes releases merozoites into the circulation to initiate further cycles of asexual replication. This one cycle takes place over an approximately 48 hour period in *P. falciparum* but the timing is different in other species.

Some parasites, at the ring stage, develop into male and female gametocytes which may be taken up by a feeding mosquito where sexual reproduction occurs. Within the mosquito, the male gametocytes undergo exflagellation to become gametes. Fertilisation occurs in the midgut of the mosquito where the male and female gametes fuse together to form a diploid zygote. After 12 to 24 hours, the zygote elongates to form an ookinete, which in turns develops into an oocyst. Sporogony in the oocyst generates sporozoites which are released when the oocyst ruptures. The developmental time in the mosquito varies according to ambient temperature but is typically in the order of 7 to 14 days.

DNA replication of the nuclear genome of *Plasmodium* takes place at various points during its life cycle. There are at least five points within the life cycle that DNA synthesis takes place: - (1) during gametogenesis, (2) after fertilisation – meiosis-associated synthesis, (3) sporogony, (4) pre-erythrocytic schizogony in hepatocytes and (5) erythrocytic schizogony. It has been shown that DNA synthesis initiates during the early trophozoite stage of asexual development and continues late into schizogony (Inselburgh & Banyal, 1984), while for the plastid DNA, its replication occurs just before the initiation of schizogony (Williamson *et al*, 1996) but presumably

also at other times prior to cell division to ensure all progeny retain a plastid through the life cycle.

1.3. Clinical features of malaria

1.3.1. Falciparum malaria

Falciparum malaria is the most severe form of the disease (Warrell, 1992). There are complications of falciparum malaria that, when left untreated, can be life threatening. The most notorious form of severe malaria is cerebral malaria, in which the patient becomes comatose before dying. Characteristics of cerebral malaria are the impairment of consciousness and convulsions in the patient. The mortality of cerebral malaria is about 15 to 20 % if good ospital care is provided, while in developing countries, the mortality rate can be as high as 95%.

Other features of severe falciparum malaria include anaemia, which is common in pregnant women, and hepatic dysfunction. The latter is more common in adults where the liver is enlarged and tender. Hypoglycaemia is also a common feature of falciparum malaria where the patient feels anxious, breathless and may suffer from seizures. Another complication of the disease and the most dreaded is pulmonary oedema, which is commonly associated as a terminal event.

1.3.2. Treatment of malaria

There is a pressing need for effective, safe, practicable therapeutic treatment for malaria as the number of cases of malaria around the world is increasing. The available range of standard anti-malarial drugs is narrow. There are four classes of compounds used as antimalarials: - 4-aminoquinolines, amino-alcohols, artemisinin derivatives, and antifolates. Not only are there a limited number of drugs to use against

malaria, there is also a lack of affordable new drugs coupled with the spread of drug resistant *Plasmodium*. Therefore, there is a strong need to develop new therapeutic treatments by searching for new drugs and also re-accessing old, forgotten drugs.

The amino alcohols include quinine (QN) and mefloquine and are effective against blood stage parasites. Quinine is used mainly in cases of severe malaria and also in combination with antibiotics like doxycycline. It is an erythrocytic drug and has no effect on the exo-erythrocytic phase or the gametocytic phase (Rimchala *et al* 1996). Mefloquine, which is structurally related to quinine, is used in both prophylaxis and therapy for complicated malaria. Mefloquine works by interfering with the transportation of haemoglobin products and other substances from the host cell to the parasite's food vacuole (Hellgren *et al*, 1997).

The 4-aminoquinolines, which include chloroquine, are effective against blood stages of the parasite. Chloroquine has been used as the front line drug in chemotherapy for decades as it is cheap, safe and practical for outpatient use. It is a very potent schizonticidal drug and is also effective against erythrocytic stage of all the four *Plasmodium* species. It has no effect on sporozoites, hypnozoites or gametocytes. It is a weak base, and concentrates itself in the parasite's food vacuole. It works by upsetting the transportation of toxic haem digestion waste from the parasite, which accumulates in the parasite and brings upon its demise. However, over usage and mismanagement of chloroquine have contributed to the extensive spread of resistance to this drug (Warhust, 2001).

Another group of drugs are the antifolates which affect the synthesis and utilisation of folate. These include pyrimethamine (2,4,diaminopyrimidine), a dihydrofolate reductase inhibitor and proguanil. They act by inhibiting the dihydrofolate reductase necessary for synthesis of tetrahydrofolate, a precursor in the parasite DNA synthesis. Sulphonamides (e.g. sulphadoxine) and sulphones (dapsone) act by competing for enzyme, dihydropteroate synthetase with para-aminobenzoic acid and therefore inhibit folate synthesis. They act on erythrocytic *P.falciparum*, but not sporozoites. Pyrimethamine is used together with sulphadoxine, in a combination to combat chloroquine-resistant strains of *P. falciparum*. Unfortunately, resistance to this drug combination has risen already (Sibley *et al*, 2001; Warhurst, 2002). Pyrimethamine and other antifolate drugs can also be combined with other sulpha drugs, and with Atovaquone (Malarone) and mefloquine.

The last group - Artemisinin and its derivatives kill all erythrocytic stages of the malaria parasites. It is also reported to be effective towards gametocytes (White, 1997). They are effective against both uncomplicated and severe malaria (Meshnik, 2002). It produces ultra-structural changes to the growing trophozoite parasite. A whorl is produced in the food vacuole and the parasite's mitochondria proliferate. This reduces the parasite's survival (Hien & White 1993).

There are other new drug combinations available against malaria like atovaquone-proguanil, artemether-lumefantrine and pyronaridine but more work is needed to fully validate their efficacy. In addition, antibiotics now are also roped in to combat malaria. Antibiotics like tetracycline and doxycycline are often combined with pyrimethamine or quinine for 100% cure. Clindamycin is also another candidate

antibiotic on clinical trials for use as an antimalarial drug (Lell & Kremsner, 2002). Multiple strategies need to be adopted to try to tackle not only the treatment but also the prevention of malaria. With the availability of both *P. falciparum* and *Anopheles gambiae* genomes, it is hoped that this new information will facilitate identification of novel drug targets. More information on the basis of resistance can also be used to facilitate the development of combinations in future to reduce the likelihood of the development of drug resistance.

1.4. Molecular biology of *Plasmodium*

1.4.1. The Genome of *Plasmodium*

The *P. falciparum* 3D7 nuclear genome is composed of 22.8 Mb of DNA distributed among 14 chromosomes ranging in size from approximately 0.6 to 3.3 Mb. The genome has been fully sequenced (Gardner *et al*, 2002) and is found to be 80.6% A-T rich. (*E. coli* is approximately 50% A-T and the human nuclear DNA contains 63% A-T.) Such an A-T rich genome is reflected in a skewed codon usage in *P. falciparum* (Saul & Battistutta, 1988; Weber, 1987). Most of the third positions of codons in *P. falciparum* contain either an A or a T where this position can vary without changing the amino acid.

The *P. falciparum* genome is predicted to encode 5,268 gene products which include proteins, tRNA and rRNA, (Gardner *et al*, 2002) with a mean gene length of approximately 2.3 kb. Other characteristics of the *P. falciparum* genome are summarised in Table 1.1 (Adapted from Gardner *et al*, 2002).

Feature	*P. falciparum*
Size of genome	22.8 Mb
AT content (%)	80.6
No. of genes	5268
Mean gene length excluding introns	2.3 kb
Gene density (kb per gene)	4.3
% coding	52.6
Genes with introns (%)	53.9

Table 1.1. Summary of characteristics of the *P. falciparum* nuclear genome.

An unusual feature of *Plasmodium* genome is the presence of genes combined to give bifunctional proteins. Many of these proteins are found in other organisms as single functional entities. For example, there is the bifunctional dihydrofolate reductase-thymidylate synthase enzyme (DHFR-TS) (Bzik *et al*, 1987) while both DHFR and TS exist as distinct, monofunctional enzymes in bacteriophages, bacteria and mammals (Blakey & Benkovic, 1984). These enzymes are involved in the folate metabolic pathway. There are at least another two bifunctional enzymes in *P. falciparum* that are also involved in the same pathway. The first is the dihydropteroate synthetase-dihydro-6-hydroxymethylpterin pyrophosphokinase (Triglia & Cowman, 1994) and the second is the dihydrofolate synthetase-folylpolyglutamate synthetase (DHFS-FPGS) (Salcedo *et al*, 2001). Other bifunctional enzymes include the ornithine decarboxylase-S-adenosylmethionine decarboxylase (ODC-AdoMetDC) (Müller *et al*, 2000) which is involved in polyamine biosynthesis, and the glucose-6-phosphate

dehydrogenase-6-phosphogluconolactonase (G6PD-6PGL) (Clarke *et al*, 2001), which is involved in the first two steps of the pentose phosphate pathway. All of the examples given above are involved in the metabolic pathways, other examples include two large integral membrane proteins which possess guanylyl cyclase and adenyl cyclase activities (Carucci *et al*, 2000).

With all these examples of bifunctional proteins found in *P. falciparum*, one might wonder about the evolution of the genes encoding these proteins. Apparently, it seems that gene fusion in *P. falciparum* is relatively common. It has been speculated that there is biological advantage for bifunctional proteins in metabolic pathways, as this arrangement optimises substrate channelling and the formation of products with minimum regulation involved (Ivanetich & Santi, 1990).

1.4.2. Extrachromosomal DNAs

Other than the nuclear genome, *Plasmodium* possesses two distinct extrachromosomal DNAs or episomes. One of these is a multi-copy 6 kb element, also known as the mitochondrial DNA (Feagin, 1992). The other is a 35 kb circular episome (Gardner *et al*, 1988) that has been determined to be similar to the plastid genome of plants but was once thought to be of mitochondrial nature (Feagin *et al*, 1991). This non-photosynthetic 'chloroplast'-like genome was isolated in *P. falciparum* (Gardner *et al*, 1988) and then fully sequenced (Wilson *et al*, 1996).

The mitochondrial DNA was first discovered as tandem repeats in *P. yoelii* (Vaidya & Arasu, 1987). It is present in multi-copies within *Plasmodium*, ranging from 15 per cell in *P. gallinaceum* (Joseph *et al*, 1989) to 20 per cell in *P. falciparum* (Preiser

et al, 1996) and 150 per cell in *P. yoelii* (Vaidya & Arasu, 1987). The mitochondrial genome of *P. falciparum* has been shown to carry genes for some characteristically mitochondrial proteins like cytochrome b and subunit I of cytochrome oxidase (Vaidya *et al*, 1989). It is the smallest known mitochondrial genome.

1.4.2.1. Plastid DNA

Unlike the mitochondrial DNA, the plastid DNA is only found as either one or two copies in *P. falciparum* (Wilson & Williamson, 1997). When first discovered, some scientists mistook it to be associated with the mitochondrial DNA, being part of a multipartite mitochondrial system (Feagin *et al*, 1991). The plastid DNA has been fully sequenced (Wilson *et al*, 1996) (Figure 1.3) and on closer examination, this 35 kb circle bears no homology to mitochondrial DNA. Instead, its ribosomal RNA (rRNA) genes are arranged in a chloroplast-like inverted repeats format (Gardner *et al*, 1991a, b). The inverted repeat (IR) covers about a third of the plastid DNA and encodes the duplicated large and small subunit rRNA genes (Gardner *et al*, 1994). The total length of the unit repeat is approximately 5.1 kb. The two repeats are designated IR_A and IR_B – using the nomenclature previously established for chloroplast DNA (Gardner *et al*, 1993). DNA replication is believed to initiate within these repeats (Singh *et al*, 2003).

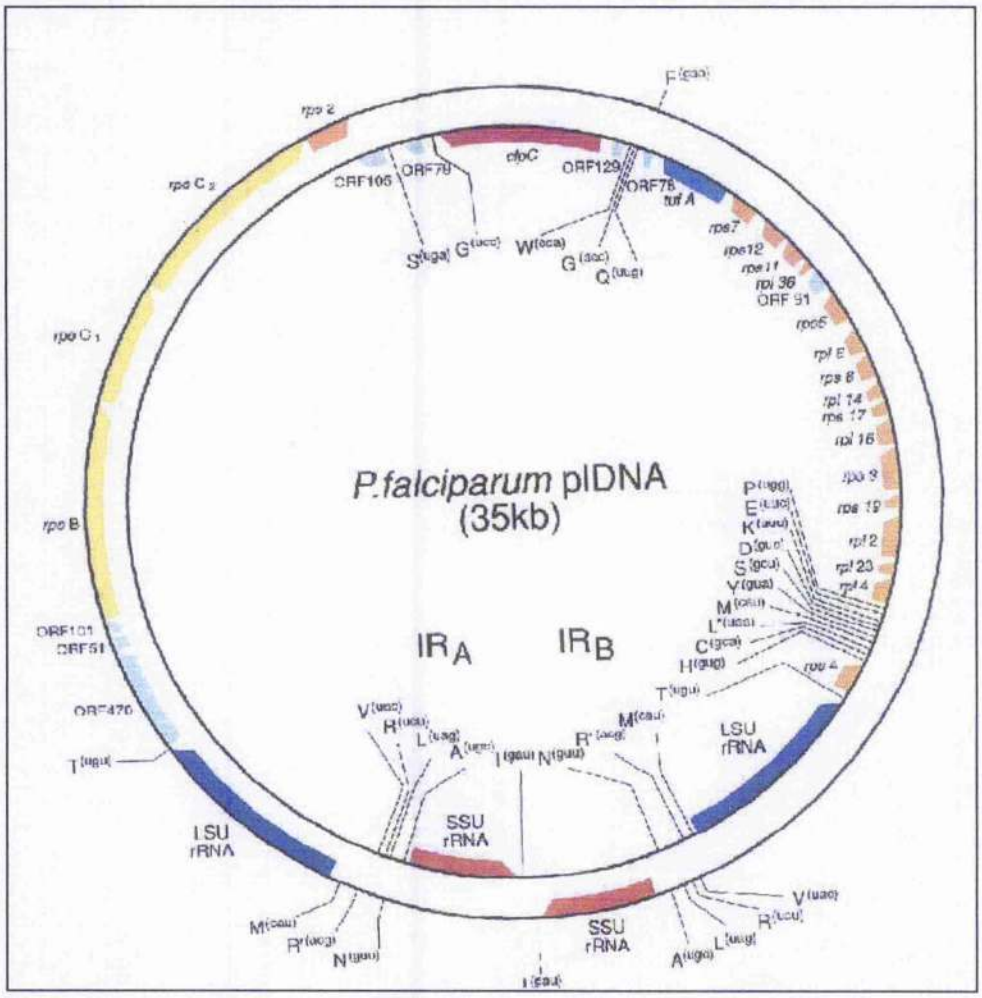

Figure 1.3. Gene map of the plastid DNA of *P. falciparum*. Colour-coded genes:- yellow- RNA polymerases, light blue – unknown ORFs, orange – putative ribosomal proteins, dark blue – large subunit rRNA, red – small subunit rRNA. (Source: Wilson *et al*, 1996).

A prominent feature of the plastid is found along the IR_B region where a string of 15 putative ribosomal protein (*rp*) genes is found. These genes are found along a 7 kb stretch where they are found to be important in the initial assembly of the 30S ribosomal subunit (Wittmann, 1983). The *rpoB* and *rpoC* genes that are found on the IR_A region have helped to ascertain the plastid origin of the 35 kb circle (Gardner *et al*, 1991a, b). Other plastid genes include the *tufA* which codes for the protein synthesis factor, Tu and downstream to it is an open reading frame that appears to code for a gene homologous to the *clpC* belonging to a molecular chaperone family.

1.4.3. DNA replication

In all cellular organisms from bacteria to humans (but excluding a variety of viral species), genetic information is locked within a double helix formed by two anti-parallel DNA stands. Thus, all replication processes involve the melting of these two stands of DNA followed by the polymerisation of each complementary strand on the resulting single-stranded templates (Kornberg & Baker, 1992). The level of complexity involved in the enzymatic machinery required for DNA replication is considerably greater than might have been expected. The enzymes involved in DNA replication will be discussed in detail later. The processes that are common to most DNA replication pathways are detailed below.

DNA replication usually starts at the origin of DNA replication, a particular sequence which increases the efficiency of initiation of DNA replication. It provides a locus for the assembly of a multi-protein complex which includes various enzymes, proteins and accessory factors required for DNA synthesis to take place. The initiation of DNA replication involves three sequential steps. The first step involves specific proteins binding to the origin of replication. In *E. coli*, it is the DnaA protein that binds the replication origin (Ori C). OriC is highly conserved among Enterobacteria (Zyskind *et al*, 1983) and has several distinctive features. These include the presence of DnaA boxes which are repetitive 9mers with sequences 5'-TTATC/ACAC/AA-3' in the form of two inverted repeats. The positions of these DnaA boxes are highly conserved too (Zyskind *et al*, 1983). These are responsible for binding to the DnaA protein (Fuller & Kornberg, 1983; Matsui *et al*, 1985). Located to the left of the DnaA boxes, are a series of AT- rich 13mers. These are arranged in a series of three and they are involved in the process of localized denaturation required to initiate DNA replication.

The DnaA protein serves at least two functions. The first is to initiate DNA unwinding using a DNA helicase while the second function is to guide other replication proteins to the origin. The DnaA protein itself is an ATPase that requires the presence of ATP (which is hydrolysed to release ADP) in order to bind to OriC. Therefore, initiation of DNA replication starts with the DnaA protein binding to the DnaA box sequences found at OriC, forming an initial open complex. Next, the unwinding of the 13mers takes place, leading to the second step of DNA replication, which is the DNA unwinding of the two complementary DNA strands. The enzyme involved in this step is a DNA helicase. DnaA is responsible for guiding the DNA helicase to the open complex. In *E. coli*, the DNA helicase responsible for the replication is called DnaB.

DNA unwinding usually begins at an easily unwound DNA sequence, referred to as the DNA unwinding element (DUE). A DUE is identified by *cis*-acting mutations that increase the stability of the double helix (Umek & Kowalski, 1990). These DUEs, it seems, do not have consensus sequences. It was observed that the binding of proteins to OriC, results in DNA unwinding in the DUEs in *E. coli* (Kowalski & Eddy, 1989) before DnaB can start the unwinding of the double helix.

The initial opening of the duplex allows the establishment of a replication fork. The most important step in this process is the loading of a DNA helicase onto the DNA strands. In *E. coli*, one molecule of DnaB, a hexamer of identical subunits, clamps around each of the two single-stranded DNA in the open complex formed between OriC and DnaA. This is now called the pre-priming complex. Along with the DNA helicase, DNA unwinding is also facilitated by single-stranded specific DNA binding proteins (SSB), which bind to single-stranded DNA fibres and prevent them from reannealing;

and topoisomerase I, which releases torsional stress generated by the unwinding of the DNA double helix (Figure 1.4). The DNA helicase, using energy provided by NTP hydrolysis, 'translocates' along the DNA strand, melting the hydrogen bonds that keep the DNA strand in association with its complementary strand.

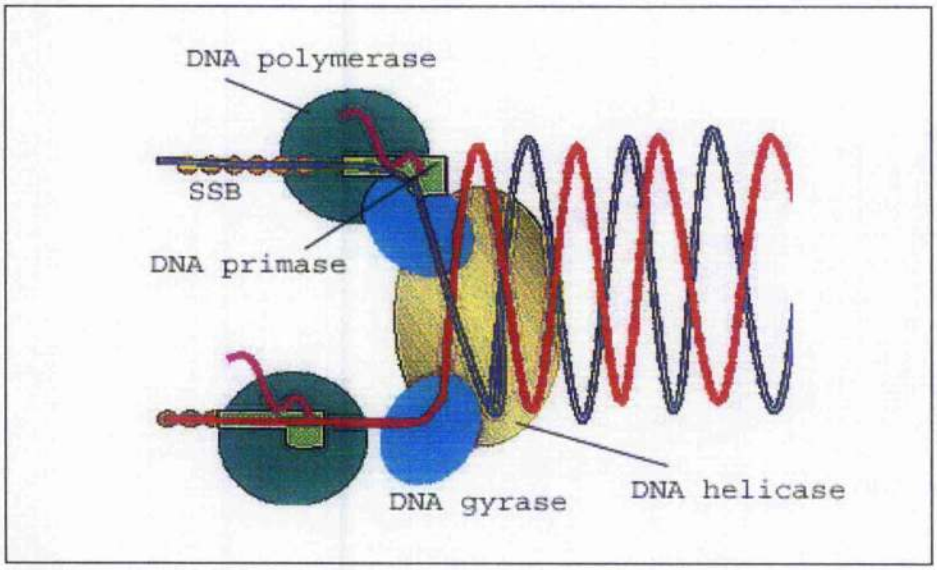

Figure 1.4. A DNA replication fork whereby DNA unwinding is facilitated by a DNA helicase, a topoisomerase (DNA gyrase) and single-strand binding proteins (SSB). DNA primase then make short RNA primers that are used by DNA polymerase to begin synthesising complementary strand.

The final step to the initiation of DNA replication is the commencement of DNA synthesis. This involves several replication proteins, including DNA primase and DNA polymerase. The unwound DNA strands need to be primed by a DNA primase so that the DNA polymerase can elongate the primer strands. In most eukaryotic cells and some prokaryotic cells, DNA synthesis is generally primed by short RNA chains. The DNA primase known as DnaG, is responsible for the synthesis of this primer in *E. coli*.

The primase is usually recruited to a segment of single-stranded DNA by first binding to the DnaB hexamer. This complex is called a primosome. Once the DNA primase synthesises the short primer RNA molecules complementary to the DNA, it dissociates from the primosome complex.

Now that most of the enzymes are assembled, a replication fork is formed; and the elongation of the new DNA fibres begins. The DNA polymerase responsible for replication in *E. coli* is the DNA polymerase III. DNA replication proceeds by a semi-continuous mechanism where one DNA strand (the leading strand) is elongated continuously from a single primer, whereas the other DNA strand (the lagging strand) is constructed from many short DNA chains elongated from multiple primers. Polymerisation of the leading strand occurs in the same direction as the replication fork movement while the lagging strand is synthesised in the opposite direction (Figure 1.5). The leading strand is synthesized in the 5' - 3' direction continuously, while the lagging strand synthesis is more complicated. Since DNA polymerase can only add nucleotides to the 3' end of a primer or DNA strand, the elongation of the lagging strand is also in the *p+4X5'-3' direction, although the overall direction of the lagging strand is from its 3'end towards the 5' end. For this to occur, short fragments called Okazaki fragments synthesised in the 5'-3' direction, are made discontinuously from many RNA primers after which the fragments are joined by DNA ligase.

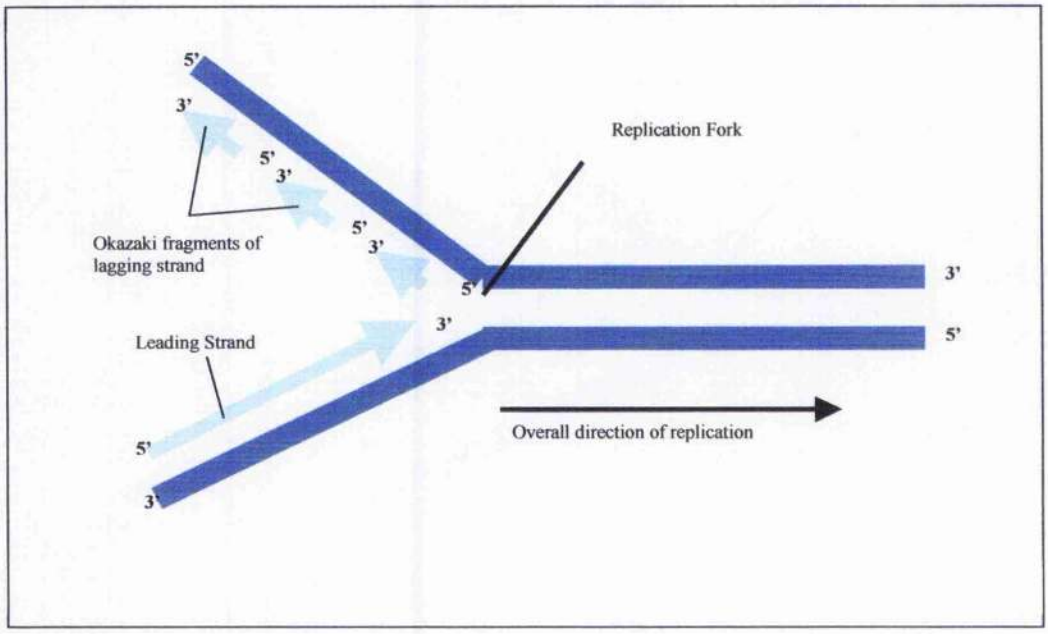

Figure 1.5. Replication fork showing the leading strand and the lagging strand and their direction of strand elongation.

There have been two models proposed for the movement of DNA replication – the factory model versus the tracking model. The tracking model proposes that the DNA replisome moves along the DNA template while the factory model proposes that the DNA replisome is in a fixed position and only the unreplicated DNA is pulled through the stationary replisome (Dingman, 1974; Pardoll *et al*, 1980). The tracking model seems unlikely, as DNA replication based on free moving molecules would result in chaotic entanglement of the newly synthesised DNA strands. The factory model on the other hand, allows the two newly replicated DNA strands to move bidirectionally, away from the unreplicated DNA, thus preventing entanglement. Additionally, both the DNA polymerase and DNA helicase are 'powerful' motors, and as such may be able to provide the force responsible for the movement of the DNA strands. Experimental evidence has been obtained to support the factory model (Lemon & Grossman, 1998)

1.4.3.1. Enzymes involved in DNA Replication

From prokaryotes to eukaryotes, the double stranded nature of DNA provides an elegant structure to ensure the accurate duplication and repair of DNA. This is due to the complementary base pairing of the DNA, which also poses a problem as the hydrogen bonds that hold the double helix together must be disrupted. In order to achieve this, a full repertoire of proteins works together. The main proteins involved are DNA helicase, DNA primase and DNA polymerase. Their functions and roles are detailed below.

1.4.3.1.1. DNA helicases

All key processes that are essential for the maintenance and faithful transmission of DNA ranging from DNA replication, repair and recombination requires the unwinding of the DNA double helix to provide single-stranded DNA as a template. DNA helicases are the enzymes responsible for the catalysis of the unwinding of the double helix. They are molecular motors that couple the energy of nucleoside-5'-triphosphate (NTP) hydrolysis to the transient disruption of hydrogen bonds formed between the Watson-Crick base pairs of the DNA double helix. Hence, helicases are also NTPases.

The first DNA helicase isolated on the basis of its nucleic acid unwinding activity was in 1976 (Abdel Monem & Hoffman-Berling, 1976). It was identified in *E. coli*, and was designated as DNA helicase I. DNA helicase I is encoded by the *traI* gene of the F episome (Abdel-Monem *et al*, 1983) and is required to unwind the DNA that is transferred during conjugation. Since then, multiple helicases have been identified from prokaryotes (Matson & Kaiser-Rogers, 1990) and eukaryotes (Thommes & Hubscher,

1992). Some of these are putative DNA helicases that have been identified from genome sequence projects while a handful with helicase activities have been isolated and characterised. The omnipresence of these DNA helicases in many sources suggests that these enzymes are ubiquitous in nature. Moreover, it seems that different DNA helicases have specific functions resulting in the presence of multiple DNA helicases in a single organism. For example, in *E. coli*, there are at least 11 distinct DNA helicases (Matson, 1991), eight in calf thymus and four in yeast (Thommes & Hubscher, 1992).

The basic biochemical reaction catalysed by DNA helicase is the hydrolysis of NTP and it is based on this activity that DNA helicases are often characterised. The DNA helicase assays follow the conversion of double-stranded DNA into single strands. The most common assay employs a DNA substrate that is labelled and incubated with Mg^{2+} and an NTP. The DNA substrate is usually a ^{32}P-labelled oligonucleotide annealed to a larger single-stranded DNA molecular such as M13 viral DNA. The products of the reaction are resolved either on an acrylamide or agarose gel. The radioactive substrate and product molecules differ greatly in size so that the quantity of the substrate that has been rendered single stranded by the helicase can be evaluated.

Many DNA helicases require a region of single-stranded DNA adjacent to the duplex region to serve as an initial binding site. This site also serves to facilitate the formation of an initiation complex. Based on the requirement for a single-stranded overhang, different DNA helicases show different preferences for the polarity of this overhang. Some DNA helicases show a strong preference to utilise a 3' terminated single-stranded DNA. These are the 3'-5' DNA helicases. Others prefer a 5' overhang. These are the 5'-3' DNA helicase group. There are of course exceptions to the case such

as the *E. coli* RecBCD protein, a recombination helicase which does not require a single-stranded DNA overhang but prefers to unwind blunt-ended DNA (Taylor & Smith, 1985). Interestingly, RecB alone without RecC and D subunits, prefers to unwind a 3' single-stranded DNA overhang (Boehmer & Emmerson, 1992).

1.4.3.1.1.1.Molecular biology of DNA helicases

DNA Helicases are divided into five main superfamilies and families based on the presence and composition of conserved amino acid residues (Helicase signatures) (Figure 1.6). Comparison of the DNA helicase sequences has revealed various categories of sequence homology. Three vast superfamilies and two smaller families have been identified (Gorbalenya & Koonin, 1993). The superfamilies 1 and 2 (SF1 & SF2) are the largest groups, containing the majority of DNA helicases including examples from viral, prokaryotic and eukaryotic organisms. The members from both families are identified by the presence of six conserved amino acid motifs (I-VI) (Gorbalenya & Koonin, 1993). A seventh motif, termed Ia, is found only in a subset of helicases within the superfamilies and has a poorly defined consensus sequence.

Superfamily 3 (SF3) is much smaller and the members of this superfamily possess only three conserved motifs (Gorbalenya & Koonin, 1993). These DNA helicases are generally found in small DNA and RNA viruses (Gorbalenya *et al*, 1990). Family 4 is a smaller family group which comprises of DNA helicases found in the bacterial and bacteriophage systems. These helicases are always associated physically with DNA primases (Ilyina *et al*, 1992). This group is also known as the DnaB-like helicases, because the type-member of this group is the DnaB protein from *E. coli* other family 4 members share homology to the DnaB helicase. They have three distinct

conserved motifs (Ilyina *et al*, 1992), in addition to the Walker A and B sequences. The last family of helicases are the DNA-RNA helicases that could not be grouped with the other 4 families (Gorbalenya & Koonin, 1993). An example is the bacterial transcription termination factor, Rho (Brennan & Dombroski, 1997).

The two motifs that are present in all known DNA helicases were first described as the Walker A and B sequences (Motif I and II respectively). The Walker motifs are found in all NTP-binding proteins (Walker *et al*, 1982). The residues in the Walker A and B sequences are believed to interact with Mg^{2+}NTP/Mg^{2+}NDP. The Walker A motif has a consensus sequence of GxxxxGKT (Walker *et al*, 1982) (Figure 1.7) where the last three residues form an essential part (GKT/S) of the motif. It was suggested that the amino group of the lysine interacts with the phosphates of Mg^{2+}NTP/Mg^{2+}NDP while the hydroxyl group of the threonine/serine complexes with the Mg^{2+} ion (Walker *et al* 1982). The Walker B motif has a consensus sequence of DExx where the carboxyl group of the aspartate functions to co-ordinate the Mg^{2+} ion of Mg^{2+}NTP/Mg^{2+}NDP while the glutamate is suggested to act as a catalytic base during NTP hydrolysis. Through X-ray crystal structure studies, it was noted that other residues within the Walker B motif also have a role to play, extending the consensus sequence of the Walker B motif to DE(Y/F/A)QD (Figure 1.7) where the aspartate in the fifth position is observed to form a salt bridge with the glutamine residue found in motif VI (Caruthers *et al*, 2000; Korolev *et al*, 1997). This is only observed in helicases from SF1 (Soultanas *et al*, 1999; Velankar *et al*, 1999). Among helicases from SF2, the Walker B consensus sequence is depicted as – DEx(D/H).

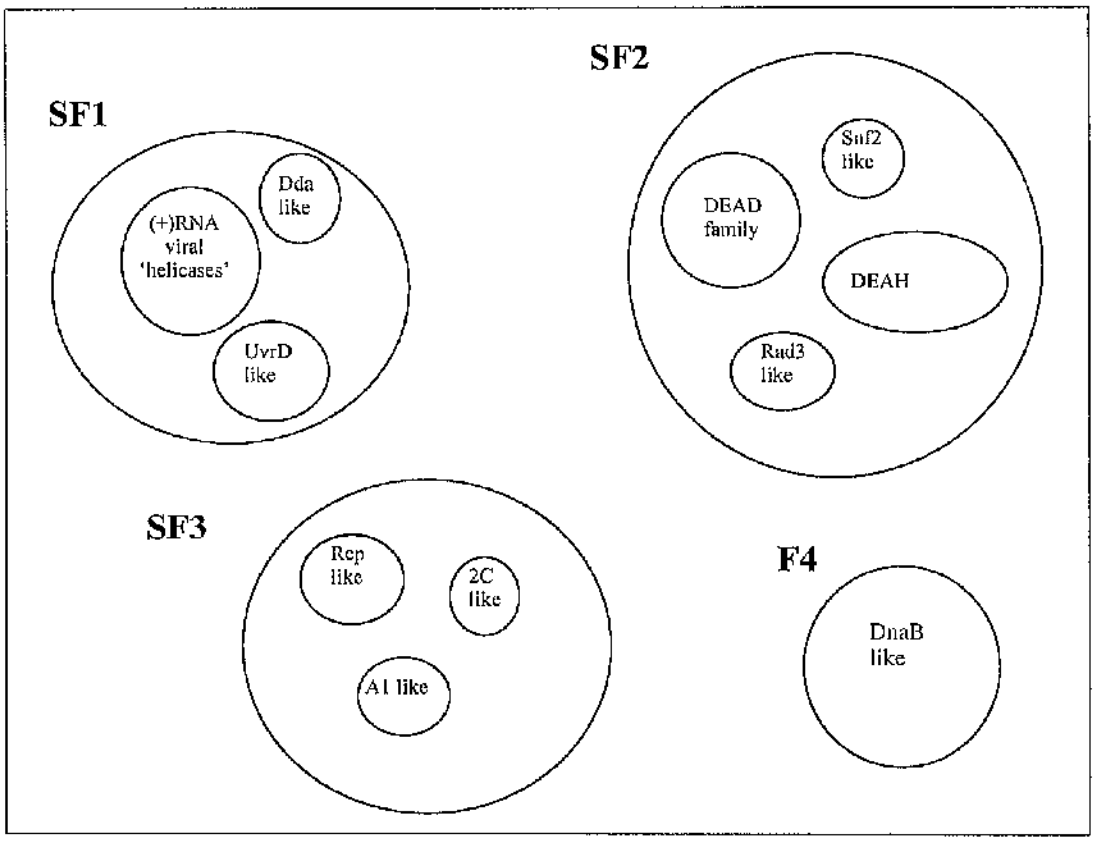

Figure 1.6. The main groups of DNA helicases. There are four groups of helicases (SF1-SF3, F4). (Source: adapted from Gorbalenya & Koonin, 1993).

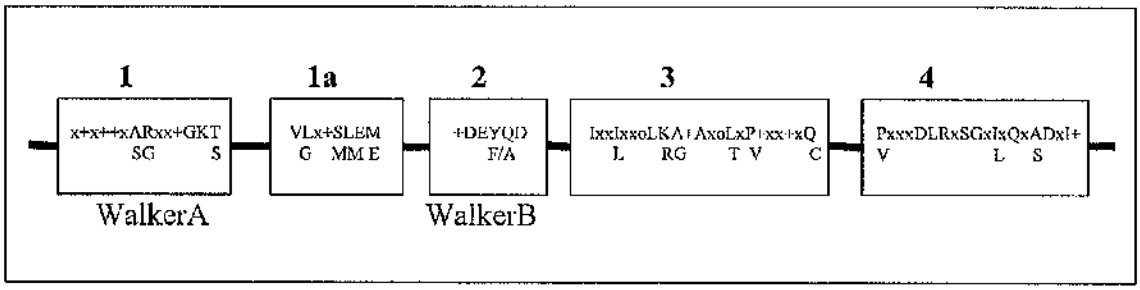

Figure 1.7. A schematic diagram representing the motifs of DnaB like helicases. Open boxes represent the conserved motifs, and the letters inside the boxes are the consensus amino acid sequences of each motif. Labels above the open boxes are the names assigned to the motifs. The consensus sequences were derived from Ilyina *et al*, 1992. Single-letter amino acid abbreviations were used. The '+' represents a hydrophobic residue, an 'o' represents a hydrophilic residue and an 'x' represents a residue that is not restricted to being hydrophobic or hydrophilic. (Adapted from Hall & Matson, 1999).

1.4.3.1.1.2.Molecular biology of DnaB-like helicases

The members of this family consist of bacterial and bacteriophage helicases. The DNA helicase in PfPREX shows the strongest homology to this group of DNA helicases. Therefore, this section gives more details of this group of DNA helicases.

The key representative type-member of this family is DnaB from *E. coli*. Ilyina *et al* (1992) carried out an alignment of DnaB-related helicases and found that they possess five distinct motifs of which two are the Walker A and B sequences (H1 and H2 respectively). Other examples of family members are T7 gene 4 helicase and T4 gene 41 helicase. They belong to the group of hexameric helicases whereby six helicase subunits assemble into a hexameric ring with a central channel to unwind double-stranded DNA. The process involves one strand passing through the channel while the other passes outside the ring (West, 1996). The other three motifs (H1a, H3 and H4) also play key roles too in the unwinding of DNA. Motif H1a contains a glutamate that has been suggested to play a role in catalysis (Sawaya *et al*, 1999). Motif H3 has been suggested to participate in the interaction of Mg^{2+} in NTP/NDP hydrolysis and contributes to the binding of oligonucleotides (Caruthers & McKay, 2002). Finally motif H4 has a role linked with DNA binding (Gorbalenya & Koonin, 1993; Washington *et al*, 1996).

1.4.3.1.2. DNA primases

DNA primases are another essential component of the DNA replication machinery. Since all DNA polymerases are unable to initiate polymerisation *de novo*, they require a primer molecule to provide a 3'-OH to which the first nucleotide is added (Kornberg & Baker, 1992). DNA primase synthesises short RNA molecules which then

serve as primers for both the initiation of leading stand replication at the origin of replication and of Okazaki fragments on the lagging strand (Kornberg & Baker, 1992). DNA primases have been identified in bacteria, viruses and eukaryotes. With the recent explosion in genome sequencing, a multitude of proteins have been discovered that show homology to known DNA primases.

DNA primases can be classified into two groups (Frick & Richardson, 2001). The first group contains DNA primases from bacteria and bacteriophages, while the second is made up of eukaryotic DNA primases. The two groups differ in their structure and their relationship with other proteins in the replication complex.

1.4.3.1.2.1.Prokaryotic DNA primases

Prokaryotic DNA primases include proteins from bacteria and bacteriophages. The prototypical bacterial primase is the enzyme, DnaG from *E. coli* (Kornberg & Baker, 1992). All other known bacterial primases, as well as the bacteriophage primases, are homologous to DnaG. They all possess similar functional characteristics. Proteolytic digestions of DnaG from *E. coli* and phage T7 primase have shown that the prokaryotic DNA primases are composed of three regions (Marians, 2000; Washington *et al*, 1996), an N-terminal zinc-binding domain, an oligonucleotide synthesis site and either a helicase or a region that interacts with a helicase.

The zinc-binding domain contains the "zinc motif" which is defined as two pairs of residues, made up by either cysteines or histidines or both (Motif 1) (Figure 1.8). The configuration of the zinc motif allows for the formation of a zinc finger which is essential for primase activity. This zinc motif is present in many primases from both

prokaryotic and eukaryotic sources (Ilyina *et al*, 1992; Mendelmann *et al*, 1994; Toh, 1986). The position of the zinc-binding domain varies between different classes of primases. In prokaryotic primases, the zinc-binding domain is located at the N-terminus of the polypeptide while it is found at the C-terminus of primases of eukaryotic viruses. For standard eukaryotic primases, the domain is located in the central catalytic domain (Figure 1.8).

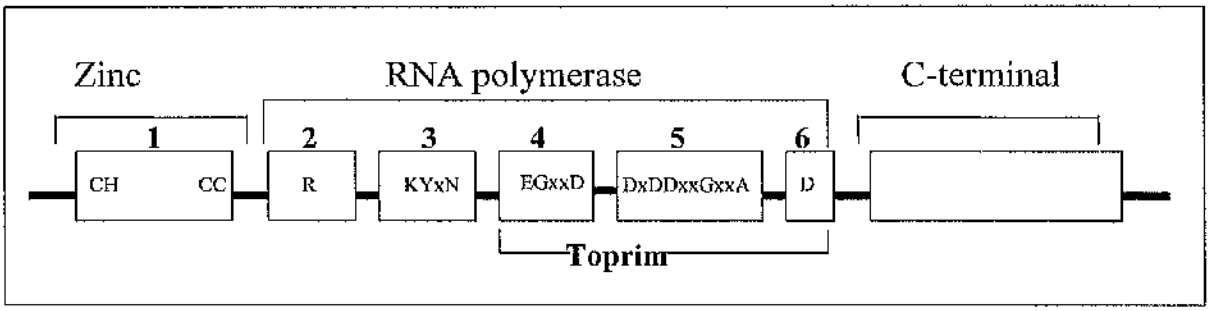

Figure 1.8. Schematic diagram of the domain structure and the conserved residues in DnaG-like primase. The six consensus sequences identified by Ilyina *et al*, 1992 are numbered at the top of the boxes.

The importance of the zinc-binding domain to the primase activity is demonstrated in the phage T7 gene 4 protein which codes for both a DNA primase and helicase (Mendelmann *et al*, 1994). When the zinc motif is disrupted in the protein, priming activity is lost. The same loss of activity is observed with the phage P4 primase when the two cysteine residues in the zinc motif are replaced by glycine residues (Ziegelin *et al*, 1995).

The central domain or catalytic domain contains the majority of the conserved motifs (Salas, 1991). This domain is also known as the RNA synthesis domain, which is responsible for synthesis of the primer strand. It contains five conserved motifs (Motifs 3-6). Motif 2 is the only motif for which no functional or

structural role has yet been assigned. Motifs 3-6 contain residues that appear to play roles in NTP binding and oligonucleotide synthesis. Additional charged residues in the proximity of motif 3 are shared among several prokaryotic and eukaryotic RNA polymerases (Versalovic & Lupski, 1993). Experiments using *E. coli* DnaG confirmed that this region plays a role in RNA synthesis. Motifs 4 to 6 may play roles in the coordination of NTP and Mg^{2+} ions. Motifs 4 and 5 contain conserved negatively charged residues that are preceded by runs of hydrophobic residues. Within this arrangement, the residues are predicted to form beta strands which resemble motifs involved in Mg^{2+}-mediated NTP binding observed in ATPases (Fry *et al*, 1986, Gorbalenya & Koonin, 1989). Motif 4 has the consensus sequence of EGxxD where the glutamate residue is predicted to be essential for primer synthesis (Strack *et al*, 1992). Aravind *et al* (1998) predicted that the same glutamate is needed to facilitate nucleotide polymerisation. Motif 5 has a consensus sequence of DxDxxGxxA where the DxD sequence acts to coordinate Mg^{2+} (Aravind *et al*, 1998). The same DxD sequence can also be located on motif 6, where it is conserved in all DnaG-like bacterial primases (Szafranski *et al*, 1997) but only the first aspartate is present in phage primases.

Parts of the catalytic domain seem to have structural relationships with otherwise unrelated proteins such as some DNA topoisomerases and several nucleases (Aravind *et al*, 1998). This shared region is named the TOPRIM domain (for topoisomerase/primase). The TOPRIM domains in primases are smaller than those in topoisomerases (~80 residues as compared to ~120 residues in topoisomerase) (Podobnik *et al*, 2000). Motifs 4 and 5 are found within the TOPRIM domain and the DxD dyad is central to this region.

The C-terminal domains of prokaryotic primases are not evolutionary conserved. This region is required for the association with a helicase or itself is a helicase. Therefore, other than where the C-terminus is a helicase, conserved motifs are not generally present within this domain. Those that possess a helicase at the C-terminus include bacteriophage T7 and P4 primases while those that do not, include phage T4 primase and *E. coli* DnaG. *E. coli* DnaG has been shown to interact with DnaB helicase via this region (Tougu *et al*, 1994). When the C-terminal domain of DnaG is removed by proteolysis, the protein can still synthesise primer strands but is unable to engage in any helicase activity (Tougu *et al*, 1994) because the DnaG no longer associates with DnaB.

1.4.3.1.3. DNA polymerases

DNA polymerases are essential enzymes for DNA replication, recombination and repair. They are involved in the catalysis of the synthesis of DNA in a sequence-independent manner that results in a faithful copy of the original DNA molecule. Because DNA polymerases are involved in many separate functions, an extreme diversity of DNA polymerases exists, not just among different organisms but also within individual organisms. For example, in *Saccharomyces cerevisiae*, there are at least eight different DNA polymerases (Hubscher *et al*, 2000). These enzymes can function alone or with accessory factors. They can vary not only in their fidelity, speed and processivity with which they replicate DNA but also in the functions that they perform.

Based on their functions, DNA polymerases can be broadly classified into two groups; the first are the replicative DNA polymerases and the second, the repair polymerases. Replicative DNA polymerases are responsible for DNA duplication while repair polymerases fix damaged DNA. The discovery of *E. coli* DNA polymerase I in 1956 (Kornberg, 1960) yielded the first insight into the structure and mechanisms of this group of enzymes. Recently, with the explosion of genome sequencing projects, more DNA polymerase sequences have been discovered which allows us to use this information to further understand the workings of the enzyme.

Name	DNA polymerase family	Function
pol (alpha) α	B	Replication
pol (beta) β	X	Repair
pol (gamma) γ	A	Mitochondrial replication and repair
pol (delta) δ	B	Replication, repair
pol (epsilon) ε	B	Replication, repair
pol (zeta) ζ	B	Translesion synthesis
pol (eta) η	Y	Translesion synthesis
pol (theta)θ	A	Cross-link repair
pol (iota) ι	Y	Translesion synthesis
pol (kappa) κ	Y	unknown
pol (mu) μ	X	Somatic hypermutation
pol (lambda) λ	X	Meiotic mutation.

Table 1.2. Classification of DNA polymerases. (Adapted from Friedberg *et al*, 2000).

The DNA polymerases have also been grouped into different families based on their amino acid sequence homologies to *E. coli* DNA polymerases (Ito & Braithwaite, 1991). Family A polymerases are homologous to the *polA* gene product, *E. coli* DNA polymerase I. Other members include bacterial and bacteriophage polymerases like *Thermus aquaticus* DNA polymerase I, phage T7 DNA polymerase, eukaryotic mitochondrial DNA polymerase gamma (γ) and DNA polymerase theta (θ).

DNA polymerase θ is a polymerase that was identified in *Drosophila melanogaster* as Mus308 that is shown to be involved in the repair of DNA crosslinks (Harris *et al*, 1996) and later the human homologue of Mus308 was identified too (Sharief *et al*, 1999). Like DNA polymerase θ, the family A DNA polymerases function in repair (e.g. PolI in nucleotide excision repair (Sancar, 1996) and also in replication (e.g. phage T7 DNA polymerase (Fuller & Richardson, 1985). Family A DNA polymerases contain three conserved motifs (A-C) (Sousa *et al*, 1996), where motifs A and C are found in the catalytic site of the enzyme while motif B is involved in the binding of dNTP.

Family B DNA polymerases comprise bacterial, bacteriophage and eukaryotic enzymes, which are homologous to the *E. coli* DNA polymerase B (pol II). Members include eukaryotic replication polymerases like polymerase alpha (α), polymerase delta (δ) and polymerase epsilon (ε) (Hubscher *et al*, 2000) and also phage T4 replicative polymerase (Karam & Konigsberg, 2000). In type B polymerases, there are six conserved motifs identified. Motifs I and II are found in the catalytic site. These two motifs are considered to be equivalent to family A polymerase motifs C and A respectively (Joyce, 1997; Steitz, 1999).

There are other polymerase families like the family C DNA polymerases and family X polymerases. Family C polymerases are homologous to *E. coli* polymerase C (pol III) (Kelman & O'Donnell, 1995) while family X members do not share significant sequence similarity with DNA polymerases but are related to terminal transferases. Members of family C comprise most of the bacterial replication polymerases while family X members includes eukaryotic DNA polymerase beta (β), lambda (λ) (Garcia-Diaz *et al*, 2000) and mu (μ) (Dominguez *et al*, 2000). With the ever-growing size and

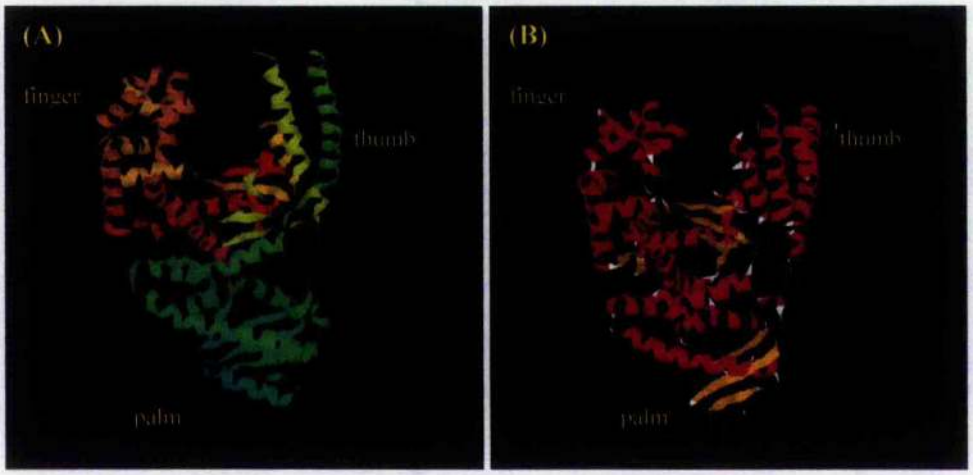

Figure 1.9. 3D structure of *E. coli* Klenow fragment and *Thermus aquaticus* Taq polymerase. (Source:Klenow- PDB file 1KFD, Beese *et al,* 1993 and Taq –PDB file 1KTQ, Korolev *et al*, 1995). Both structures possess similar overall structure which comprise the characteristic finger, thumb and palm.

Other residues including Arg 754, Arg 682, Lys 758 and His 734 have been implicated in the interaction with dNTPs. These sets of residues are well conserved among family A DNA polymerases. They are all positively-charged residues and are thought to interact with the phosphate backbone of dNTPs (Astatke *et al*, 1995). Residues that are important and play roles in primer strand attachment are Glu 611, Thr 609, Asn 678, Asn 675, Lys 635 and Arg 631 (Basu *et al*, 1988).

The detailed structure of the *E. coli* DNA polymerase provides a platform for the functional studies of other DNA polymerases I. Still only a small area of the structure has been studied. More has to be carried out to study the interactions of the various residues with the dNTPs, DNA template, primer and other replication proteins found on the replication fork.

1.4.3.2. DNA Replication in *Plasmodium*

One reason that the replication of DNA in malaria parasites is the subject of research is because it provides a gateway for potential therapeutic applications. DNA replication occurs at several points during the life cycle of the parasite. One time point is when after parasites invade hepatocytes of the host and undergo exo-erythrocytic schizogony. DNA replication also occurs during both erythrocytic schizogony and gametogenesis, and during sporogony in the mosquito. In fact, DNA replication during gametogenesis and exflagellation appears to be one of the most rapid known examples of DNA replication. It would be of interest to understand this process in more detail.

In *P. falciparum*, two distinct DNA polymerase classes were purified (Chavalitshewinkoon *et al*, 1993), one being aphidicolin-sensitive (A^S) and the other aphidicolin-resistant (A^R). To further characterise the two polymerases, they were treated with concentrations of different compounds to obtain IC_{50} values. The A^R polymerase was sensitive to N-ethylmaleimide (NEM) and dideoxy-TTP (ddTTP) while the A^S polymerase was sensitive to 1-β-D-arabinofuranosyladenine-5'-triphosphate (araATP). The IC_{50} values obtained for both polymerase classes suggested that the A^R fraction resembled the eukaryotic mitochondrial DNA polymerase γ while the A^S fraction possessed primase activity and is classified as DNA polymerase α. In *P. berghei*, three distinct DNA polymerase classes were purified (De Vries *et al*, 1991), two being A^S and one A^R. However, unlike in *P. falciparum*, the fraction that was shown to be processive was able to use an RNA-primed template but lacked primase activity. It was thus classified as a DNA pol α-like enzyme. Based on the inhibition profile of the second A^S fraction, it was classified as DNA polymerase δ. The A^R

fraction of *P. berghei* unlike the *P. falciparum* fraction was resistant to both ddTTP and NEM and was classified as a DNA polymerase β.

Inhibitors of DNA polymerase have been investigated as potential therapeutic agents. For example acyclic nucleoside analogues, which are related to the S-9-(3-hydroxy-2-phosphoryl methoxy-propyl)adenine (HPMPA), were shown to strongly inhibit the growth of *P. falciparum* (De Vries *et al*, 1991). A single injection of HPMPA prevents any increase in parasitaemia in mice infected with *P. berghei* (De Vries *et* al, 1991) for several days. Repeated drug administration of HPMPA blocked parasite growth for long periods but when treatment was stopped, parasitaemia returned.

Nuclear DNA replication is much better understood than organellar DNA replication. However, it is critical to understand this latter process as enzymes of organellar DNA replication provide good targets for drugs against the parasites, especially if they are of plastid and cyanobacterial/prokaryotic origin and as such, likely to be different from the host's DNA replication enzymes. As yet, plastid DNA replication has not been well explored or understood in *Plasmodium*. Even information from the conventional plastid genomes is of little help. What is known is that the malaria plastid DNA does not carry any genes for plastid DNA replication. They are most probably carried by the nuclear genome but had not been identified prior to this thesis.

1.4.4. Plastid DNA replication

Until recently, nothing much was known about the replication of the *Plasmodium* plastid DNA. The plastid DNA, during the erythrocytic cycle, replicates early in schizogony at about the same time as the nuclear and mitochondrial DNA. The pattern of replication was presumed to be similar to higher plant chloroplast, i.e. the plastid replicates bidirectionally using the rolling circle mode of replication. Williamson *et al*, (2002) discovered that the plastid of *Plasmodium* in fact replicates by two different mechanisms, one that adopts the rolling circle strategy, initiating at an unknown location while the second mechanism, which initiates at the twin D-loops located in the large inverted repeat. This mechanism is relatively sensitive to the topoisomerase inhibitor, ciprofloxacin unlike the first mechanism which is less sensitive to it.

The enzymology of plastid replication is not well studied. There are only two replication genes that have been found that are associated with plastid DNA replication. The genes are *gyrA* and *gyrB* which encode gyrase subunits have been shown to be nuclear encoded plastid proteins (Wilson *et al*, 2002). Therefore, they are most probably involved in the plastid DNA replication. White & Kilbey (1996) proposed that the aphidicolin-insensitive DNA polymerase identified by De Vries *et al* (1991) could play a role in plastid DNA replication. As yet though, no other direct evidence has been obtained or enzymes isolated that have been implicated directly in the replication of the plastid DNA, the enzymology of which remains elusive.

1.5. Apicoplast

1.5.1. Introduction

Plastids include the photosynthetic chloroplasts of plants, the rhodoplasts of red algae and the chromoplasts of brown algae. The apicoplast also belongs to this family of organelles. The apicoplast is found in a group of parasites which belong to the phylum Apicomplexa. The members of the Apicomplexa include *Toxoplasma*, *Plasmodium* and *Theileria* among many other groups. Several of them cause severe diseases in livestock and humans such as theileriosis, toxoplasmosis and malaria.

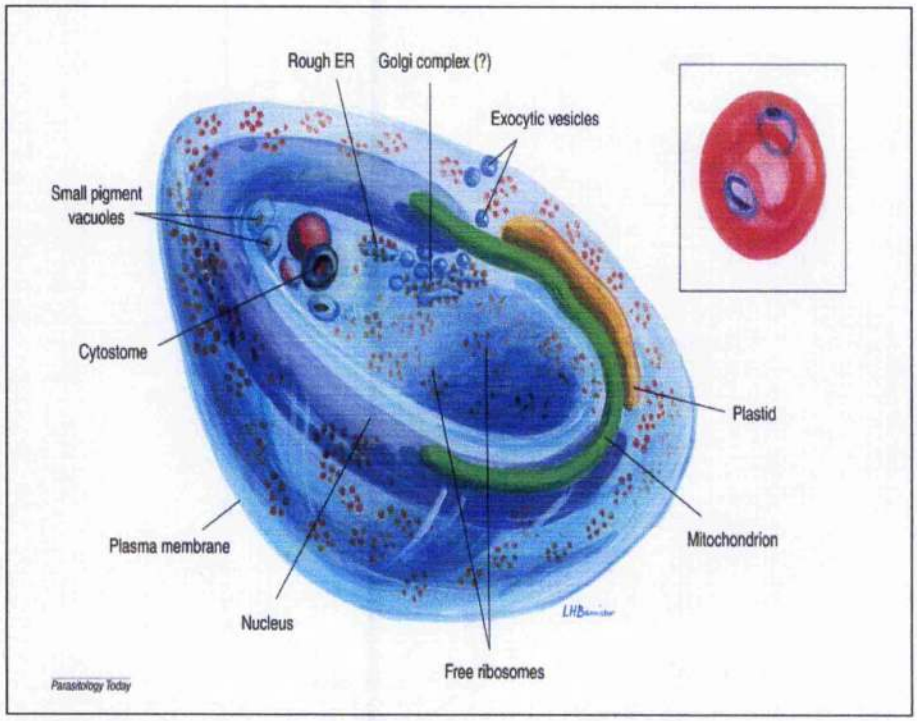

Figure 1.10. Ultrastructure of a ring stage *Plasmodium falciparum* showing the various organelles like the plastid and mitochondrion. (Source: Bannister *et al*,2000)

When the non-photosynthetic plastid was first discovered in apicomplexan parasites, it attracted a lot of interest for its potential as a drug target. Its evolutionary

history indicates that an ancestor of the apicomplexan parasite must have endocytosed a symbiotic alga. A great deal of work has been carried out to learn and understand more of this interesting organelle.

1.5.2. Origin and evolution of the apicoplast

The apicomplexan plastid is thought to be a product of a secondary endosymbiotic event where instead of engulfing a cyanobacterial prokaryote, the apicomplexan ancestor gained its plastid by taking up a eukaryote that had already acquired a primary plastid. Ultrastructural and molecular data support the notion that the apicoplast originated from such an event. Hopkins *et al* (1999) postulated that three membranes surround the *Plasmodium* plastid while others have shown that there are four membranes surrounding the plastid (Kohler *et al*, 1997). The two inner membranes correspond to the typical plastid envelopes, while the outermost membrane belongs to the host endomembrane system. Regardless of the finer details, the plastid does seem to originate from a serial endosymbiotic event (Delwiche & Palmer, 1997).

However, there seems to be confusion over the precise origin of the plastid in Apicomplexa. There are arguments over whether the plastid originated from a red alga or green alga. Early evidence supported the green alga lineage where phylogenies constructed from ribosomal RNAs and ribosomal proteins suggested an evolutionary affiliation with the euglenoid plastids (Gardner *et al*, 1994; Howe, 1992). Sequence analysis of the *tuf*A gene, coding for protein synthesis factor, Tu, has placed the

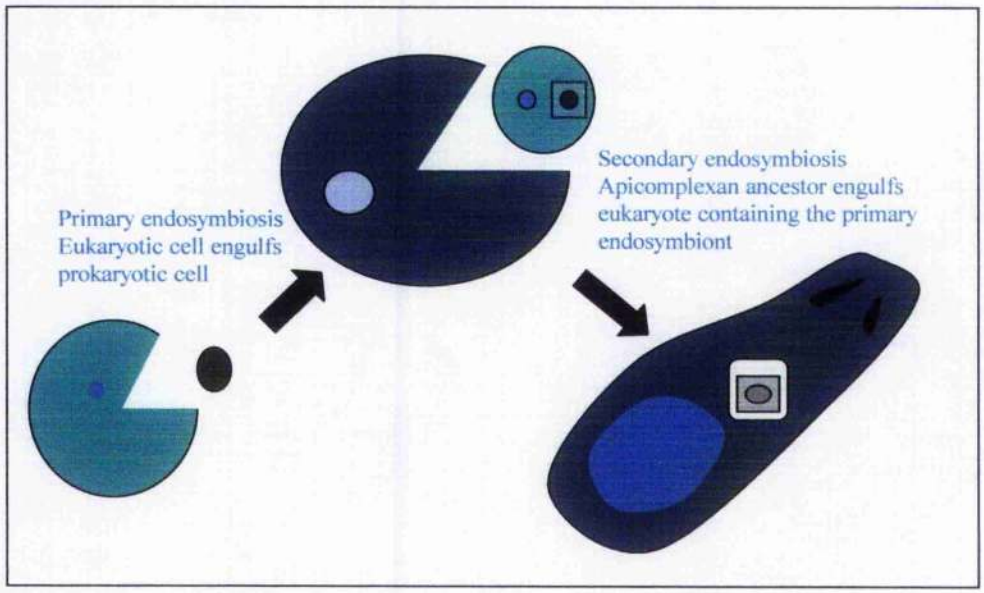

Figure 1.11. Secondary endosymbiotic event where the apicomplexan ancestor engulfed a eukaryote that already harboured a plastid. (Source: adapted from Roos *et al*, 1999).

apicomplexan plastid with the green alga lineage. Unfortunately, these studies were flawed because of a common problem; the apicomplexan plastid genome is very A-T rich, thus skewing both the ribosomal RNA sequences and amino acid composition of proteins (Kohler *et al*, 1997; Wilson *et al*, 1996) which posed a serious problem for sequence analysis and weakened the interpretation of the data obtained.

The presence of a gene, *orf470*, on the *P. falciparum* plastid DNA was the key that led to the proposal of a red alga origin (Williamson *et al*, 1994; Wilson, 1993). The same gene is found on the plastid genome of red algae, where it is designated *ycf24* (Law *et al*, 2000; Williamson *et al*, 1994; Wilson, 1993). The support of a red algal origin of the apicoplast is stronger than that of a green algal lineage (McFadden *et al*, 1997; Zhang *et al*, 2000).

1.5.3. Protein targeting to the apicoplast

The apicoplast genome contains a total of 57 genes (Table 1.3), the majority of which are involved in gene expression. There are genes encoding three subunits of RNA polymerase, 17 ribosomal proteins, elongation factor Tu, duplicated large and small subunit rRNAs and 25 tRNAs. There are also nine open reading frames, one of which encodes a subunit similar to the Clp family of molecular chaperones, one is a conserved ORF found in red algal plastids and the rest are of unknown function. These genes are not sufficient to provide all the required elements for the maintenance and survival of the plastid. During the evolutionary development of plastids, many of the genes that encode proteins that are essential to plastid function have been transferred to the nucleus of the host. The same scenario is observed in plants where it is estimated

Class	Genes
Ribosomal RNA	16S, 23S
Transfer RNA	A^{UGC}, C^{GCA}, D^{GUC}, E^{UUU}, F^{GAA}, G^{ACC}, G^{UCC}, H^{GUG}, I^{GAU}, K^{UUU}, L^{UAG}, L^{UAA}, M^{CAU}, M^{CAU}, N^{GUU}, P^{UGG}, Q^{UUG}, R^{UCU}, R^{ACG}, S^{GCU}, S^{UGA}, T^{UGU}, V^{UAC}, W^{CCA}, Y^{GUA}
Ribosomal proteins	*rps* 2, 3, 4, 5, 7, 8, 11, 12, 17, 19 *rpl* 2, 4, 6, 14, 16, 23, 36
RNA polymerase	*rpoB*, C_1, C_2
Other proteins	*clpC*, *tufA*, ORF430
Unassigned ORFs	51, 78,79, 91, 101, 105, 129

Table 1.3. Gene content of the 35 kb circular DNA of *P. falciparum*. (Source: Wilson *et al*, 1996).

that between 1,000 to 5,000 chloroplast proteins are encoded by nuclear genes (Martin & Herrmann, 1998). These nuclear encoded proteins must be imported back into the

plastid. In order for import, plastid targeted proteins possess N-terminal extensions called transit peptides.

Due to the fact that the apicomplexan plastids are of secondary endosymbiotic origin, protein targeting is more complex because of the presence of multiple membrane layers for the proteins to cross. Therefore, a two-part targeting system is used for plastid entry. Instead of having just a transit peptide, these plastids possess bipartite presequences (Waller *et al*, 1998). These bipartite presequences of proteins that are targeted to the apicoplast have two functional domains:- a signal peptide and a transit peptide. The signal peptide consists of a short run of hydrophobic residues folowed by a cleavage motif (Nielsen *et al*, 1997). The transit peptide domain carries a net positive charge (Waller *et al*, 1998). Recently, the *Plasmodium* transit peptide has been defined (Foth *et al*, 2003) and it also contains a net positive charge due to the high number of lysine residues found within the domain. It is also depleted in acidic residues (glutamate and aspartate) among its first 20 amino acids. In addition, *Plasmodium* transit peptides are enriched in isoleucine while possessing low numbers of small apolar amino acids like glycine, valine, alanine and leucine. With this consensus in mind, Foth *et al* (2003) identified 466 putative apicoplast-targeted proteins in the *P. falciparum* genome.

The presence of a bipartite presequence means that the protein targeting process involves at least two steps. The apicoplast-targeted protein with the help of the signal peptide, first enters into the secretory pathway At some point in this pathway, the transit peptide mediates the transfer committing to, and allowing entry into, the apicoplast (Waller *et al*, 2000). As for the exact mechanism and proteins involved in

this transport process, they are unknown. In plant chloroplasts, protein targeting is mediated through a system called the Tic-Toc system. The translocon outer chloroplast complex (Toc) and the translocon inner chloroplast complex (Tic) are located on the outer and inner membrane of the chloroplast respectively (Soll & Tien, 1998), where they are responsible for translocating proteins across the chloroplast membrane into its interior. Instead of two membranes, the apicoplast is surrounded by at least three membranes. Therefore, the tic-toc system cannot operate precisely as in plants to ensure the translocation of apicoplast-targeted proteins. However, Tic and Toc homologues have been identified in *P. falciparum* (vanDooren *et al*, 2000) which suggests that the protein translocation system in *Plasmodium* is probably related to the tic-toc system known to operate in plant chloroplasts.

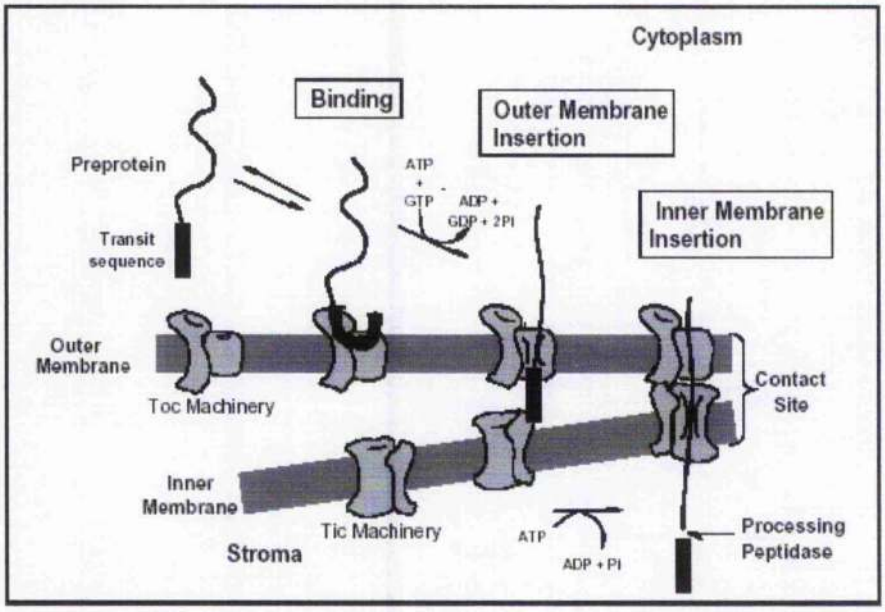

Figure 1.12. Diagrammatic representation of the chloroplast protein transport system (Tic-Toc). (Source: Fuks & Schnell *et al*, 1997)

1.5.4. Functions of the apicoplast

Various experiments have shown that the apicoplast is indispensable for the survival of the apicomplexan parasites (Fichera & Roos, 1997; McConkey *et al*, 1997; McFadden & Roos, 1999). As the apicomplexan plastid is non-photosynthetic, a question arises to its precise cellular function. Since there are estimated to be 466 putative nuclear-encoded plastid targeted proteins – the net plastid proteome could point to its function. Several laboratories have successfully demonstrated the presence of key metabolic activity taking place in the apicoplast. Key pathways include *de novo* fatty acid biosynthesis (Jelenska *et al*, 2001; Waller *et al*, 1998; 2000), isoprenoid biosynthesis (Jomaa *et al*, 1999; Wiesner *et al*, 2000) and haem synthesis (Sato & Wilson, 2002; van Dooren *et al*, 2002). The principal features of these pathways are outlined below.

1.5.4.1. Fatty acid synthesis

Fatty acid synthesis is a process where two-carbon precursors are assembled into fatty acids. Two important cofactors involved in the process are coenzyme A (CoA) and the acyl carrier protein (ACP). Even though it was previously thought that *P. falciparum* does not synthesise fatty acids *de novo* (Matesanz *et al*, 1999), several proteins that are involved in the process including ACP, β-ketoacyl-ACP synthase III (FabH) and acetyl coA carboxylase (ACC) have been shown to localise to the apicoplast (Jelenska *et al*, 2001; Waller *et al*, 1998; 2000). In addition, using radilabelled precursors, Surolia & Surolia (2001) have shown that they are incorporated into fatty acids by *P. falciparum*. The evidence therefore suggests that *P. falciparum* does possess a *de novo* fatty acid synthesis pathway. Judging by the presence of apicoplast-targeted enzymes responsible for fatty acid synthesis, the

apicoplast is likely to be site for fatty acid synthesis. These fatty acids can then be incorporated into phosphoglycerides, sphingolipids and glycosylphosphatidylinositols (GPI).

1.5.4.2. Isoprenoid synthesis

Isoprenoids are a group of natural products that include sterols, carotenoids and terpenoids. They are usually incorporated into proteins that are involved in signal transduction, protein-protein interactions and membrane-associated protein trafficking. A 1-deoxy-D-xylulose-5-phosphate (DOXP) pathway or non-mevalonate isoprenoid biosynthesis pathway in *P. falciparum* linked the apicoplast with the plastids in plants and algae which also possess the DOXP pathway. The DOXP pathway provides a pathway to isoprenoids that is distinct from the pathway in eukaryotes. In *P. falciparum*, the genes encoding DOXP synthase and DOXP reductoisomerase have been found (Jomaa *et al*, 1999) and they contain plastid-targeting domains.

1.5.4.3. Haem synthesis

Haem is the prosthetic group of oxygen-carrying electron-transferring proteins (for example cytochromes). In *P. falciparum*, protein synthesis appears to be haem-dependent (Surolia & Padmanaban, 1991; 1992). *Plasmodium* also appears to encode its own enzyme δ-aminolevulinate dehydratase (ALAD) which is involved in the condensation of two molecules of δ-aminolevulinate to give porphobilinogen (Sato *et al*, 2000; Sato & Wilson, 2002). The gene encoding ALAD possesses a putative apicoplast-targeting leader sequence (Sato & Wilson, 2002), thus it appears that it might be active within the apicoplast. However, there is no evidence for the presence of another important protein, δ-aminolevulinate synthetase (ALAS) which is responsible

for the formation of δ-aminolevulinate from other precursors. Therefore, there is still a need for further clarification to the precise role that the apicoplast plays in haem synthesis.

1.5.5. The apicoplast as a potential drug target

The discovery of the presence of a relict endosymbiont within the apicomplexan parasites has opened up doors for novel chemotherapies exploiting the apicoplast as a drug target. Even though the true function of the apicoplast has yet to be established, it has been shown to be indispensable to the parasite (Fichera & Roos, 1997). Interestingly though, when *Toxoplasma gondii* parasites lose apicoplast function, they do not perish immediately, instead they fail to invade new host cells (He *et al*, 2001). This suggests that the apicoplast may play a role in the invasion of the host cell. In addition, due its prokaryotic origin, the apicoplast contains key cellular processes such as DNA replication, transcription, translation, catabolism and metabolism differ substantially from similar processes in their host. Therefore, the apicoplast can make a good drug target. In the next section, several pathways that have already been targeted by compounds that lead to parasite death are discussed.

1.5.5.1. Fatty acid synthesis

As reviewed in Section 1.5.4.1, the presence of a fatty acid synthetic pathway in *Plasmodium* has been noted. The plasmodial pathway appears to be similar to the type II fatty acid pathway present in bacteria and chloroplasts which uses distinctive enzyme systems when compared with eukaryotic pathways. Several antibiotics target these type II fatty acid biosynthetic enzymes. For example β-ketoacyl ACP synthase (FabH) is a target for thiolactomycin (Waller *et al*, 1998) and triclosan

targets enoyl-ACP reductase (FabI) (Surolia & Surolia, 2001). Both of these antibiotics show anti-plasmodial activity.

1.5.5.2. Isoprenoid synthesis

The DOXP reductoisomerase has been identified in *P. falciparum* and has been shown to be a target of fosmidomycin (Jomaa *et al*, 1999). Furthermore, fosmidomycin can inhibit the growth of *P. falciparum* in culture (Jomaa *et al*, 1999). Many other inhibitors of the DOXP pathway are being tested against bacterial (Altincicek *et al*, 2000) and plant (Zeidler *et al*, 2000) systems which may be of use to test for antimalarial activity.

1.5.5.3. DNA replication and transcription

Since the apicoplast is indispensable for the apicomplexan parasite, inhibitors of DNA replication of its genome will affect the well-being of the parasite itself. Ciprofloxacin blocks prokaryotic DNA replication by inhibiting DNA gyrase, a prokaryotic type II topoisomerase. This antibiotic also inhibits plastid DNA replication in *P. falciparum* (Weissig *et al*, 1997). Interestingly in *T. gondii*, the antibiotic does not kill the parasite immediately but progressively reduces the copy number of the plastid genome, and it affects the ability of the parasite to invade host cells (Fichera & Roos, 1997). As yet, other than *gyrA* and *gyrB* (two components of the DNA topoisomerase system), no other plastid DNA replication related genes have been described. However, enzymes involved in plastid DNA replication and maintenance should be good targets for antimalarials.

Plastid transcription uses prokaryotic-like RNA polymerase homologues (Gray & Lang, 1998). Antibiotics that inhibit transcription can be used against these

parasites. For example, rifampicin inhibits the function of prokaryotic type RNA polymerase B, is effective against apicoplast transcription (Wilson *et al*, 1996) and has activity against *Plasmodium*.

Aims of the project

The discovery of a gene that encodes a putative DNA polymerase, DNA helicase and DNA primase activity, and which possesses a putative apicoplast-targeting presequence, underlies the aims of this project. The main aim of the project was to determine and clarify the true status of this gene, *PfPREX*. My PhD project aimed to clone and express the gene and to determine whether it encodes all of the predicted functions. Moreover, the project aimed to investigate the origins of *PfPREX*, and the evolutionary route that has led to it now functioning in *P. falciparum*.

Chapter II

Materials and Methods

2.1. Materials

All chemicals used were reagent grade and were purchased from Sigma, unless otherwise stated. DNA restriction and modification enzymes were from Promega. Ribo- and deoxyribonucleoside triphosphates were purchased from both Invitrogen and Sigma. Oligonucleotides were synthesised by Invitrogen and MWG Biotech. All radioactive materials were purchased from Perkin Elmer. Poly (dT) from Sigma, had an average length of 200-300 nucleotides. Bacteriophage M13mp18 single-stranded DNA was obtained from New England Biolabs. The recombinant helicase, PcrA was purchased from Cambio Science. Klenow fragment, *Taq* and *Pfu* DNA polymerases were purchased from Promega. The Gateway Cloning kits and competent cells, DH5α and BL21si were obtained from Invitrogen.

2.2. Parasite lines/clones and culture

Plasmodium falciparum clone 3D7 was cultured *in vitro* in a class I sterile hood using the method of Jensen & Trager (1978) with some modifications. The parasites were grown at 5% haematocrit in RPMI 1640 medium (Gibco BRL), supplemented with 5.94 g/l HEPES, 42 ml/l 5% (w/v) sodium bicarbonate and 10% pooled heat-inactivated human serum (group AB). Whole blood was obtained from the Blood Transfusion Service. The cultures were gassed with a mixture of 3% CO_2, 1% O_2, 96% N_2 and incubated at 37°C. The culture was kept at between 1 – 5% parasitaemia. If the parasitaemia exceeded 5%, the culture was diluted to a lower parasitaemia level in fresh supplemented RPMI 1640 medium.

2.3. Bacterial strains and cultures

Several *E. coli* strains were used for cloning, sub-cloning and expression studies. *E. coli* JM109 (Promega) and DH5α (Invitrogen) were used for standard sub-cloning experiments. For the expression studies, the *E. coli* BL21si (Invitrogen) strain was used. The liquid cultures of *E. coli* were grown in Luria-Bertani (LB)(Appendix A.1) broth at 37°C with shaking while for BL21si strains were grown in LB broth with no NaCl.

Antibiotics were used at final concentrations of 30 μg/ml for kanamycin (km) and 50 μg/ml for ampicillin (amp) depending on particular experiments. Stock solutions of the antibiotics were made at 100 mg/ml with water for ampicillin and 30 mg/ml for kanamycin and were kept at –20°C.

2.4. Basic molecular biology techniques

2.4.1. Preparation of parasite extracts

For the preparation of extracts from the malarial parasites, 1 ml of parasite culture (5% haematocrit and 5% parasitaemia) was used. The infected red blood cells were pelleted by spinning at 800 g for 5 minutes. The pelleted red blood cells were lysed by the addition of 0.15% saponin in PBS. The suspension was incubated at room temperature for 15 minutes, followed by centrifugation at 800 g for 10 minutes. The pellet was further washed twice with 1 ml of PBS (Appendix A.2). The parasite pellets were stored at –20°C until use in Western blot experiments.

2.4.2. Preparation of genomic DNA from *P. falciparum*

Genomic DNA from *P. falciparum* 3D7 was isolated from 10^8 mixed asexual erythrocytic stage parasites using the Bio-Rad InstaGene™ whole blood kit. Asynchronous cultures of 3D7 were spun down to obtain the red blood cell pellet and genomic DNA extraction was carried out according to the manufacturer's instructions.

The kit consisted of the lysis buffer and a suspension of InstaGene™ matrix. The cell membrane was broken up by the addition of the lysis buffer and the haemoglobin was released from the red blood cells along with the nuclei from the white blood cells. The white blood cell nuclei were pelleted by centrifugation and the InstaGene™ matrix was added. The matrix is a polyvalent cation-chelating resin which binds cations that would catalyse the degradation of DNA at high temperature. The parasite nuclei were lysed by incubation at 60°C. After centrifugation, the DNA released from the nuclei localised to the supernatant while the debris was in the matrix pellet. The DNA obtained does not need further purification and can be used straight for PCR and other applications.

2.4.3. Preparation of total RNA from *P. falciparum*

Total parasite RNA was prepared using the TRIzol® Reagent (Invitrogen). The TRizol® Reagent is a mono-phasic solution of phenol and guanidine isothiocyanate and the RNA extraction using this reagent was carried out based on the method developed by Chomczynski & Sacchi (1987). The rbc pellet was lysed by the addition of 1 ml of the reagent followed by repetitive pipetting. The rest of the extraction was carried out according to the manufacturer's instructions. The RNA obtained was dissolved in DEPC-treated water and stored at –70°C until use.

2.4.4. Preparation of plasmid DNA from *E. coli*

Plasmid DNA was prepared from 5 ml of overnight bacterial cultures by alkaline lysis. Overnight cultures were harvested at 3,000 g for 15 minutes. Plasmids were extracted using QIAprep spin Mini Prep kit from Qiagen according to the manufacturer's instructions. The plasmid DNA was resuspended in sterile water and stored at -20°C until use.

2.4.5. Restriction digestion of plasmid DNA

Plasmid DNA was digested with various restriction enzymes (Promega). Approximately 0.2 – 2 μg of plasmid DNA was cut using 10 units of enzyme in 1X of the corresponding reaction buffer and left at 37°C for 1 – 2 hours. The digestions were stopped by inactivating the enzyme at 68°C for 10 minutes when using heat-sensitive restriction endonucleases.

2.4.6. Agarose gel electrophoresis of DNA

The DNA samples were separated on 0.8 – 1.0 % agarose (Gibco BRL) prepared in 1X TAE buffer (Appendix A). The gel was cast on a standard gel apparatus (Horizon ® Gibco BRL) and DNA samples containing 1X loading buffer (Appendix A.3) were loaded into the wells of the gel submerged in 1X TAE. 500 ng of 1 kb DNA ladder (Promega) was loaded alongside the samples on the same gel as a DNA size marker. Electrophoresis was carried out at 10 V/cm. The gel was then stained with EtBr (0.5 μg/ml) for at least 15 minutes and viewed under the short range UV transilluminator (Hoefer) and photographed.

2.4.7. Polymerase chain reaction (PCR)

The PCR reactions were carried out in 100 µl volumes containing 200 µM of each dNTP, various concentrations of $MgCl_2$ ranging from 1.5 mM to 3.0 mM, 10 µl of 10X *Pfu* polymerase buffer (Promega), 0 to 10 % DMSO, 1U of *Pfu* polymerase (Promega) and 50 ng of *P. falciparum* 3D7 genomic DNA. The typical amplification profile for the PCR for 25 or 40 rounds was as follows: - denaturation step at 94°C for 30 seconds; annealing step at the appropriate annealing temperature for 30 seconds, followed by an extension step at 62°C for 2 – 10 minutes depending on the end product to be obtained and a final elongation step at 72°C for 5 minutes. The PCR amplifications were performed on the DNA engine Gradient Cycler (MJ Research). 10 µl of the amplified products were analysed on the appropriate percentage agarose gel.

Primer Name	Gene region	Gene-specific primer sequence
GWpolF1	Polymerase	5'-ATCAAGAAATGGAAAAGAATAAC-3'
GWpolR1	Polymerase	5'-ATCATTCCATGGGAACATTT-3'
GWHeliSignalF1	Helicase/Primase	5'-TTCTATGATATACTACCATGCTTTTG-3'
GWHeliHingeR1	Helicase/Primase	5'-TGTTTTGATTCATATTCATCATCAGCTA-3'
GWHeliF4	Helicase	5'-ATGCGAATGATTGTTTGAAACAT-3'
GWHeliR4	Helicase	5'-TCTCTAAACTATCCACATA-3'
GWPriF1	Primase	5'-GTCATAGATGTGGATATAAAGGA-3'
GWPriR1	Primase	5'-TGGCATCAATTTCTCCTTCTGT-3'
GWHingeF1	Hinge	5'-ATGAGCATGTAGTTTCAAATACT-3'
GWHingeR2	Hinge	5'-TACTACTACTGTTCTTATTCTTATT-3'
AttB1		5'-GGGGACAAGTTTGTACAAAAAAGCAGGCT-3'
AttB2		5'-GGGGACCACTTTGTACAAGAAAGCTGGGT-3'
Add attB1 sequence to forward primers and attB2 to reverse primers		
ssurRNAF1	ssurRNA	5'-GATCCTAGCTCAGAATTAAACGCT-3'
ssurRNAR1	ssurRNA	5'-GTAAGGTTTATCGTGTTGCATC-3'

Table 2.1. Primers used for all PCR reactions are listed in this table.

2.4.8. DNA extraction from low-melting point agarose gels

The DNA products were analysed first on a 1% low-melting agarose gel. Gel fragments of the desired size were cut from the gel and incubated with equal volume of TE buffer (0.1M) (Appendix A.2) at 37°C for 30 minutes after disrupting the gel piece with a wide-bore needle. One unit of Agarace (Promega) was added and the suspension was incubated for a further 45 minutes at 37°C. An equal volume of phenol was added and the suspension incubated on ice for 20 minutes. This was followed by centrifugation at 13,000 x g at 4°C for 30 minutes. The upper aqueous layer was removed and the DNA was recovered by standard ethanol precipitation (Sambrook *et al*, 1989)

2.4.9. Reverse-transcriptase PCR amplification (RT-PCR)

2.4.9.1 First strand cDNA synthesis

The RNA used was treated with 2 µl (1 U/µl)(Sigma) of DNase I at room temperature for 15 minutes. 2 µl of RNase inhibitor (10 U/µl) (Gibco Life Technologies) and 2 µl of 200 ng/µl oligo dTs were added to 20 µl of DNase-treated RNA. The RNA was denatured by incubating the mix at 80°C for 10 minutes and then cooled rapidly on ice. After the addition of 4 µl of 0.1 M DTT, 8 µl 5X FSB and 2 µl of 10 mM dNTPs, 20 µl of the mixed solution was removed as a negative control (minus reverse transcriptase). To the rest of the mixture, 1 µl of superscript II (Gibco) was added to make the first strand of cDNA. The primer extension was carried out at 42°C for 1 hour.

Primer Name	Gene region	Primer sequence	Product size (bp)	Tm (°C)
RTHeliF1	Primase	5'-GCTCGTACATTTGTCGTTATGC	-	59
RTHeliF2	Helicase	5'-AAGAAGCTGAAAACGCAAGG-3'	453	59
RTHeliR2		5'-TGGCATCAATTTCTCCTTCTG-3'		60
RTHingeF1	Hinge	5'-TCGGCACAAAATAACATTCC-3'	420	58
RTHingeR1		5'-TCCATCACCGATGTTAGATCC-3'		59
RTPolF1	Polyme-rase	5'-CAACAGGTTTAGAAGTGTTCGATG-3'	400	60
RTPolR1		5'-CAACTAGAATCACGAGCAGCA-3'		59

Table 2.2. Primer sequences used for the RT-PCR reactions.

2.4.9.2. Reverse transcriptase-PCR

The cDNA was amplified using various oligonucleotides, for 40 cycles: 94°C –30 seconds, 50°C –30 seconds, 62°C –2-5 minutes. The amplification products were analysed on an agarose gel using ethidium bromide according to standard procedures.

2.4.10. Formaldehyde gel electrophoresis of RNA

A formaldehyde gel was made by adding a solution containing 16 ml of formaldehyde, 5 ml of 20X Northern gel buffer (Appendix A.4) and 29 ml of DEPC-treated ddH_2O to a solution of 50 ml of 2% agarose melted in a microwave and allowed to set in a standard gel apparatus (Horizon ® Gibco BRL). A 1X Northern Gel buffer was prepared by mixing 50 ml 20X Northern Gel buffer, 88 ml formaldehyde and 860 ml DEPC-treated ddH_2O.

The RNA samples were prepared in a final volume of 20 µl by adding to the RNA sample, 1 µl of 20X Northern gel buffer, 3.5 µl formaldehyde, 10 µl of formamide and DEPC-treated ddH_2O to 20 µl. The mixture was heated at 55°C for 15 minutes, then chilled on ice and 2 µl of RNAse-free loading buffer (Appendix A.4) was added before loading the samples on the gel. The gel was run at 60V for 4 to 5 hours with a magnetic stirrer placed inside the box once the RNA samples had entered the gel matrix. The stirrer keeps the buffer circulated.

2.4.11. Northern Hybridisation

RNA was extracted and approximately 10 µg was electrophoresed using denaturing conditions on a formaldehyde gel. The gel was then directly blotted on to a nylon membrane (Hybond N, Amersham) according to the technique described in Sambrook *et al* (1989), using 20x SSC.

2.4.11.1. Labelling of DNA probes

DNA probes were labelled using the Prime-It random primer labelling kit (Stratagene). The probes were labelled according to the manufacturer's instructions. The procedure relies on the use of random hexanucleotides that anneal to multiple sites along the DNA template. 25 µg of purified DNA templates were boiled for 5 minutes in the presence of the random oligonucleotides in a final volume of 34 µl. The mix was then allowed to cool and 10 µl of 5x primer buffer, 5 µl of [α^{32}P] ATP (3000 Ci/mmol, 10 mCi/ml, NEN Life Science Products), and 1 µl of Klenow fragment (5U/ml) was added. The reaction was incubated to 37°C for 10 minutes and stopped by adding 2 µl of stop mix. The probe was then purified to separate the unincorporated dATP from the

labelled probe using a microspin column (Sigma). The labelled DNA was then denatured by boiling for 5 minutes.

2.4.12. Chemical transformation of *E. coli*

The cells used for chemical transformation were either DH5α (Promega) or BL21si (Invitrogen) and a standard heat shock method was employed (Sambrook *et al*, 1989). 50 µl of cells were used. The cells were pre-incubated with about 1 – 50 ng of DNA to be transformed on ice for 30 minutes. This was to allow the DNA to attach itself to the cells. This was followed by heat shocking the cells at 42°C for 45 seconds. The cells were placed immediately on ice for 2 minutes for the cells to recover before the addition of 450 µl SOC medium (Appendix A.1). The cells were then allowed to multiply at 37°C for 1 hour. 100 µl of the cell suspension was plated onto LB plates containing the appropriate antibiotics and incubated at 37°C overnight.

2.5. Molecular cloning techniques for PfPREX

2.5.1. Gateway cloning technology

Gateway cloning technology (Invitrogen) is a powerful system. It provides a faster and more efficient route to traditional cloning methods. It is based on the lambda phage site-specific recombination. This system allows the transfer of DNA fragments between vectors with compatible recombination sites while maintaining orientation. Therefore, it is a versatile system which allows the simple relocation of a gene of interest into any number of different expression vectors for expression in a variety of hosts. The Gateway Cloning Strategy involves two steps, the first of which is to insert the gene of interest into an entry vector. The second step involves the shuffling of the gene fragment into a destination vector to generate an expression clone.

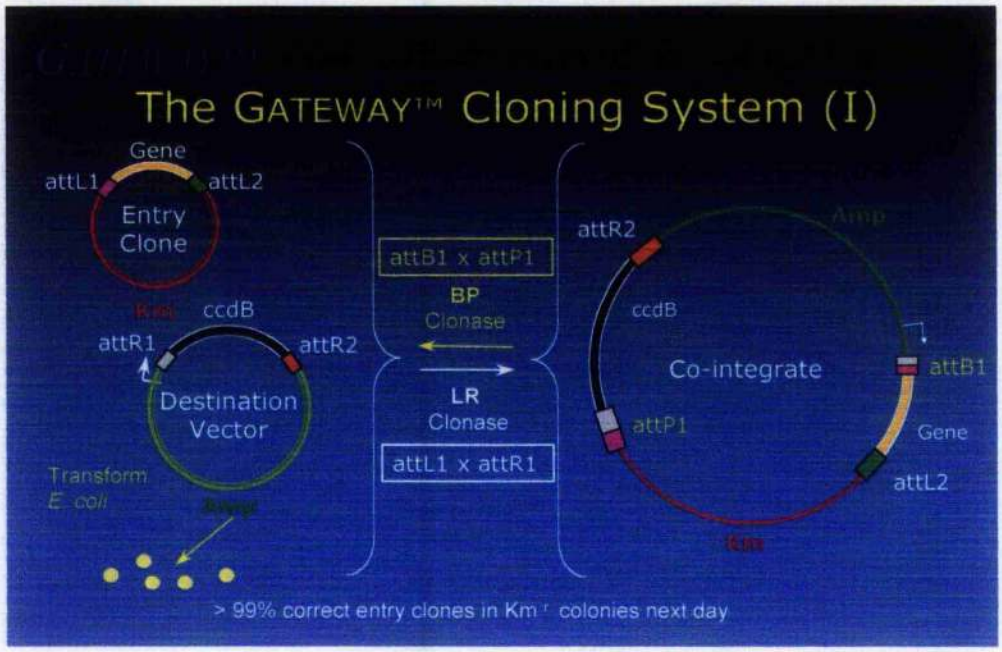

Figure 2.1. Schematic representation of the Gateway cloning technology. The diagram shows the two key reactions for Gateway cloning, the BP reaction and the LR reaction. (Source: Invitrogen)

With our intended genes of interest, we anticipated problems with expression due to the high A-T content of the *Plasmodium* genome. Therefore, this system was selected because it is ideal for us to attempt to clone our gene into different expression vectors with the minimum number of passages through *E. coli* and also permits one to express the recombinant proteins in various expression systems with minimal sub-cloning.

2.5.2. Generation of expression constructs

2.5.2.1. Generation of entry clones

The generation of an entry clone is achieved by designing primers that contain *att*B recombination sites. From the PCR, one obtains PCR fragments containing

the *att*B sites which are then converted into entry clones by recombining into the *att*P sites of pDONR201.

2.5.2.1.1. Preparation of *att*-PCR products

The PCR primers used for the amplification were obtained from Invitrogen. The forward and reverse primers contain additional sequences of *att*B recombination sites at the 5' ends which are $attB_1$ and $attB_2$ respectively. The *attB* sites are specific recombination sites that are normally present in *E.coli* which will recombine with *attP* sites found on the lambda phage for integration process to proceed. The PCR reactions were carried out as stated in Section 2.4.7.

2.5.2.1.2. 'BP' reaction for the generation of the entry clones

The BP reaction involves the generation of the entry clones, it starts with the mixing of the specially generated PCR products containing the gene of interest and the entry vector of your choice. More specifically, the BP reaction facilitates the recombination of the *att*B-containing substrate (*att*B-PCR product) with an *att*P substrate (pDONR201- Donor vector), which gives the reaction the name BP. This reaction is catalysed by the BP Clonase™ enzymes mix.

The *attP* containing entry vector, pDONR201 (300 ng) was mixed with 2 µl of the purified PCR product. It was added to a reaction mixture of 20 µl, containing 4 µl of the BP clonase (mixture containing both the lambda phage integrase and the *E. coli* protein, IHF). After incubation at 25°C for 1 hour, proteinase K (4 µg in 2 µl) was added to inactivate the BP clonase by incubating the mixture at 37°C for a further 20 minutes. 2 µl aliquots were transformed into *E. coli* DH5α (library efficient strain)

(Invitrogen) and plated onto Kanamycin (100 μg/ml) containing LB plates. Since the Gateway reaction has a high efficiency of generation of positive clones (usually > 99%), it minimises the need for screening.

2.5.2.2. Generation of destination clones

2.5.2.2.1. 'LR' reaction for the generation of destination clones

The second step of Gateway Cloning involves the LR reaction. This reaction facilitates the recombination of the *att*L containing entry clone with a *att*R containing destination vector. This reaction is catalysed by the LR Clonase™ enzyme mix.

For the LR reaction, the entry clones obtained from the BP reaction were used. The destination vectors used were pDEST15 (GST-Tag) and pDEST17 (His-Tag). Approximately 200 ng of entry clone was added to 300 ng of destination vector in 20 μl reactions containing 4 μl of LR Clonase™ (which contains lambda recombination proteins Int, Xis and an *E. coli*-encoded protein IHF). The reaction mixture was incubated at 25°C for 60 minutes. Proteinase K was added and the reaction was further incubated at 37°C for 20 minutes. 2 μl aliquots of each reaction were transformed into *E. coli* (DH5α) and plated onto LB-Amp plates (100 μg/ml). Colonies were picked and minipreps to extract the plasmids were performed to identify positive clones.

2.6. Protein analysis

2.6.1. Sodium dodecyl sulphate polyacrylamide gel electrophoresis (SDS-PAGE)

The purified proteins or parasite extracts were prepared by the addition of an equal volume of 2X sample buffer (Appendix A.5). The samples were boiled for five

minutes before being loaded onto a gel system (Laemmli, 1970) consisting of a 10% resolving gel and a 5% stacking gl (Appendix A.5). The gel was run at 150V on a mini-protean dual slab gel electrophoresis apparatus (Bio-Rad) in 1X running buffer (Appendix A.5).

After electrophoresis, the gels were immersed in a Coomassie Blue staining solution (Appendix A.5) for 1 hour at room temperature with shaking. Excess dye is then allowed to diffuse from the gels by immersing the gel in the destain solution (Appendix A.5) for one hour.

2.6.2. Western blotting

The proteins were size-fractionated by electrophoresis on SDS-PAGE gels and transferred to Hybond nitrocellulose membranes (ECL) using the Bio-Rad mini-trans blot electrophoretic transfer cell at 100 V for 1 hour. The membrane was blocked with 5% skimmed milk containing 0.2% Tween 20 in 1X TBS (Appendix A.6). It was probed with a dilution of the primary antibody at 4°C overnight with shaking in 1% skimmed milk with 0.1% Tween 20 in TBS. The membrane was then washed 4 times with 1X TBS, 1% skimmed milk. After washing the membrane, it was probed with horseradish peroxidase-labelled secondary antibody (Diagnostics Scotland), diluted to 1:2000 in 10X TBS and 1% skimmed milk. The membrane was incubated with the secondary antibody at room temperature for 2 hours with shaking, followed by 3 washes for 30 minutes. The immunoreactive proteins were detected using the enhanced chemiluminscence protocol (Pierce). Blots were exposed to film for between 30 seconds to 15 minutes depending on the signal intensity.

2.6.3. Protein quantification

The protein concentrations were determined using the Bio-Rad protein assay which is based on the method of Bradford (Bradford, 1976). It involves the addition of an acidic dye to a protein solution where the colour change is determined by measurement at 595 nm with a spectrophotometer. Protein standards using bovine serum albumin (BSA) were prepared within the range of 0.5 to 5 μg of proteins. The dye reagent (Bio-Rad) was diluted 1:4 with distilled water and filtered to remove particulate matter. 10 ml of each standard and sample solution were pipetted into separate microtiter plate wells. 200 μl of the diluted dye reagent was added to each well and mixed thoroughly. The plate was then incubated at room temperature for at least 5 minutes when the absorbance was read at 595 nm using the microplate reader (Titertek Multiskan® MCC/340). The protein concentrations were calculated with reference to the standard curve drawn with the values obtained from the protein standards prepared.

2.7. Expression and purification of recombinant proteins

2.7.1 Expression and purification of His-tagged recombinant proteins

The polymerase domain (PfPREXpol) was first cloned into an entry vector, pDONR201 then transferred into the Gateway vector pDEST17 (Invitrogen) to give a hexahistidine amino-terminal fusion protein. This was to allow the ease of purification of the recombinant protein. The pDEST17 vector has salt-inducible T_7 promoter, therefore expression of the fusion protein was carried out in *Escherichia coli* strain BL21si (Invitrogen) which enables differential expression in response to salt.

Positive colonies were inoculated onto LB without salt with ampicillin (100 μg/ml). From an overnight culture of 5 ml of LBamp without NaCl, 1 in 100 dilution of

the culture was transferred to fresh LBamp without NaCl, containing the respective antibiotics and incubated at 37°C until OD_{590} was approximately 0.3. Expression of the recombinant protein was induced by the addition of 5 M NaCl to a final concentration of 0.3 M and incubated at 37°C for a further 4 hours. The culture was then harvested and resuspended in the lysis buffer (1 mM EDTA, 50 mM Tris-HCl, pH 8.0, 1 mM DTT). The cells were lysed by sonication (20 microns, 30s on, 30s off for 6 cycles). Lysates were cleared by centrifugation at 13,000 x g for 20 minutes at 4°C. The cell lysates were filtered using a 0.2 μm syringe filter (Sartorius). The recombinant protein was then purified using a Nickel-chelate column through the BioCad purification system, which allowed high-pressure affinity chromatography to be carried out. A wash was carried out at the beginning with 50 mM of imidazole to remove non-specific binding of *E. coli* proteins from the column. Elution of the His-tag proteins was performed at an imidazole gradient ranging from 50 mM to 500 mM with 1.5 ml fractions over 10 fractions. Fractions containing the eluted recombinant protein were collected and pooled together. The pooled fractions were concentrated using a stirred cell concentrator (Amicon) and a cellulose membrane of 30 kDa cut off size (Flowgen). Concentration of at least 15 fold was achieved. The purified proteins were then checked for purity by running on a protein SDS-PAGE gel.

2.7.2 Expression and purification of GST-tagged recombinant proteins

The helicase/primase domain was also cloned into pDONR201 to make the entry clones and then transferred to the pDEST15 vector to give a N-terminal GST-Tagged fusion protein. Like the pDEST17 vector, the pDEST15 vector has a salt-inducible T7 promoter for which the induction of expression of the fusion protein was carried out in the *E. coli* BL21si strain (Invitrogen).

The positive colonies were plated on LB plates without salt with ampicillin (100 μg/ml) and the procedure for the induction of expression of the recombinant protein was essentially the same for the His-Tagged recombinant protein.

The purification of the GST-Tagged recombinant proteins was performed using the GST-purification kit from Novagen. The GST purification resin slurry (50%) was provided with the kit. A 2 ml bed volume column was made and the 20% ethanol was allowed to drain from the column. The column was allowed to equilibrate in 5 volumes of 1X GST wash buffer provided in the kit. Subsequent washing steps using 10 volumes of 1X GST wash buffer was carried out. For the elution of the GST-Tagged proteins, the 1X elution buffer containing reduced glutathione (10 mM) was used. Three eluted fractions of 2 ml volume were collected and the fractions were concentrated using a stirred cell concentrator (Amicon) and a cellulose membrane of 10 kDa cut off size (Flowgen). Concentration of at least 5 fold was achieved. The purified protein quality was checked by SDS-PAGE.

2.7.3. Production of antibodies

For the production of anti-serum against the polymerase domain, the recombinant polymerase was sent to 'Diagnostics Scotland'. The polyclonal antiserum was raised in rabbit by the inoculation of 4 aliquots of the recombinant polymerase (100 μg per aliquot of 1 ml).

For the production of the antisera against the hinge, primase and helicase domains, new primers were designed for those domains to clone them into Gateway pDEST15 vector to generate the new recombinant proteins. The GST-Tagged fusion

proteins were purified as stated in the previous section and four aliquots of proteins were sent to Diagnostics Scotland to have polyclonal antisera raised in rabbits.

All the antisera (with the exception of the GST-tagged helicase domain antisera due to time constraint) were all checked using dot blotting method against the corresponding recombinant proteins to ensure the presence of antibodies in the antisera specific for the proteins in question. In addition, negative controls were carried out to ensure that first there was no non-specific cross-reaction between the antisera produced and non-related proteins and that the pre-immune sera also did not produce any reaction to the corresponding recombinant proteins.

2.8. Functional analysis of the recombinant proteins

2.8.1. DNA primase activity assays

Reaction buffer for the DNA primase assay contained 50 mM NaCl, 2 mM $MgCl_2$, 200 μM ATP, 0.2 mg/ml BSA, 50 mM Tris (pH 7.5). An appropriate amount (1 μg) of primase was added to the reaction buffer alongside 500 ng of poly (dT) and incubated at 30°C for 15 minutes. Subsequently, buffer exchange was performed to remove the salts from the previous reaction buffer in buffer-exchange columns (Amersham). The flow-through from the buffer exchange columns was then used for the next step of the assay whereby 1 U of Klenow fragment (Promega) and 10 μCi of [^{3}H]-dATP (15 Ci/mmol, Perkin Elmer), along with the buffer provided with the Klenow fragment were added. The reaction mixture was incubated at 30°C for 30 minutes before it was terminated by the addition of 10 μl of 0.5 M EDTA. The unincorporated radionucleotides were removed using either microspin G-50 columns (Amersham Biosciences) or the Sigma Spin Post-reaction spin columns, spun at 750 x g

for 2 minutes. The flow-through was then counted for 1 minute in a beta-scintillation counter (Perkin Elmer Wallace Trilus 1450 Microbeta). Negative controls were carried out using the recombinant PfPREXpol. This was carried to ensure that the activity observed was due to DNA primase alone and not some *E. coli* contaminating protein that may be present in the purified recombinant protein.

2.8.2. DNA helicase activity assays

DNA helicase activity was characterised using the Helicase [^{3}H] scintillation proximity enzyme assay (SPA) system (Amersham Life Science). The SPA system uses a weak beta-emitter like [^{3}H]. On contact with the SPA beads, the deceleration of its particles will emit a light signal which can be measured. The starting material of the assay is a M13 single-stranded DNA bound to a [^{3}H]-oligonucleotide. If a helicase is present, the oligonucleotide will be unwound from the M13 single-stranded DNA. The [^{3}H] -oligonucleotide is then free to bind to a biotinylated complementary oligonucleotide. At this point streptavidin-SPA beads are added to the reaction buffer which will bind to the biotinylated/[^{3}H]-oligonucleotide (Figure 2.2). This association of all the appropriate molecules will lead to a production of a signal which can be measured by a scintillation counter.

The assay is set up using 20 µl of the assay buffer containing 30 mM Tris-HCl, pH 7.6, 5 mM ATP (or various other nucleotides), 5 mM $MgCl_2$, 0.075% (v/v) Triton X-100, 0.05% (w/v) sodium azide to which 10 µl of the diluted (1:10) substrate solution which contains 10 mM Tris-HCl, pH 8.0, 25 mM NaCl, 1 mM EDTA and 0.05% (w/v) sodium azide and 0.08 µCi of [^{3}H]-dNMPs was added. 10 µl of the purified recombinant helicase (approximately 1 µg) was added to the reaction mixture.

The reaction was started by incubating the tubes at 33°C for 1 hour. The reaction was terminated by the addition of 10 µl of the stop/capture reagent and incubated for a further 15 minutes at 33°C. To the mixtures, 200 µl of streptavidin SPA bead suspension was added and incubated at room temperature for 15 minutes. The tubes were then counted for 1 minute in a beta-scintillation counter (Perkin Elmer Wallace Trilus 1450 Microbeta). All reactions were carried out in triplicate.

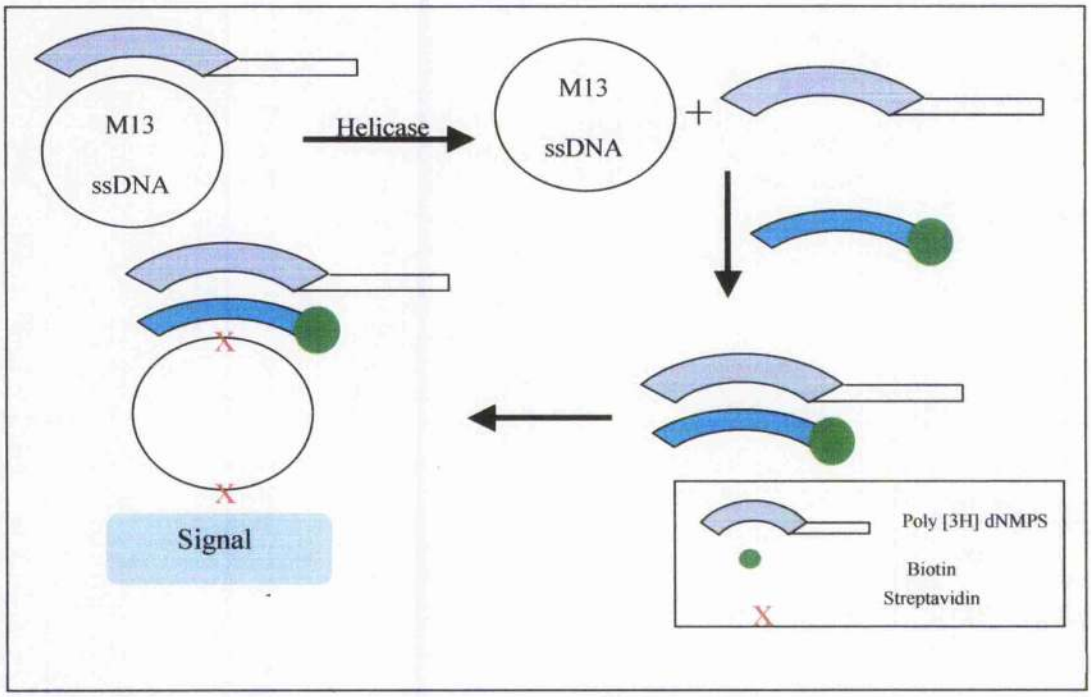

Figure 2.2. Helicase [^{3}H] Scintillation proximity enzyme(SPA) assay (Amersham). (Adapted from Amersham Bioscience).

2.8.3. DNA polymerase activity assays

Reaction mixtures contained 20 mM Tris-HCl, pH 8.0, 1 mM DTT, 5 mM $MgCl_2$, 20 µg BSA, 100 µM each of dCTP, dTTP, dGTP and 10 µCi [^{3}H]-dATP (15 Ci/mmol, Perkin Elmer) (method adapted from Huang & Levin, 2001). The template

used for the assay was M13mp18 single-stranded DNA (1.2 pmol), annealed to 1.6 pmol of M13 specific primer (5'-TTCCCAGTCACGACGTTGTAAAACGACGG-3'). A volume of 1.2 µl of the annealed primer-template mixture was added to the reaction mixture along with 5 µg of the recombinant enzyme. The mixture was incubated for 1 hour at 37°C. The unincorporated radionucleotides were removed using either microspin G-50 columns (Amersham Biosciences) or the Sigma Spin Post-reaction spin columns (Sigma), spun at 750 x g for 2 minutes. The radioactivity that passed through the column representing incorporated nucleotides, was then counted in a liquid scintillation counter (LKB Wallace 1219 Rack Beta). The relative activity in any given experiment is defined as a percentage relative to the highest activity recorded in a given experiment.

The DNA polymerase activity was also evaluated in the presence of various concentrations of $MgCl_2$, KCl and various pHs and temperature variations are recorded the relevant sections. The effect of aphidicolin was also examined by the addition of various concentrations of the inhibitor. All reactions were carried out in triplicate.

2.8.4. 3'-5' exonuclease activity assays

The substrate for the 3'-5' assay was prepared similarly to the reaction mixtures for the DNA polymerase activity assays (method adapted from Huang & Levin, 2001). Reaction mixtures contained 50 mM Tris-HCl, pH 8.0, 1 mM DTT, 5 mM $MgCl_2$, 20 µg BSA, 100 µM of each of dCTP, dTTP, dGTP, 50 µCi α-^{32}P-dATP and 5 pmol of M13-ssDNA to a final volume of 50 µl. Five units of Klenow fragment were added to catalyse the reaction and the mixture was incubated at 37°C for 1 hour. The unincorporated radionucleotides were removed using microspin G-50 columns. This labelled, double-stranded DNA substrate was then used for the exonuclease assay.

For the assay, the labelled DNA substrate was added to 50 mM Tris-HCl, pH 8.0, 1 mM DTT, 20 μg BSA and 5 μg of purified recombinant polymerase. The reaction mixture (25 μl) was incubated at 37°C for 1 hour in the absence of deoxyribonucleotide triphosphates. The reaction was stopped by the addition of 5 μl of 0.5 M EDTA, pH 8.0. DNA was precipitated by the addition of 10 μl of 100% TCA and by centrifugation at 13,000 x g for 30 minutes. The radioactivity of the supernatant fraction that contained the released nucleotides, was determined in a liquid scintillation counter. A control reaction where the recombinant protein was not added was also carried out. All reactions were carried out in triplicate.

2.8.5. Nucleotide hydrolysis assays

DNA helicase activity requires the hydrolysis of NTP substrates to release the free phosphate to power its actions. NTP hydrolysis was measured using the method adapted from Tseng *et al* (2000). The method used is colorimetric and involves the detection of the released phosphate by the absorption of a 'molybdate blue' complex which forms upon the reduction of an ammonium molybdate-phosphate complex in strong acid solution.

The reaction was carried out in a 96-well plate in a 30 μl assay volume which contained the assay buffer (50 mM Tris-HCl, pH 7.6, 10 mM $MgCl_2$, 0.2mg/ml BSA, 2.0 mM of individual NTPs/ dNTPs and M13 ssDDNA (17 μg/ml)). The reaction was incubated at 37°C for one hour after which 125 μl of a 1:1 mixture of 1.4% ascorbic acid in 1M H_2SO_4 and 0.36 % in 1M H_2SO_4 was added. The reaction was incubated at 37°C for 15 minutes for colour development to take place. Negative

controls were carried out where no enzyme was added to detect if there was spontaneous hydrolysis of the dNTPs. The plate was then read at A_{690} using a microplate reader (Titertek).

2.9. Subcellular localisation of *PfPREX* gene products

2.9.1. Indirect immunofluorescence

For experiments with mitotracker staining, the live *Plasmodium* infected erythrocytes were incubated in the presence of 100 nM of Mitotracker® Red CMXRos (Molecular Probes) for 15 minutes at 37°C and washed 2 times in PBS, after which, normal blood smears with parasitised red blood cells were performed on slides that were then air-dried for 10 minutes. The slides were fixed in acetone and allowed to air dry. Later, the slides were blocked in blocking buffer for 20 minutes at room temperature. The slides were then incubated with the appropriate primary and secondary antibodies. Secondary antibodies were fluorescein isothiocyanate (FITC)-coupled anti-rabbit IgG (Diagnostics Scotland). Primary antibodies included those raised to the DNA polymerase domain, the DNA primase region and the DNA helicase region (peptide fused to GST – more details included in the results section).

The primary and secondary antibodies were diluted appropriately in the immunobuffer. Dilutions are detailed in the results section.. In between incubation with the primary or secondary antibodies, the slides were washed twice in 1X PBS containing 0.2% Tween 20. Where indicated, slides were stained in 5 mM 4,6-diamidino-2-phenylindole (DAPI) (Sigma) for 30 minutes at 37°C. Coverslips were mounted with the anti-fade agent AF2 (Citifluor).

2.9.2. *In situ* hybridisation

2.9.2.1. DNA probe preparation

The ssurRNA PCR product was amplified using the ssurRNAF1 and ssurRNAR1 primers (Table 2.1). The appropriate PCR product was used as the DNA probes for the *in situ* hybridisation were denatured at 80°C for 2 minutes. The probes were then allowed to cool slowly down to 42°C. Approximately 75 ng of DNA probed was added to the same volume of 50% formamide for use in the experiment.

2.9.2.2. *In situ* hybridisation

Slides were prepared and fixed as stated in section 2.9.1. The slides were prehybridised in the hybridisation buffer (HB) for 2 hours at 42°C. Once the excess hybridisation buffer was removed, the DNA probe was added (6 µl in 24 µl HB) was added. The coverslips were mounted and the slides were incubated overnight at 42°C on a PCR machine (Hybrid).

The slides were washed 3 times in 0.1X SSC for 30 minutes at 42°C, followed by 2 washes in 1X SSC for 10 minutes at room temperature. Finally, the slides were washed in 1X PBS for 5 minutes.

2.9.2.3. Fluorescent detection of the *in situ* hybridisation DNA probe

The slides were placed in detection buffer for 5 minutes. The slides were blocked in BSA blocking buffer (2% (w/v) BSA in Detection buffer) at 37°C for 30 minutes in the dark. After the blocking step, the detection solution (10 µg/ml of Streptavidin-Texas red in BSA blocking buffer) was added and the slides were incubated at 37°C for 1 hour. Three washes in detection buffer were done at 42°C for 20

minutes. Coverslips were mounted with the anti-fade agent for viewing under the microscope.

2.9.3. Fluorescent Microscopy

Slides prepared were viewed using a Zeiss Axiovert 35 inverted microscope equipped with a 100W Mercury-vapour lamp. The microscope was equipped with a Axiovision camera Axiovision Software (Zeiss). The DAPI filter had an excitation and emission peaks of 360 nm and 460 nm, the Texas red filter- 560 nm and 630 nm and the FITC filter- 484 nm and 510 nm respectively. Image analysis was performed using Axiovert software (Axiovert). The images were merged using the Adobe Photoshop 6.0 software.

2.10. DNA sequencing

Plasmids that contained the cloned PCR fragments were sent to MWG-BIOTECH (Milton Keynes, UK) for sequencing. The plasmids were sequenced in both directions to confirm their sequences. The data obtained was then analysed by comparing chromatograms using Vector NTI version 6 (Informax, Inc.).

2.11. Software

Prism version 3.02 (Graphpad software) (http://www.graphpad.com/prism/Prism.htm) was used to handle all the biochemical graph-fitted data.

The Vector NTI suite 6 (http://www.informaxinc.com) package was used to handle DNA and protein sequences. The suite contains different functional modules like AlignX® for carrying out alignments and ContigExpress® for the construction of contigs from shorter sequences.

ClustalX version 1.81 (Jeanmougin *et al,* 1998) was used to do the protein multiple alignments where stated. Specific parameters for the protein alignments are described the relevant results sections.

Mega (Molecular evolution and genetic analysis) version 2.1 (http://www.megasoftware.net) was used to build all phylogenetic trees. There are four different tree-building methods available with the software – Neighbour Joining (NJ), Unweighted Paired Group Method with Arithmetric Mean (UPGMA), Minimum Evolution (ME) and Maximum Parsimony (MP). The default settings used for tree generation are discussed in the relevant result sections.

VMD (Visual Molecular Dynamics) version 1.8.1

(http://www.ks.uiuc.edu/Research/vmd/) was used to visualise 3D structures of proteins.

A number of different databases were used to clarify *PREX* homologues, predominantly using BLAST servers associated with the sites listed below: -

Databases

- TIGR databases: http://www.tigr.org/tdb/parasites
- Parasite-genome (European Bioinformatic Institute): http://www.ebi.ac.uk/blast2/parasites.html
- The Sanger Center: http://www.sanger.ac.uk/Projects/
- NCBI: http://www.ncbi.nlm.nih.gov/BLAST
- Plasmodb: http://www.plasmodb.org

Alignment programme

- DIALIGN: http://www.genomatix.de/cgi-bin/dialign/dialign.pl (Morgenstern *et al*, 1996). The parameters used for the protein alignments:- Threshold T =0 (DIALIGN uses diagonals to construct an alignment. Therefore, the threshold *T* influences the set of used diagonals: with $T > 0$, a diagonal is considered for alignment only if its *weight* exceeds this threshold. Regions of lower similarity are not aligned.)

Prediction of the presence of signal peptide

- SignalP: http://www.cbs.dtu.dk/services/SignalP/#submission (Nielsen *et al*, 1997).

Prediction of apicoplast-targeted *Plasmodium* proteins

- PlasmoAP: http://www.plasmodb.org/restricted/PlasmoAPcgi.shtml (Foth *et al*, 2003).
- PATS (Prediction of apicoplast targeted sequences) : http://gecco.org.chemie.uni-frankfurt.de/pats/pats-index.php (Zuegge *et al*, 2001).

ORF prediction software

- ORF finder : http://www.ncbi.nlm.nih.gov/gorf/gorf.html

Chapter III

Identification of a novel gene, *PfPREX*, from *Plasmodium falciparum*

3.1. Introduction - background to the discovery of the gene, *PfPREX*.

During a study carried out by Dr P.Neuville with Professor RS Phillips, (University of Glasgow) analysing antigenic variation in *P. chabaudi* AS strain, a gene with a putative role in this process was identified and named *Pom*I (Genbank accession No: AAA84746.1). The gene was identified using hyperimmune serum raised in mice against antigenically distinct variants of *P. chabaudi*, one from the parent AS clone and a second raised from a recrudescent variant clone. The serum was used to screen phage λ gt 11 expression libraries of cDNA from the parasite and several clones were recognised by the sera. The clones were all sequenced and one particular clone of 597 bp translated to give a putative protein containing an ATP-binding site (*Pom*I). The *Pom*I sequence was used in BLAST searches against the *P. falciparum* genome database (Sanger Center, TIGR and Stanford University). The search gave a longer sequence (an apparently full-length open reading frame, ORF of 6057 bp) in *P. falciparum*. On further investigation, it was revealed that it contained a single open reading frame encoding 2016 amino acids (Genbank accession No: AAN36724.1) with a predicted molecular mass of 235.8 kDa. Since work reported in this thesis indicates that the gene encodes proteins involved in plastid DNA replication, it was named *PfPREX* (*P. falciparum* Plastid Replication/Repair Enzyme Complex)

This chapter describes the work involved in elucidating the properties and arrangement of the *PfPREX* gene. The purpose of this chapter is to provide insight into the nature of the gene and also the background to the predicted functions based on sequence information.

3.2. Identification of the gene and sequence analysis

The nucleotide sequence of the gene studied in this thesis has been termed *PfPREX*. The predicted amino acid sequence, PfPREX was used in BLASTP searches in the NCBI website (http://www.ncbi.nlm.gov/blast) against non-redundant protein databases. Initially, the C-terminal domain of PfPREX produced a match to a thermostable DNA polymerase from *Aquifex aeolicus* (Genbank accession Number: AAC07735.1) with an E value of $1x10^{-53}$ (Figure 3.1a). The N-terminus of PfPREX showed homology to DNA helicases and primases from bacteriophages (E values of $7x10^{-7}$ - $4x10^{-5}$) and bacteria (Figure 3.1b). It seems that the *PfPREX* sequence encodes for a polypeptide with more than one functional domain (Figure 3.2). Therefore, it was decided to split the *PfPREX* sequence into separate regions to do more detailed homology modelling to provide a clearer indication of the roles of different domains of PfPREX.

3.2.1. Identification of a DNA polymerase-like domain in the *PfPREX* sequence

The C-terminal end of the sequence, which has been designated PfPREXpol, was used in a BLASTP search against the non-redundant protein database (Figure 3.1a) The predicted sequence shares 25-30% identity and 40-46% similarity with prokaryotic DNA polymerases from the family A group (Section 1.4.3.1.3). The results gave E values of $1x10^{-53}$ to $6x10^{-7}$ with the highest significant homology to the DNA polymerase of *Aquifex aeolicus* (Genbank accession Number: AAC07735.1). The other matches all belong to the members of the family A group such as *E. coli* DNA polymerase I, *Thermus aquaticus* DNA polymerase I and T7 DNA polymerase I.

(a)

sp|O67779|DPO1_AQUAE DNA POLYMERASE I (POL I) >gi|7514773|p...	213	1e-53
sp|O51498|DPO1_BORBU DNA POLYMERASE I (POL I) >gi|7434818|p...	189	2e-46
pir||E72232 DNA-directed DNA polymerase I - Thermotoga mari...	175	4e-42
sp|P00582|DPO1_ECOLI DNA POLYMERASE I (POL I) >gi|67054|pir...	159	4e-37
pdb|1KFD| Dna Polymerase I (Klenow Fragment) (E.C.2.7.7....	159	4e-37
pdb|2KFN|A Chain A, Klenow Fragment With Bridging-Sulfur Su...	159	4e-37
sp|Q59156|DPO1_ANATH DNA POLYMERASE I (POL I) >gi|1405438|e...	158	6e-37
pdb|1KLN|A Chain A, Dna Polymerase I (Klenow Fragment) (E.C...	157	2e-36
sp|P43741|DPO1_HAEIN DNA POLYMERASE I (POL I) >gi|1074025|p...	155	4e-36
pdb|1D8Y|A Chain A, Crystal Structure Of The Complex Of Dna...	155	6e-36
sp|O05949|DPO1_RICPR DNA POLYMERASE I (POL I) >gi|7434819|p...	154	8e-36
emb|CAB72805.1| (AL139074) DNA polymerase I [Campylobacter ...	154	8e-36

(b)

gi|9627449|ref|NP_041977.1|	gene 4B/helicase [14,15] [Enter...	59	7e-07
gi|30387470|ref|NP_848279.1|	primase/helicase protein [Yers...	58	1e-06
gi|9627447|ref|NP_041975.1|	gene 4A, primase/helicase [14,1...	58	1e-06
gi|17570807|ref|NP_523316.1|	helicase [Bacteriophage T3] >g...	55	7e-06
gi|17570806|ref|NP_523315.1|	DNA primase/helicase [Bacterio...	55	7e-06
gi|9634014|ref|NP_052088.1|	helicase [Bacteriophage phiYeO3...	55	1e-05
gi|9634013|ref|NP_052087.1|	DNA primase/helicase [Bacteriop...	55	1e-05
gi|9964622|ref|NP_064752.1|	RFprimase/helicase [Roseophage ...	54	3e-05
gi|29366716|ref|NP_813761.1|	putative primase/helicase [Pse...	53	4e-05

(c)

gi|23509333|ref|NP_702000.1|	POM1, putative [Plasmodium fal...	1779	0.0
gi|1142660|gb|AAA84746.1|	POM1 [Plasmodium chabaudi chabaudi]	495	e-138
gi|23487175|gb|EAA20985.1|	POM1 [Plasmodium yoelii yoelii]	493	e-137
gi|27684485|ref|XP_219939.1|	similar to twinkle [Mus muscul...	245	3e-63
gi|11141909|ref|NP_068602.1|	twinkle; likely ortholog of mo...	244	8e-63
gi|14582616|gb|AAK69558.1|AF292004_1	putative T7-like mitoc...	244	8e-63
gi|24962647|ref|NP_722491.2|	twinkle [Mus musculus] >gi|244...	244	1e-62
gi|21294867|gb|EAA07012.1|	ENSANGP00000000580 [Anopheles ga...	239	3e-61
gi|24583154|ref|NP_609318.1|	CG5924-PA [Drosophila melanoga...	231	7e-59
gi|20976892|gb|AAM27521.1|	LD38710p [Drosophila melanogaster]	228	5e-58
gi|14582618|gb|AAK69559.1|AF292005_1	truncated putative T7-...	206	3e-51
gi|22028196|gb|AAH34909.1|	Twinl protein [Mus musculus]	198	6e-49

Figure 3.1. BLAST results with the description consisting of four columns (from the left): (1) identifier for the database sequence (Genbank Entry); (2) brief description of the sequence; (3) the (bit) score of the highest-scoring HSP (High Scoring Pairs) found for each database sequence; (4) the E value. (a) BLASTP results using PfPREX against non-redundant protein database (http://www.ncbi.nlm.nih.gov/BLAST) showing matches to prokaryotic DNA polymerases. (b) BLASTP results using PfPREX against non-redundant protein database (pre-2001) showing matches to DNA helicases and primases. (c) More recent BLASTP (post-2001) results showing matches to 'Twinkle' and its homologues. The BLAST results obtained has changed since the beginning of the project with newer entries into the database in which our sequence is homologous to, as shown in part b and c in this figure.

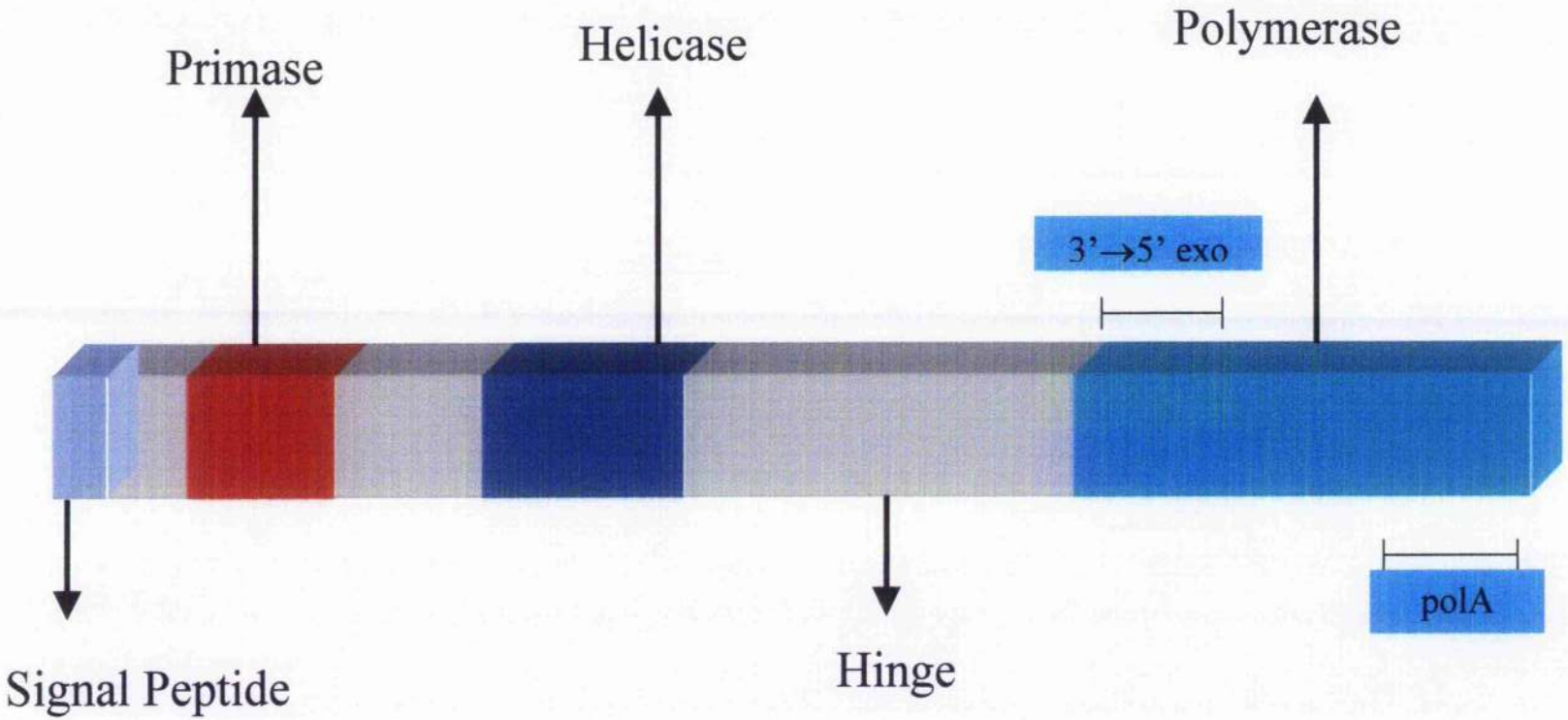

Figure 3.2. Diagrammatic representation of PfPREX protein with the different functional domains it encodes for. A signal peptide at the extreme N-terminus end followed by a DNA primase and DNA helicase domain, separated by a hinge region, and a DNA polymerase domain.

3.2.2. The family A group of DNA polymerases

The DNA polymerases from family A group have diverse roles such as gap filling, DNA repair and DNA replication (Albà, 2001; Burgers, 1998; Hubscher *et al.*, 2000) (Figure 3.3). Most DNA polymerases from this family, exemplified by *E. coli* DNA polymerase I, possess three domains which include a 5'-3' exonuclease domain, a central 3'-5' exonuclease domain and a C-terminal polymerase domain. Not all members of the family have all three domains (Figure 3.3). Sequence alignments of PfPREXpol with other family A DNA polymerases (Figure 3.4) indicated the absence of a 5'-3' exonuclease domain while the 3'-5' exonuclease and polymerase domains were observed. This is similar to the phage T5 DNA polymerase I and *Aquifex aeolicus* DNA polymerase I, neither of which have the 5'-3' exonuclease domain. The Klenow fragment of *E.* coli Pol I is obtained by protease cleavage which remove the 5'-3' exonuclease domain (Klenow & Overgaard-Hansen, 1970).

3.2.3 3'-5' exonuclease domain

The 3'-5' exonuclease activity usually provides proofreading for the DNA polymerase and this helps to enhance the accuracy of the DNA synthesis activity of the DNA polymerase which helps to enhance genome stability. The exonuclease functions by catalysing the excision of the nucleoside monophosphate (dNMP) from the 3' end of the DNA. Within the PfPREXpol domain, we have located all three conserved motifs (Exo I-III) of the 3'-5' exonuclease activity (Figure 3.5). The conserved motifs are DxET in the Exo I region, NX_2YD in the Exo II region and YX_3D in the Exo III region. The aspartate residues found in all three Exo regions and the glutamate in Exo I are thought to be essential for divalent metal ion binding which participate in the catalysis of phosphoryl transfer (Beese & Steitz, 1991; Bernad *et al.*, 1989; Derbyshire *et al.*,

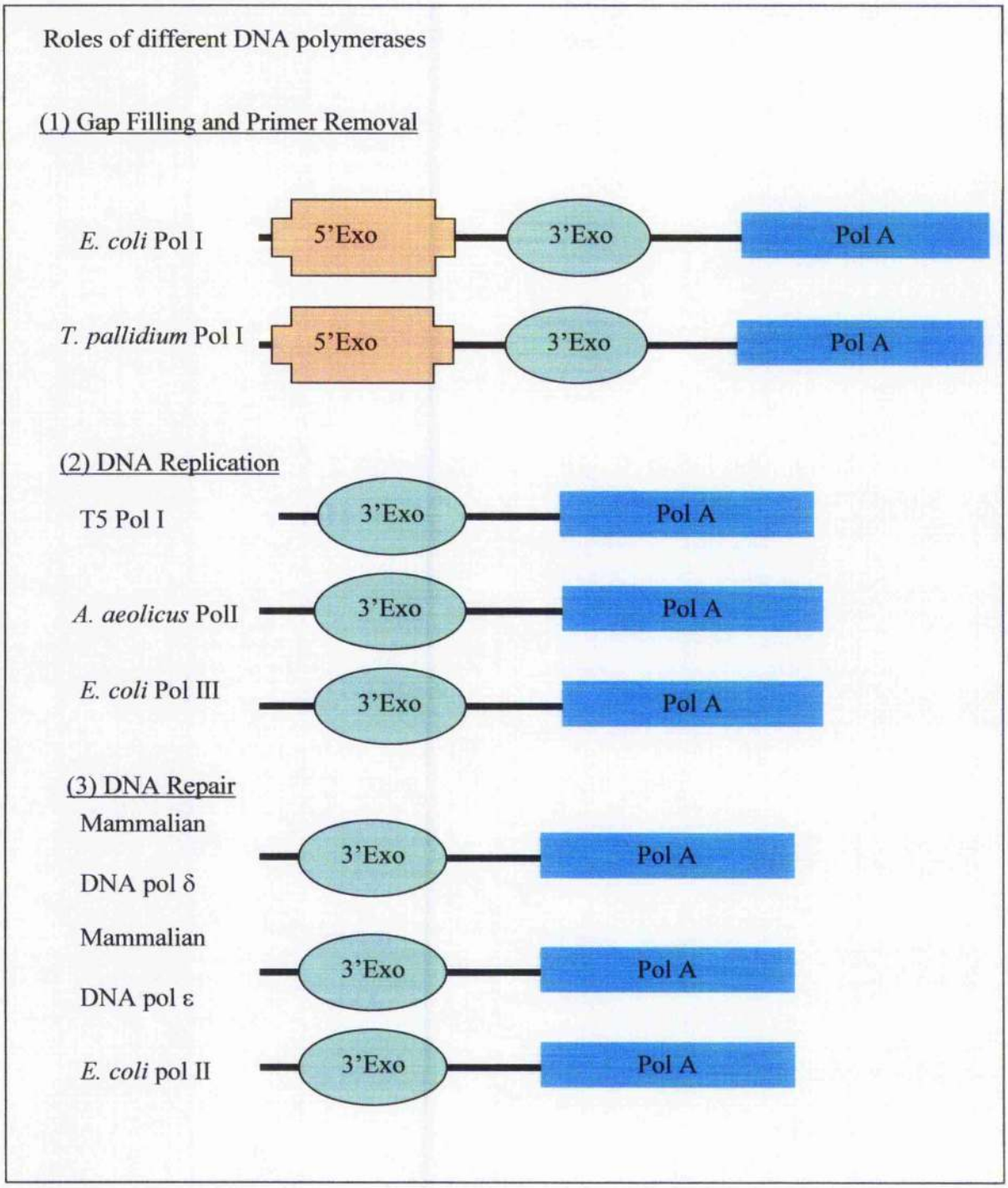

Figure 3.3. Diagrammatic representations of the roles of different members of the family A group of DNA polymerases. 5'Exo box represents the 5'3' exonuclease domain, the 3'Exo box represents the 3'5' exonuclease domain and the Pol A box represents the polymerase domain.

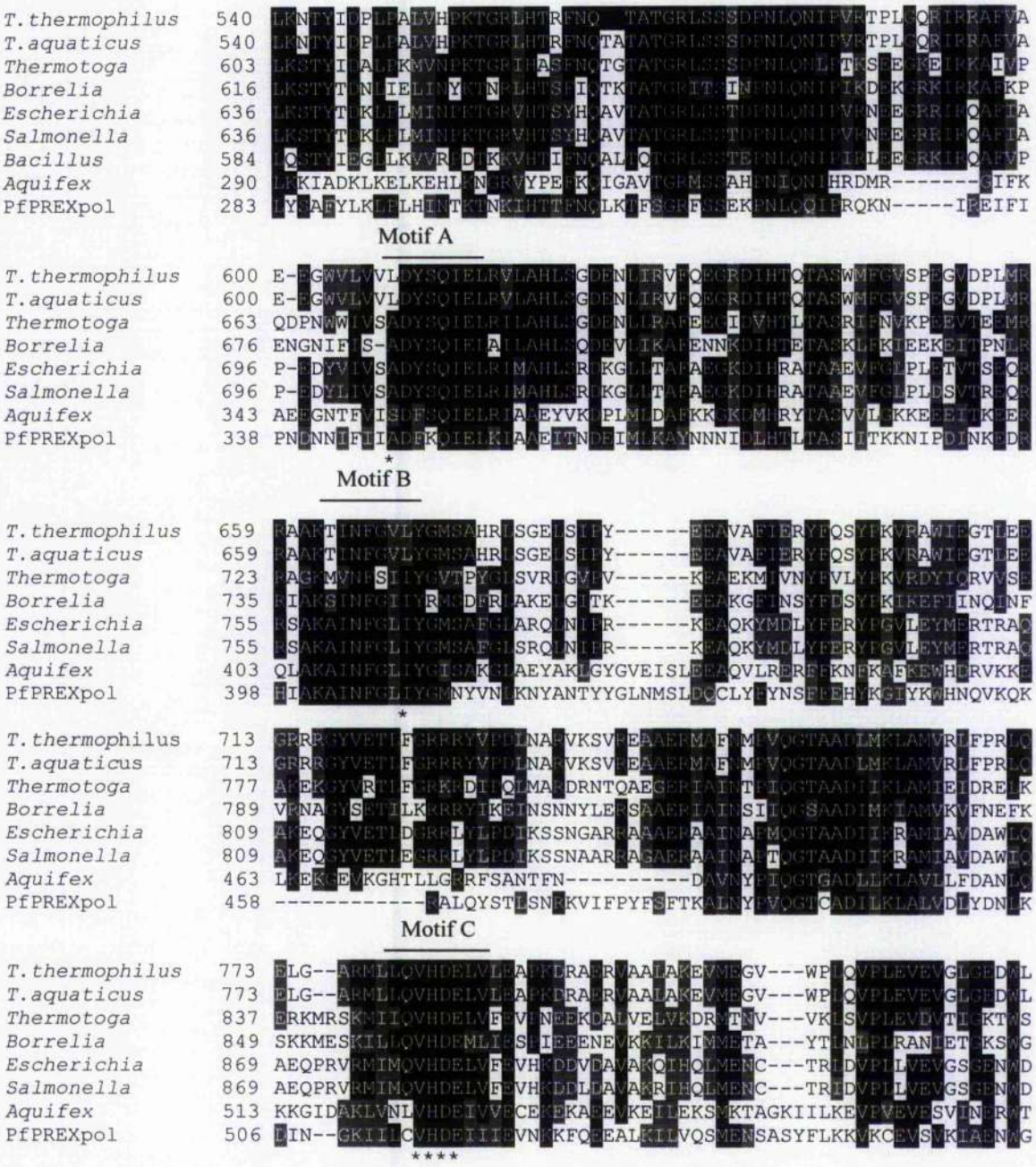

Figure 3.4. Alignments of deduced amino acid sequence of the polA domain of DNA polymerases from family A. Sequences used are as follows: *Thermus thermophilus* (Genbank accession no:- CAA46900.1), *Thermus aquaticus* (Genbank accession no:- AAA27505.1), *Thermogata maritime* (Genbank accession no:- AAD36686.1), *Borrelia burgdorfei* (Genbank accession no:- AAC66909.1), *Escherichia coli* (Genbank accession no:- CAA23607.1), *Salmonella typhimurium* (Genbank accession no:- AAG43170.1), *Aquifex aeolicus* (Genbank accession no:- AAC07735.1) and the PfPREXpol sequence. These sequences were aligned using ClustalX 1.81. Black shading indicates identical amino acid, grey shading indicates conserved amino acid substitutions. The numberings on the left hand side shows the relative position of the amino acids in the respective sequences. The alignment has been culled to show the regions where the three conserved boxes are found, they are shown as motifs A, B and C above the sequence. Key residues involved in enzymatic activity are denoted below with an asterisk.

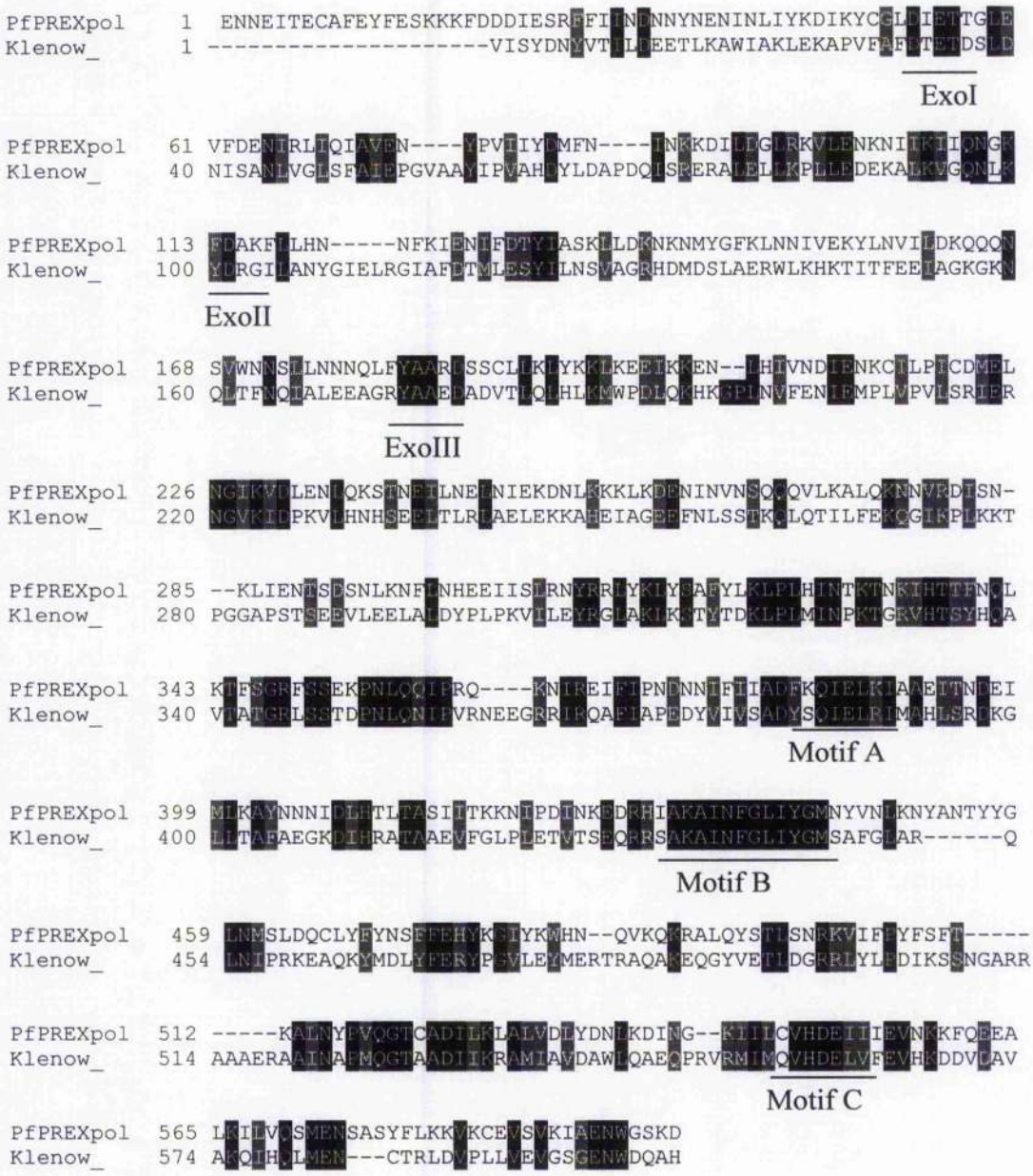

Figure 3.5. Pairwise alignment of the amino acid sequences of the Klenow fragment of *E. coli* and PfPREXpol using ClustalX 1.81 with default settings. The numbers on the left refer to the amino acid number of the individual sequence. Black shading indicates identical amino acids; grey shading indicates conserved amino acid substitutions. The various motifs are indicated with underlined text – Exo I-III (3'-5' exonuclease activity) and Motif A-C (DNA Polymerase activity).

1995; Morrison *et al.*, 1991). The conservation of these essential residues in the PfPREX sequence suggests that it contains a functional 3'-5' exonuclease domain.

3.2.4 The DNA polymerase domain

Several amino acid motifs are conserved among all family A DNA polymerases. These conserved motifs have been defined in different DNA polymerase families based on sequence comparisons and mutation analyses (Joyce & Steitz, 1994; 1995). The PfPREXpol domain contains the A (DFKQIELK), B (AINFGLIYGM) and C (LCVHDE) motifs (Delarue *et al*, 1990) (Figure 3.4), which are found in the polymerase domain. Motif A and C are part of the catalytic site of the polymerase. Motif A also forms a pocket for the incoming dNTP. The two aspartate residues present within them help to coordinate the two Mg^{2+} ions that stabilise the transition state of the enzyme and facilitate phosphoryl transfer (Steitz, 1998). The presence of all these essential residues in the PfPREXpol sequence suggests that it does encode a functional polymerase.

3.3. Identification of DNA helicase and DNA primase domains

Database searches using the N-terminal half of the PfPREX sequence revealed it to share homology to both a DNA helicase and a DNA primase. BLAST searches performed in 2001 or later revealed a new sequence added to the database that showed substantial similarity with the N-terminal half of PfPREX. That protein is called 'Twinkle' from rat (Genbank accession no: - XP_219939.1 Swissprot) (E value - $3x10^{-63}$). The same domain also showed similarity to DNA helicases and primases from bacteriophages like T7 and cyanophages at E values of $7x10^{-7}$ to $4x10^{-5}$. In these bacteriophages, the DNA G-like primases are fused to DNA B-like helicases. This is the same scenario observed with the T-odd bacteriophages.

3.3.1. The DNA helicase domain of PfPREX

The sequence alignment of the DNA helicase-like domain (termed PfPREXheli), revealed motifs conserved among the DNA helicases. DNA helicases are responsible for the unwinding of double-stranded DNA using energy from NTP hydrolysis. A key characteristic of these enzymes is the presence of conserved domains responsible for helicase function (Ilyina *et al*, 1992). There are several of these motifs which are essential for several biochemical features including nucleic acid binding, NTP binding and hydrolysis. The 'Walker motif', which encompasses the motifs A (H1) and B (H2), contains a typical purine NTP-binding pattern. This 'Walker motif' can be found in all helicases and also *p+16Xother NTP-utilizing enzymes. The 'Walker motif' can also be located in our PfPREXheli sequence (Figure 3.6). The Walker 'A' motif is the phosphate-binding loop ('P' loop). The Walker 'B' motif is involved in the dNTP binding. The residues responsible for this interaction are a conserved arginine and lysine. An aspartate found in the Walker 'B' motif is important as its carboxyl group is responsible for coordinating the Mg^{2+} ion, which forms a complex with the ATP/ADP through the outer sphere interactions.

In addition to the 'Walker motif', there are three other conserved motifs (H1a, H3 and H4) that can be located in DNA helicases, also present in the PfPREXheli sequence. Motif H1a contains a glutamic acid that has been suggested to play a role in catalysis (Sawaya *et al*, 1999). The role of motif H3 is unclear. It is hypothesised, based on studies of the T7 gp4 DNA helicase that it is involved in energy transduction (Sawaya *et al*, 1999). It has also been suggested the motif H3 participates in the interaction of Mg^{2+} with ATP/ADP and contributes to the binding of oligonucleotides (Caruthers & McKay, 2002).

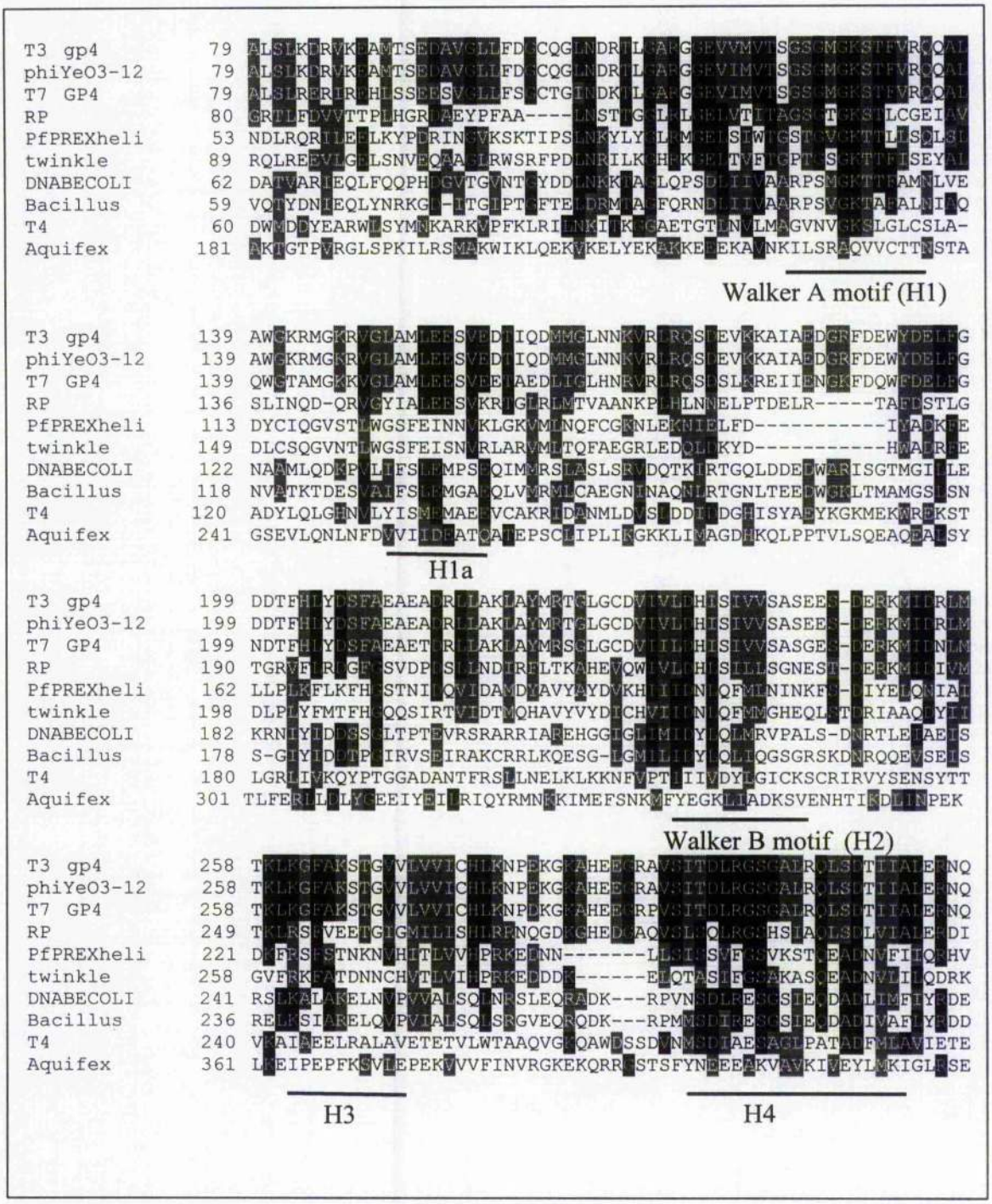

Figure 3.6. Alignments of deduced amino acid sequences of DNA helicases. Sequences are as follows: These full-length sequences were aligned using ClustalX 1.81. Sequences used are as follows: T3 gp4 (Genbank accession no: - CAA35135.1), phiYe03-12 (Genbank accession no: - CAB63608.1), RP (Roseophage, Genbank accession no: - AAL73266.1), twinkle (*Mus musculus*, Genbank accession no: - AAL27647.1), DNABECOLI (Genbank accession no: - AAA23689.1), Bacillus (*B. subtilis*, Genbank accession no: - BAA05176.1), T4 (Genbank accession no: - AAD42466.1), Aquifex (*A. aeolicus*, Genbank accession no: - AAC07803.1). Black shading indicates identical amino acids; grey shading indicates conserved amino acid substitutions. The numberings on the left hand side is the relative position of the amino acid in the respective sequences. Alignment has been culled to show the region where the five conserved boxes are found; they are shown as motif H1-H4.

Finally, motif H4 has a role that may be linked with DNA binding (Gorbalenya & Konin, 1993; Washington *et al*, 1996). The presence of these conserved motifs suggests that PfPREX encodes for a functional DNA helicase.

3.3.2. The DNA primase domain of PfPREX

The DNA primase domain of PfPREX revealed less sequence homology to the T7 phage gene4 like protein products than the DNA helicase domain. As automated alignment failed to identify all motifs, potentially significant sequence similarity was checked by eye. Key motifs, thought to be important for DNA primase activity were found in the PfPREX sequence (Ilyina *et al.*, 1992). The best probability match obtained during the BLASTP search was to the T7 gene 4 protein (Genbank accession no: CAA24405.1) at $7x10^{-7}$, which itself encodes for a combined DNA helicase /DNA primase.

3.3.2.1. Conserved features of DNA primases

The multiple alignment of the DNA primase domain of PfPREX (termed PfPREXpri), along with various primases of prokaryotic origin consisting of both bacterial and phage primases, revealed the presence of several motifs conserved among the group (Figure 3.7). PfPREXpri also contains these motifs. DNA primase is actually a specialised RNA polymerase, which synthesises a short RNA strand which DNA polymerase then uses for strand elongation. Among DNA primases, there are key motifs responsible for function. Prokaryotic DNA primases consist of three key domains (Figure 3.8): - (1) a zinc binding domain (Kusakabe & Richardson, 1996), (2) a catalytic domain (Aravind *et al.*, 1998) and (3) either a helicase domain or a region for the interaction with a helicase (Tougu *et al.*, 1994). PfPREXpri contains all three domains; the helicase domain (PfPREXheli) will be discussed in the next section.

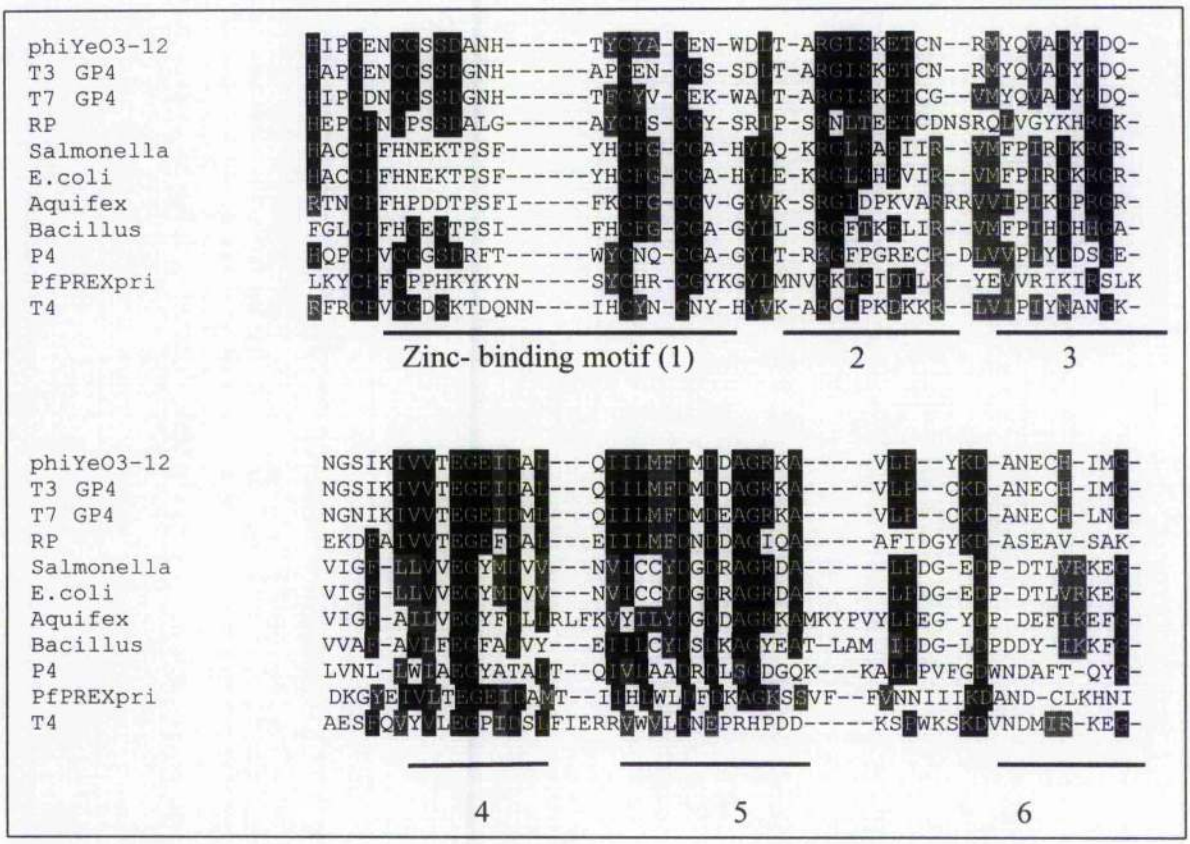

Figure 3.7. Alignments of deduced amino acid sequences of DNA primases. Sequences are as follows: phiYe03-12 (Genbank accession no: - CAB63608.1), T3 gp4 (Genbank accession no: - CAA35135.1), T7 gp4 (Genbank accession no: - CAA24405.1), RP (Roseophage, Genbank accession no: - AAL73266.1), Salmonella (*S. typhimurium* LT2, Genbank accession no: - AAL22084.1), E.coli (*E. coli* DnaG, Genbank accession no: -CAA23531.1), Aquifex (*A. aeolicus* DnaG, Genbank accession no: - AAC07430.1), T4 (Genbank accession no: - AAA32554.1). Sequences were aligned using ClustalX 1.81. Black shading indicates identical amino acids; grey shading indicates conserved amino acid substitutions. The alignment has been culled to show the region where the six conserved boxes are found; they are shown as motif 1-6.

From the alignment, it is evident that two pairs of cysteine residues, a key feature of zinc finger/zinc-binding motifs, are found within the first domain. This zinc motif is present in other primases from both prokaryotic and eukaryotic sources. Among prokaryotes, the zinc-binding motifs are found near the N-terminus of the protein. It was shown in T7 gp4 protein, when the zinc motif was disrupted (Mendelman *et al.*, 1994) or in the P4 primase (Ziegelin *et al.*, 1995) where the two cysteine residues were replaced by glycine residues, priming activity was lost. The zinc motif is therefore

postulated to be essential for the primase activity. Work with T7 gp4 suggested that the zinc motif might be involved in priming site recognition on the template DNA (Berstein & Richardson, 1988; Mendelman *et al.*, 1994). In the case of PREXpri, the two pairs of cysteine residues, which make up the zinc-binding motif, are found (Figure 3.7).

In addition to the zinc-binding motif, five other motifs conserved among PfPREXpri and other prokaryotic primases (Ilyina *et al.*, 1992) are observed in the alignment. These five motifs are found within the catalytic domain (also known as the RNA polymerase domain). Motif 2 is the only motif for which no functional or structural role has been yet assigned. Motifs 3 to 6 have been implicated to play roles in primer synthesis. A glutamate residue in motif 4 is predicted to be essential for primer synthesis (Strack *et al.*, 1992). More specifically, this glutamate residue provides a base to facilitate nucleotide polymerisation (Aravind *et al.*, 1998).

The key characteristic of motif 5 is an aspartate dyad (DxD) that it is believed is involved to be in the coordination of the Mg^{2+} ion (Aravind *et al.*, 1998). An additional aspartate dyad (DxD) is found in motif 6 among all bacterial DNA G-like sequences while among bacteriophage sequences, only the first aspartate is present. There is only one aspartate residue in PfPREXpri, similar to the bacteriophage primases. Motifs 4 and 5 are especially important because they contain these conserved acidic residues which are glutamate and aspartate respectively. They are preceded by runs of hydrophobic regions predicted to form beta strands. Motifs 4 and 5 comprise the TOPRIM domain which is so named because the two motifs are found conserved not only in DNA primases (DNA G-like) but also among DNA topoisomerases. The DxD motif is central to the TOPRIM domain, as it is required for the activity of all TOPRIM-

containing enzymes. Since all the important domains for a functional primase are found on PfPREX sequence, it is likely that it may encode for a functional primase.

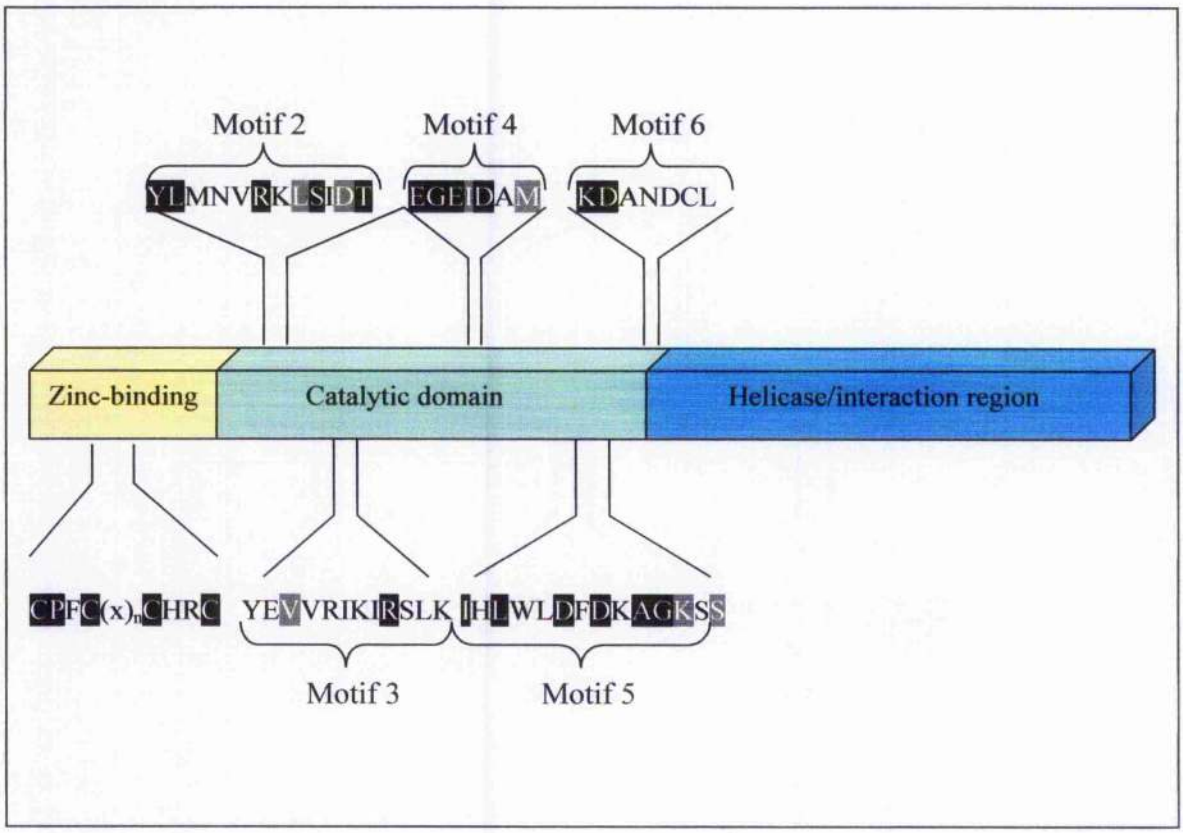

Figure 3.8. Diagrammatic representation of the 3 key domains in prokaryotic DNA primase consisting of a zinc-binding domain, a catalytic domain and a helicase or helicase-interaction region. In addition, the conserved motifs of PfPREXpri in those regions are shown based on the conserved motifs discovered by Ilyina *et al* (1992).

3.4. The hinge domain of PfPREX

There is a region of sequence between the helicase and the polymerase (994 a.a to 1392 a.a) that does not have any marked similarity to any protein sequence within the database as judged by BLASTP searching. This region that separates the DNA primase/helicase and DNA polymerase domains has been termed the hinge region. Other multifunctional proteins (at least five have been characterised) from *P. falciparum* have hinge regions that appear to be involved in the proper folding of the protein. One example is the bifunctional ornithine decarboxylase S-adenosylmethionine decarboxylase (Krause *et al.*, 2000; Müller *et al.*, 2000) (ODC/AdoMetDC). It is not clear whether a similar role is played by this sequence in the PREX protein – indeed evidence presented later suggests that it may play a role in the processing of the protein rather than merely a hinge separating domain.

3.5. Identification of a transit peptide at the extreme N-terminal domain

The first 50 amino acid sequence from the N-terminal domain of PfPREX sequence was entered into the SignalP online server at http://www.cbs.dtu.dk/services/SignalP that uses the von Heijne algorithm (Nielsen *et al*, 1997) to predict the presence and location of signal peptides. A signal sequence and a cleavage site between amino acid position 19 (Cysteine) and 20 (Isoleucine) in PfPREX were detected. In addition, the N-terminal amino acid sequence was seen to possess the characteristics of a bipartite transit sequence, which consists of 2 functional domains, a signal sequence followed by a targeting sequence, where the signal sequence is responsible for channelling the protein into the secretory pathway while the transit sequence is responsible for targeting the protein into the correct compartment. On the other hand, chloroplast-targeted proteins (Bruce, 2000) only possess transit sequences. Typically in an apicoplast bipartite transit sequences, the signal sequence part contains a

short run of hydrophobic residues, followed by the von Heijne cleavage site. The apicoplast targeting sequence carries an overall positive charge, very much like in the plant plastid targeting sequences (Waller *et al*, 1998). It is also known that *Plasmodium* apicoplast targeting sequences have a net positive charge due to the large number of lysine residues. They also possess a large number of asparagine residues (Foth *et al*, 2003). These features are evident in PfPREX putative apicoplast targeting sequence. Therefore, PfPREX has the key characteristics consistent with it being an apicoplast-targeted protein.

To confirm its status, we submitted the first 50 amino acids to PATS (Prediction of Apicoplast-Targeted Sequences) (Zuegge *et al*, 2001) and PlasmoAP (Foth *et al*, 2003), two programmes designed to specifically determine potential *Plasmodium* apicoplast targeting sequences. Both programmes returned results that indicated the presence of an apicoplast targeting sequence in PfPREX (Figure 3.9).

In addition, we wanted to test whether the programmes are sufficiently robust to detect apicoplast targeting sequences and differentiate them from other targeting sequences such as mitochondrion-targeting sequences. Both programmes were therefore tested with other known targeting sequences including the leader sequence of HSP60 from *Plasmodium*, which has been shown to target to the mitochondrion (Sato *et al*, 2003). Both PATS and PlasmoAP predicted this sequence to lack apicoplast targeting potential. The leader sequence from acyl carrier protein (ACP) from *Plasmodium*, which has been shown experimentally (Waller *et al*, 2000) to be targeted to the apicoplast, was also analysed by the two programmes, both predicted the presence of an apicoplast targeting sequence. Therefore, both programmes seem to be

Apicoplast targeting peptide prediction

Query sequence: (Please note, that only the first 150 AA have been taken into account for the analysis.)
>query
MLLYKFYFLYFLLVHLSLCIRYRNQNKTDSYLKTNYKLLK
KRKKYENRRY

Result:
The protein has a good signal sequence.
The submitted peptide sequence seems to have an apicoplast-targeting sequence.

Complete PlasmoAP output for query :

Criterion	Value	Decision
apicoplast-targeting	5 of 5 tests positive	++
Ruleset 1		
Ratio acidic/basic residues in first 22 amino acids <=0.7	0.143	yes
Does a KN-enriched region exist (40 AA with min. 9 K or N) with a ratio acidic/basic <=0.9	0.167	yes
Ruleset 2		
number of acidic residues in first 15 amino acids (<=2)	1	yes
Does a KN-enriched region exist (40 AA with min. 9 K or N) ? Ratio acidic/basic residues in this region <0.6	0.167	yes
Is the first charged amino acid basic ?		yes

Figure 3.9. Result of the PlasmoAP (Foth *et al*, 2003) apicoplast targeting peptide prediction where the first 50 amino acids from PfPREX were entered.

sufficiently robust to differentiate between selected proteins that target to the apicoplast and those targeted to the mitochondrion, PfPREX therefore does appear to possess a putative apicoplast targeting sequence at its extreme N-terminus.

3.6. PREX homologues in other Apicomplexans

3.6.1. Homologues in *Plasmodium*

Since the partial *PREX* gene (formerly known as *POMI*) was discovered in *P. chabaudi*, indicating that the gene was conserved in the genus *Plasmodium*, it was decided to explore other apicomplexan genome databases to search for the presence of a full-length sequences corresponding to the *PREX* gene. The predicted amino acid sequence of PfPREX was used in a TBLASTN search using the Plasmodb database (http://www.plasmodb.org) to search for other *Plasmodium* homologues. Full length PREX homologues were found in *P. vivax*, *P. yoelii*, *P. knowlesi* and *P. berghei* while partial PREX sequences were found in *P. chabaudi* and *P. reichenowi*.

Full-length sequences of the homologues from other *Plasmodium* species from the genome databases were acquired (Appendix C). The full-length sequence of PyPREX from *P. yoelii* was retrieved from the NCBI protein database with the Genbank accession number of EAA20985 (Carlton *et al*, 2002). The PyPREX is 1813 amino acids in length and has a sequence identity to PfPREX of 65%. The homologues from *P. knowlesi* and *P. berghei* were assembled from contigs obtained from the *Plasmodium* genome database from the Sanger centre website (http://www.sanger.ac.uk). The PkPREX (*P. knowlesi*) is 1861 amino acids in length and has a sequence identity to PfPREX of 65%. Like PfPREX, it does not appear to contain any introns. PbPREX from *P. berghei* is 1770 amino acids in length and is 63% similar to PfPREX. PbPREX sequence is interrupted by at least 3 introns (based on the

ORF finder http://www.ncbi.nlm.nih.gov/gorf.html). For *P. vivax* homologues, a TBLASTN search was carried out against the 5X contig database on the TIGR website (http://www.tigr.org). A full length PvPREX was assembled and is 1860 amino acids in length with no intron and has 64% similarity to PfPREX (Table 3.1). For *P. chabaudi*, it appears to possess a PREX homologue but only a partial sequence (1345 amino acids) was obtained. As more genome sequence is entered into the database, a full-length sequence of PcPREX will be assembled when more sequence data is available.

Since PfPREX contains an N-terminal bipartite apicoplast targeting sequence, it was also of interest to check whether the homologues from other *Plasmodium* species also possess a similar bipartite plastid targeting sequence. We submitted the first 50 amino acids of all the six *Plasmodium* PREX homologues into PlasmoAP (Foth *et al*, 2003) to search for the presence of such sequences. PlasmoAP first determines the number of acidic amino acids in the first 15 amino acids. The minimum number of acidic amino acids considered for inclusion as a potential targeting sequence is two. The ratio of basic to acidic amino acids among the first 22 residues must be greater than seven or equal to 10. The presence of at least nine lysine or asparagine residues and a basic to acidic residues ratio in this stretch must be either greater than or equal to 10/9 (ruleset 1) or 5/3 (ruleset 2) respectively (Figure 3.9). Finally, PlasmoAP checks for the charge of the first charged amino acid which should be basic. Table 3.2 shows the summary of the results obtained from PlasmoAP of the six *Plasmodium* PREX homologues. All of the *Plasmodium* homologues possess an N-terminal bipartite apicoplast targeting sequence.

All of the homologues (except for *P. berghei* and *P. chabaudi* – because we do not have the full *PcPREX* sequence) also have the same cleavage point, between position 19 and 20 in spite of divergent sequences. There seems to be a consensus sequence at the cleavage point among the homologues (Table 3.2) xLx-I/VR.

3.6.2. PREX homologues in other Apicomplexans

In the previous section, it has been shown that different *Plasmodium* species possess PREX, all of which contain an N-terminal bipartite plastid targeting sequence. Whether other apicomplexans also possess PREX homologues has also been assessed.

TBLASTN searches using PfPREX amino acid sequence against the various apicomplexan genome databases. The *Theileria* genome database was sed and a PREX homologue was found. Dr Shigeharu Sato (NIMR, Mill Hill) found PREX homologues in both the *T. annulata* (Ta) and *T. parva* (Tp) genome databases and assembled the full-length sequence from the contigs. Ta and Tp homologues (TaPREX and TpPREX) have 33% and 34% sequence identity respectively to the PfPREX peptide sequence (Table 3.1). The TaPREX is 1786 amino acids in length while the TpPREX is 2060 amino acids in length.

Attempts were also made to find PREX homologues in *Eimeria tenella*, *Babesia bovis*, *Cryptosporidium parvum* and *Toxoplasma gondii*. For *Eimeria tenella*, insufficient genome information prevented a robust search for a PREX homologue. For *B. bovis* and *C. parvum*, short fragments with homology to PfPREX were isolated but there is also insufficient sequence information to enable derivation of full-length sequences for either. For *T. gondii*, we found significant matches to data available in the

T. gondii genome database but we were not able to obtain the full length PREX homologue from *T. gondii* which appears to be highly interrupted with introns.

	PcPREX	PkPREX	TaPREX	TpPREX	PyPREX	PfPREX	PvPREX	PbPREX
PcPREX	100	51	32	33	71	46	51	72
PkPREX		100	38	38	69	65	87	68
TaPREX			100	90	41	33	37	41
TpPREX				100	42	34	38	42
PyPREX					100	64	69	94
PfPREX						100	64	63
PvPREX							100	68
PbPREX								100

Table 3.1. Similarity table of PREX homologues from *Plasmodium* and other apicomplexans. Abbreviations: *P. falciparum* (Pf), *P. berghei* (Pb), *P. chabaudi* (Pc), *P. knowlesi* (Pk), *Theileria annulata* (Ta), *T. parvum* (Tp), *P. vivax* (Pv) and *P. yoelii* (Py). The numbers represent the percentage similarity between each pair of proteins.

Homologue	Signal Sequence	Apicoplast	Cleavage site	Cleavage sequence
PyPREX	+	+	19/20	ALG-IR
PbPREX	-	+	-	-
PkPREX	+	+	19/20	VLA-VR
PvPREX	+	+	19/20	ALA-VR
PcPREX	NA	NA	NA	NA
PfPREX	+	+	19/20	SLC-IR

Table 3.2. Table showing the *Plasmodium* PREX homologues and the presence of a signal sequence and apicoplast targeting sequence. Included also is the cleavage site of the signal sequence and the cleavage sequence for all the homologues. Abbreviations: *P. falciparum* (Pf), *P. berghei* (Pb), *P. chabaudi* (Pc) *P. knowlesi* (Pk), *P. vivax* (Pv) and *P. yoelii* (Py). NA- sequence is not available.

3.7. Determination of the arrangement of the different domains within PfPREX

Sequence similarity predictions have indicated that PfPREX encodes for several different activities. Alignment with the other PREX homologues showed variation in the degree of similarity across the protein which might indicate the structural arrangement of the functional domains within the sequence.

A multiple alignment of all of the PREX homologues allowed for the determination of the approximate limits of each individual domain based on the regions of best conservation (Figure 3.10). From the alignment, it is predicted that the DNA primase domain of PfPREX spans from position 114 to 470. Within this region, a high degree of similarity among the different PREX homologues and the conservation of the key primase conserved residues are observed. After this region, there is an area where there is less conservation before the helicase domain starts. The helicase domain is predicted to start at position 511 and runs to position 684 in PfPREX. This domain again is very well conserved among the PREX homologues.

The hinge region of PREX, shows less conservation overall. However in more or less the middle of the hinge, there is an area that is relatively well conserved. The hinge region did not show homology to any known proteins in the BLAST searches. The hinge region in PfPREX spans from position 1000 to 1360. The conserved domain within the hinge region, which spans from 1228 amino acids to 1264 in PfPREX, might be functionally relevant. However in the absence of homology to other proteins, that function remains speculative. As demonstrated later, the DNA primase/helicase and DNA polymerase domains appear to be separated by cleavage

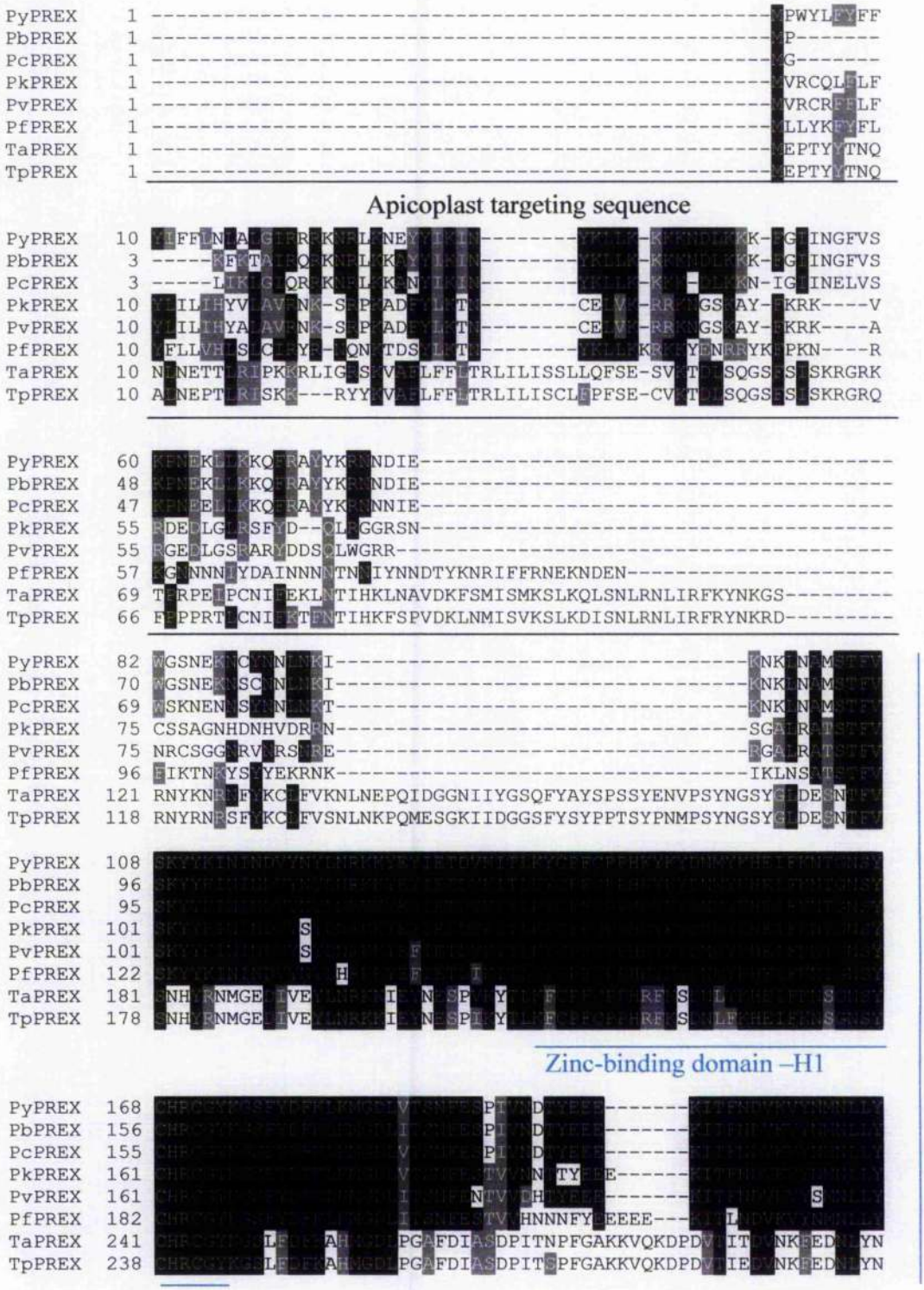
Apicoplast targeting sequence
Zinc-binding domain –H1

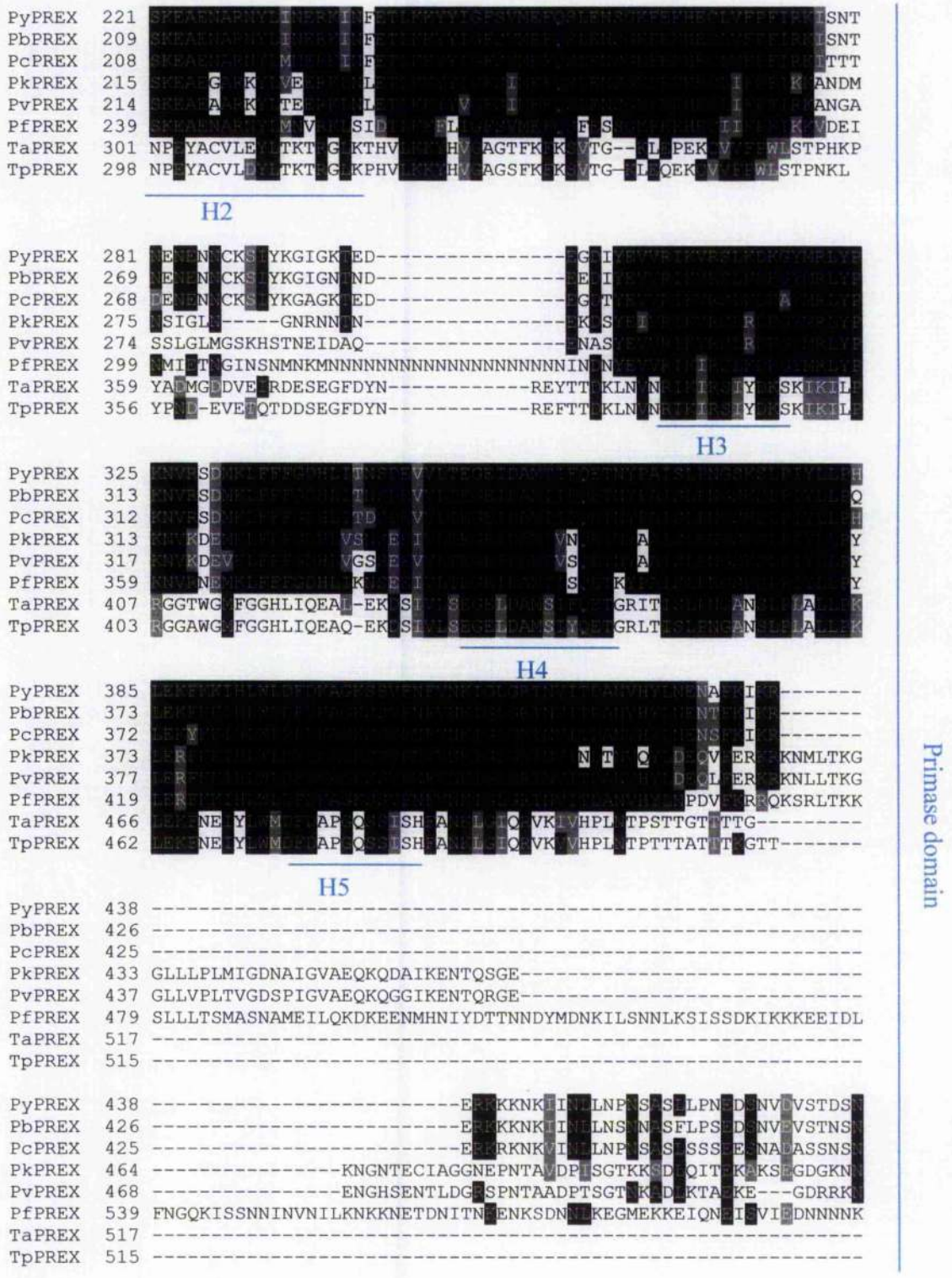
PyPREX 221
PbPREX 209
PcPREX 208
PkPREX 215
PvPREX 214
PfPREX 239
TaPREX 301
TpPREX 298
H2
PyPREX 281
PbPREX 269
PcPREX 268
PkPREX 275
PvPREX 274
PfPREX 299
TaPREX 359
TpPREX 356
H3
PyPREX 325
PbPREX 313
PcPREX 312
PkPREX 313
PvPREX 317
PfPREX 359
TaPREX 407
TpPREX 403
H4
PyPREX 385
PbPREX 373
PcPREX 372
PkPREX 373
PvPREX 377
PfPREX 419
TaPREX 466
TpPREX 462
H5
PyPREX 438
PbPREX 426
PcPREX 425
PkPREX 433
PvPREX 437
PfPREX 479
TaPREX 517
TpPREX 515
PyPREX 438
PbPREX 426
PcPREX 425
PkPREX 464
PvPREX 468
PfPREX 539
TaPREX 517
TpPREX 515
Primase domain

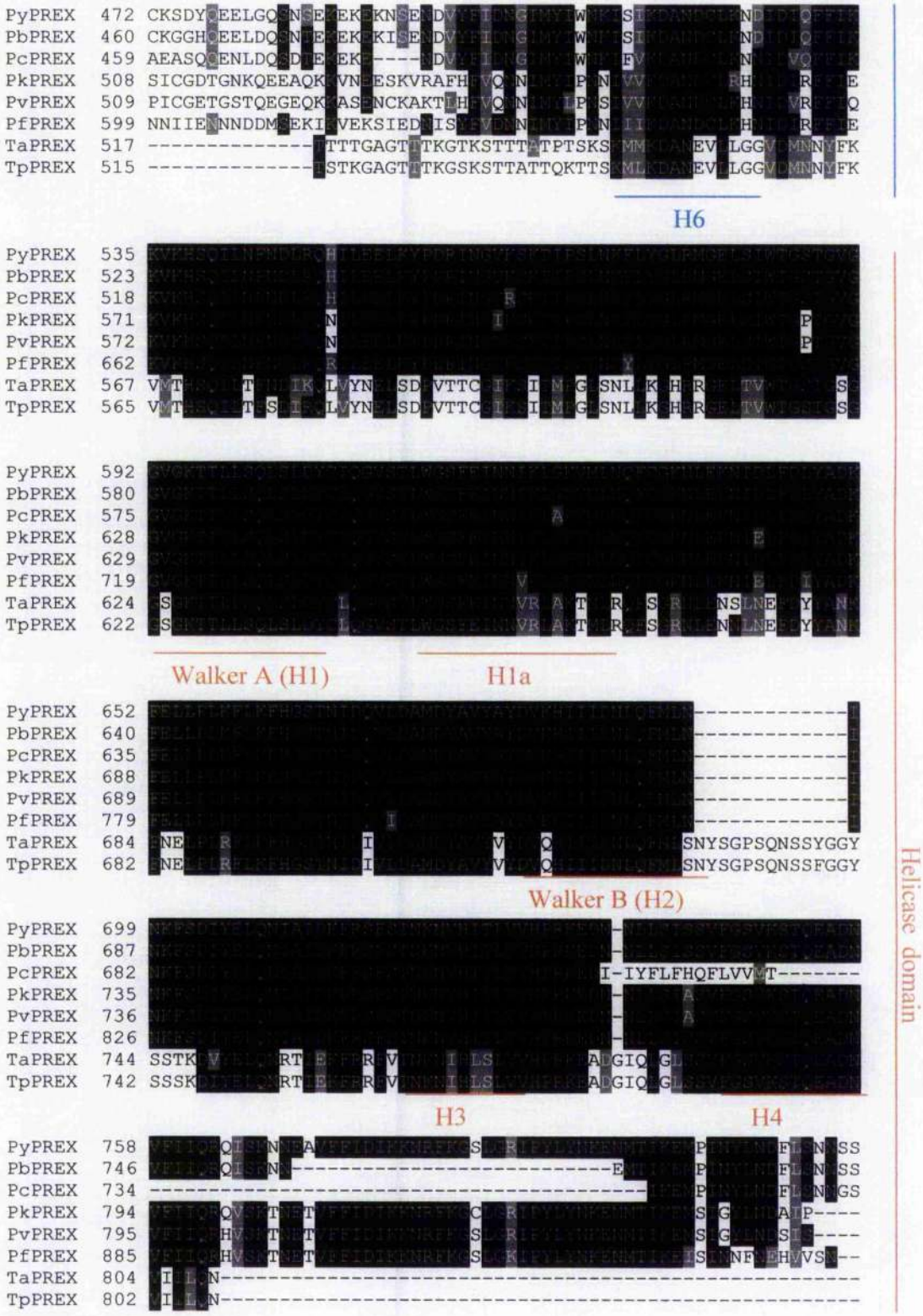
H6
Walker A (H1)
H1a
Walker B (H2)
H3
H4
Helicase domain

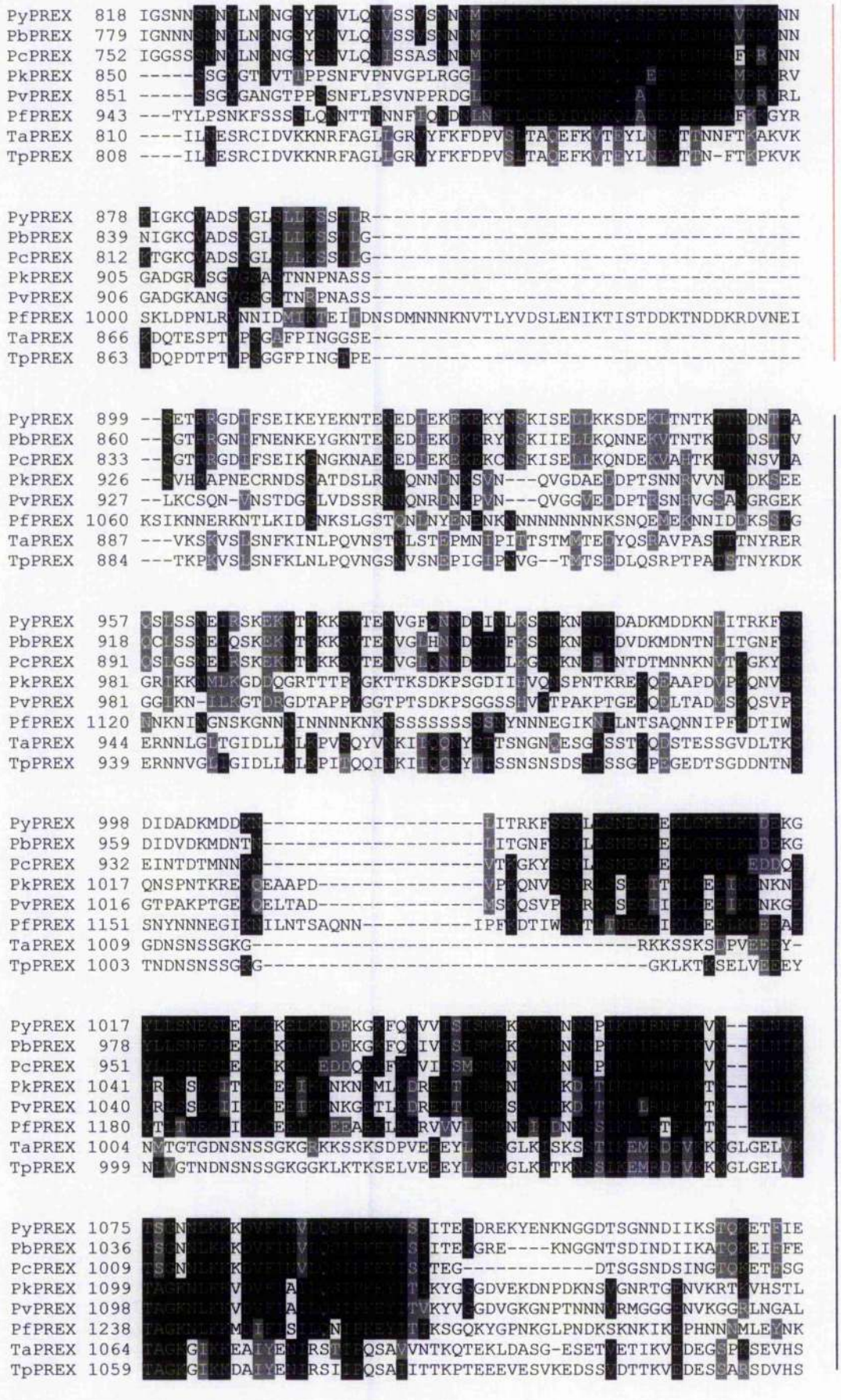

Hinge Domain

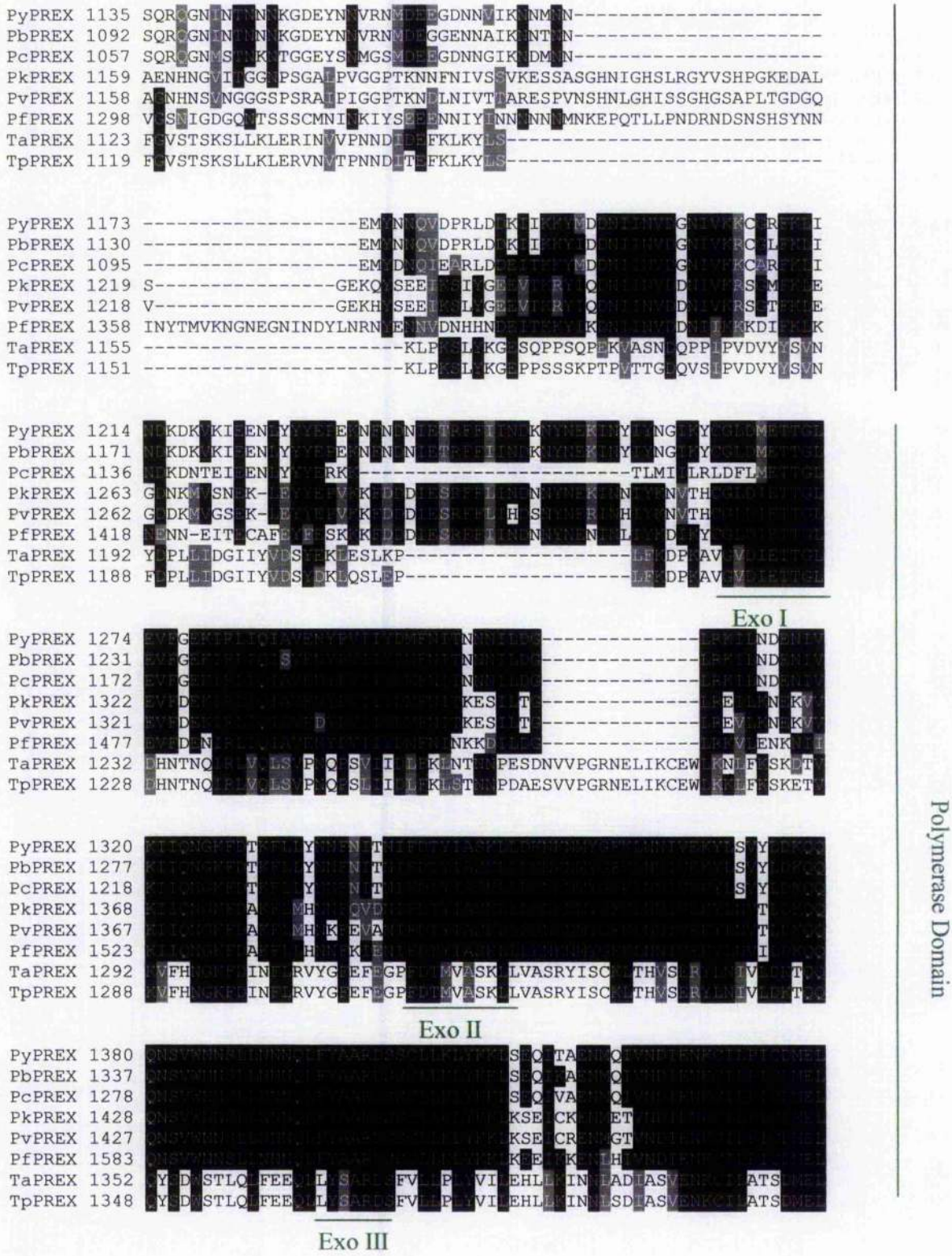
PyPREX 1135
PbPREX 1092
PcPREX 1057
PkPREX 1159
PvPREX 1158
PfPREX 1298
TaPREX 1123
TpPREX 1119
PyPREX 1173
PbPREX 1130
PcPREX 1095
PkPREX 1219
PvPREX 1218
PfPREX 1358
TaPREX 1155
TpPREX 1151
PyPREX 1214
PbPREX 1171
PcPREX 1136
PkPREX 1263
PvPREX 1262
PfPREX 1418
TaPREX 1192
TpPREX 1188
Exo I
PyPREX 1274
PbPREX 1231
PcPREX 1172
PkPREX 1322
PvPREX 1321
PfPREX 1477
TaPREX 1232
TpPREX 1228
PyPREX 1320
PbPREX 1277
PcPREX 1218
PkPREX 1368
PvPREX 1367
PfPREX 1523
TaPREX 1292
TpPREX 1288
Exo II
PyPREX 1380
PbPREX 1337
PcPREX 1278
PkPREX 1428
PvPREX 1427
PfPREX 1583
TaPREX 1352
TpPREX 1348
Exo III
Polymerase Domain

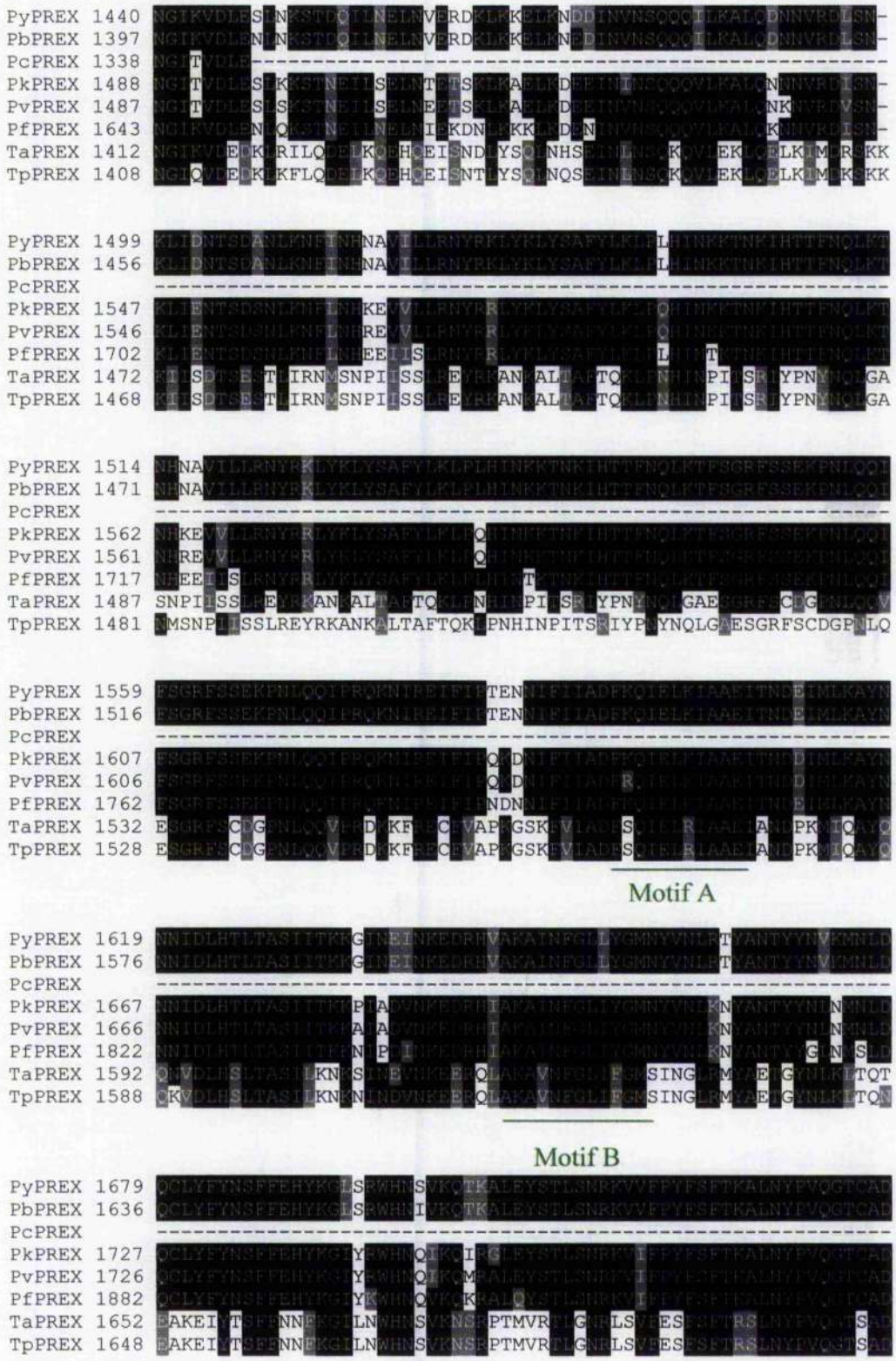
PyPREX 1440
PbPREX 1397
PcPREX 1338
PkPREX 1488
PvPREX 1487
PfPREX 1643
TaPREX 1412
TpPREX 1408
PyPREX 1499
PbPREX 1456
PcPREX
PkPREX 1547
PvPREX 1546
PfPREX 1702
TaPREX 1472
TpPREX 1468
PyPREX 1514
PbPREX 1471
PcPREX
PkPREX 1562
PvPREX 1561
PfPREX 1717
TaPREX 1487
TpPREX 1481
PyPREX 1559
PbPREX 1516
PcPREX
PkPREX 1607
PvPREX 1606
PfPREX 1762
TaPREX 1532
TpPREX 1528
Motif A
PyPREX 1619
PbPREX 1576
PcPREX
PkPREX 1667
PvPREX 1666
PfPREX 1822
TaPREX 1592
TpPREX 1588
Motif B
PyPREX 1679
PbPREX 1636
PcPREX
PkPREX 1727
PvPREX 1726
PfPREX 1882
TaPREX 1652
TpPREX 1648

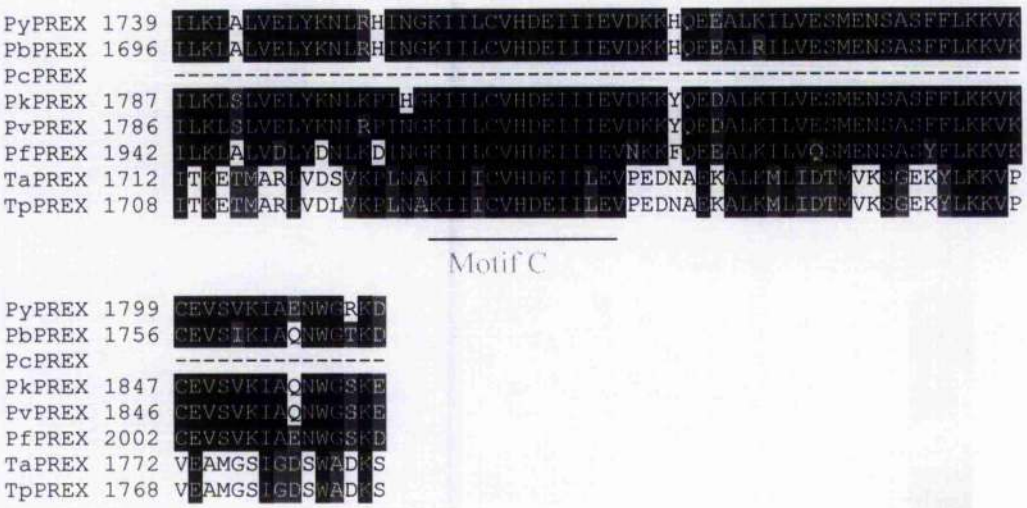

Figure 3.10. Multiple alignment of the PREX homologues using ClustalX 1.81 with default settings. The numbers in the brackets refer to the amino acid number of the individual sequence. Black shading indicates identical amino acids, grey shading indicates conserved amino acid substitutions. The various motifs are indicated with underlined text. Blue – primase domain , pink – helicase domain; black - hinge domain and green – polymerase domain.

during maturation. The conserved domain of the hinge region might play a role in this cleavage.

The DNA polymerase start site is predicted to begin at amino acid 1389 and stretches to the stop codon at position 2016. Yet again, the region shows a high degree of conservation among all of the homologues. All PREX homologues contain the key residues known to be essential for the function of the DNA polymerase. Figure 3.11 illustrates the PfPREX with its different domains colour-coded.

Figure 3.11. Putative amino acid of PfPREX which is colour coded for the different functional domains. Colour coding :- Red font- signal sequence (cleavage site between aa 19 and 20). Red-Hinge with box of conserved residues between *Theilera* and *Plasmodium,* Yellow background – primase domain, Green background – helicase domain, Pink-Polymerase domain, black words within polymerase domain –3'-5' exonuclease domain, blue words within polymerase domain- pol A domain, Boxes show conserved signature motifs found within primase, helicase and polymerase domains.

3.8. Phylogenetic relationship between PREX homologues in apicomplexans

From the multiple alignments of the apicomplexan PREX homologues, the phylogenetic relationship between them could be determined. The alignment was used to obtain a phylogenetic tree by various methods. In addition to that, the genetic distances between the PREX amino acid sequences were obtained. The distances and trees were calculated and generated by the MEGA (Molecular Evolutionary Genetic Analysis) software (Kumar *et al*, 2001). The genetic distances were calculated with Poisson correction for amino acids (Table 3.3). Genetic distance is a measure of the difference between two sequences. The genetic distances obtained ranges from 0.0486 (between *P. berghei* and *P. yoelii*) and 0.3817 (between *P. vivax* and *P. falciparum*). This value is relatively high if you compare it with a glycolytic protein e.g. aldolase (Cloonan *et al*, 2001) where the genetic distance between *P. vivax* and *P. falciparum* is 0.140. However, its evolutionary rate is comparable to other proteins including adenylsuccinate lyase (ASL) (Kedzierski *et al*, 2002) or cysteine proteinase (Rosenthal, 1996) where the genetic distances between *P. vivax* and *P. falciparum* are 0.4577 and 0.425 respectively. Therefore, based on this result, PfPREX seems to have a rate of evolution similar to ASL.

Phylogenetic trees were constructed using the MEGA software using all 4 available methods Unweighted Paired Group Method with Arithmetric Mean (UPGMA), Neighbour-Joining (NJ), Minimum Evolution (ME) and Maximum Parsimony (MP). All 4 methods gave a similar topology (Figure 3.12). The *Plasmodium* species PREX homologues are grouped into 2 distinct clades. One branch contains the rodent malaria species, *P. berghei, P. yoelii* and *P. chabaudi*. It was also

```
[1] #PyPREX
[2] #PbPREX
[3] #PcPREX
[4] #PkPREX
[5] #PvPREX
[6] #PfPREX

[     1       2       3       4       5       6       ]
[1]
[2]  0.0486
[3]  0.1292 0.1438
[4]  0.3743 0.3767 0.4634
[5]  0.3760 0.3818 0.4695 0.1563
[6]  0.3675 0.3669 0.4739 0.3650 0.3817
```

Table 3.3. Genetic distances between the PREX homologues of six *Plasmodium* species. The distances were calculated with Poisson correction for amino acid residues. Abbreviations: *P. berghei* (Pb), *P. yoelii* (Py), *P. chabaudi* (Pc), *P. knowlesi* (Pk), *P. vivax* (Pv) and *P.falciparum* (Pf).

observed that *P. berghei* and *P. yoelii* are closely related with a bootstrap support of 100 (depending on the method used), which is in agreement with previous findings (Killick-Kendrick, 1978). The other branch groups the primate malaria species *P. knowlesi* and the human parasite, *P. vivax* together. This is fully supported by a bootstrap of 100. This is also observed by Kedzierski *et al*'s (2002) study with the ASL sequences. The bootstrap value for the node where *P. falciparum* joins the primate clade in the UPGMA tree is weaker (52-74) as opposed to the 100 bootstrap values for the other nodes but the bootstrap values indicate the relationships are robust.

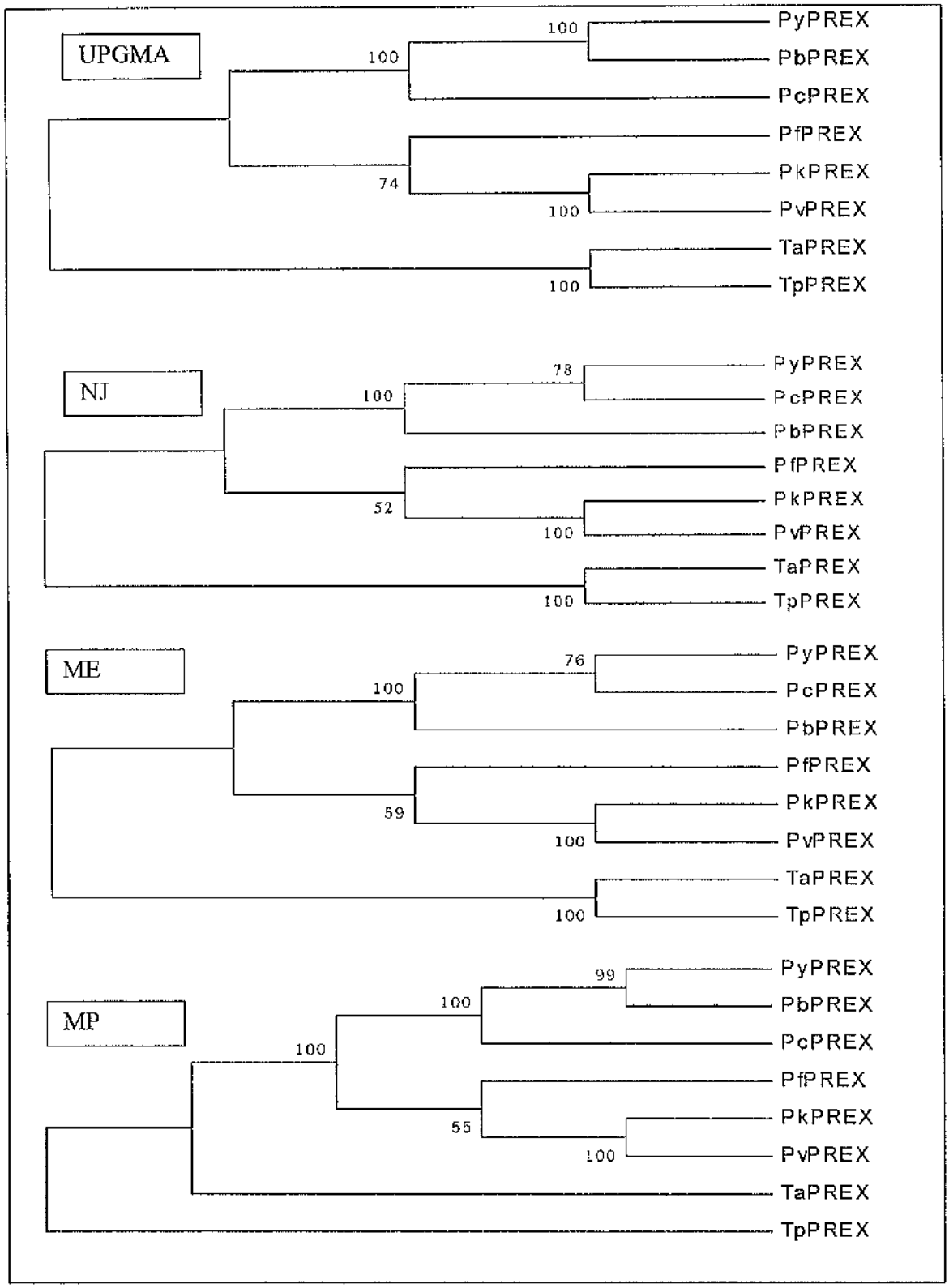

Figure 3.12. Phylogenetic Trees for PREX homologues. The trees were generated using MEGA 2.1 for Unweighted Pair Group Method with Arithmetic Mean (UPGMA), Neighbour-joining (NJ), Minimum Evolution (ME) and Maximum parsimony (MP) methods. Bootstrap values correspond to 100 random runs. Abbreviations: *P.falciparum* (Pf), *P. berghei* (Pb), *P. chabaudi* (Pc), *P. knowlesi* (Pk), *Theileria annulata* (Ta), *T. parvum* (Tp), *P. vivax* (Pv) and *P. yoelii* (Py).

3.9. Discussion

The sequence analysis carried out so far seems to suggest that the PfPREX is composed of three putative domains, a DNA primase, DNA helicase and DNA polymerase. The C-terminal domain resembles a DNA polymerase domain. The homology search carried out identified the three key motifs characteristic of family A DNA polymerases. Therefore, to prove that indeed the C-terminal domain does encode an active polymerase, functional studies have to be carried out. The N-terminal domain resembles DNA primase and DNA helicase domains, very similar to the DNA primase/helicase complex of the T7 bacteriophage group. Homology searches carried out also identified the key motifs characteristic of both the DNA helicase and DNA primase. Since PfPREX possesses all of these key motifs, it is likely that it might code for functional DNA primase and helicase.

An interesting point is the presence of an apicoplast-targeting sequence located at the extreme N-terminus. Prediction programmes that are specific for locating such sequences in *P. falciparum* have returned positive results indicating that the sequence is involved in apicoplast-targeting. Therefore, PfPREX is most probably targeted to the apicoplast where it is postulated that it may have a role to play in plastid replication.

Homologues of PfPREX can be found in other *Plasmodium* species with very high similarity between the sequences. Furthermore, PfPREX homologues are also found in other apicomplexans ranging from *Theileria*, where the full PREX sequences have been assembled, to *Toxoplasma gondii* (partial sequences only). This seems to suggest that PREX was already present in the common ancestor of apicomplexans.

Based on amino acid homologies among the PREX homologues, we were able to use that information to determine the putative boundaries of the various domains on PfPREX. This information is useful for the design of primers for the cloning of the individual domains. In addition to this, the PREX homologues were used to make genetic distance calculations and phylogenetic analysis. The results obtained were as expected and compared to a study carried out on adenylsuccinate lyase, PREX seems to have a rate of evolution that is similar to ASL, information which can be used to contribute to studies to determine evolutionary history of *Plasmodium* species.

The information obtained from the bioinformatic studies has given insight into the function of the PfPREX and also allows the opportunity to further explore PfPREX. The main aim of this project has been to demonstrate whether PfPREX does encode a functional plastid replicase. The remaining chapters of this thesis describe the functional characterisation of this protein.

Chapter IV

Functional analysis and subcellular localisation of theDNA polymerase (PfPREXpol) domain encoded by the *PfPREX* gene

4.1. Introduction

Propagation of a species depends upon the faithful replication of its genome. In order for cells to achieve this, they require an efficient machinery to maintain genome integrity during cell division, DNA repair, DNA recombination and also when confronted with DNA damage. A key enzyme involved in all of these processes is DNA polymerase. Multiple DNA polymerases have been identified in mammals, yeast and prokaryotes. A particular DNA polymerase may have multiple roles to play in a cell and a particular part of the DNA metabolic process may need more than one polymerase. So far 12 classes of DNA polymerase have been classified, α, β, γ, δ, ε, ζ, η, θ, ι, κ, λ, μ, (Dominguez *et al*, 2000, Friedberg *et al*, 2000, Gibbs *et al*, 1998, Harris *et al*, 1996, Hubscher *et al*, 2000, Masutani *et al*, 1999, Nagasawa *et al*, 2000, Nelson *et al*, 1996, Ohashi *et al*, 2000, Tissier *et al*, 2000) (Table 1.2) where each has a different role to play in the DNA metabolic processes. Based on sequence relationships, these enzymes are classified into five families designated A, B, C, X and Y (Burgers *et al*, 2001). The family A group of polymerases are typified by the *E. coli* PolI; for family B members include the mammalian pol α, δ, ε and *E. coli* pol IV. *E. coli* pol III exemplifies family C and mammalian pol β is the best known member of family X . Finally *E. coli* pol V represents family Y.

In *Plasmodium berghei*, seven DNA polymerases have been identified using classical biochemical characterisation (De Vries *et al*, 1991). Five of them are aphidicolin-sensitive while two are resistant. Aphidicolin is a natural product derived from the fungus, *Nigrospora oryzae*, and it is widely used to distinguish between prokaryotic and eukaryotic DNA polymerase activities (Spadari *et al*, 1984). The two DNA polymerases, which are aphidicolin-sensitive, were hypothesised to be DNA

polymerase alpha (α) and DNA polymerase gamma (γ). Among those which are aphidicolin-insensitive, two of which are believed to be either a DNA polymerase beta (β) or delta (δ). For *P. falciparum*, at least two distinct DNA polymerase activities were detected (Chavalitshewinkoon *et al*, 1993). The aphidicolin-sensitive fraction was postulated to contain DNA polymerase α activity while the aphidicolin-insensitive fraction might contain a DNA polymerase γ. To date, only the subunits of DNA polymerase alpha and delta have been cloned and characterised from *P. falciparum* (Ridley *et al*, 1991).

The *P. falciparum* genome has been fully sequenced (Gardner *et al*, 2002). This provides the opportunity to explore the database to identify DNA polymerase gene sequences within the *P. falciparum* genome. BLAST searches using the Plasmodb database (Version 4.1) and also a query search of 'polymerase' of the annotated gene database were performed. To be more specific, the query was carried out at the Plasmodb website (www.plasmodb.org), using a GO-function assignment search for function of DNA-directed DNA polymerase (GO_ID 3887). GO stands for gene ontology where it organises different proteins based on 3 principles:- (1) molecular function, (2) biological process and (3) cellular component (Ashburner *et al*, 2000). Table 4.1 shows the results from the query search through the annotated gene database (Plasmodb Version 4.1). We have found at least five different DNA polymerases:- a DNA polymerase delta (δ) catalytic subunit, small subunit to a DNA polymerase alpha (α), a DNA polymerase epsilon (ε), a DNA polymerase zeta (ζ) catalytic subunit and a DNA polymerase I. These DNA polymerases from *P. falciparum* do not possess any apicoplast-targeting sequence.

	gene identifier	location	description	references
1	PFC0340w	pfal_chr3: 350224-351720	DNA polymerase delta small subunit, putative	Horrocks *et al*, 1996; Ridley *et al*, 1991
2	PFD0590c	pfal_chr4: 535089-541382	DNA polymerase alpha	White *et al*, 1993
3	MAL6P1.175	chr6: 1071327-1075661	DNA polymerase 1, putative	-
4	PF10_0165	chr10: 685577-688861	DNA polymerase delta catalytic subunit	Horrocks *et al*, 1996; Ridley *et al*, 1991
5	PF10_0362	chr10: 1464928-1472132	DNA polymerase zeta catalytic subunit, putative	-
6	PFL1285c	chr12: 1077858-1078766	proliferating cell nuclear antigen, putative	Horrocks *et al*, 1996; Kilbey *et al*, 1993
7	PF14_0112	chr14: 461400-467450	POM1, putative	-
8	PF14_0234	chr14: 989361-993071	DNA-directed DNA polymerase, putative	-
9	PF14_0602	chr14: 2571936-2573555	DNA polymerase alpha subunit, putative	White *et al*, 1993
10	MAL6P1.125	chr6: 1304902-1314100	DNA polymerase epsilon, catalytic subunit a, putative	-

Table 4.1. GO function search using Plasmodb for DNA-directed DNA polymerases in the *Plasmodium falciparum* database. The table consists of four columns, (1) Gene identifier, (2) Gene location which shows which chromosome the gene is located on, (3) Description which shows the class of DNA polymerase and (4) References from which work on the gene had been reported. Number 7 entry is *PfPREX*.

We also performed BLASTP and TBLASTN searches using the sequence of DNA polymerase gamma (γ) from *Drosophila melanogaster* which encodes a polymerase that replicates mitochondrion DNA (Lewis *et al*, 1996) in many eukaryotes. However the *P. falciparum* genome database did not appear to possess genes with homology to this sequence. Therefore, it seems that *P. falciparum* either does not possess a DNA polymerase gamma (γ) or that the gene is highly disrupted by introns and therefore not identified by classical BLAST analysis.

In addition, no DNA replication protein, i.e. the DNA polymerase involved in the replication of the *Plasmodium* plastid, has been previously isolated. The *PfPREX* sequence that is found on chromosome 14 (Genbank accession number: AAN36724.1), has homology to a prokaryotic DNA polymerase-I like sequences. The same ORF also encodes a typical plastid-targeting domain (Section 3.5). Therefore, we hypothesised that *PfPREX* may be responsible for plastid DNA replication/repair. Since the total *PfPREX* gene is over 6 kb in length and, like other *Plasmodium* genes, it is highly A-T rich, cloning and expression of the entire gene was deemed too difficult to warrant effort. Therefore, an approach was undertaken to clone and express the DNA polymerase domain in isolation from the DNA helicase and primase domains. This chapter is dedicated to reporting the cloning, expression and characterisation of the DNA polymerase domain of the *PfPREX* gene.

4.2. Results

4.2.1. Cloning of the PfPREXpol domain of the *PfPREX* gene

The DNA polymerase domain of the *PfPREX* gene spans a region of approximately 1,878 bp at the C-terminal domain of the gene. It was amplified using gene-specific primers, designed specifically for the use in the Gateway Cloning system (Invitrogen). The primers used were GWPolF1 as the forward primer and GWPolR1 as the reverse primer (Table 2.1). The forward primer was designed to overlap partially with the hinge domain of the gene. Figure 4.1 shows the relative positions of the primers in accordance to the PfPREXpol domain. The expected size of the PCR product was 2.9 kb (Figure 4.2). The primers used contained the *att* sites to permit of recombination with the Gateway Cloning system that was used.

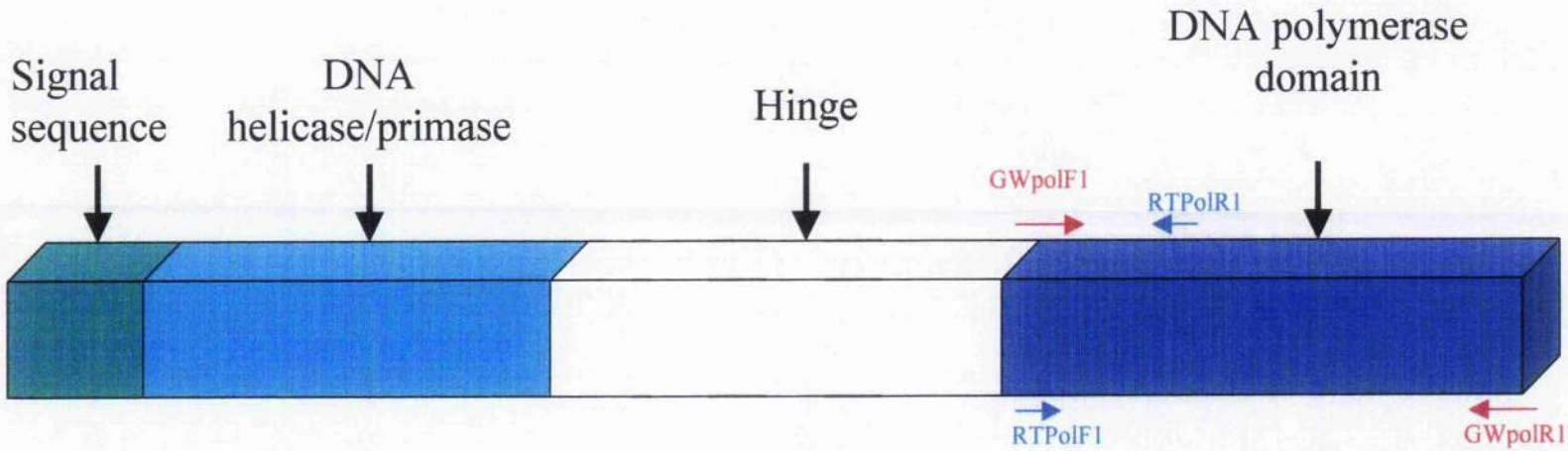

Figure 4.1. Diagrammatic representation of the PfPREX showing the gene specific primers GWpolF1 and GWpolR1 for amplifying the PfPREXpol domain and RT-PCR primers for the same domain RTPolF1 and RTPolR1. The GWpolF1 and GWpolR1 primers are shown with red arrows while the RT-PCR primers are shown with blue arrows.

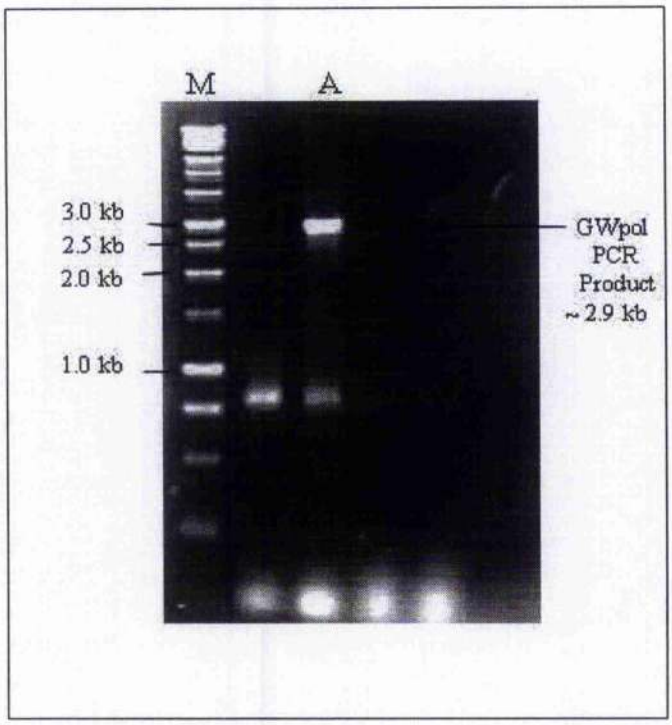

Figure 4.2. PCR amplification products of the polymerase domain of PfPREX amplified from *P. falciparum* 3D7 genomic DNA using specific primers (GWPolF1 and GWPolR1) (Table 2.1) separated on a 0.8% agarose gel. The PCR product is approximately 2.9 kb in size (Lane A).

The 2.9 kb PCR product was first cloned into the pDONR201 donor vector before it was transferred into the destination vector (or expression vector), pDEST17 that adds an N-terminal His-tag to the protein to facilitate purification of the expressed protein (Figure 4.3).

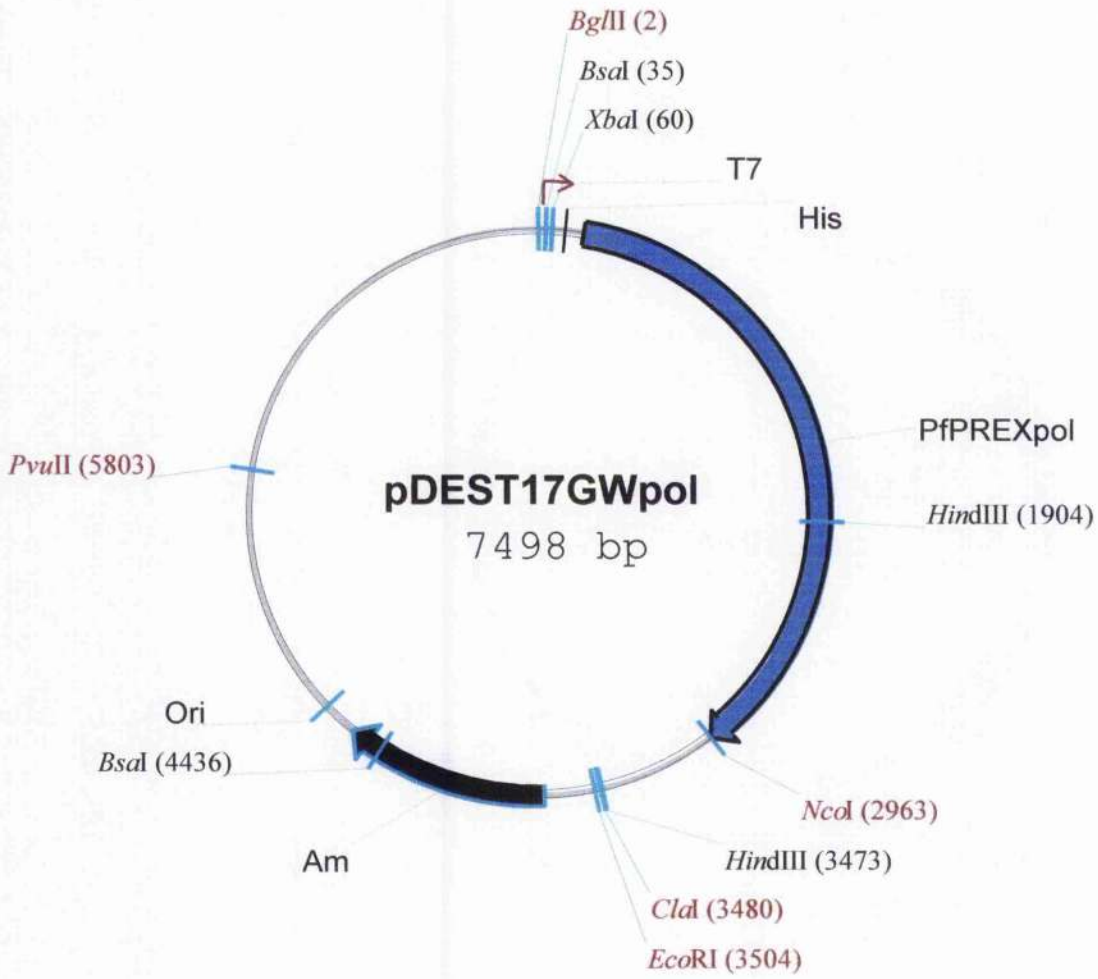

Figure 4.3. The pDEST17GWpol expression construct. The Gateway PCR product GWpol DNA polymerase domain (GWPolF1 and GWPolR1) (Table 2.1) was cloned into the specific recombination sites of pDEST17 (His-Tag) (Invitrogen) expression vector. The pDEST17 vector contains an ampicillin-resistance gene (Amp) and a T7 promoter. Selected restriction enzyme sites are shown, as are the positions of the T7 promoter (T7), the His-tag (His), the ampicillin resistance gene (Amp) and the plasmid origin (ori).

4.2.2 Expression and purification of PfPREXpol

The *E. coli* BL21si strain was used to host the expression of PfPREXpol. Induction of expression of the recombinant protein was performed at 37°C (Section 2.7.1). The calculated mass of the PfPREXpol domain is 107 kDa (Figure 4.4). Since the expressed recombinant protein contains an N-terminal His-tag, it was purified using a nickel-affinity column on a BIO-CAD 700E workstation (PE Biosystems). Cultures were lysed and prepared for the purification of the His-tagged recombinant protein. The purification was carried out as detailed in section 2.7.1. Approximately 10 mg of soluble recombinant protein was obtained from one litre of *E. coli* culture. The purified protein was analysed by SDS-PAGE. The apparent size of the protein on the gel was 90 kDa, lower than its predicted molecular weight.

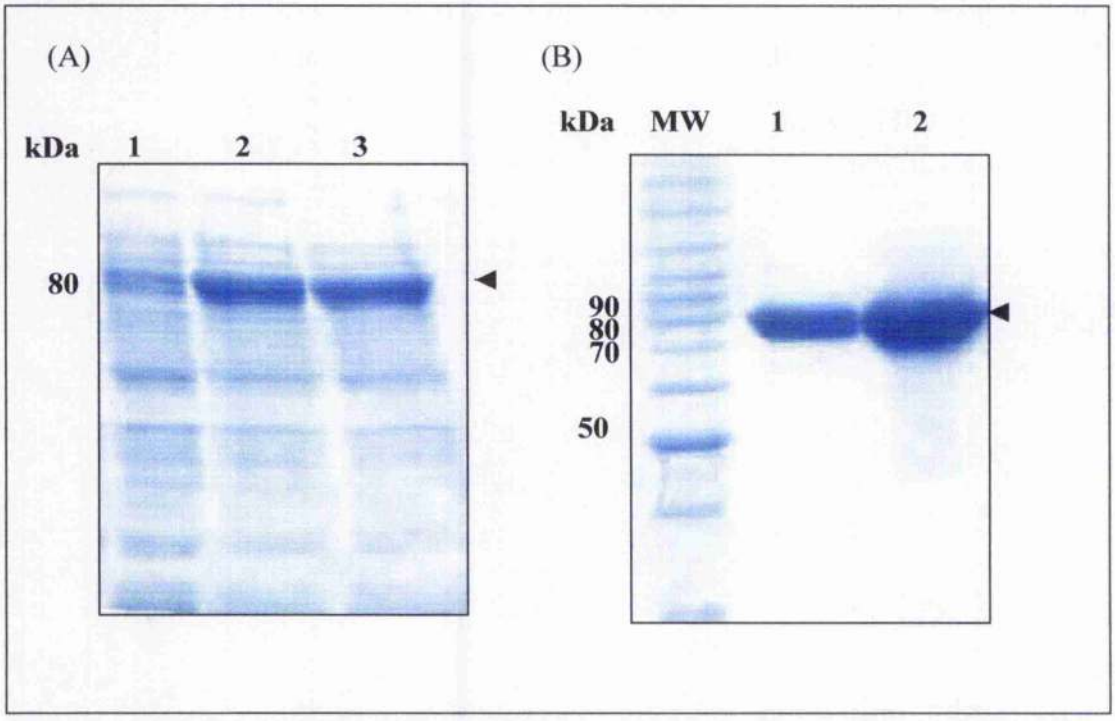

Figure 4.4. Coomassie blue-stained SDS-polyacrylamide gel of expressed and purified PfPREXpol. (A) Coomassie blue-stained SDS-polyacrylamide gel of uninduced (Lane 1) and NaCl induced cells carrying the cloned *PfPREXpol* gene fragment (lanes 2 and 3). (B) Coomassie blue-stained SDS-polyacrylamide gel of nickel affinity purified protein, PfPREXpol, as indicated by the arrow (lanes 1 and 2).

4.2.3. Functional characterisation of PfPREXpol

To determine whether the PfPREXpol protein has DNA polymerase activity, the expressed and purified recombinant protein was used in DNA polymerase activity assays (Section 2.8.3). In addition, the recombinant protein was also checked for the presence of 3'-5' exonuclease activity (Section 2.8.4) because it was observed to possess key structural motifs for that activity (Section 3.2.3).

4.2.3.1. DNA polymerase activity

DNA polymerases catalyse the template-directed incorporation of dNTPs into DNA by addition at the 3'OH termini of primer strands. Polymerase activity is assayed by measuring the incorporation of radiolabelled dNTPs into DNA. Primed single-stranded M13 DNA is frequently used as the template and is the template of choice for the DNA polymerase assays carried out (Section 2.8.3).

DNA polymerase activity was detected in the purified PfPREXpol protein (Figure 4.5a). Different conditions known to influence DNA polymerase activity were investigated. Control experiments were also carried out. Commercial Klenow (*E. coli* DNA polymerase I) (Promega) was used as a positive control for template elongation while a negative control using just distilled water was used as a blank to determine background counts from radiolabel that non-specifically reached the product collection tube. Another negative control was carried out using the recombinant PfPREXprihcli. This control helped to check if the presence of DNA polymerase activity is specific to the recombinant PfPREXpol and not from contaminating proteins in *E. coli*. Typical radioactivity counts obtained from the polymerase activity assays were as such:- the negative controls counts per minute (cpm) range from 747.17 to 1402.76, positive

controls gave cpm of greater than 30,000 while PfPREXpol samples gave a cpm range from 2209.78 to 26,750.

First the effect of pH on the enzyme activity was measured using buffers calibrated to different pH values between 6.0 and 9.0. The buffers used were 50 mM MOPS-NaOH (pH 6.0 -6.5), 50 mM Tris-HCl (pH 7.0 to 9.0). The enzyme has an optimum catalytic activity at pH 7.0 but is inhibited at acidic pH. At alkaline pH, its activity also decreased drastically (Figure 4.5b). Experiments were also performed to determine the effect of temperature on the polymerase activity between 25°C and 90°C. The optimum activity of the polymerase was observed at a surprising 75°C and decreases thereafter (Figure 4.5c). Interestingly, the PfPREXpol protein has most similarity to a DNA polymerase from the thermophilic bacteria *Aquifex aquaticus* (Table 4.2)

DNA polymerases require divalent cations for activity as the cations are involved in stabilising of the transition state of the enzyme and facilitating phosphoryl transfer (Steitz, 1998). Therefore, the effect of Mg^{2+} concentration on the polymerase was tested. The optimal Mg^{2+} concentration for activity was at 5 mM (Figure 4.5d). The effect of KCl concentration on the polymerase activity was also investigated because when salt concentration is high, it affects the dynamics of protein-DNA complex interaction. This results in electrostatic interactions which can contribute to the stability of the complex. For PfPREXpol, the optimum concentration of KCl for activity is 50 mM. Higher concentrations of KCl were inhibitory to the DNA polymerase activity (Figure 4.5e). Its range of activities is comparable to other recombinant DNA polymerases from other organisms (Table 4.2).

DNA Polymerase Source	Temperature optima	pH optima	Optimum Mg^{2+} conc (mM)	Reference
Rhodothermus marinus	55°C	7	5	Blöndal *et al*, 2001
Pisum sativum	N.A	7.5	8	Gaikwad *et al*, 2002
E. coli	N.A	7.5	10-20	Huang & Levin, 2001
Spodoptera littoralis nucleopolyhedrovirus	N.A	7.5	10-20	Huang & Levin, 2001
Cauliflower inflorescence	37°C	7.0	1	Seto *et al*, 1998
Thermus filiformis	70-72.5°C	8.4-9.0	4	*Choi et al*, 1999
Streptococcus pnemoniae	37°C	N.A	6.5	Pons *et al*, 1991
Aquifex aeolicus	70°C	6.8-7.2	4-5	Chang *et al*, 2001
PfPREXpol *P. falciparum*	75°C	7.0	5	

Table 4.2. Characteristics of other DNA polymerase I-like proteins from other sources of organisms. N.A stands for not available.

(A)

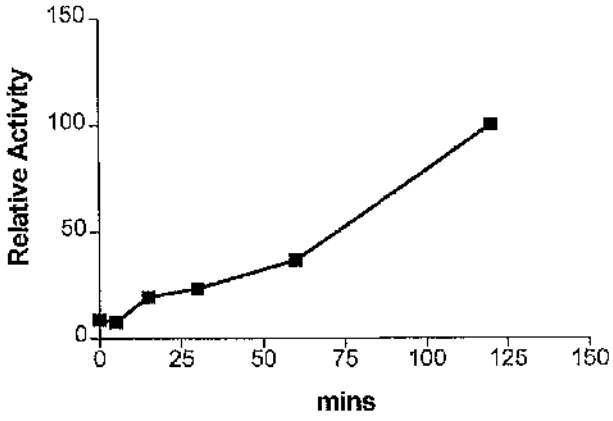
150
100
50
0
Relative Activity
0
25
50
75
100
125
150
mins

(B)

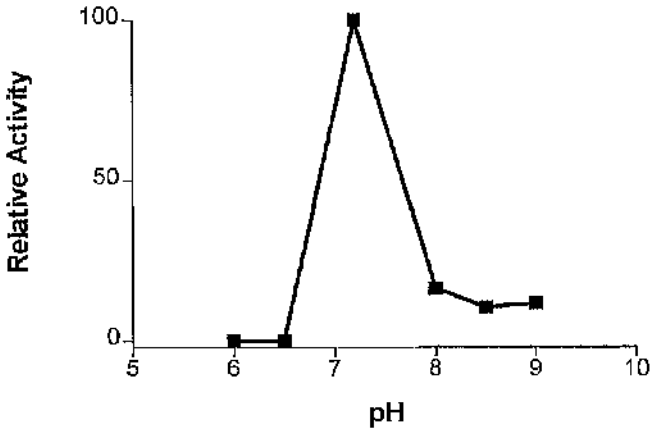
100
50
0
Relative Activity
5
6
7
8
9
10
pH

(C)

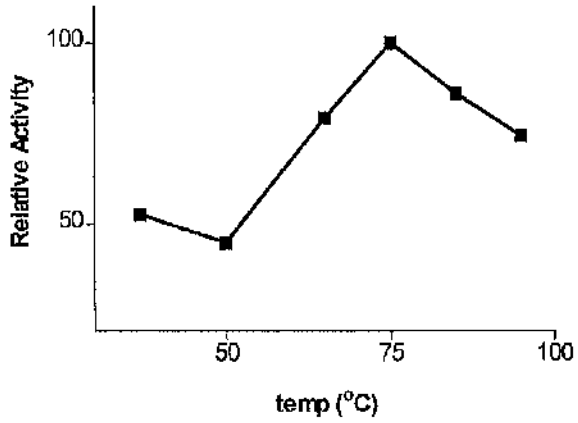
100
50
Relative Activity
50
75
100
temp (°C)

(D)

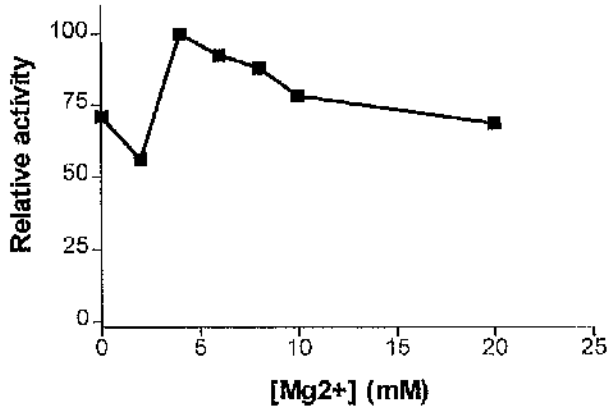

(E)

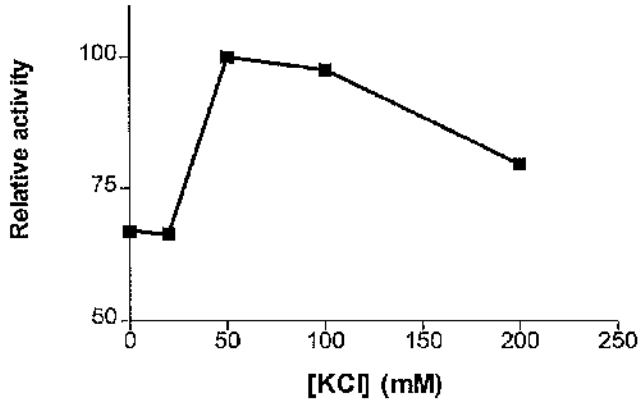

Figure 4.5. Characterisation of DNA polymerase activity of PfPREXpol and the effects of different conditions on its activity. The activity is expressed as relative activity (100%) with respect to different conditions. The experiments were carried out in triplicate over three individual experiments (n=9) and the average was taken to draw the graphs using the Prism software (Graphpad) (a) Time course experiment with PfPREXpol, (b) pH profile of PfPREXpol (c) Temperature profile of PfPREXpol, (d) Effect of Mg^{2+} ions on PfPREXpol activity and (e) Effect of KCl concentration of PfPREXpol activity. No error bars are shown due to the wide range of CPM obtained from each experiment, instead the results are represented as mean relative activity.

Aphidicolin, an inhibitor of most eukaryotic DNA polymerases was also tested for its effect on the recombinant polymerase. Aphidicolin was added to the reaction mixture at various concentrations up to 160 mg/ml but no inhibition was seen, indicating that the recombinant DNA polymerase is not sensitive to aphidicolin. A control experiment was also carried out to test aphidicolin on *E. coli* Klenow (Promega) and it is also insensitive to aphidicolin. Other prokaryotic DNA polymerases and the mitochondrial DNA polymerase of eukaryotes are also aphidicolin-insensitive while most types of eukaryotic DNA polymerases are aphidicolin-sensitive. Unfortunately, we were not able to obtain any eukaryotic DNA polymerases to use as a control to verify whether the batch of aphidicolin used here was functional.

4.2.3.2. 3'-5' exonuclease activity

The domain that has been classified as the DNA polymerase domain of PfPREX (PfPREXpol) also has significant homology towards its N-terminus with 3'-5' exonucleases. The three key structural motifs common among these enzymes can all be found within PfPREXpol. The 3'-5' exonuclease activity of the PfPREXpol was investigated (Section 2.8.4). 3'-5' exonuclease activity was detected, however it was slow-acting over a period of time. Our time course experiments were conducted for up to 2 hours (Figure 4.6), during which the activity of the 3'-5' exonuclease did not reach a plateau. This could be due to the non-optimal conditions used for the assay. For example, the temperature optimum obtained for DNA polymerase activity was at 75°C but the temperature used for this assay was 37°C. Its pH profile was also investigated but further experiments established that there was a spontaneous degradation of the double stranded fragments as the pH of the reaction buffer was increased. Therefore, no further characterisation of the 3'-5' exonuclease was carried out.

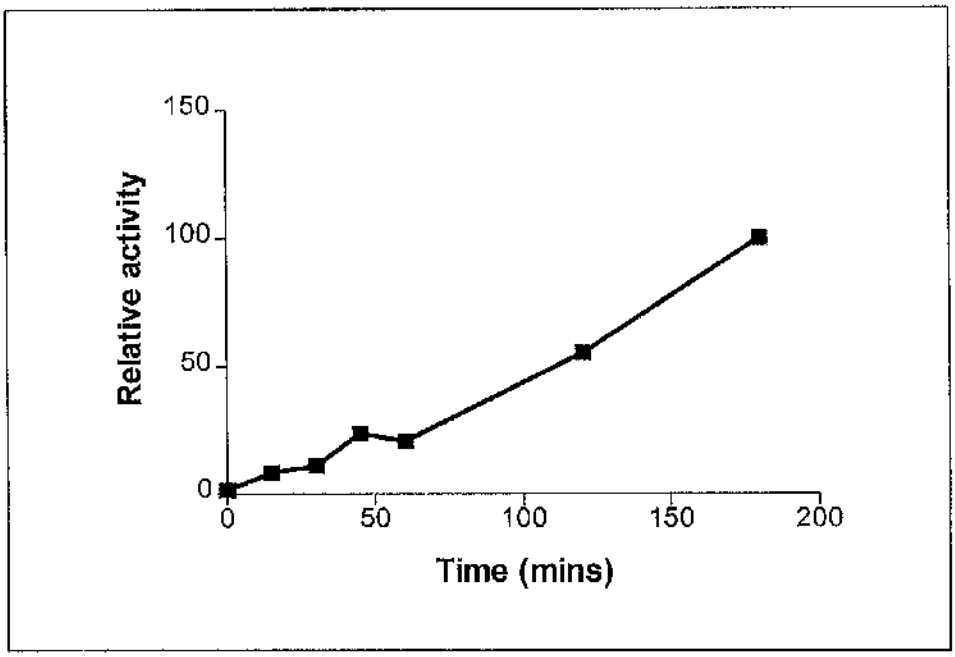

Figure 4.6. Time course experiment of 3'-5' exonuclease domain of PfPREXpol. The activity is expressed as relative activity (100%). The experiments were carried out in triplicate and the average was taken to draw the graphs using Prism software (Graphpad). No error bars are shown because of the large range of CPM obtained from each experiment, instead the results are represented as mean relative activity.

4.2.4. Expression of PfPREXpol in *P. falciparum*

RT-PCR and Western blotting were used to investigate the expression pattern of the *PfPREX* gene and its product in *P. falciparum*. The PfPREX protein is predicted to be 235.8 kDa in its entirety. Whether the PfPREX is indeed translated as a single polypeptide has implication for the topological aspects of the molecule. Production of such a large protein could pose a problem when it comes to ensuring the proper folding and function of the final molecule.

To investigate the transcription of the *PfPREXpol* gene in *P. falciparum*, RT-PCR was performed. Northern blotting using total RNA from asynchronous culture

failed to reveal a signal. Therefore, total RNA from an asynchronous culture of *P. falciparum* was obtained and RT-PCR primers for the PfPREXpol region (Table 2.1) were used (Figure 4.1) to amplify cDNA obtained from *P. falciparum* (Section 2.4.9.2). The results of the RT-PCR (Figure 4.7) showed a band of the predicted size of 400 bp. From the result obtained, it appears that the *PfPREXpol* domain is transcribed. Controls using no reverse transcriptase confirmed that there was no genomic DNA contamination in the RT-PCR samples.

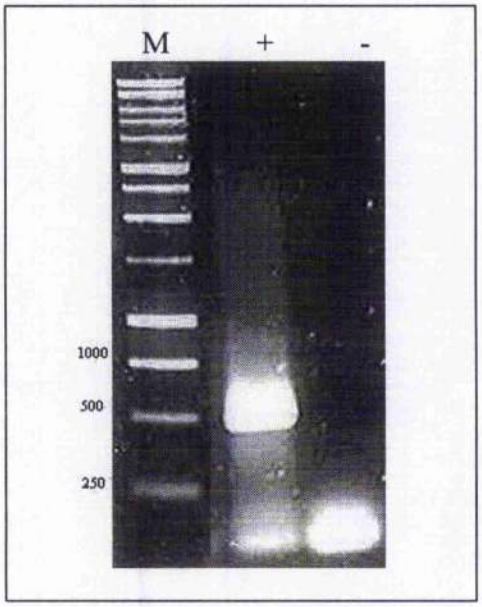

Figure 4.7. RT-PCR amplification of the *PfPREX* transcript from *P. falciparum* 3D7 total RNA. PCR was carried out for 40 cycles; + and – indicate reactions wih and without reverse transcriptase, respectively as a control to check for genomic DNA contamination. PCR amplification was carried out on total RNA obtained from *P. falciparum* 3D7, using primers specific for DNA polymerase region RTPolF1 and RTPolR1. The expected size of the band is approximately 400 bp.

Western blots were also carried to determine whether the PfPREXpol is translated in *P. falciparum*. The recombinant purified PfPREXpol (Section 2.7.1) was used to generate anti-serum made in rabbits (Section 2.7.3). The anti-serum was used to probe blots of parasitised rbc lysates and non-parasitised samples. All Western blots were performed at least three times to check for reproducibility of results. Since *PfPREX* comprises a single ORF which translates to a predicted protein size of approximately 2016 amino acids, the size of the PfPREX protein was estimated at 235.8 kDa. Anti-sera to PfPREXpol, however, identified a single band of approximately 91 kDa in infected but not uninfected rbc on the Western blot (Figure 4.8). The Western blot was repeated at least three times which showed that the result obtained was reproducible. Thus, this result suggests that the PfPREXpol is cleaved from the precursor PfPREX protein. The size of the identified band coincides with just the polymerase domain. It may be that the PREX protein is transported to the apicoplast, and then the C-terminal end (PfPREXpol domain) is cleaved post-translationally. Alternatively, cleavage could occur prior to apicoplast entry, or differential splicing could occur. However, it has not been possible to distinguish these different scenarios during the course of this thesis.

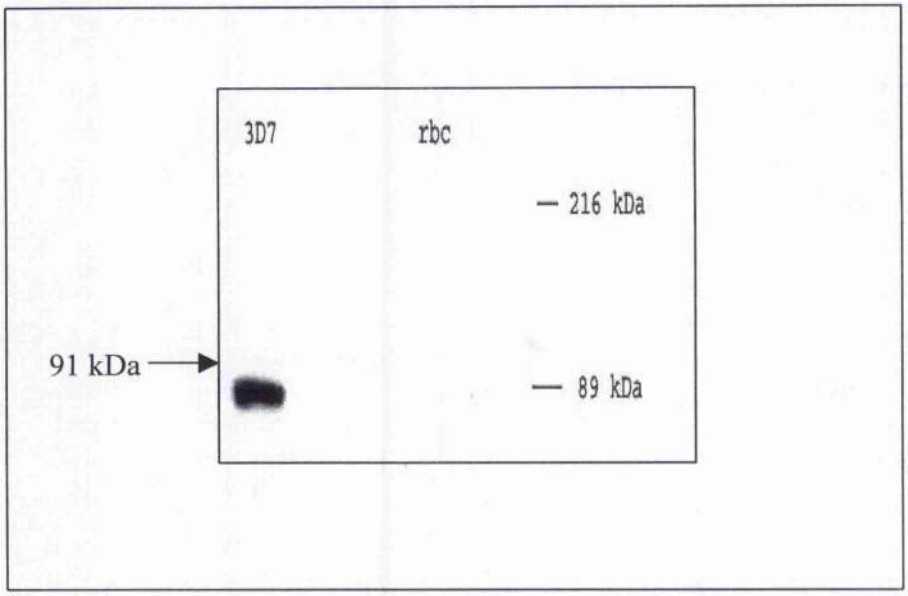

Figure 4.8. Western Blot of parasitised rbc (3D7) and non-parasitised rbc lysates probed with anti-PfPREXpol (1:2000) anti-sera. A single band was observed in the 3D7 lane of approximate size of 91 kDa.

4.2.5. Homology modelling of PfPREXpol

Homology modelling was carried with the PfPREXpol amino acid sequence. Due to the similarity of PfPREXpol to the Klenow fragment, we were able to send the PfPREXpol amino acid sequence to the Swiss Model First Approach (Schwede *et al*, 2003) website (http://swissmodel.expasy.org) to obtain a putative 3D structure of PfPREXpol based on the known crystal structure of Klenow fragment of *E. coli* (PDB no:- 1KFD) (Beese *et al*, 1993).

4.2.5.1 A modelled 3D structure of PfPREXpol protein

Like the Klenow fragment, the engineered protein representing the DNA polymerase I, PfPREXpol, consists of a 3'-5' exonuclease domain at its N-terminal end and the DNA polymerase domain at its C-terminal end. PfPREXpol shares 38.1%

similarity and 24.5% identity with the *E. coli* Klenow fragment which shows that they share a high degree of conservation. The alignment of PfPREXpol alongside the *E.* coli Klenow fragment (Figure 3.5) shows the degree of conservation especially in the key motifs involved in both 3'-5' exonuclease activity and DNA polymerase activity. The Swiss Model service of the Expasy server (Guex & Peitsch, 1997; Ollis *et al*, 1985; Peitsch, 1996) was used.

The modelling result suggests that there is a high degree of conservation of structure between PfPREXpol and *E. coli* Klenow fragment. The key thumb-finger-palm structure, characteristic of the Klenow fragment, is also observed in the predicted PfPREXpol 3D structure alongside the 3'-5'exonuclease domain (Figure 4.9).

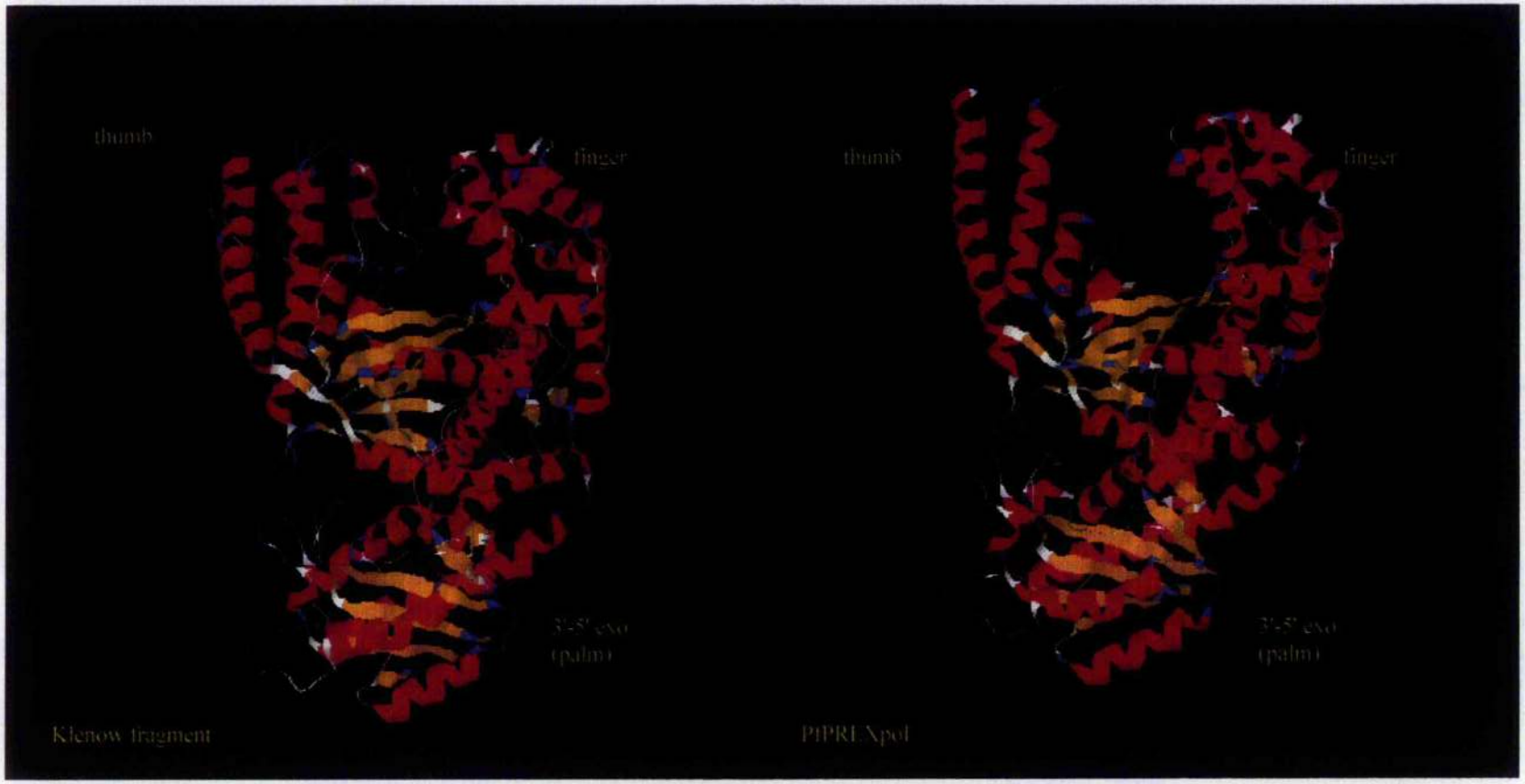

Figure 4.9. 3D structure of Klenow fragment from *E. coli* and PfPREXpol which was modelled on the Klenow fragment. The two structures look strikingly similar consisting of key characteristic features of DNA polymerase I. It consists of a thumb-finger structure and a 3'-5' exonuclease domain.

4.2.5.2. Comparison of PfPREXpol and *E. coli* Klenow fragment 3D structures

Figure 4.9 shows the putative 3D structure of PfPREXpol and the solved 3D structure of *E. coli* Klenow. As in Klenow polI, the structure of PfPREXpol consists of three domains (the thumb, the palm and the fingers). When the amino acid sequence entered into the Swissmodel First Approach, it only contained the predicted PfPREXpol domain. Only a partial 3D structure was obtained. Only when the hinge domain is included in the amino acid sequence used for prediction of 3D structure, was a full 3D structure of PfPREXpol was obtained. Therefore, we hypothesised that the hinge domain of PfPREXpol may have a role to play to ensure the proper folding of the DNA polymerase domain.

In addition, it was considered of interest to compare the amino acid residues that are shown to be important in the various aspects of DNA polymerase activity in Klenow fragment with amino acids occupying the same positions in the modelled structure of PfPREXpol. Previous experiments, which dealt with dNTP binding to the polymerase site, revealed that incoming dNTPs interact with Arg 754, Arg 682 and Lys 758 (Basu & Modak, 1987). These residues are highly conserved in the family A of DNA polymerases and interact with the phosphate backbone of incoming dNTPs as these residues are all positively charged. When the same positions were checked on PfPREXpol, they were found to comprise the same residues. The corresponding residues are conserved between the *E.* coli and *P. falciparum* except for Arg 682 in Klenow is replaced conservatively as a Lys 205 in PfPREXpol. Essentially in this case, the positive charge remains in place for interaction with dNTPs. Figure 4.10 shows the stereodiagrams with these sites highlighted. The sites in both enzymes are in similar positions for the interaction with dNTPs.

(A) Residues involved in dNTP interactions

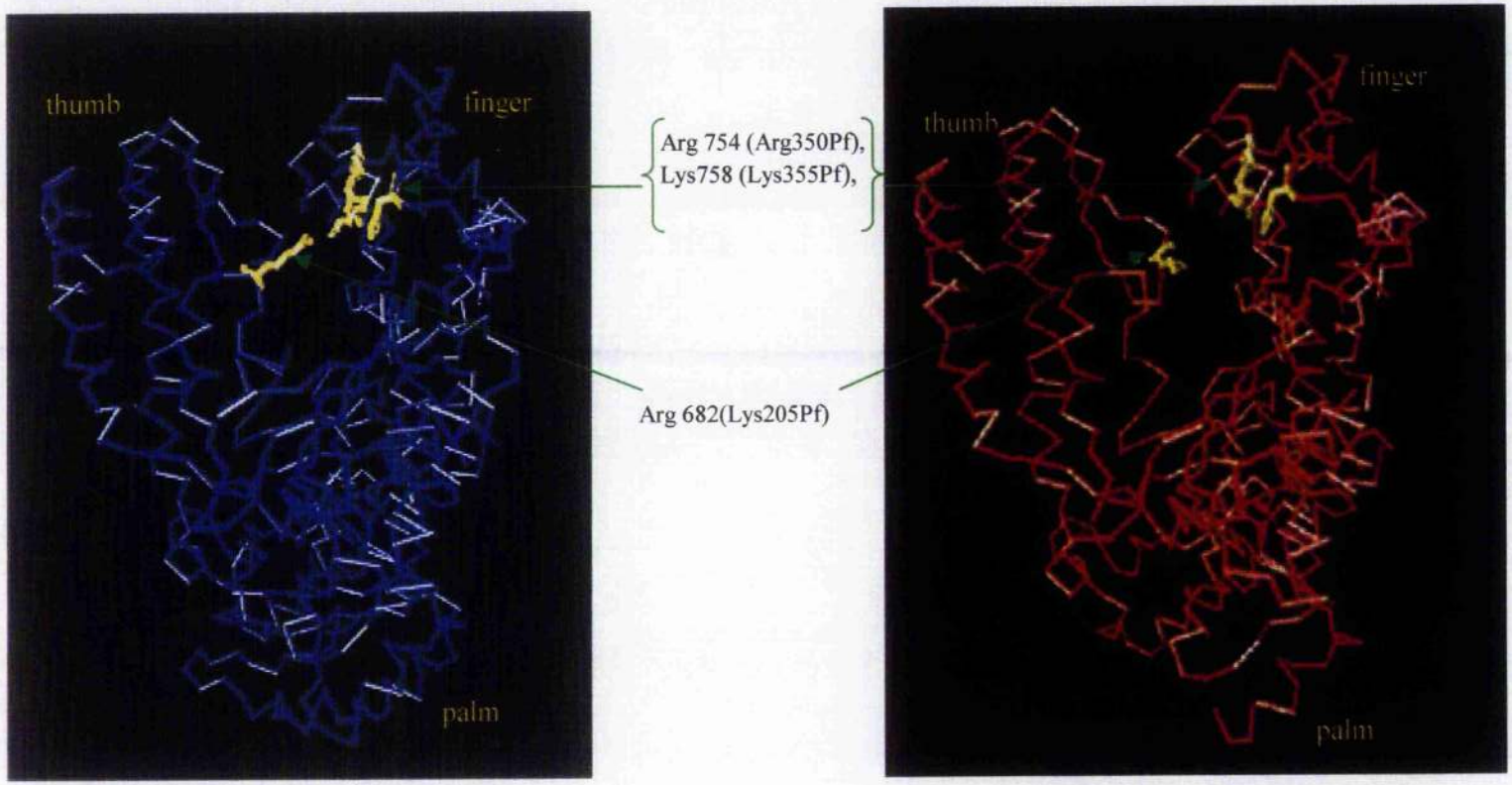

(B) Residues involved in dNTP binding.

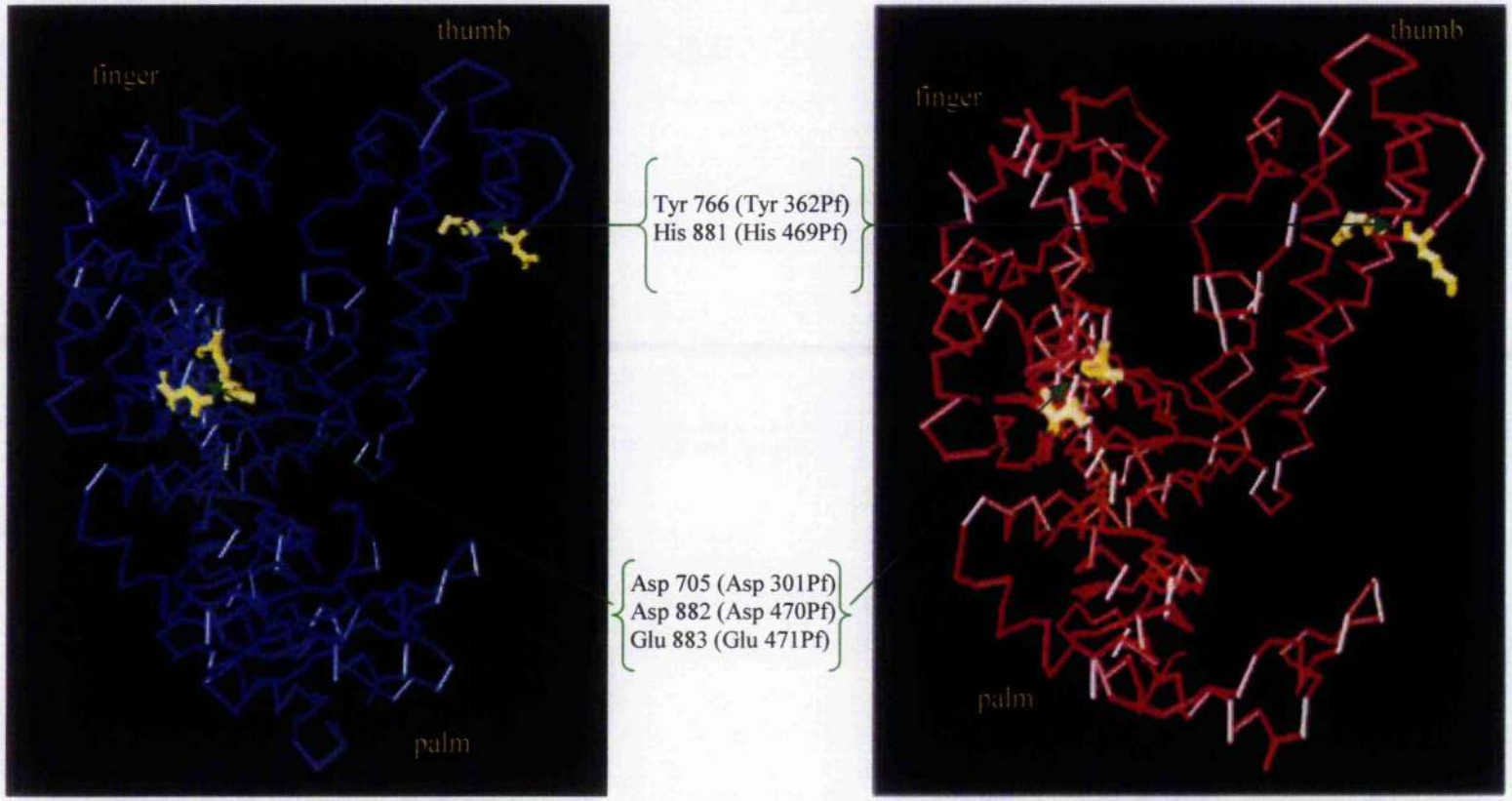

(C) Residues involved in primer attachment

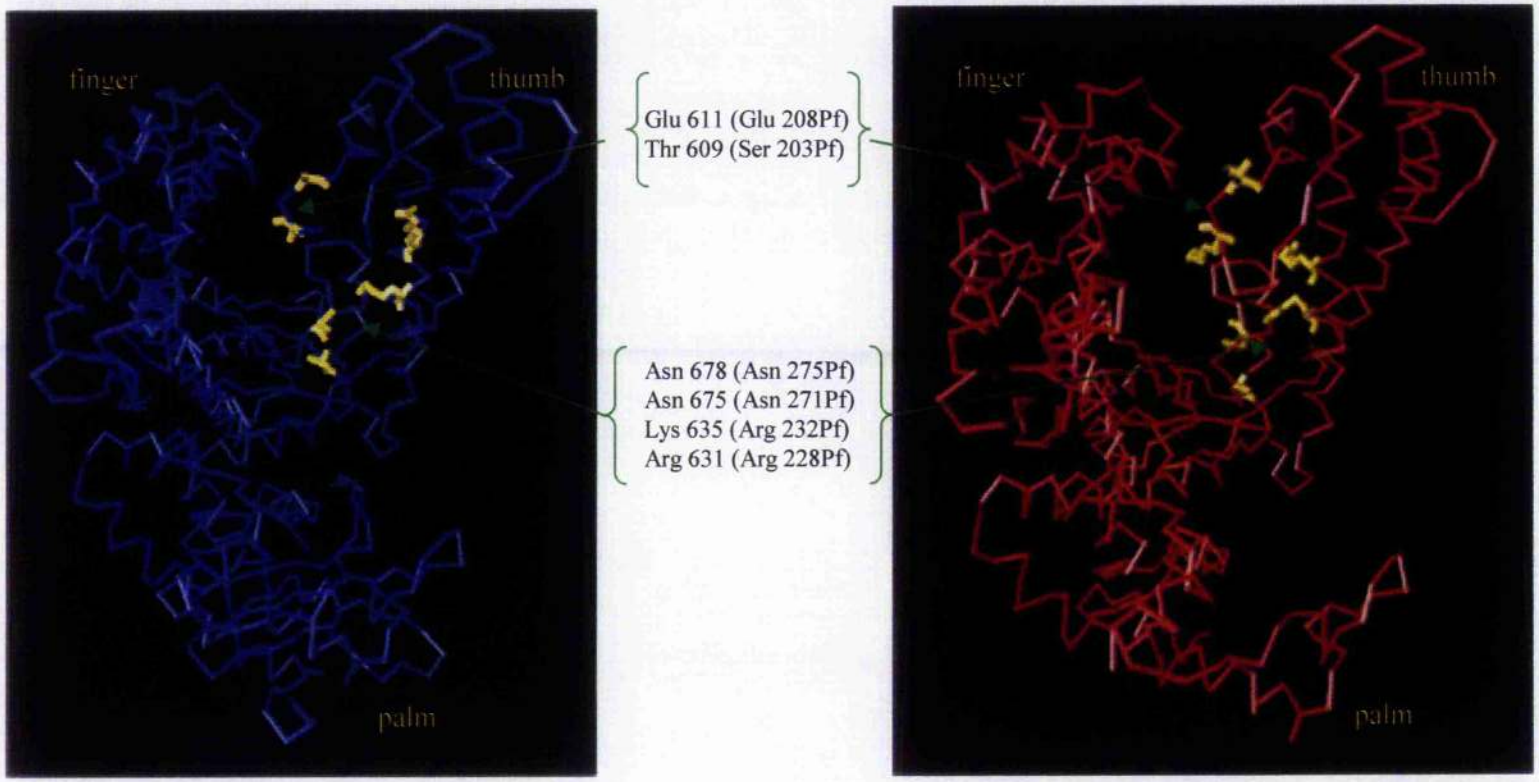

(D) Residues involved in catalysis

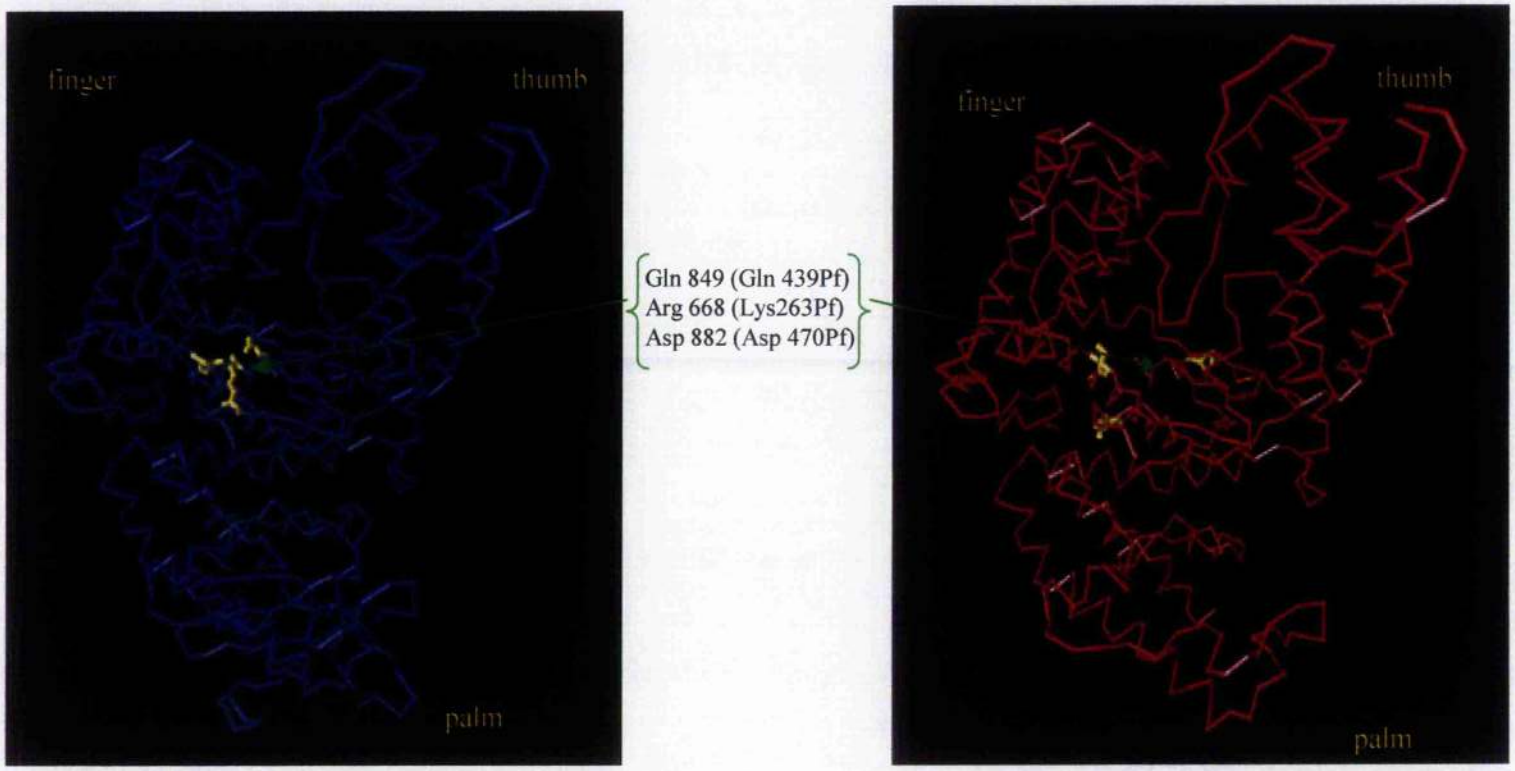

Figure 4.10. Comparison of the structures of Klenow and PfPREXpol. Superimposed stereodiagrams of the structures of both enzymes. Klenow is shown with the blue line while PfPREXpol is shown with the red line. (A) shows highlighted residues involved in dNTP interactions, (B) shows highlighted residues involved in dNTP binding and (C) shows highlighted residues involved in primer attachment and (D) shows highlighted residues involved in catalysis. Key Residues for Klenow are labelled while the residues for PfPREXpol are in labelled in brackets.

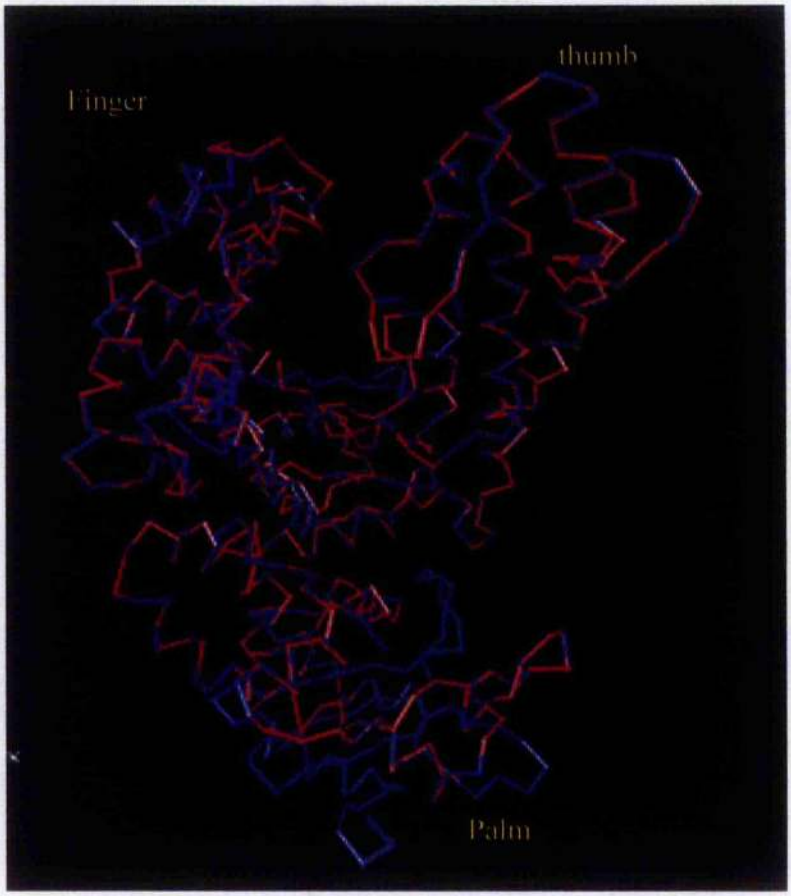

Figure 4.11. Comparison of the structures of Klenow and PfPREXpol. Superimposed stereodiagrams of the structures of both enzymes. Klenow is shown with the blue line while PfPREXpol is shown with the red line.

Previous experiments and X-ray crystallography data have shown that Tyr 766, Arg 841, Asn 845, Asp 882, Asp 705, Glu 883 and His 881 (Joyce & Steitz, 1994; Pandey *et al*, 1987; Polesky *et al*, 1990) are all involved in binding and directing the incoming dNTP. The corresponding residues in PfPREXpol are also well conserved (Table 4.3). Asp 882 (Asp 482) and Asp 705 (Asp 301) correspond to the residues in motif C and A respectively which are shown to be involved in dNTP binding. In addition, they have been shown be involved in the binding of divalent metal cations (Joyce & Steitz, 1994). Other residues which are required for primer attachment and catalysis are observed to be well conserved between Klenow and PfPREXpol. The palm domain contains the catalytic centre where the residues important for catalysis are Asp 882 (Asp 470), Arg 668 (Lys 263) and Gln 849(Gln 439) (Polesky *et al*, 1990). The thumb domain contains highly conserved residues that are involved in primer attachment. These residues are well conserved across the PolI family. Arg 631 (Arg 228), Lys 635 (Arg 235), Asn 675 (Asn 271) and Asn 678 (Asn 275). Table 4.3 shows all the conserved residues important in DNA polymerase activity.

Sites Involvement	Klenow residues	PfPREXpol residues	References
dNTP interaction	Arg 754	Arg 350	Basu & Modak, 1987
	Arg 682	*Lys 250	Pandey *et al*, 1990
	Lys 758	Lys 355	Beese *et al*, 1993a
dNTP binding	Tyr 766	Tyr 362	Pandey *et al*, 1987
	Asp 882	Asp 470	Joyce & Steitz, 1997
	Asp 705	Asp 301	Beese *et al*, 1993a
	Glu 883	Glu 471	
	His 881	His 469	
	Arg 841	*Lys 432	
	Asn 845	Asn 435	
Catalysis	Gln 849	Gln 439	Polesky *et al*, 1990
	Arg 668	*Lys 263	
	Asp 882	Asp 470	
primer attachment	Glu 611	Glu 208	Beese *et al*, 1993b
	Asn 678	Asn 275	
	Asn 675	Asn 271	
	Lys 635	*Arg 232	
	Arg 631	Arg 228	

Table 4.3. Comparison of key residues on Klenow and PfPREXpol. The key residues involve in dNTP interaction, dNTP binding, primer attachment, catalysis and template attachment for both Klenow and PfPREXpol. Asterisk next to the residue represents a conservative replacement of amino acids.

4.2.6. Subcellular localisation of the *PfPREXpol* gene product

With reference to the presence of the plastid-targeting sequence in the N-terminus of PfPREX, we wanted to confirm the subcellular localisation of PfPREXpol domain. To do this, we used the PfPREXpol anti-serum and performed some indirect immunofluorescence (IDF) and some *in situ* hybridisation using a plastid specific DNA probe to give us co-localisation data. This first approach was taken to use a plastid-specific DNA probe to target the plastid DNA in *P. falciparum* using *in situ* hybridisation. PCR primers specific for the *ssurRNA*, a gene found on the plastid DNA in *P. falciparum*, were used to generate a PCR product (Section 2.9.2.1). The PCR product had biotinylated dUTP incorporated which will bind to Streptavidin-Texas red for fluorescent detection under phase contrast microscopy. The protocol was in addition to IDF which was carried out after the *in situ* hybridisation step. The protocol could not be optimised to give satisfactory results. No red fluorescence could be observed, apparently the DNA probe was either not binding to the target DNA as expected or it was being washed off during the subsequent steps carried out in the protocol.

Therefore, another approach was taken. Instead of targeting the plastid DNA, we used a stain, Mitotracker® Red CMXRos (Molecular Probes) that is taken up by the mitochondrion. This was carried out to check if PfPREX is localised to the mitochondrion. The stain was used alongside DAPI (Sigma) which stains the nucleus and immunofluorescence using the anti-PfPREXpol anti-sera. To optimise the IDF protocol, various dilutions of the anti-sera were used, ranging from 1:50 to 1:1000. The optimum dilution of the anti-sera to be used was 1:500 alongside 1:400 dilution of the secondary antibody (anti-rabbit FITC, Diagnostics Scotland) (Figure 4.13). From the figure, there appears to be no overlay between the mitotracker and the FITC (anti-

PfPREXpol). This suggested that the PfPREXpol did not localise to the mitochondrion in *P. falciparum*. However, it was not clear whether the anti-sera localised to the plastid. The DAPI stains both nuclear and plastid DNA, but it is difficult to see the plastid under the highest available magnification. Therefore, another approach was undertaken in order to show whether PfPREX localised to the plastid. A collaboration was set up with Iain Wilson and Shigeharu Sato (NIMR, MRC) to make green fluorescent protein (GFP) constructs using the PfPREX leader sequence to check for targeting. This work is beyond the context of the thesis itself, since these localisation experiments were the work of Dr Sato. However, the results of Dr Sato's work will be discussed briefly in chapter 7.

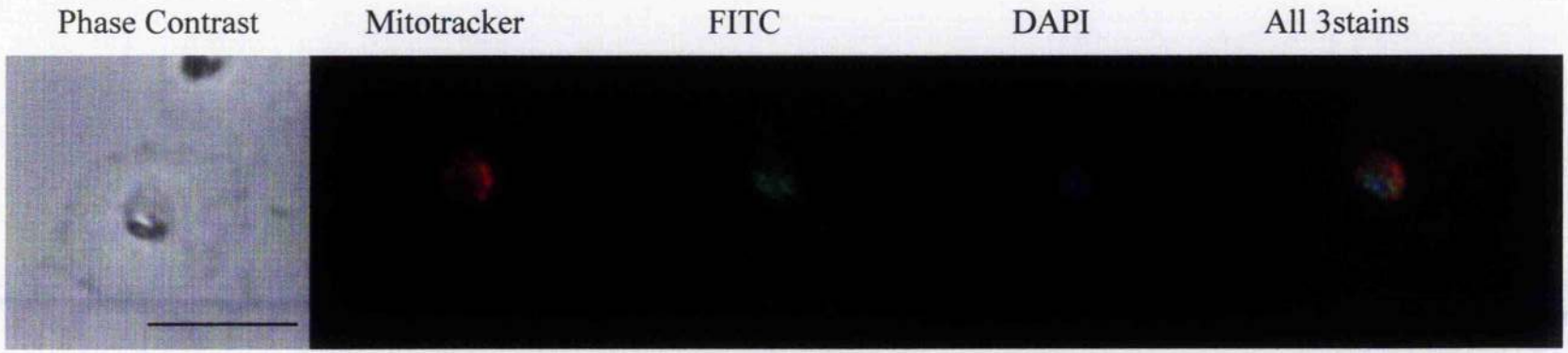

Figure 4.12. Subcellular localisation of PfPREXpol using immunofluorescence technique. The first diagram is a phase contrast microscopy picture of a red blood cell infected with a ring-form parasite, followed by the same cell viewed under fluorescence using the Texas red filter of an excitation and emission peak of 560 and 630 nm respectively. The three picture shows the same cell viewed under fluorescence using the FITC filter of an excitation and emission peak of 484 and 510 nm respectively, followed by DAPI filter of 360 and 460 nm respectively and finally with all pictures merged together. The mitotracker stain shows the locality of the mitochondrion DNA, FITC shows where the anti-PfPREXpol antisera have bound and DAPI stains specifically nuclear and apicoplast DNA. Scale bar, 5 μm.

4.3. Discussion

The experimental findings and sequence analysis suggested that PfPREX possesses a DNA polymerase functional domain. The C-terminal domain resembles a DNA polymerase domain (Chapter 3) homologous to family A DNA polymerases. Homology searches identified the three key structural motifs conserved among family A DNA polymerases. Furthermore, the presence of the three 3'-5' exonuclease motifs also suggested the presence of that enzymatic activity. Therefore, attempts were made to clone and express the PfPREXpol domain. This was successful, as purified PfPREXpol was obtained. Functional characterisation was carried out to show that the PfPREXpol is a functional DNA polymerase. It has characteristics similar to other family A DNA polymerases (Table 4.2) including its Mg^{2+} requirements and pH optimum. One interesting point to note is that its temperature optimum was high (75°C). The temperature optimum of PfPREXpol is similar to thermophilic *Aquifex aquaticus* DNA polymerase at 70°C. It is noteworthy that the enzyme closest in sequence similarity to PfPREXpol is also the same DNA polymerase of *Aquifex aquaticus*. This raises the possibility that the plasmodial DNA polymerase may be a recent acquisition through horizontal gene transfer from a thermophilic bacterium closely related to the *Aquifex* family.

Transcription of the PfPREXpol domain was also shown in *P. falciparum*, although failure to identify the transcript by Northern blot analysis indicates it is in very low abundance. Recent transcriptome analysis (Le Roch *et al*, 2003) has shown *PfPREX* to be expressed predominantly in replicative time points of the life cycle in mammalian blood. In addition, experimental findings with the Western blots carried out, suggests that PfPREX may be post-translationally cleaved. The PfPREXpol domain was detected

as a 91 kDa band on a Western blot of parasite lysates probed with anti-PfPREXpol anti-sera, rather than a larger band of 235.8 kDa, which is the size of the full polypeptide. The size of the band 91 kDa, coincides approximately with the predicted size of the PfPREXpol domain. This result seems to suggest that the PfPREXpol domain is cleaved. Topologically, it may be necessary to cleave from the full polypeptide to ensure proper folding and for function.

Homology modelling of PfPREXpol structure was carried out based on its similarity to the Klenow fragment of *E. coli*. The 3D structure obtained from PfPREXpol had a similar structure to the Klenow fragment of *E. coli* which is composed of 3 regions (thumb, finger and palm). We were able to compare the key residues and their positions within the structures of Klenow and PfPREXpol. The results obtained suggests that PfPREXpol is indeed similar to Klenow in terms of its structural composition.

Unfortunately, the results obtained from the subcellular localisation studies here were inconclusive. The *in situ* hybridisation experiments were designed such that the biotinylated plastid-specific DNA probe would bind to the plastid DNA which in turn binds to streptavidin Texas red, so that it could be used to give some co-localisation data. If the anti-PfPREXpol antisera localised to the plastid, the two fluorescence signals would overlay on each other. It seemed though that the DNA probe was not binding to the plastid. Instead, when viewed under texas-red filter under confocal microscopy, no red fluorescence was observed. It could be due to the fault of the DNA probe that it is not a good probe or that the protocol used had too many washing steps such that the DNA probe had been washed away. Due to time constraints, the protocol

could not be fine-tuned and new probes were not made due to the time limitations in efforts to get better results.

Based on the results obtained with the immunofluorescence experiments, we cannot conclude on the localisation of PfPREXpol. Careful analysis of the FITC staining pattern obtained with the anti-PfPREXpol (Figure 4.12) suggested a staining pattern typical of compartmental localisation. The green fluorescence was found in spots around the infected red blood cell. If PfPREXpol is located in the cytoplasm, a uniform green fluorescence pattern would be expected. The pattern observed has a spot-like characteristic. Dr Sato (NIMR, Mill Hill) then used GFP technology to help find out the exact location of PfPREX and concluded a plastid localisation (discussed later in Chapter 7).

Chapter V

Functional analysis and subcellular localisation of the DNA primase/helicase (PfPREXpriheli) domain of the *PfPREX* gene

5.1. Introduction

DNA helicases are ubiquitous in nature. Multiple DNA helicases, each with different functions, are present within a single organism. All DNA helicases are NTPases and they share common biochemical properties including nucleic acid binding, NTP binding and NTP hydrolysis. Common amino acid motifs can identify putative DNA helicases. We have detected the presence of multiple motifs that are known to be important for DNA helicase function in PfPREX suggesting that *PfPREX* may encode a functional DNA helicase. In addition to this DNA helicase, *Plasmodium* may also possess other helicases (*E. coli* has at least 11 DNA helicases). Therefore, a GO function search, similar to the one carried out for DNA polymerase in chapter 4, was carried out to search for other helicases in *P. falciparum*. Table 5.1 shows the DNA helicases that have been detected in the *P. falciparum* genome database. At least nine putative helicase genes have been annotated in the *P. falciparum* genome but none of these correspond to the DNA helicase on PfPREX.

DNA primases are often associated with DNA helicases (Ilyina *et al*, 1992). This may be the case with PfPREX, which also contains a region with similarity to a DNA primase. DNA primases are responsible for synthesising short RNA strands for DNA polymerase to use to elongate DNA during DNA replication. DNA primases also possess key motifs required for activity; these include a zinc motif, and two DxD (aspartate) dyad motifs that can be located in PfPREX. In addition, three other motifs important for DNA primase activity were detected on PfPREX which suggest that it may possess a functional DNA primase activity. A GO function search was also carried out to check for the presence of other DNA primases in *P. falciparum* (Table 5.1). Only

two other DNA primases are found, neither of which correspond to the DNA primase identified on PfPREX.

	gene	location	description
1	PFB0730w	pfal_chr2: 658636-664629	DNA helicase, putative
2		chr6: 248857-254350	DNA helicase, putative
3	PFI0910w	pfal_chr9: 764838-767024	DNA helicase, putative
4		chr13_1: 1690520-1695332	DNA helicase, putative
5	PF13_0308	chr13_1: 2189979-2192699	DNA helicase
6		chr13_1: 2386358-2387809	ATP-dependent DNA helicase, putative
7	PF14_0081	chr14: 313974-317456	DNA repair helicase, putative
8		chr14: 1175723-1180045	ATP-dependent DNA helicase, putative
9	PF08_0100	chr8: 841194-843300	ruvB like DNA helicase, putative
10	PFI0530c	pfal_chr9: 496141-497718	DNA primase, large subunit, putative
11		chr14: 1563530-1566794	small subunit DNA primase

Table 5.1. Putative genes found using a GO function search through the *Plasmodium falciparum* genome using DNA helicase and DNA primase function searches in Plasmodb version 4.1. Genes 1 to 9 shows the putative DNA helicases found and genes 10 and 11 shows the putative DNA primases found through GO function search.

The GO function search for both DNA helicase and DNA primase failed to detect the putative DNA helicase or DNA primase of PfPREX. This could be due to the nature of algorithms of the search programme which were not able to pick up the key amino acid motifs found on each of them.

In this chapter, the cloning and expression of the DNA helicase and DNA primase domains together is described. The two domains were chosen to be cloned and expressed as a single entity because they showed most similarity to the phage T7 gene 4 which is a combined DNA primase-DNA helicase. Therefore, the possibility exists that the DNA primase and helicase need to be together to fold or function correctly.

5.2. Results

5.2.1. Cloning of the *PfPREXpriheli* domain of the *PfPREX* gene

The DNA primase/helicase domain of the *PfPREX* gene spans a region of approximately 2,721 bp over the N-terminal domain of the gene. It was amplified using gene-specific primers, designed specifically for use in the Gateway Cloning system (Invitrogen). The primers used were GWHcliSignalF1 as the forward primer and GWHcliHingeR1 as the reverse primer (Table 2.1). The reverse primer was designed to overlap partially with the hinge domain (~ 400 bp) of the gene while the forward primer precedes the primase domain at the extreme N-terminus within the predicted plastid-targeting domain. Figure 5.1 shows the relative positions of the primers in accordance to the PfPREXpriheli domain. Therefore, the expected size of the PCR product was 3.2 kb (Figure 5.2). The primers used contained the *att* sites for ease of recombination with the Gateway Cloning system (Invitrogen) that was used for expression (Section 2.5.1).

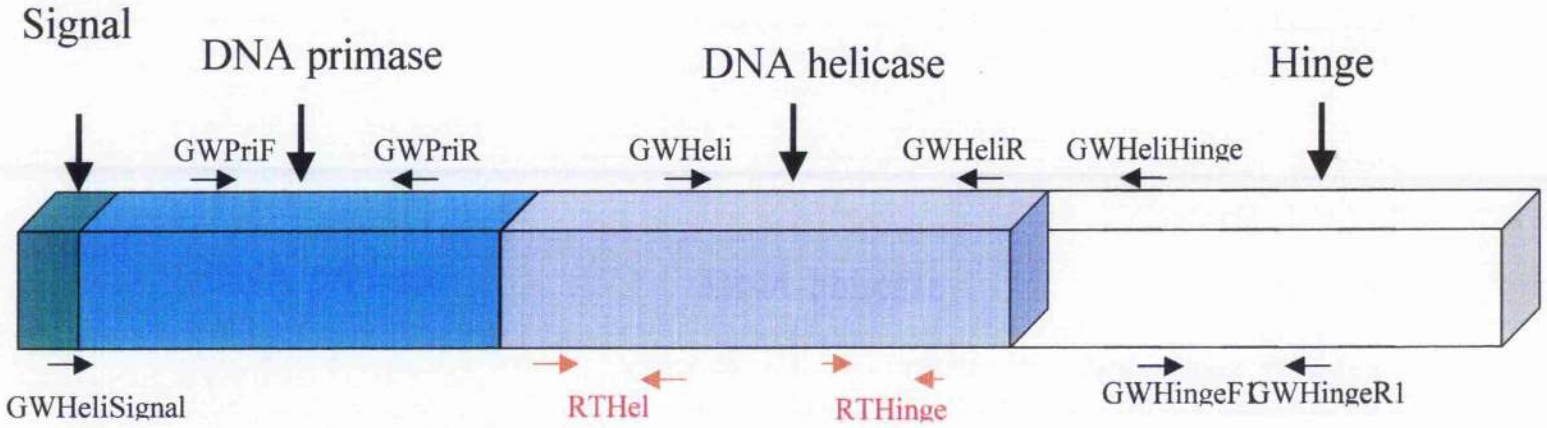

Figure 5.1. Schematic diagram showing the location of the primers used on the gene *PfPREX*. The black arrows show the primers used in the PCR amplification of the fragments used for cloning. The red arrows show the primers used for RT-PCR experiments.

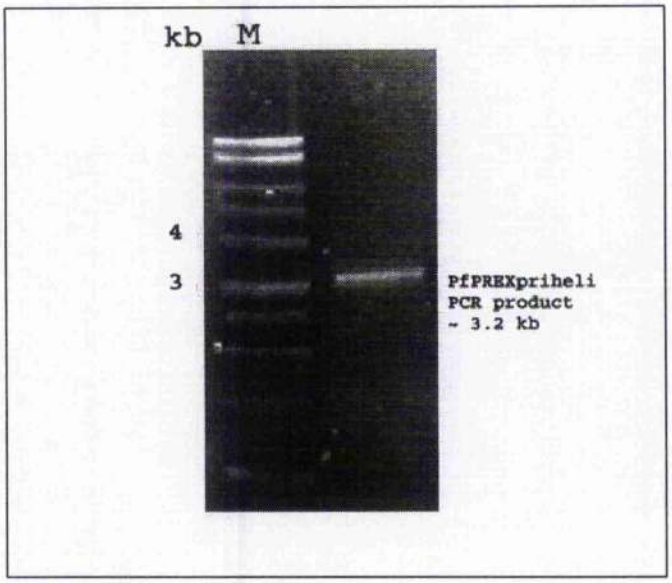

Figure 5.2. Cloning of recombinant His_6-tagged PfPREXpriheli DNA helicase/primase. The PCR amplification product was analysed on a 0.8% agarose gel.

In addition, attempts to clone and express fragments of the DNA helicase, DNA primase and the hinge domains as fusion proteins, separately for the purpose of generating anti-sera for localisation studies were carried out. The primers used for all three domains are listed in Table 2.1. The expected sizes of the three PCR products from the DNA primase, helicase and hinge domains were 500 bp, 420 bp and 600 bp respectively (Figure 5.3).

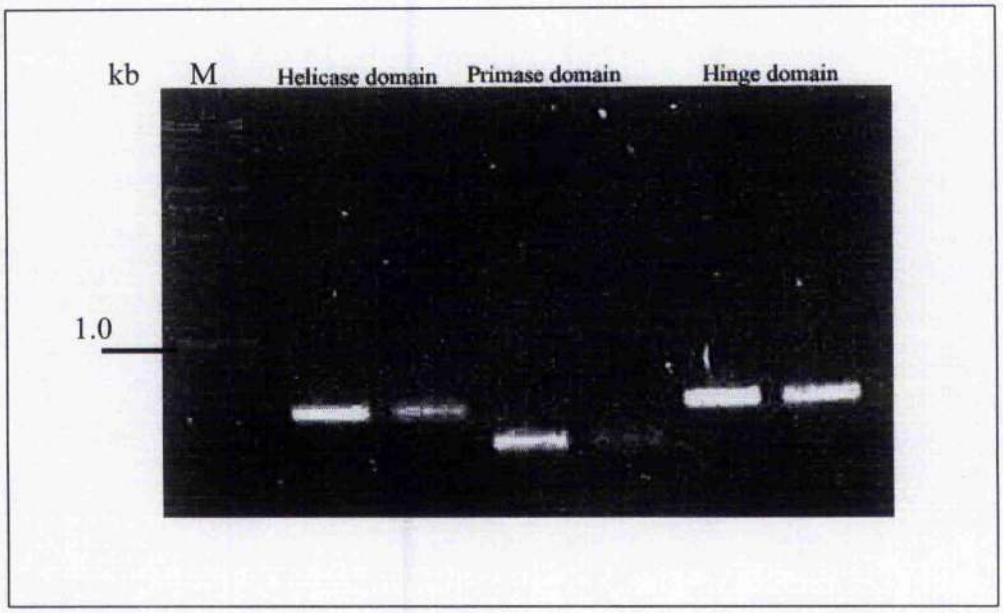

Figure 5.3. PCR amplification products of the fragments from the DNA primase, DNA helicase and hinge domains of *PfPREX*. Fragments of the three domains were amplified using gene-specific primers as detailed in Table 2.1. The PCR products were analysed on a 0.8% agarose gel. The PCR product of the helicase domain has an expected size of 500 bp, the primase domain - 450 bp and the hinge domain - 600 bp.

The PCR products obtained were then cloned into pDONR201 donor vector before they were transferred into destination vectors (expression vectors). The PfPREXpriheli PCR product was transferred into a pDEST15 vector which added an N-terminal GST-tag to the protein to facilitate purification. The other three PCR products were also subcloned into pDEST15.

5.2.2. Expression and purification of DNA primase/helicase and hinge recombinant proteins

The *E. coli* BL21si strain was used to host the expression of the recombinant proteins. Induction of expression of the recombinant proteins was performed at 16°C overnight and soluble proteins were obtained from *E. coli*. The calculated mass of the PfPREXpriheli recombinant protein is approximately 120 kDa. Since the expressed recombinant protein contains an N-terminal GST-tag, it was purified as detailed in Section 2.7.2 in chapter 2. A significantly lower quantity of recombinant protein was obtained with the PfPREXpriheli than with the PfPREXpol protein. The purified protein was analysed on an SDS-PAGE but it ran on the gel as a band at 97 kDa (Figure 5.4), significantly lower than its predicted molecular weight. This could be due to the basic nature of the protein where its predicted pI is 9.13. The three GST-fusion proteins analysed on SDS-PAGE, ran at their expected sizes: - primase domain (22 kDa), helicase domain (20 kDa) and hinge domain (23kDa) (Figure 5.5).

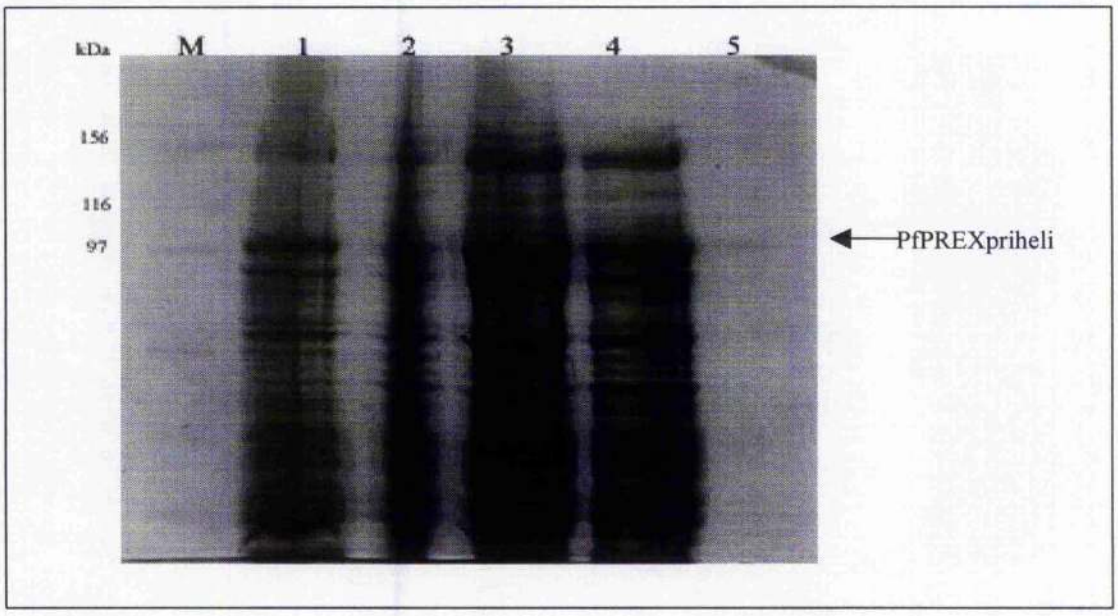

Figure 5.4. Coomassie Blue-stained SDS-polyacrylamide gel of nickel affinity purified proteins. PfPREXpriheli, as indicated by the arrow. Lane (M) indicates the marker, (1) Uninduced fraction, (2) induced fraction (3) + (4) purification flow through fraction and (5) purified PfPREXpriheli.

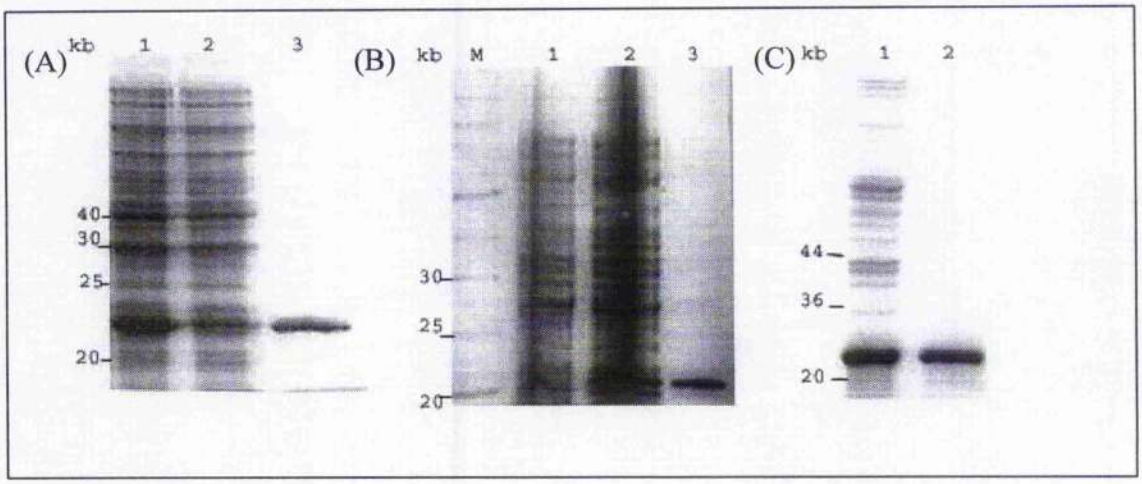

Figure 5.5. Coomassie Blue-stained SDS-polyacrylamide gel. (A) pDEST15pri, the recombinant primase protein. Lanes (1) extract from induced cells, (2) flow-through fraction from GST purification column and (3) purified protein; (B) pDEST15Hinge, the recombinant hinge protein. Lanes (M) marker protein, (1) extract from uninduced cells, (2) extract from induced cells and (3) purified hinge protein; (C) pDEST15Heli, the recombinant helicase protein. Lanes (1) total induced cell lysate and (2) purified protein.

5.2.3. Functional characterisation of PfPREXpriheli

To determine whether the PfPREXpriheli protein has DNA primase and DNA helicase activities, the expressed, purified recombinant protein was used in activity assays (Section 2.8).

5.2.3.1. DNA primase activity

DNA primase activity was detected in the purified PfPREXpriheli protein (Figure 5.6). Different conditions that can affect the DNA primase activity were investigated (Section 2.8.1). In addition, control experiments were carried out. First the purified recombinant PfPREXpol was used as a negative control in both the DNA primase and DNA helicase assays. This was to check for the presence of contaminant *E. coli* proteins that possess either DNA primase or DNA helicase activity so that if either activity was observed, it was due to PfPREXpriheli and not an *E. coli* contaminant

protein. Typical radioactivity counts obtained from the DNA primase activity assays were as such :- the negative controls gave average cpm of 723.73 and PfPREXpri samples gave cpm ranging from 1637.26 to 26,206.53.

Different concentrations of PfPREXpriheli were added to the enzyme assays to see the effect of increased quantity of enzyme on the activity. There was a proportional increase of DNA primase activity with increase in the quantity of enzyme added. Next, a time course experiment with the recombinant protein was carried out. The rate of activity stayed constant, yielding increasing quantities of primer-product over time. The effect of Mg^{2+} on DNA primase activity was also studied. The enzyme activity was at its optimum when the Mg^{2+} concentration was between 4.0 and 6.0 mM (Figure 5.6c). Finally, the effect of pH on primase activity was studied. It appears that the enzyme is most active at alkaline pH (pH 7.5-9.0). Unfortunately, time constraints and the limiting quantity of protein prevented us from trying higher pH values to see if the primase activity is inhibited by more alkaline conditions. Moreover, the other parameters were measured at pH 7.5, which is apparently suboptimal for activity. Notwithstanding this, the activity is clearly present, dose dependent and also dependent on Mg^{2+} concentration and pH.

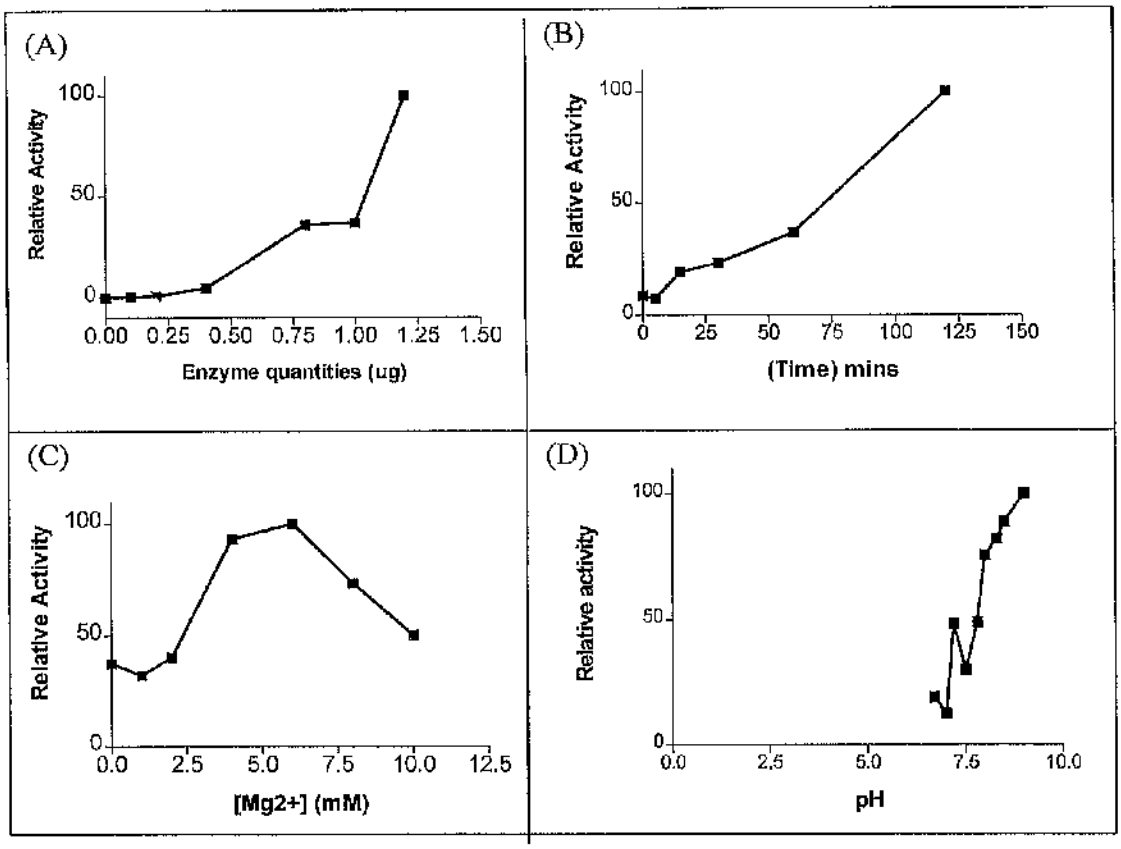

Figure 5.6 Characterisation of the DNA primase activity of PfPREXpriheli and the effects of different conditions on its activity. The activity is expressed as relative activity with respect to different conditions. The experiments were carried out in triplicate (n=9) and the average was taken to draw the graphs using Prism software (Graphpad). The experiment was carried to checked for DNA primase activity based on different conditions: - (A) increasing quantities (µg) of PfPREXpriheli, (B) time course experiment, (C) effect of Mg^{2+} ions on DNA primase activity and (D) pH profile of PfPREXpriheli.

5.2.3.2. DNA helicase activity

Using the SPA helicase assay (Amersham), we were able to determine the presence of unwinding activity in the recombinant PfPREXpriheli. Control experiments were carried out. The purified PfPREXpol recombinant protein was used as a negative control to check for any contaminating *E. coli* proteins and to confirm that any presence of unwinding activity was due to the the recombinant PfPREXpriheli. In addition, *E. coli* DnaB helicase, a gift from E Biswas (University of Medicine & Dentistry of New Jersey) was used as a positive control. Very little unwinding activity was observed in either the positive control or PfPREXpriheli. Therefore, a second positive control was

obtained to check if the problem was with the kit or our enzymes. The new positive control was PcrA (a DNA helicase from *Bacillus stearothermophilus*) (Cambio Science). Typical radioactivity counts obtained from the DNA helicase assays were as such :- the negative controls average cpm were 312.9, PcrA positive controls average cpm were 2801.14 and PfPREXheli samples cpm range from 459.3 to 1081.3.

First, different amounts of the recombinant enzymes were added to the assays which yielded an increase in unwinding activity (Figure 5.7a). This was followed by a time course experiment where we saw an initial time lag in the rate of unwinding activity. The rate of unwinding activity increased after one hour of incubation at 33°C and thereafter (Figure 5.7b). Other conditions that affected the unwinding activity of PfPREXpriheli were investigated too. The Mg^{2+} concentration that was optimum for its unwinding acitivity was found to be between 2.0 to 3.0 mM (Figure 5.8a) while the optimal temperature is at 37°C (Figure 5.8b). Finally, the pH at which the enzyme activity is optimal at pH 6.8 (Figure 5.8c).

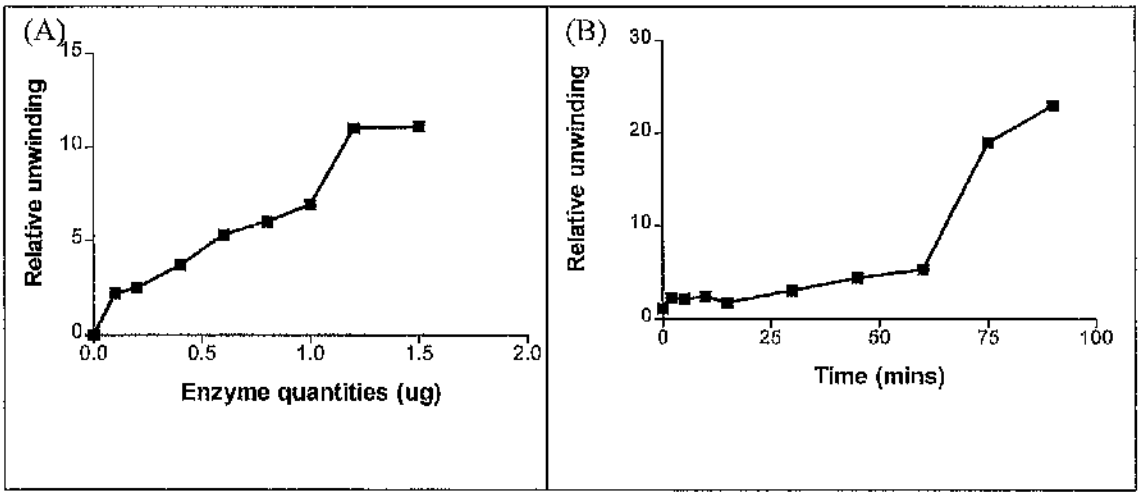

Figure 5.7. Characterisation of DNA helicase activity of PfPREXpriheli and the effects of enzyme quantities on its activity and its time course. The activity is expressed as relative unwinding. The experiments were carried out in triplicate over three individual experiments (n=6) and the average was taken to draw the graphs using Prism software (Graphpad). The experiment was carried:- (A) Increased quantities of PfPREXpriheli, (B) Time course experiment.

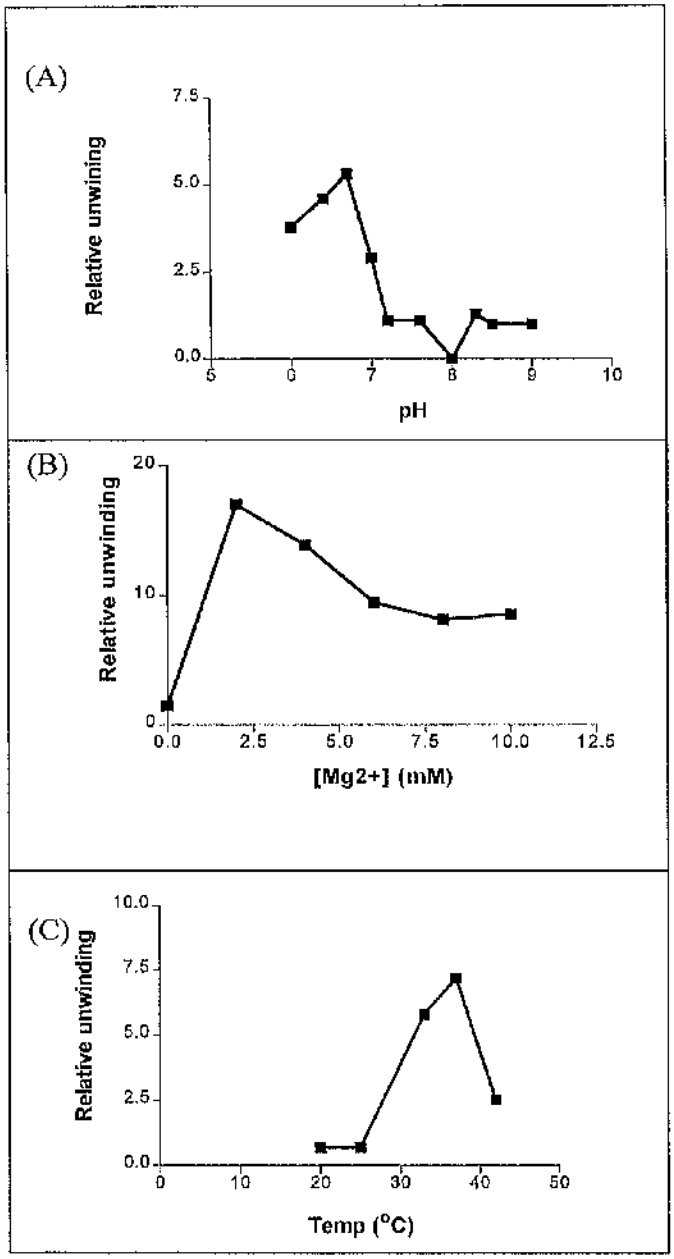

Figure 5.8. Characterisation of DNA helicase activity of PfPREXpriheli and the effects of different conditions on its activity. The activity is expressed as relative unwinding with respect to different conditions. The experiments were carried out in triplicate over three individual experiments (n=6) and the average was taken to draw the graphs using Prism software (Graphpad). The following conditions were tested against the activity of PfPREXpriheli: - (A) effect of Mg^{2+} ions on DNA helicase activity, (B) temperature profile of PfPREXpriheli and (C) the pH profile of PfPREXpriheli.

5.2.3.2.1. Nucleotide Hydrolysis Assay

A nucleotide hydrolysis assay was carried out to analyse the NTPase activity of the enzyme (Section 2.8.5). All helicases are NTPases as they require the hydrolysis of NTPs to energise the unwinding of DNA. Whether the helicase displays a preference for the use of a particular NTP was analysed, as it has been previously shown that many helicases have preferences for the NTP that they hydrolyse. For example, T7 DNA helicase prefers TTP and can utilise all NTPs except CTP while T4 DNA helicase can use all NTPs and dNTPs (Matson & Kaiser-Roger, 1990). The results obtained indicated seem to suggest that PfPREXpriheli has no preference of nucleotide used for hydrolysis (Figure 5.9). However, an important negative control with another recombinant protein to check for the presence of a contaminanting NTPase was not carried out during the course of the experiment. Therefore, a full interpretation of the data could not be carried out.

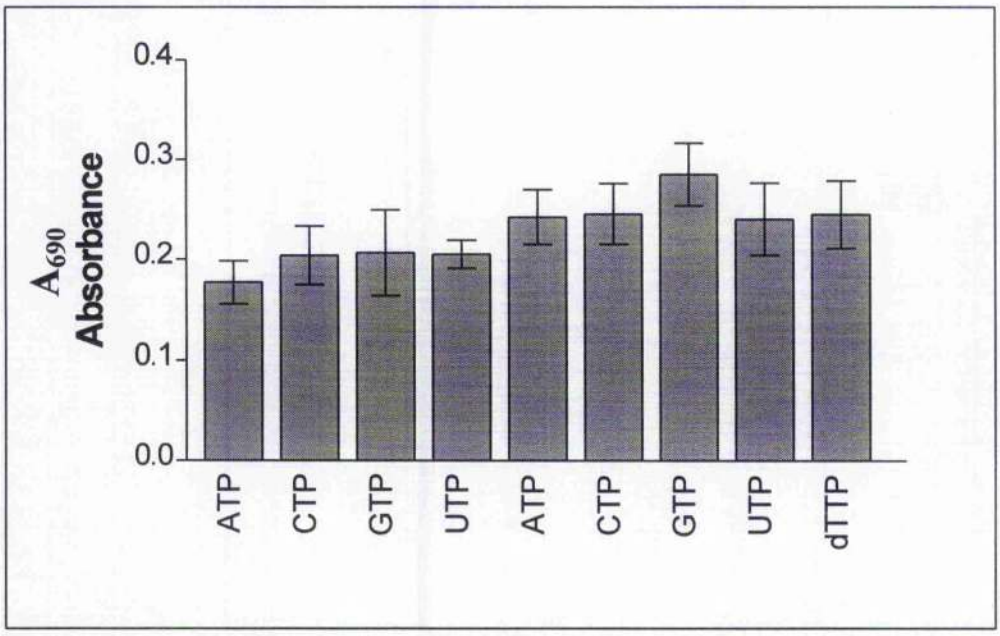

Figure 5.9. Nucleotide hydrolysis assay of PfPREXpriheli. Different NTPs and dNTPS were used as the substrate to check for NTP preference of PfPREXpriheli. The experiment was carried out in triplicate and the averages ± standard errors of four individual experiments (n=12) were used to draw the graph using Prism (Graphpad) software. The change in absorbance was measured as an indication of the release of the phosphate by the absorption of a 'molybdate blue' complex. The more phosphate is released the more complex is formed which results in the increase in absorbance at A_{690}.

5.2.4. Expression of PfPREXpriheli in *P. falciparum*

To determine whether *PfPREXpriheli* in *P. falciparum* is transcribed, RT-PCR was performed. Total RNA from an asynchronous culture of *P. falciparum* was obtained and RT-PCR primers designed in the region of PfPREXpriheli were used (Figure 5.2). Two sets of primers were used. One set (RTHeliF2 and RTHeliR2) of primers was used to check if the DNA helicase domain was transcribed and the other set (RTHingeF1 and RTHingeR1) was used to check for the hinge domain. The results of the RT-PCR (Figure 5.10a) showed bands of the predicted sizes of 453 bp and 420 bp respectively. Thus, we can conclude that both the helicase and hinge domains are transcribed. In addition, we had controls with no reverse transcriptase added to confirm that we have no genomic DNA contamination in the RNA samples.

However, these results are unable to tell us if the whole *PfPREX* is transcribed in a single transcript. Therefore, different combinations of RT-PCR primers were used to investigate this, where overlapping amplicons would suggest that *PfPREX* is transcribed as a single transcript. RTHeliF1 (within the primase region) was used in combination with RTHingeR1 which covers the whole of the DNA primase and helicase domain and into the hinge. Another set of primers used was RTHeliF2 and RTPolR1. This set of primers covers the region that overlaps the hinge region of the previous primer set and into the polymerase region. The results of the RT-PCR (Figure 5.10b) showed bands of the predicted sizes of 3.9 kb and 3.2 kb. The two bands had a region of 360 bp that overlapped (hinge domain). This suggests that *PfPREX* is transcribed as a single transcript. However, these results do not indicate the size of the

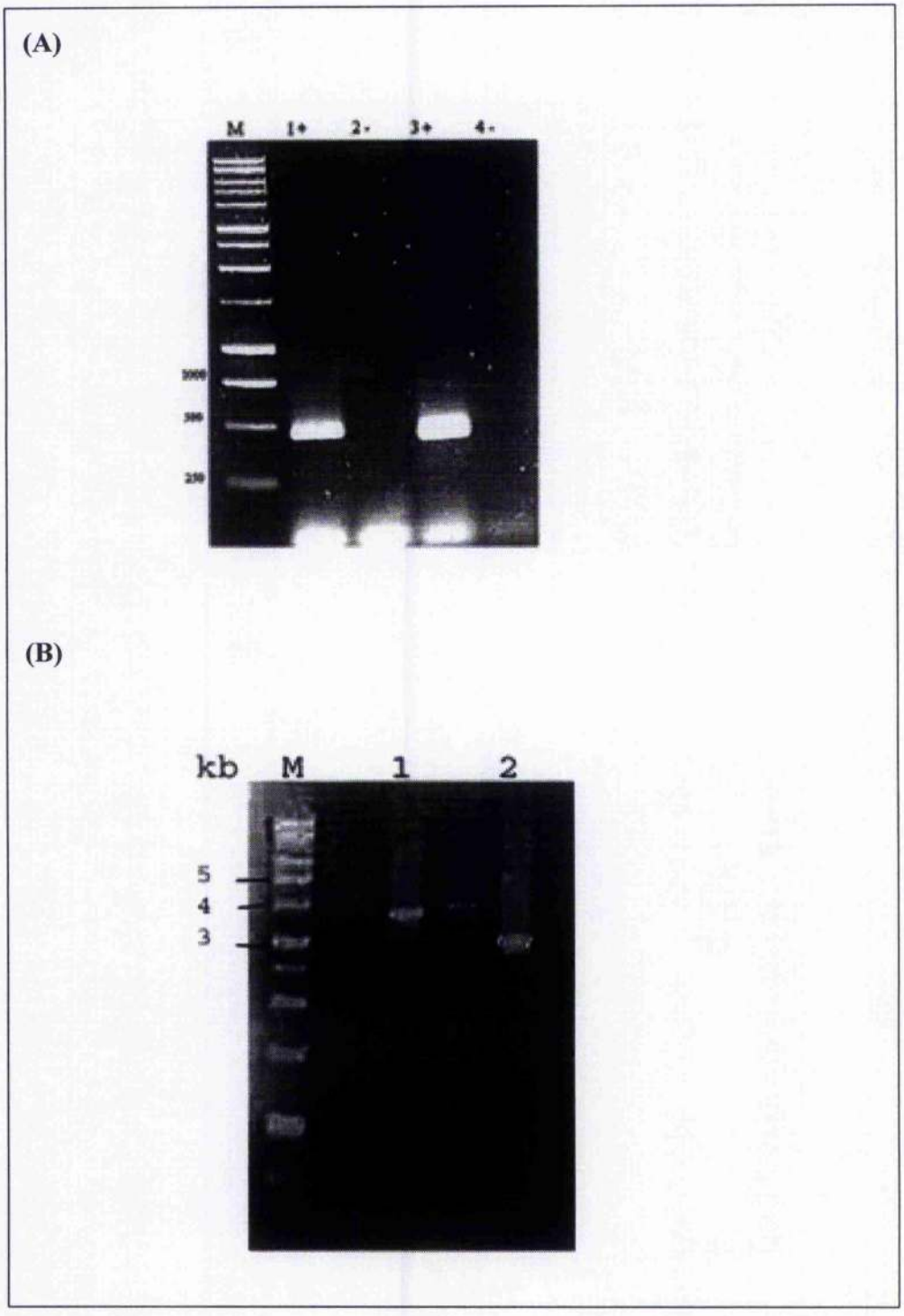

Figure 5.10. RT-PCR amplification of the *PfPREX* transcript from *P. falciparum* 3D7 total RNA. PCR was carried out for 40 cycles; + and – indicate reactions with and without reverse transcriptase, respectively as a control to check for genomic DNA contamination. PCR amplification using (A) primers specific for the DNA helicase region (Lane 1, 2), for the hinge region (Lane 3, 4). (B) primers specific for the region between primase and hinge region (Lane 1) and between the hinge and polymerase region (Lane 2). PCR products encompassing the primase and hinge and the polymerase and hinge overlap, indicating that the *PfPREX* gene is transcribed as a whole fragment.

PfPREX transcript and multiple attempts to get results from Northern Blots were unsuccessful indicating that the stable transcript is not abundant and is below a level detectable by Northern blot analysis in asexual stages of the life-cycle. Data from elsewhere indicates that in *P. chabaudi PfPREX* is transcribed as a 7 Kb mRNA in asexual bloodstream form stages (C. Janssen, personal communication).

Western blots were also performed to yield more information about whether the *PfPREXpriheli* is translated in *P. falciparum*. Antisera were made against the DNA helicase, primase and hinge domains separately as fusion proteins (Section 2.7.3). The antisera were used to probe blots of parasitised red blood cell lysates and non-parasitised samples. All Western blots were performed at least three times to check for reproducibility of results. Since PfPREX represents a single ORF encoding a predicted protein of approximately 2016 amino acids, the estimated size of the PfPREX protein is 235.8 kDa. If *PfPREX* is translated as a whole polypeptide, a single band of approximately 235.8 kDa would be expected on the blot using any of the antisera. Instead, the anti-PfPREXpol antisera, indicated a post-translational cleavage of PfPREX (Section 4.2.4). The anti-PfPREXhinge revealed no bands on the Western blots, while the anti-PfPREXpri antisera bound to a band of approximately 88 kDa, slightly smaller than the band obtained with anti-PfPREXpol. Several bands were obtained on the blot probed with anti-PfPREXpri antisera. There were two other high molecular weight bands observed in both the 3D7 and red blood cell lysates. The bands could be a cross-reaction between the polyclonal antisera and a host polypeptide found within the red blood cell lysates. Using the anti-PfPREXheli antisera to probe the Western blot, several bands were observed on the blot. There was a low molecular weight band on the red blood cell lysate which was not present in the 3D7 lysate. This could be a cross-

reaction with a protein found in just red blood cells but not in infected red blood cells. On the 3D7 lane, multiple bands were observed. There were an approximately 150 kDa band, followed by a 80 kDa and a 50 kDa band.

The result obtained from the anti-PfPREXpri together with the result obtained from the anti-PfPREXpol, both suggest that PfPREX may be post-translationally cleaved to give separate DNA polymerase domain from the DNA primase/helicase domain. The size of the band (88 kDa) obtained with the anti-PfPREXpri antisera is consistent with the primase/helicase domain being together (as seen for the bacteriophage T7). However, the size detected with the anti-PfPREXheli antisera disagrees with that. Both antisera should identify the same band if the DNA primase/helicase are together. The different size bands obtained with the anti-PfPREXheli suggest that the some of the DNA primase/helicase are also cleaved into several different fragment sizes. Further experiments, possibly with additional antisera, would be required to resolve the ultimate processing pathway of PfPREX.

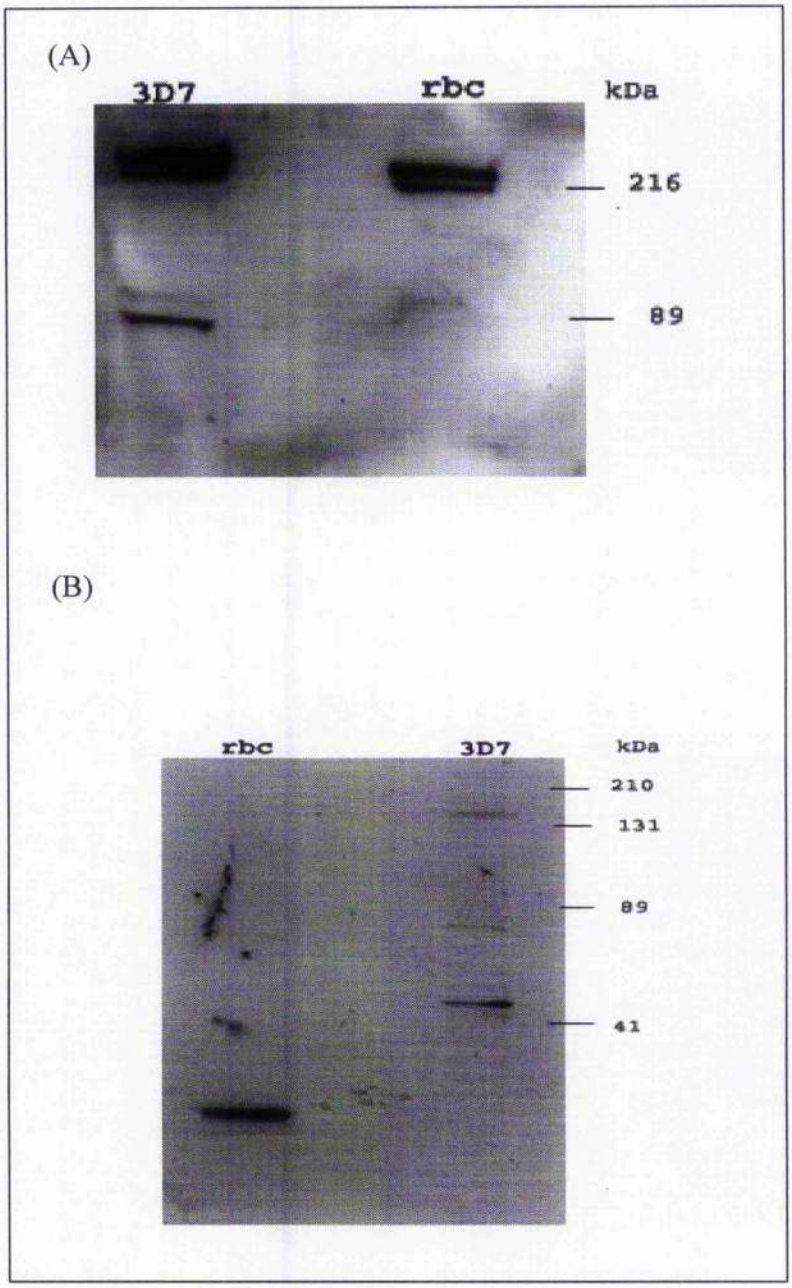

Figure 5.11. Western Blot of parasitised rbc (3D7) and non-parasitised rbc lysates probed with anti-PfPREXpri and anti-PfPREXheli. (A) Western blot probed with anti-PfPREXpri (1:1000) and (B) Western blot probed with anti-PfPREXheli (1:1000).

5.2.5. Subcellular localisation of PfPREXpriheli gene product

With reference to the presence of the plastid-targeting sequence in the N-terminus of PfPREX, experiments to identify the subcellular localisation of PfPREXpriheli domain were performed. The anti-PfPREXpri, anti-PfPREXheli and anti-PfPREXhinge were used in indirect immunofluorescence microscopy experiments. Since with the previous studies using anti-PfPREXpol with *in situ* hybridisation using plastid DNA specific probes did not give satisfactory results, that approach was not used here. We also used the Mitotracker stain (Molecular Probes) to stain the mitochondria in *P. falciparum* and DAPI to counterstain the nucleus.

To optimise the IDF protocol, various dilutions of the anti-sera were used, ranging from 1:50 to 1:1000. When higher dilutions are used, no fluorescence could be observed with any of the three anti-sera and when lower dilutions (below 1:100) were used, ubiquitous fluorescence was observed. Finally, the optimum dilution of the anti-sera to be used for anti-PfPREXheli, anti-PfPREXpri and anti-PfPREXhinge was determined to be 1:100 alongside 1:400 dilution of the secondary antibody (anti-rabbit FITC, Diagnostics Scotland) (Figure 5.13). The immunofluorescence carried out with the anti-PfPREXhinge antisera did not result in any fluorescence detected in the infected red blood cells observed under the microscope. For the anti-PfPREXheli and anti-PfPREXpri results, there appears to be no overlay between the mitotracker and the FITC. This suggested that the PfPREXpriheli did not localise to the mitochondrion in *P. falciparum*. However, it was not clear whether either anti-sera localised to the plastid. The DAPI stains both nuclear and plastid DNA, but it is difficult to see the plastid under the highest available magnification.

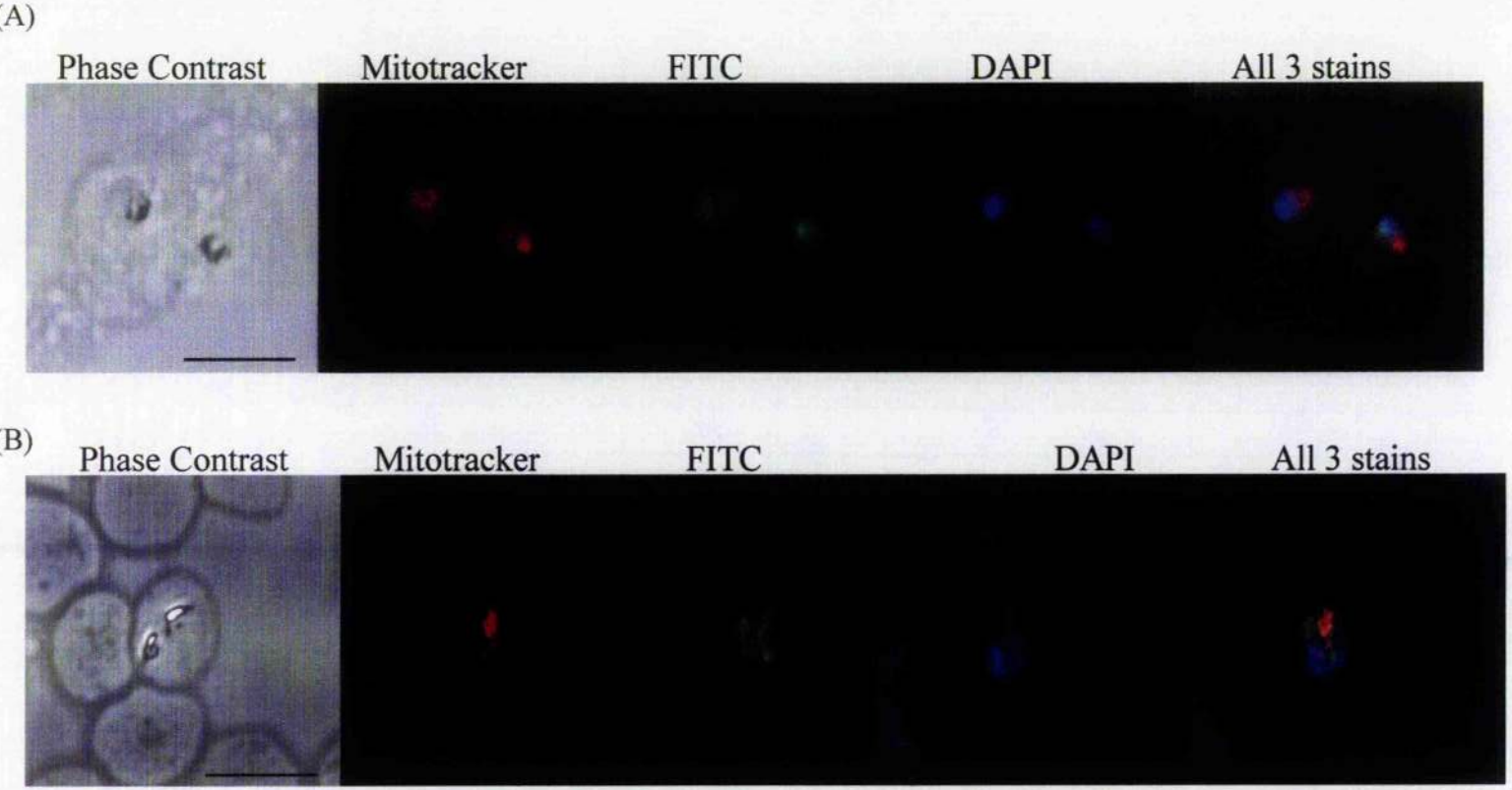

Figure 5.12. Subcellular localisation of PfPREXpol using immunofluorescence technique. The first diagram is a phase contrast microscopy picture of a red blood cell infected with a ring-form parasite, and stained with different fluorescence markers outlined in the text. The second picture shows the same cell viewed under fluorescence using the Texas red filter with an excitation and emission peaks of 560 and 630 nm respectively. The third picture shows the same cell viewed under fluorescence using the FITC filter with an excitation and emission peaks of 484 and 510 nm respectively, followed by the DAPI filter with an excitation and emission peaks of 360 and 460 nm respectively and the last set of image were all previous images merged together. The mitotracker stain shows the locality of the mitochondrion, FITC shows where the anti-PfPREXpol antisera have bound and DAPI stains specifically nuclear and apicoplast DNA. (A) shows the immunofluorescence results obtained with the anti-PfPREXpri antisera and (B) shows the immunofluorescence results with the anti-PfPREXheli antisera. Scale bars, 5 μm.

5.3. Discussion

The experimental findings and sequence analysis suggested that PfPREX consists of a DNA primase and DNA helicase functional domains. This chapter provides a functional confirmation of these activities. In addition, the reaction conditions may not be optimal for the helicase activity of PfPREX. Therefore, the DNA helicase was unwinding at suboptimal conditions, which may have been why the time lag occurred. However, one positive control, *E. coli* DnaB (a gift from Dr E Biswas) showed low unwinding activity (<30% unwinding activity). In comparison, the same quantity of the PcrA achieved unwinding activity of up to 60% over the same time course. In addition, Amersham also claimed that using *E. coli* DNA helicase I, the highest unwinding activity achieved in their labs was 75%. Therefore, the low rate of unwinding activity observed with DnaB and PfPREXpriheli was not due to a fault with the kit. Both PcrA and *E. coli* DNA helicase I, unlike DnaB, are not hexameric DNA helicases. Perhaps, the reaction conditions of the kit are not suited for hexameric DNA helicases like DnaB and possibly for PfPREXpriheli, which is most similar to DnaB helicase family and thus likely to take on a hexameric form to function. Currently we could not come up with any function reasons that could be put forward forth to explain why the assay did not work as well. Therefore, it is postuated that the conditions required for these helicases to form the correct structure for DNA unwinding were not provided, which may explain the lower than expected unwinding activity.

The NTP requirements of the DNA helicase is also investigated. It appears that PfPREXheli does not have major preference over the type of NTP it utilises for hydrolysis. This trait can also be observed with the T4 DNA helicase and T7 DNA helicase (Matson & Kaiser-Roger, 1996).

The RT-PCR results suggest that PfPREX is transcribed as a single transcript. Unfortunately, we were not able to obtain any Northern blot data to give the size of the PfPREX transcript. However, in *P. chabaudi*, a 7 kb transcript of the PcPREX homologue has been detected (C Janssen, personal communication). Towards the end of this study, Le Roch *et al* (2003) carried out a detailed transcriptome analysis of *Plasmodium falciparum*. In this study, it has shown that *PfPREX*'s transcription is upregulated (data available in Appendix B) when the ring stages are developing into trophozoites and continues into schizogony , which corresponds to the initiation of DNA synthesis as observed (Inselburg & Banyal, 1984).

The Western blot results obtained with the anti-PfPREXheli and anti-PfPREXpri anti-sera supported the conclusions of the result obtained with anti-PfPREXpol, that PfPREX is post-translationally cleaved. It was postulated that the PfPREX would be cleaved into two fragments, to give one that contains the DNA primase and DNA helicase domains and the other to contain the DNA polymerase domain. The result obtained with anti-PfPREXpol suggested that the DNA polymerase domain is on a separate fragment. If the DNA primase and helicase domains are together on a single fragment, the Western blot results obtained with both individual anti-sera would show similar size bands. However, this was not what was observed. The Western blot probed with anti-PfPREXpri anti-sera gave a band of the expected size of approximately 88 kDa, but the blot probed with PfPREXheli anti-sera gave a multitude of different bands and nothing at the 88 kDa mark. On the same blot, the anti-PfPREXheli appeared to be cross-reacting with a polypeptide present only in the uninfected red blood cell lysate. It could be that the fusion protein sent for antisera production is not pure and could be contaminated with some other proteins. In addition,

the anti-PfPREXheli antisera have not been checked against the recombinant PfPREXheli to ensure that it contains antibodies specific against the protein. Nonetheless, the other Western blot results do suggest that the post-translational cleavage of PfPREX does occur.

Finally, the subcellular localisation of PfPREXpriheli was carried out to help reveal the location of the protein *in vivo*. The immunofluorescence results obtained revealed similar conclusion as with the anti-PfPREXpol results. Both sets of results agree that PfPREX does not localise to the mitochondrion but the results were not able to tell us if PfPREX localised to the apicoplast. Due to the fact that the apicoplast is in close association with the nucleus within *Plasmodium* (Bannister *et al*, 2000), when DAPI (which stains both nuclear DNA and apicoplast DNA) is used to stain the cells, it is difficult to tell the apicoplast DNA and nuclear DNA apart. However, a similar staining pattern was observed with FITC fluorescence, where both anti-PfPREXpri and anti-PfPREXheli gave results that indicated the compartmentalisation of the products that these antisera were bound to.

Chapter VI

The Evolution of *PfPREX*

6.1. Introduction

The discovery of a gene sequence, *PfPREX* that encodes three functional domains, where each may have a role to play in the replication/repair of the plastid DNA in *P. falciparum* raises a number of questions regarding its origins and evolution. To help answer these questions, phylogenetic analysis on each of the individual domains was carried out. This analysis has shed light on the evolutionary pathway that led to the derivation of PfPREX in *P. falciparum*.

P. falciparum belongs to the phylum of parasites called the Apicomplexa. All members of the group are characterised by a complicated apical complex found at the anterior of the cell. In recent years, they have been found to harbour a relict plastid – termed the apicoplast. According to Gray (1992), all plastids ultimately derive from cyanobacterial-like, prokaryotic organisms that were retained by a phagotrophic eukaryote. They established an 'endosymbiotic' relationship whereby the 'engulfed' cell is retained in a mutually beneficial relationship with the host. In the apicomplexa, the apicoplast too was derived from such an event, but instead of the eukaryote engulfing a cyanobacterial prokaryote, it acquired a eukaryote that already harboured a plastid. This is referred to as a secondary endosymbiotic event (Delwiche & Palmer, 1997).

The fact that many plastid genes and biochemical pathways are of prokaryotic origin, agrees with the serial endosymbiosis theory of the origin of the plastid. For example, *P. falciparum* contains a type II pathway for fatty acid biosynthesis, typical of bacterial-like systems and also utilised by plants. This indicates that this pathway was inherited with the plastid in both *P. falciparum* and plants

(Harwood, 1996). Given the plastid localisation of PfPREX, it was of interest to determine whether the DNA polymerase, DNA helicase and DNA primase were derived from a prokaryotic source, particularly a cyanobacterium. Therefore, a detailed phylogenetic analysis was performed to test this hypothesis. Since PfPREX contains three functional domains, the domains were analysed separately.

6.2. Phylogenetic analysis of DNA polymerases

6.2.1. DNA polymerase families

In recent years, with the boom in genome sequencing, many gene sequences have been gathered and a large number of those encode DNA polymerases. These DNA polymerases have been studied closely and phylogenetic analyses have been carried out. They have been classified into various families and subgroups. The most cited work was carried out by Braithwaite and Ito (1993) where they have placed DNA polymerases into four distinct families (A, B, C and X). Recently, a new class (class Y) has been added (Ohmori *et al*, 2001). Braithwaite and Itos' (1993) phylogeny provided the framework for the comparative analysis reported here. Filée *et al* (2001) have attempted to analyse the evolution of DNA polymerase families and have suggested that there were multiple gene exchanges between cellular and viral proteins. These will be discussed in later sections within the chapter.

BLAST searches reported earlier (Chapter 3) indicated that the DNA polymerase domain of PfPREX (PfPREXpol) has highest similarity to the *Aquifex aeolicus* DNA polymerase (Genbank accession no: - AAC07735.1) (more recently, *Aquifex pyrophilus* DNA polymerase [Genbank accession no: AAO15360.1]) and other prokaryotic type bacterial DNA polymerase I sequences, all of which belong to the family A DNA polymerases. This preliminary data suggests that PfPREXpol groups

within the family A group of DNA polymerases to which these bacterial DNA polymerase I sequences belong (Braithwaite & Ito, 1993). Therefore, the phylogenetic analysis was carried out with DNA polymerase I sequences from members belonging to this family.

6.2.2. Alignment of DNA polymerases

The "type"-member representative of DNA polymerase family A is *E. coli* DNA polymerase I which consists of a 5'-3' exonuclease domain, a 3'-5' exonuclease domain and a DNA polymerase domain. PfPREXpol does not have a typical 5'-3' exonuclease domain. In order to produce alignments of optimal phylogenetic content, DNA polymerase I sequences that possess 5'-3' exonuclease domains used in the alignments were culled to remove their 5'-3' exonuclease sequences.

Several DNA polymerase I sequences (some are selected based on their recognition by PfPREXpol in BLAST searches) from various organisms were used for the alignment. They included bacterial homologues, DNA polymerase I sequences from bacteriophages and mitochondrial DNA polymerases gamma. A novel eukaryotic nuclear DNA polymerase/helicase (Harris *et al*, 1996), the N-terminal part of which is a prokaryotic DNA polymerase I-like sequence, was also used. This protein, Mus308 (NCBI accession number:- NP_851315) was first isolated and characterised in *Drosophila melanogaster* and is also called DNA polymerase eta (Harris *et al*, 1996). *Mus308* orthologues are found in other eukaryotes including *Homo sapiens* to *Mus musculus*. Filée suggested that the eukaryotic Mus308 could be of mitochondrial origin. Therefore, it was of interest to include this sequence in our phylogenetic analysis.

All of the sequences used in the alignment are listed and tabulated in Table 6.1. The table shows the full names of the organisms from which the DNA polymerase sequences were taken and their database accession numbers. The alignment comprises 24 sequences alongside the PfPREXpol sequence.

The sequences were aligned first using the DIALIGN version 2 programme (Morgenstern *et al*, 1996) using the default settings (Section 2.11). DIALIGN relies on the comparison of whole segments of sequence rather than single residues. Pairwise, as well as multiple, alignments are constructed from gap-free pairs of equal length segments, which are called diagonals. Thus this method is well suited to detect local similarities on otherwise unrelated sequences. This preliminary alignment was carried out to enable us to determine which part of the sequences should be culled in order to retain the most phylogenetically informative sequence. Essentially the 5'-3' exonuclease domains of some of the sequences were removed as indicated in Table 6.1. The culled alignment was realigned using ClustalX1.81 (Thompson *et* al, 1994) using the settings shown in Table 6.2. Clustal X is a global alignment program for nucleotide or amino acid sequences. It uses a progressive alignment algorithm to align sequences. In other words, it aligns more similar sequences before the distant sequences. So the pairwise and multiple parameters were set as shown. The general rule of thumb for choosing the parameters are:- the higher the gap opening (GO), the less frequent the gaps and the higher the gap extension (GE), the shorter are the gaps. Therefore, the settings were chosen to optimise our particular alignment. The full alignment is shown in Appendix D.

Phyla	Enzyme	Organism	Shortened Name	Length of sequence (a.a)	Genbank/ embl accession no.	Reference
Bacteria	polI	*Mycobacterium tuberculosis*	Myctu	904	AAB46393.1	Huberts & Mizrahi , 1995
	polI	*Thermogata maritima*	Thermogata	893	AAD36686.1+	Nelson *et al*, 1999
	polI	*Aquifex aeolicus*	A.aeolicus	574	AAC07735.1	Deckert *et al*, 1998
	polI	*Aquifex pyrophilus*	A. pyrophilus	574	AAO15360.1	Direct submission
	polI	*Escherichia coli*	E.coli	928	CAA23607.1+	Joyce *et al*, 1982
	polI	*Salmonella typhimurium*	S.typhimurium	928	AAG43170.1+	Direct submission
	polI	*Thermus aquaticus*	T.aquaticus	832	AAA27507.1+	Lawyer *et al*, 1989
	polI	*Synechocystis* sp	Synechocystis	986	BAA10748.1+	Kaneko *et al*, 1995
	polI	*Rhizobium leguminosarum*	Rhizobium	1016	AAD45559.1+	Huang *et al*, 1999
Virus	polI	SP6 phage	SP6	849	AAP48753.1	Direct submission
	polI	T7 phage	T7	704	CAA24412.1	Dunn & Studier, 1983
	polI	T3 phage	T3	704	CAC86283.1	Pajunen *et al*, 2002
	polI	phiYe03-12 phage	phiYe03-12	704	CAB63614.1	Pajunen *et al*, 2001
	polI	Cyanophage P60	Cyanophage	587	AAL73268.1	Chen & Lu, 2002
Yeast	polγ	*Saccharomyces cerevisiae*	Mip1p	1254	CAA89977.1	Direct submission
Plants	polI	*Arabidopsis thaliana*	A.thaliana	1049	AAM13892.1	Direct submission
	polI	*Oryza sativagi*	Rice	976	BAB40805.2	Kimura *et al*, 2002
Fungi	polI	*Dictyostelium discoideum*	Dictyostelium	1369	AAO12053.1+	Direct submission
Insect	polγ	*Drosophila melanogaster*	Fly	1145	AAC47290.1	Direct submission
Mammal	polγ	*Mus musculus*	Mouse	1238	AAA98977.1	Direct submission
	polγ	*Homo sapiens*	Human	1239	AAC50712.1	Direct submission
	polN	*Homo sapiens*	polN	900	AAN52116.1	Direct submission
	polη	*Homo sapiens*	eta	1154	AAD05272.1	Direct submission
	polN	*Mus musculus*	MmpolN	866	AAN39837.2	Direct submission

Table 6.1. The DNA polymerase sequences used for multiple alignment. The phyla, name of organism, number of amino acids, type of polymerase and the accession number of each DNA polymerase sequence is shown. The shortened name of each sequence used in the alignment is also shown. The + signs indicate those sequences whose 5'-3' exonuclease domains are removed from the alignment.

Step	Sequences	Pairwise parameters	Multiple parameters	a.a matrix
1	All polymerases excluding 5'-3' exonuclease domains	GO 10 GE 0.1	GO 10 GE 0.1	Gonnet
2	Step 1 sequences excluding 3'-5' exonuclease domains (motifs A-C). Large gaps are removed.	GO 10 GE 0.1	GO 10 GE 0.1	Gonnet
	DNA primase sequences	GO 10 GE 0.1	GO 10 GE 0.1	Gonnet
	DNA helicase sequences	GO 10 GE 0.1	GO 10 GE 0.1	PAM250

Table 6.2. Various parameters used in ClustalX 1.81 for the alignment of the DNA polymerase, DNA helicase and DNA primase sequences. The sequences used, pairwise and multiple parameters are shown. GO – Gap opening penalty, GE – Gap extension penalty. The amino acid substitution matrix used is shown in the right most column.

The alignment revealed that the 3'-5' exonuclease domains of the DNA polymerases were relatively poorly conserved. Conservation was only observed within the three Exo motifs. Therefore, it was decided to use only the polymerase domains, which spans the three key polymerase motifs A- C (Section 1.4.3.1.3). The alignment was checked through by eye first before it was culled and realigned for a third time using ClustalX 1.81. Positions that could not be aligned unambiguously were excluded as they carried no phylogenetically useful information. Olsen (1988) also argued that these parts of the sequences should be excluded from phylogenetic analyses. All of the sequences retained the three key polymerase motifs. The alignment was checked through manually and adjusted as necessary to improve the alignment. This final alignment was then used for later phylogenetic analysis (Figure 6.1).

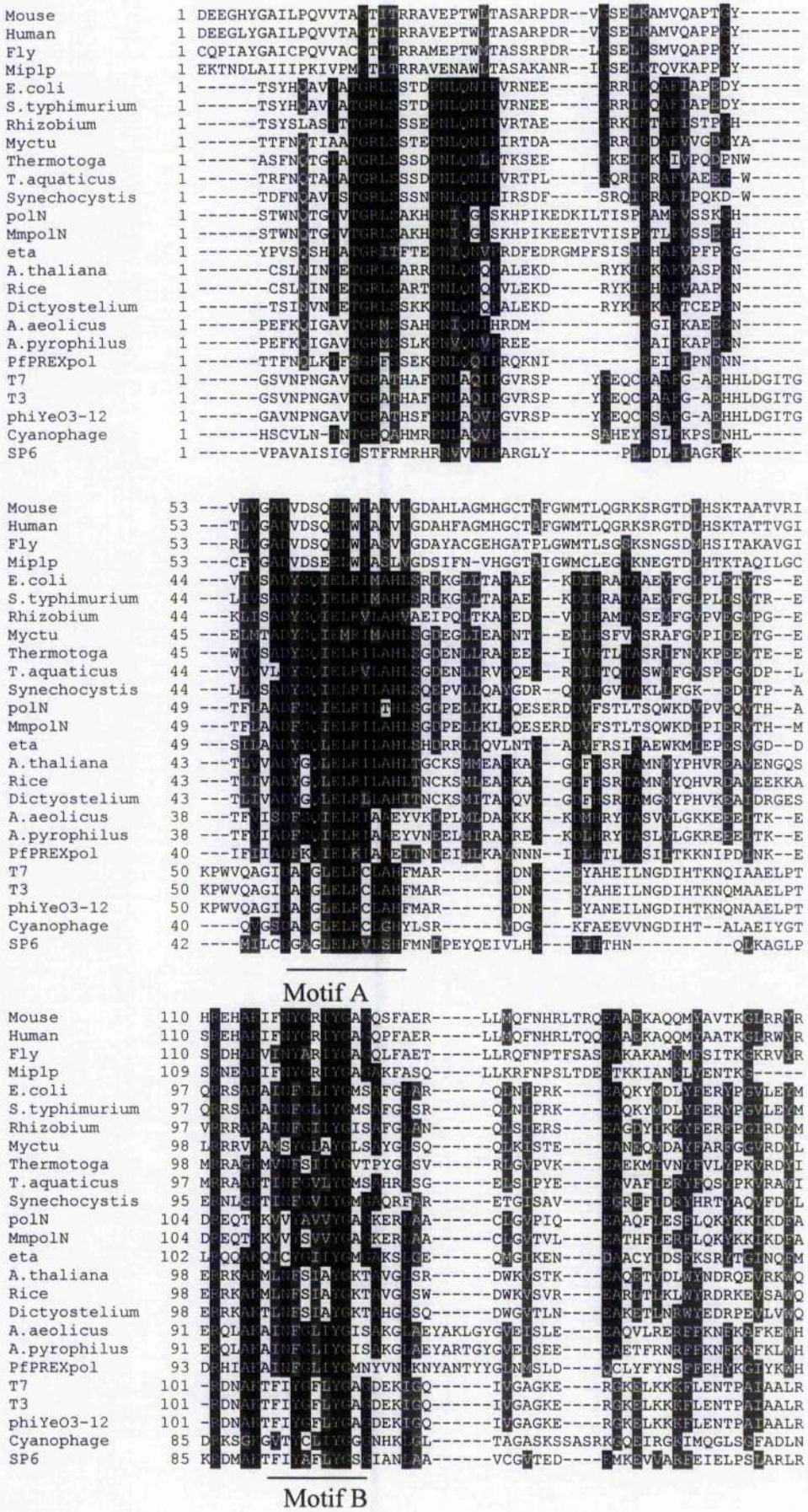
Motif A
Motif B

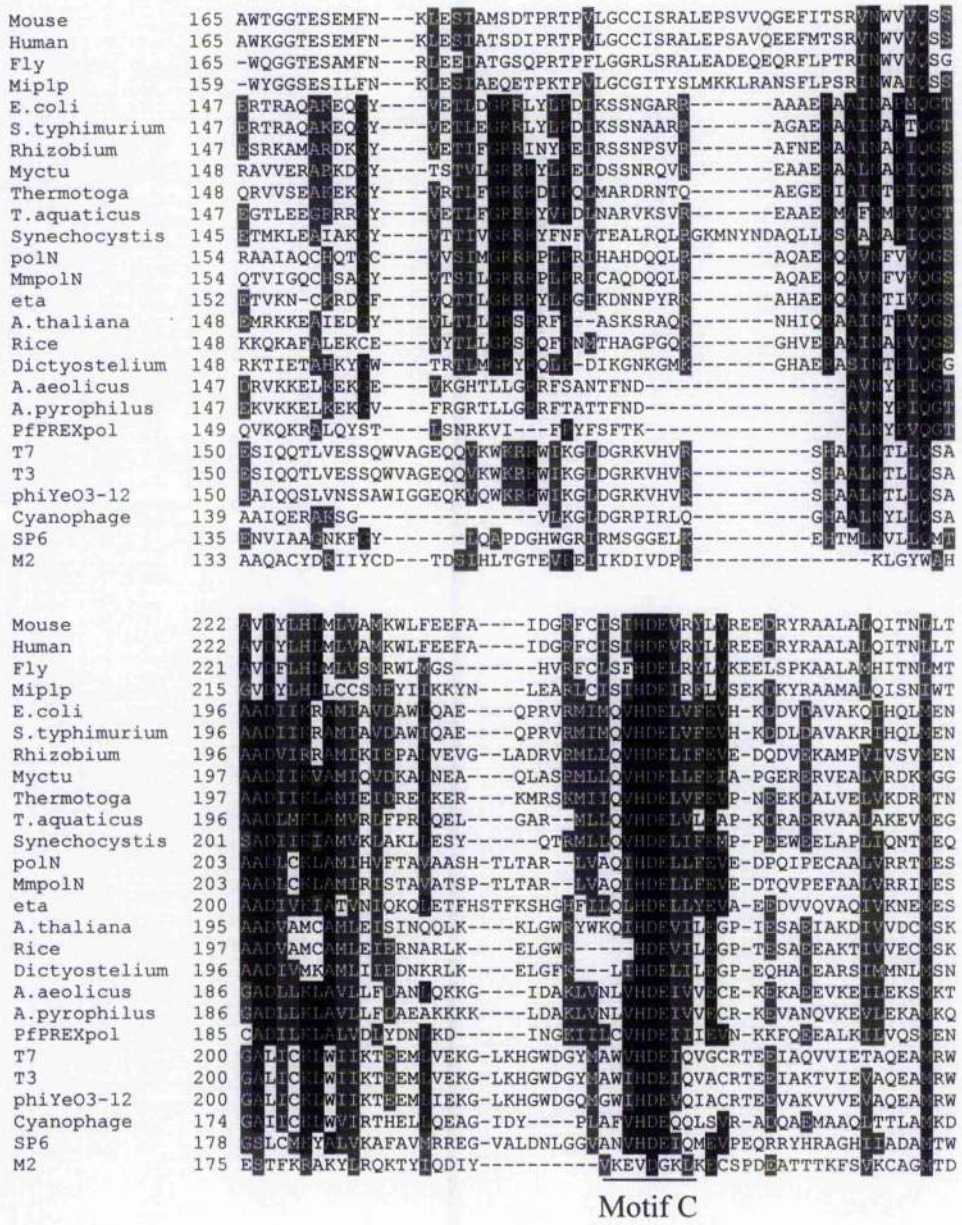

Figure 6.1. Alignment of deduced amino acid sequences of DNA polymerase domains of DNA polymerases from family A. Details of sequences used are shown in Table 6.1, alongside PfPREXpol. These sequences were aligned using ClustalX 1.81. Black shading indicates identical amino acids; grey shading indicates conserved amino acid substitutions. The numberings on the left hand side show the relative position of the amino acid in the respective sequences. Motifs A, B and C are shown with underlined text.

6.2.3. Generation of phylogenetic trees for the DNA polymerase domains

Phylogenetic trees for the family A DNA polymerases were generated using MEGA (Molecular Evolution Genetic Analysis) software version 2.1 (Kumar *et al*, 2001). The trees were created from the alignment (Figure 6.1) which comprised the three key motifs found in family A polymerases. Four different types of trees were generated with the alignment set. All trees generated were unrooted. Three trees were generated using distance methods: Unweighted Paired Group Method with Arithmetric Mean (UPGMA), Neighbour-Joining (NJ) and Minimum Evolution (ME) and one from a character-based method, Maximum Parsimony (MP). Distance methods convert aligned sequences into a pairwise distance matrix and then input that matrix into tree building while character-based methods use a specific criterion to build a tree. This criterion is then used to assign to each tree a score which is the function of the relationship between tree and data. The distance trees inferred from the amino acid sequences were computed on the basis of the Poisson correction in the MEGA programme. Poisson correction is calculated as the distance between two amino acids based on the assumption that the rate of amino acid substitution at each site follows a Poisson distribution.

The four different methods were chosen to determine the stability of the tree topologies. All four trees (Figure 6.2) showed six distinct clusters: - bacteria, plant, mammal, bacteriophage, mitochondria (γ) and *Aquifex*. The mitochondrial DNA polymerases (γ) form their own cluster and are not part of the family A cluster. However, this differs from the conclusion of Filée *et al* (2001) who noted in their trees that DNA polymerase γ was only distantly related to bacterial DNA polymerase I, (also

observed in our trees) but that it branched with the T7/T3 DNA polymerases. This was not observed with the trees obtained in our phylogenetic studies.

PfPREXpol clusters very tightly with the *Aquifex* species of DNA polymerase sequences and sits more closely to the bacterial cluster of DNA polymerases than to the eukaryote cluster. The bootstrap support for this particular branching is very strong, with values ranging from 86 to 100 for all four trees. Throughout the four trees, the topology whereby the PfPREXpol sits within the *Aquifex* cluster was maintained, which showed the stability of this branching. *Aquifex* is a thermophilic bacterium. The similarity between PfPREXpol and *Aquifex* is without precedent. Remarkably, in addition to the extraordinary similarity in sequence between the *P. falciparum* sequence and the *Aquifex* protein, the *Plasmodium* protein also encodes a thermophilic DNA polymerase with maximal activity as 75°C (Section 4.2.3.1). The optimum temperature for the activity of PfPREXpol was similar to that of the *Aquifex aeolicus* (Chang *et al*, 2001) at 75°C. These findings suggest that the origin of PfPREXpol might be from a thermophilic relative of *Aquifex* which was quite unexpected and indicative of a relatively recent horizontal gene transfer. It is also noteworthy that a DNA polymerase I analogue believed to be involved in the regulation of chloroplast DNA replication in plants (*Oryza sativagi*) is clearly more distantly related to PfPREXpol than are the *Aquifex* polymerases. This indicates that DNA polymerases involved in the apicoplast and plant chloroplast DNA replication have separate origins.

(a)

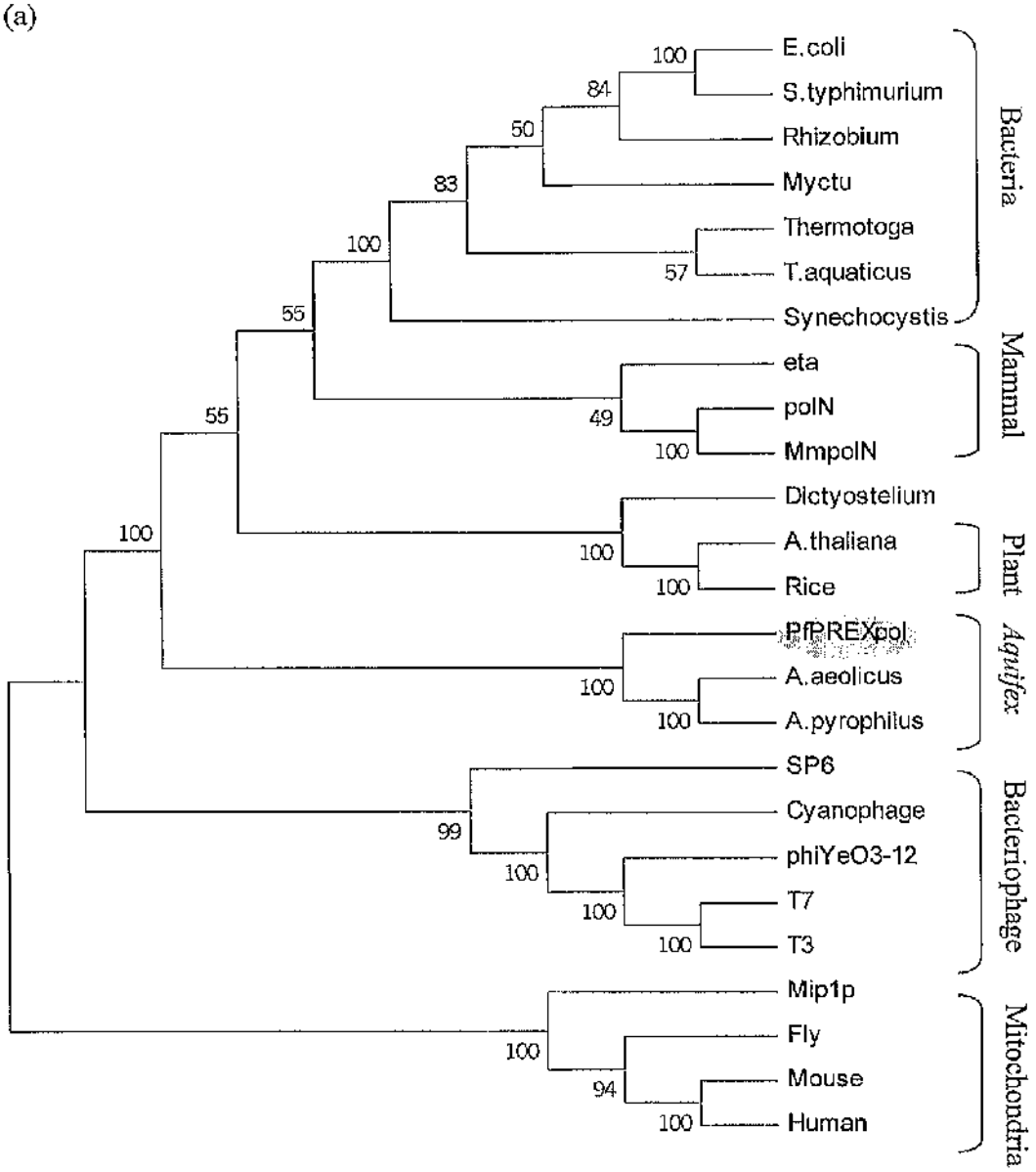
E.coli
S.typhimurium
Rhizobium
Myctu
Thermotoga
T.aquaticus
Synechocystis
eta
polN
MmpolN
Dictyostelium
A.thaliana
Rice
PfPREXpol
A.aeolicus
A.pyrophilus
SP6
Cyanophage
phiYeO3-12
T7
T3
Mip1p
Fly
Mouse
Human
100
84
50
83
100
57
55
55
49
100
100
100
100
100
100
99
100
100
100
100
94
100
Bacteria
Mammal
Plant
Aquifex
Bacteriophage
Mitochondria

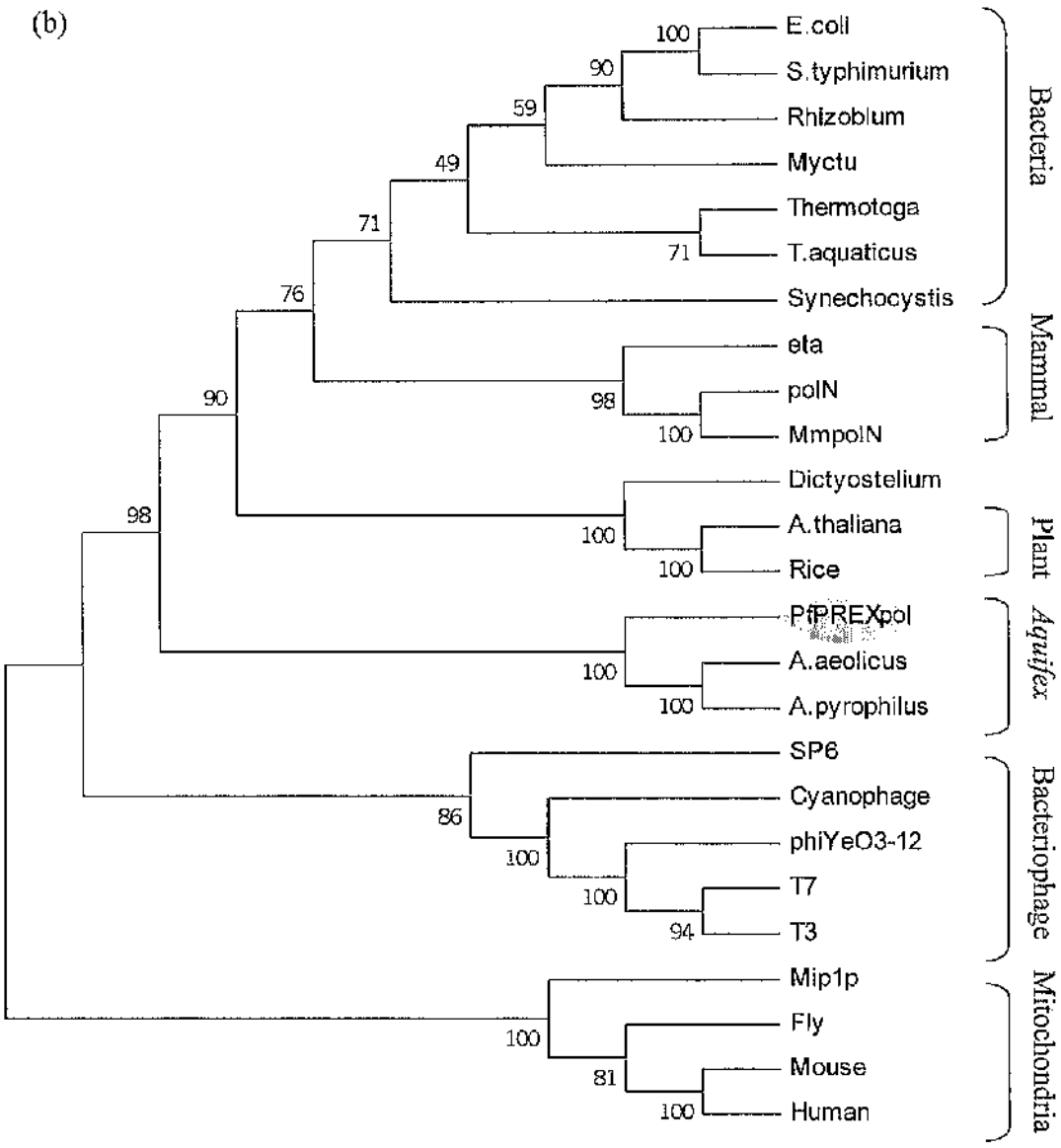
(b)
E.coli
S.typhimurium
Rhizoblum
Myctu
Thermotoga
T.aquaticus
Synechocystis
eta
polN
MmpolN
Dictyostelium
A.thaliana
Rice
PfPREXpol
A.aeolicus
A.pyrophilus
SP6
Cyanophage
phiYeO3-12
T7
T3
Mip1p
Fly
Mouse
Human
Bacteria
Mammal
Plant
Aquifex
Bacteriophage
Mitochondria
100
90
59
49
71
71
76
90
98
100
100
98
100
100
100
86
100
100
94
100
81
100

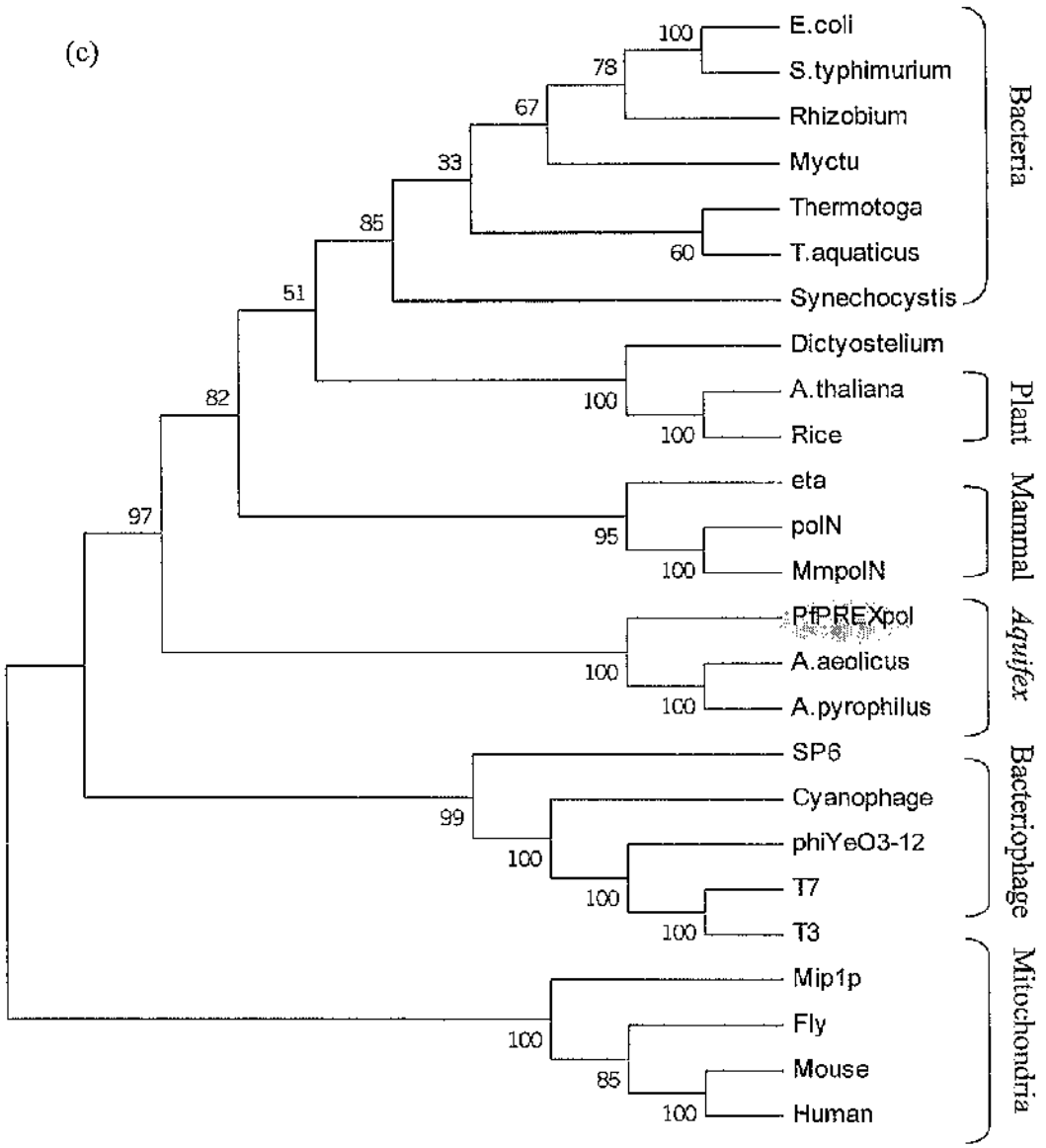
(c)
E.coli
S.typhimurium
Rhizobium
Myctu
Thermotoga
T.aquaticus
Synechocystis
Dictyostelium
A.thaliana
Rice
eta
polN
MmpolN
PfPREXpol
A.aeolicus
A.pyrophilus
SP6
Cyanophage
phiYeO3-12
T7
T3
Mip1p
Fly
Mouse
Human
Bacteria
Plant
Mammal
Aquifex
Bacteriophage
Mitochondria
100
78
67
33
85
60
51
82
100
100
97
95
100
100
100
99
100
100
100
100
85
100

(d)

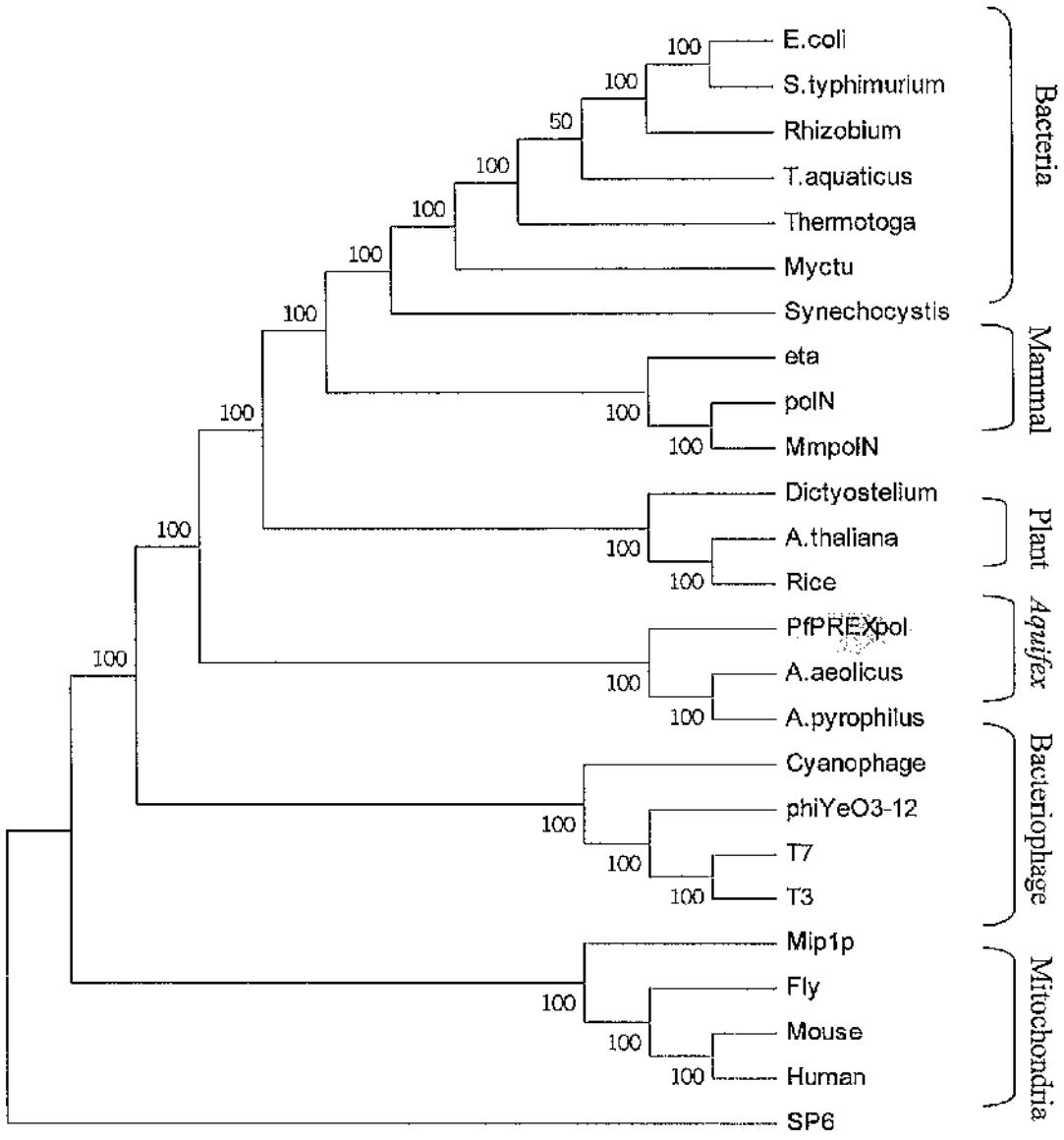

Figure 6.2. Phylogenetic trees generated by MEGA derived from the DNA polymerase alignment (Figure 6.1). The bootstrap values (100 resamplings) are indicated on the branches. Unrooted trees were generated using the distance method UPGMA (a), the NJ method (b), ME method (c) and MP method (d).

6.3. Phylogenetic analysis of the DNA helicase and DNA primase domains of PfPREX

6.3.1. DNA helicases and DNA primases

6.3.1.1. DNA primases

DNA primases are enzymes that are essential for DNA replication and their activity is required at the DNA replication fork. The activity involves the catalysis of synthesis of short oligoribonucleotides used as primers for DNA polymerases (Kornberg, 1980; 1982). Most DNA primases can be divided into 2 classes: - class I comprise bacterial and bacteriophage primases (Section 1.4.3.1.2) and class II contains heterodimeric eukaryotic type primases. The prokaryotic primases are found to be associated with replicative DNA helicases while the eukaryotic primases form a complex with DNA polymerase alpha. All DNA primases share several key motifs, all of which are found to be present in PfPREX (Section 3.3.2.1).

6.3.1.2. DNA helicases

Like the DNA primases, DNA helicases also play essential roles in DNA replication. They are responsible for the unwinding of double stranded nucleic acids before DNA replication, repair or recombination. This reaction is dependent on energy derived from nucleoside-5'-triphosphate (NTP) hydrolysis. All DNA helicases share several common motifs as discussed in Chapters 1 and 3. These motifs are also observed in PfPREX (Section 3.3.3). There are several classes of helicases including superfamily (SF) 1 to 3 and the DnaB-like group. Along with the DNA primases, I have also aimed to explore the phylogenetic relationship of PfPREXhcli alongside other helicases in the hope of shedding light on their origin and on the overall evolution of the extraordinary structure of PfPREX.

6.3.1.3. DNA Helicase/Primase Organisation

Bacteria possess separately encoded replicative DNA primase and DNA helicase. In *E. coli*, they are termed DnaG and DnaB, although their protein products join in multimeric complexes. In bacteriophages, there are two distinct types of DNA primase and DNA helicase system. One group is similar to the bacterial system (DNA primase and DNA helicase are encoded separately e.g. P22 and T4 bacteriophages). The second group comprise the T7(T3) and P4 bacteriophages in which their DNA primase and DNA helicase are found on a single polypeptide (Figure 6.3). Ilyina *et al* (1992) investigated these one and two component DNA primase/helicase systems. Pronounced

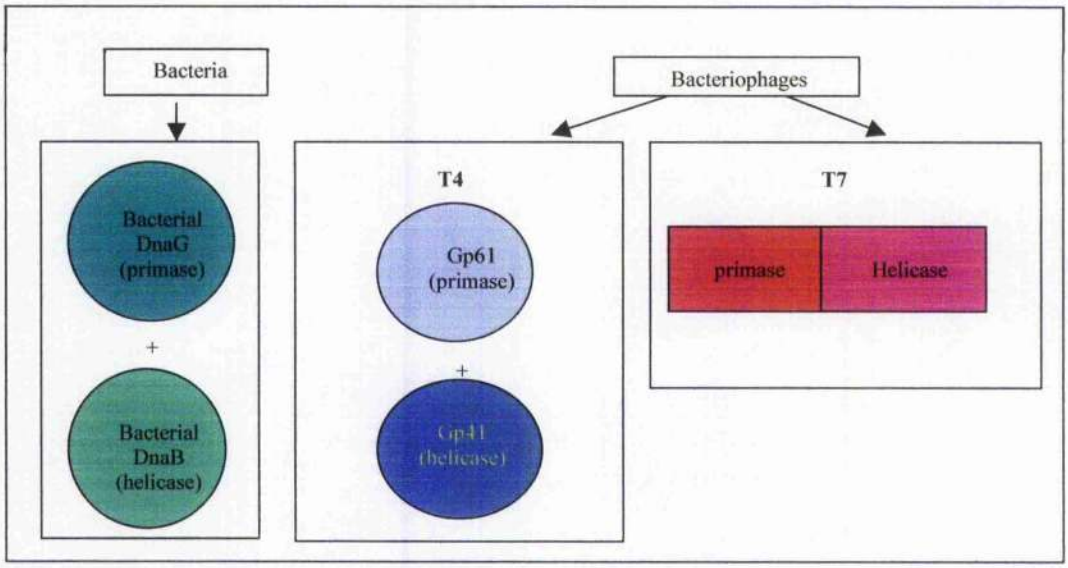

Figure 6.3. Organisation of DNA primase/helicase systems in bacteria and phages. (Adapted from Ilyina *et al*, 1992).

sequence homology was observed between the latter group and PfPREXpriheli in both the DNA primase and also the DNA helicase domains. Given also that the primase-helicase is fused and that *Plasmodium* has a tendency to fuse genes, it was of interest to determine the relatedness of this protein with the others.

6.3.2. Alignment of DNA primases

Several DNA primases from various organisms based on best homologies in BLAST searches were included in the alignment. The DNA primase sequences ranged from examples of the single component DNA primase/helicase systems of both bacteria and phages and the two component ones from phages (Table 6.3). A sequence from *Arabidopsis* was also included as it had homologues to this group. A total of 13 sequences were used in the DNA primase alignment, alongside the PfPREXpri sequence.

The sequences were aligned first using the DIALIGN version 2 programme (Morgenstern *et al*, 1996) with the default settings (Appendix D), as with the DNA polymerase alignment. The alignment was checked manually and large gaps were removed. The culled alignment was realigned using ClustalX 1.81 (Thompson *et al*, 1994) using the settings as indicated in Table 6.2 and was checked and adjusted manually.

From the alignment, a strong conservation at the N-terminus, of two pairs of Cys/Cys or Cys/His residues was observed. This conserved motif is the zinc-binding motif (Section 3.3.2). The zinc-binding motif is present throughout the bacterial and phage primases. In addition to the zinc-binding motif, the DNA primase alignment possesses another five conserved sequence motifs (Figure 6.4). This alignment was used for the generation of phylogenetic trees.

Phyla	Organism	Shortened Name	Length of sequence (a.a)	Genbank/embl accession no.	Reference
Virus	P4 phage	P4	777	CAD06954.1	Parkhill *et al*, 2001
	T7 phage	T7	566	CAA24405.1	Dunn & Studier, 1983
	T3 phage	T3	566	CAA35135.1	Direct submission
	T4 phage	T4	475	AAA32554.1	Direct submission
	phiYe03-12	phiYe03-12	566	CAB63608.1	Pajunen *et al*, 2001
	Cyanophage P60	RP	531	AAL73266.1	Chen & Lu, 2002
	Pseudomonas phage gh-1	gh-1	544	AAO73154.1	Direct submission
Eukaryote	*Arabidopsis thaliana*	Arabidopsis	709	NP_849735.1	Direct submission
Bacteria	*E. coli*	E.coli	581	CAA23531.1	Smiley *et al*, 1982
	Salmonella typhimurium	Salmonella	581	AAL22084.1	McClelland *et al*, 2001
	Bacillus subtilis	B.subtilis	603	CAB14464.1	Kunst *et al*, 1997
	Synechocystis sp	Syne	635	BAA18229.1	Kaneko *et al*, 1995
	Pseudomonas putida KT2440	Pseudomonas	544	AAN67883.1	Nelson *et al*, 2002
	Aquifex aeolicus	Aquifex	498	AAC07430.1	Deckert *et al*, 1998

Table 6.3. The DNA primase sequences used for multiple alignment. The phyla, name of organism, number of amino acids, type of polymerase and the accession number of each DNA primase sequence is shown. The shortened name of each sequence used in the alignment is also shown.

6.3.3. Alignment of DNA helicases

For the DNA helicase alignment, a total of 20 sequences were included alongside PfPREXheli (Table 6.4). These sequences include two sequences, one from a *Pseudomonas* phage gh-1 and a sequence from *Pseudmonas putida*, both of which were hits in recent BLAST results obtained with PfPREXheli. Mus308 (NCBI accession number:- NP_851315) (Harris *et* al, 1996), which was used in the DNA polymerase alignment possesses both a DNA polymerase and also a DNA helicase domain. The DNA helicase domain is called HEL308 and has been determined to be most similar to

the DNA helicases of the superfamily 2 (SF2) (Marini & Wood, 2002). Therefore, it was of interest to include this sequence in our phylogenetic analysis for use as an outgroup. The helicase moiety of a DNA primase-helicase reported in *Arabidopsis* was also included.

Phyla	Organism	Shortened Name	Length of sequence (a.a)	Genbank/embl accession no.	Reference
Virus	P22 phage	P22	458	AAM81428.1	Direct submission
	T7 phage	T7heli	566	CAA24405.1	Dunn & Studier, 1983
	T3 phage	T3heli	566	CAA35135.1	Direct submission
	T4 phage	T4heli	475	AAD42466.1	Direct submission
	phiYe03-12	phiYe03-12	566	CAB63608.1	Pajunen *et al*, 2001
	Cyanophage P60	RP	531	AAL73266.1	Chen & Lu, 2002
	Pseudomonas phage gh-1	gh-1	544	AAO73154.1	Direct submission
Bacteria	*E. coli*	E.coli	471	AAA23689.1	Nakayama *et al*, 1984
	Salmonella typhimurium	S.typhimurium	471	AAL23070.1	McClelland *et al*, 2001
	Bacillus subtilis	B.subtilis	454	BAA05176.1	Moriya *et al*, 1985
	Pseudomonas putida KT2440	P.putida	544	AAN67883.1	Nelson *et al*, 2002
	Aquifex aeolicus	Aquifex	530	AAC07803.1	Deckert *et al*, 1998
Eukaryote	*Arabidopsis thaliana*	Arabidopsis	709	NP_849735.1	Direct submission
	Drosophila melanogaster	D.melanogaster	395	AAM27521.1	Direct submission
	Caenorhabditis elegans	C.elegans	566	AAA81397.1	Direct submission
	Homo sapiens	HuTwinkle	685	AAK69558.1	Spelbrink *et al*, 2001
	Mus musculus	MmTwinkle	684	AAL27647.1	Direct submission
	Homo sapiens	HuHEL308	1101	AAL85274.1	Direct submission
	Mus musculus	MmHEL308	527	AAL85275.1	Marini & Wood, 2002
	Saccharomyces cerevisiae	S.cerevisiae	542	CAA88166.1	Direct submission

Table 6.4. The DNA helicase sequences used for multiple alignment. The phyla, name of organism, number of amino acids, type of polymerase and the accession number of each DNA helicase sequence is shown. The shortened name of each sequence used in the alignment is also shown.

The sequences were aligned first using DIALIGN and subsequently the same process was carried out as with the DNA primases (Appendix D). Large gaps were removed from the alignment and then realigned using ClustalX1.81 using the settings indicated in Table 6.2. Five conserved motifs (Ilyina *et al*, 1992) can be found among the group of DNA helicases in the alignment. Motif 1 and 2 correspond to the Walker A and B motifs (Section 3.3.3) found in all NTP-binding proteins (Walker *et al*, 1982). The alignment obtained was used for the generation of phylogenetic trees (Figure 6.5).

6.3.4. Generation of phylogenetic trees for the DNA primases

Phylogenetic trees for the DNA primase sequences were generated using MEGA (Molecular Evolution Genetic Analysis) software version 2.1 (Kumar *et al*, 2001). The trees were created from the alignment (Figure 6.4). As with the DNA polymerases, four different types of trees were generated with the alignment set to give an idea of the stability of the tree topology based on the given alignment.

All of the four trees (Figure 6.6) showed two distinct clusters:- T7/T3 group versus the bacteria/T4 group. PfPREXpri appeared to branch with the T7/T3 group with 100 bootstrap support for the maximum parsimony method while for the distance based method, bootstrap support was 74 to 100. PfPREXpri is most closely related to the cyanophage P60 (RP/Podoviridae) DNA primase (Chen & Lu, 2002). For the T4/bacteria group, the members within the cluster include the other bacterial homologues of DnaG although some of the bootstrap support within the group is not strong. Most importantly, the PfPREXpri node is well supported which implied that the relationship of PfPREXpri with the T7/T3 group is stable. It was of interest too to determine whether the PfPREXheli sequence also branches with the T7/T3 group of

DNA helicases whereby the T7/T3 bacteriophages also belong to the same family, Podoviridae as cyanophage P60.

6.3.5. Generation of phylogenetic trees for the DNA helicases

For the DNA helicases, the same four methods of tree building were used, based on the alignment shown in Figure 6.5. Phylogenetic analysis revealed that the eukaryotic T7-like Twinkle DNA helicases form a sister group branch with the T7/T3 group of DNA helicases with strong bootstrap support in all four trees. Filée *et al* (2003) had previously observed this, where the Twinkle-like sequence, including PfPREXheli sequence as a sister group with the T7/T3 phage sequences. These eukaryotic T7-like DNA helicases have been proposed to be of mitochondrial origin. Filée *et al* (2003) postulated that as mitochondria were derived from a α-proteobacterium, the Twinkle-like DNA might be derived from a horizontal gene transfer event from a T7/T3 phage. This is reminiscent of the situation observed with the mitochondrial RNA polymerase (Hedtke *et al*, 1997).

Both the DNA primase and DNA helicase of PfPREX cluster with the T7-phage like proteins. This indicates a common origin. It is possible that the DNA primase domain has been secondarily lost in other Twinkle-like DNA helicase of eukaryotic mitochondria, but is retained in *Plasmodium*. Possible evolutionary scenarios will be discussed in the next section.

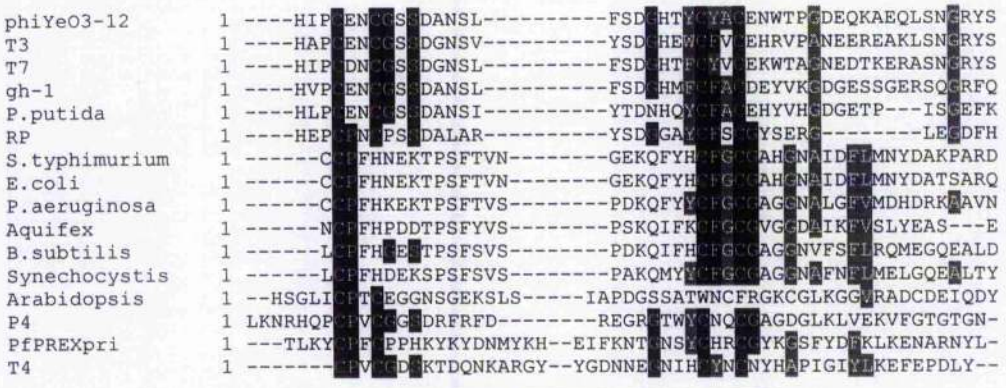
Zinc-binding motif (1)

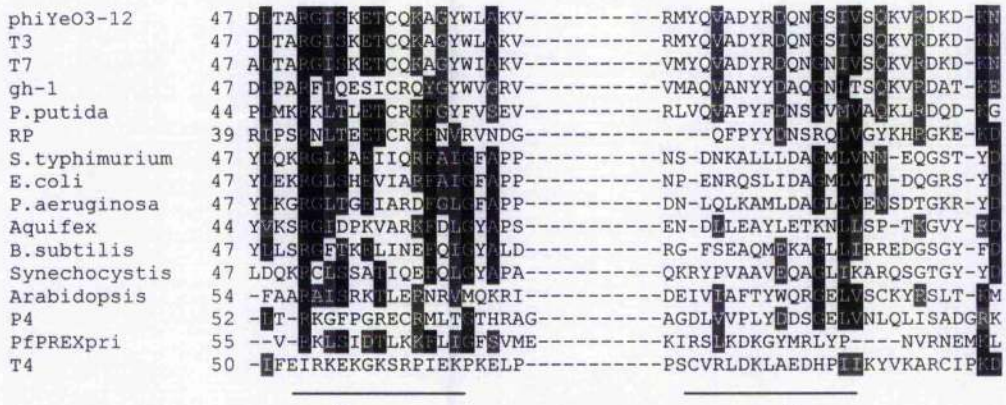
2
3

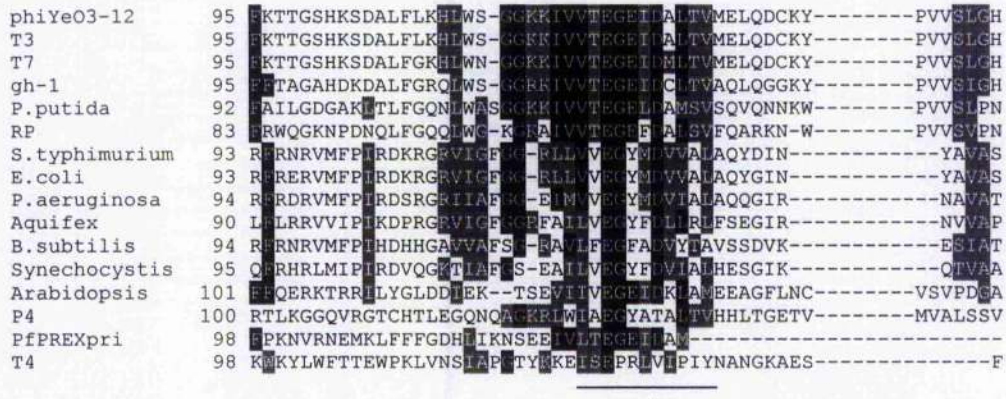
4

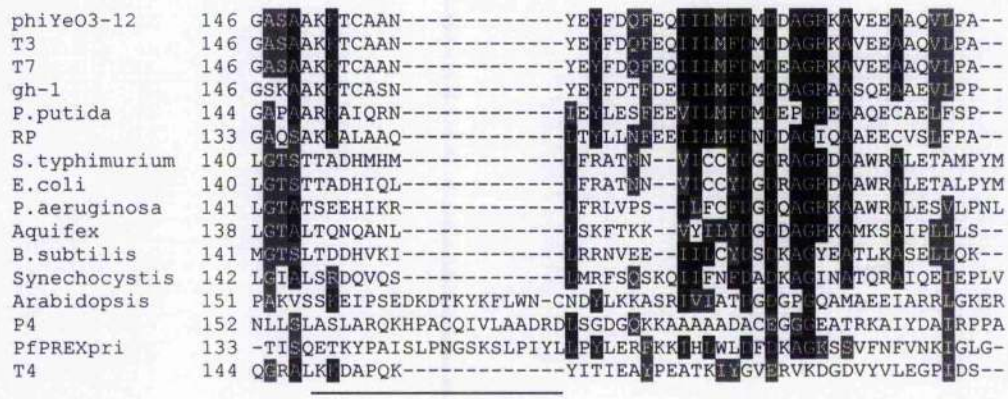
5

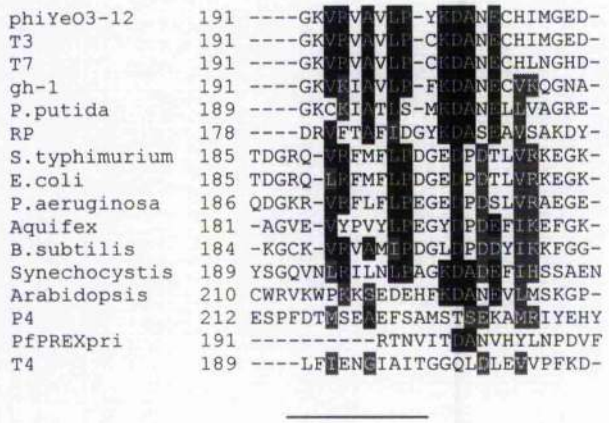

6

Figure 6.4. Alignment of deduced amino acid sequence of DNA primases. Details of sequences used are shown in Table 6.3 alongside PfPREXpri. These sequences were aligned using ClustalX 1.81. Black shading indicates identical amino acids; grey shading indicates conserved amino acid substitutions. The numberings on the left hand side are the relative positions of the amino acid in the respective sequences. Motifs 1-6 are underlined with text.

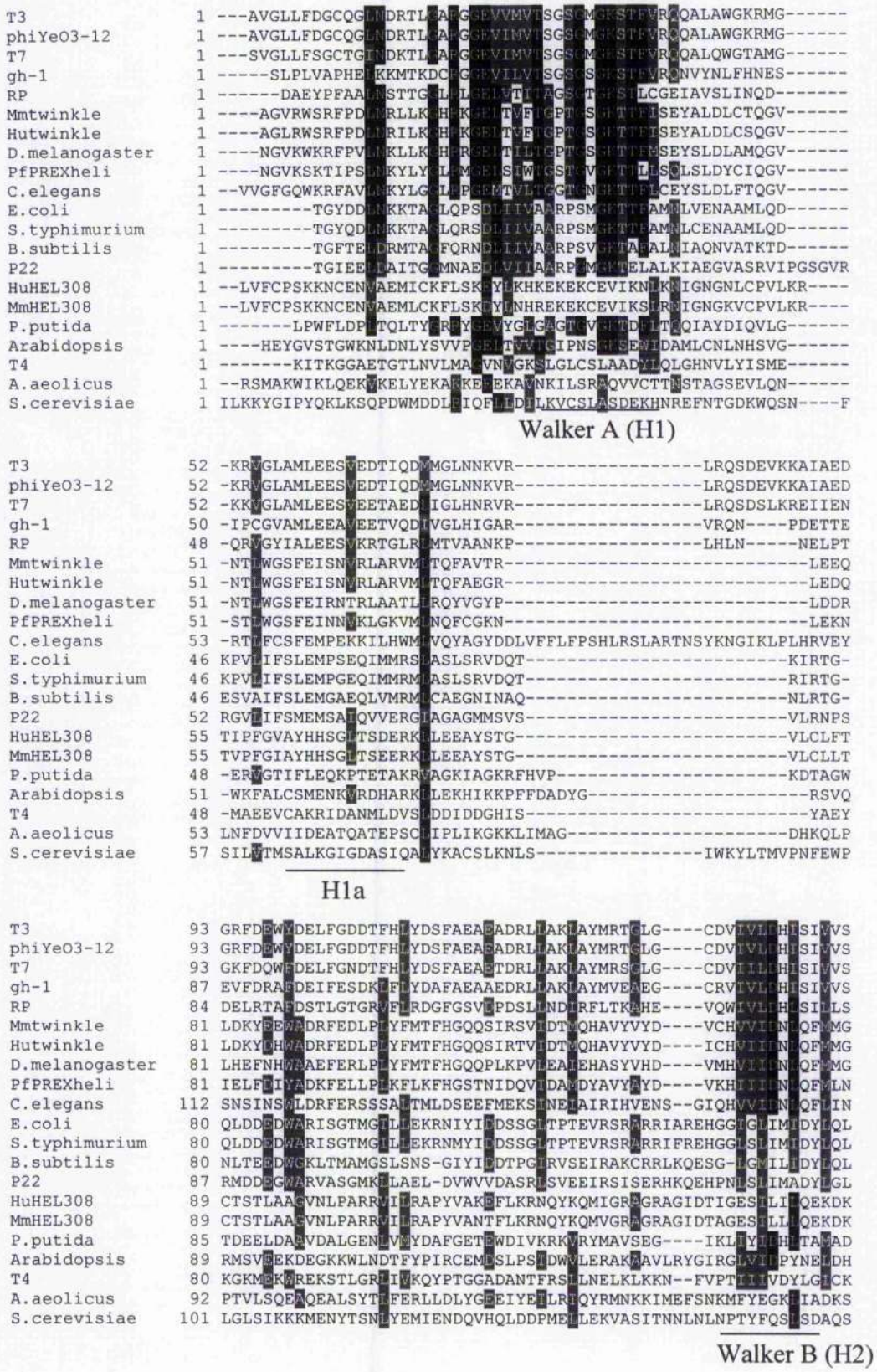
Walker A (H1)
H1a
Walker B (H2)

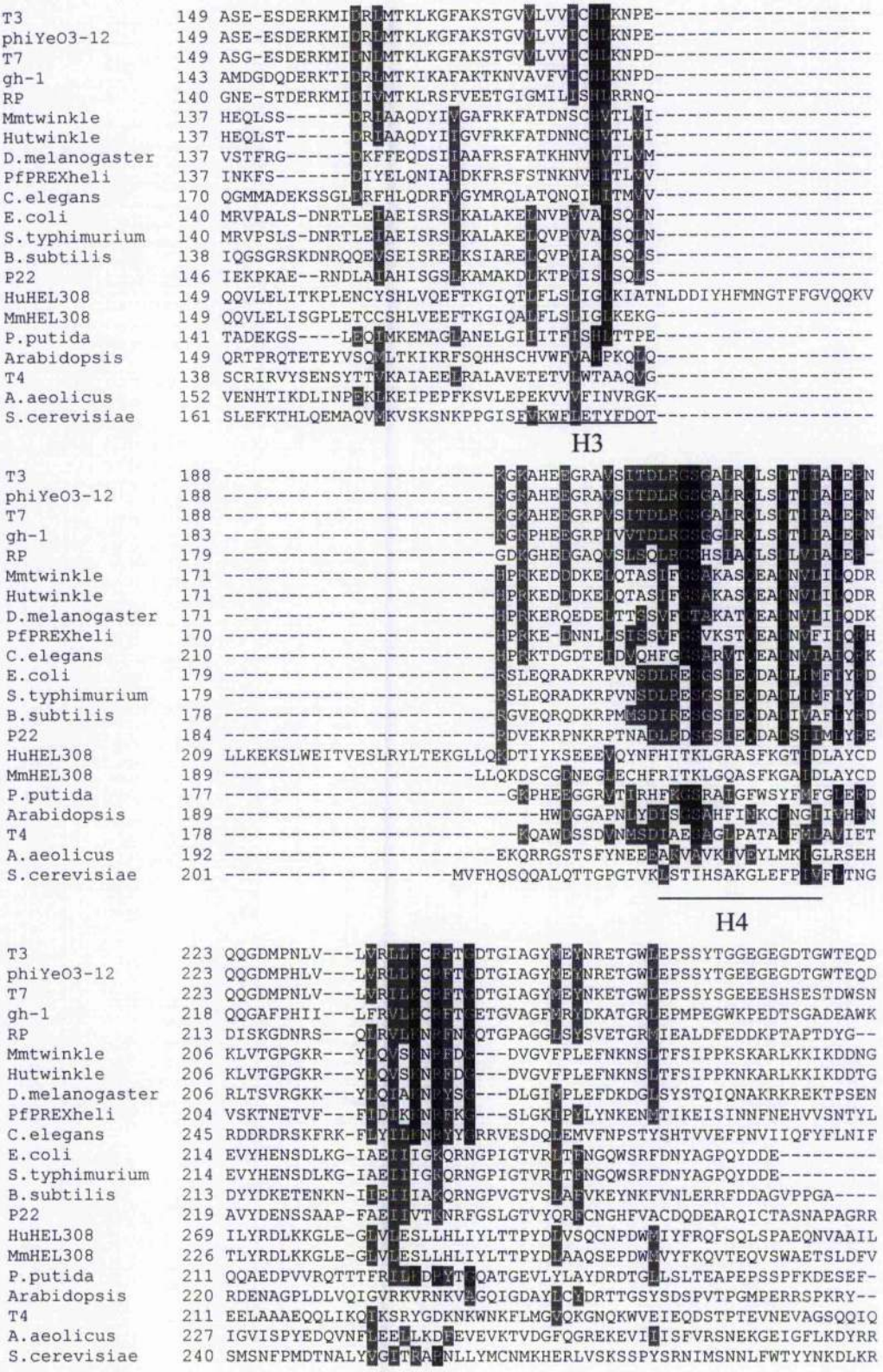

Figure 6.5. Alignment of deduced amino acid sequence of DNA helicases. Details of sequences used are shown in Table 6.4 alongside PfPREXheli. These sequences were aligned using ClustalX 1.81. Black shading indicates identical amino acids; grey shading indicates conserved amino acid substitutions. The numberings on the left hand side are the relative positions of the amino acid in the respective sequences. Motifs H1-H4 are underlined with text.

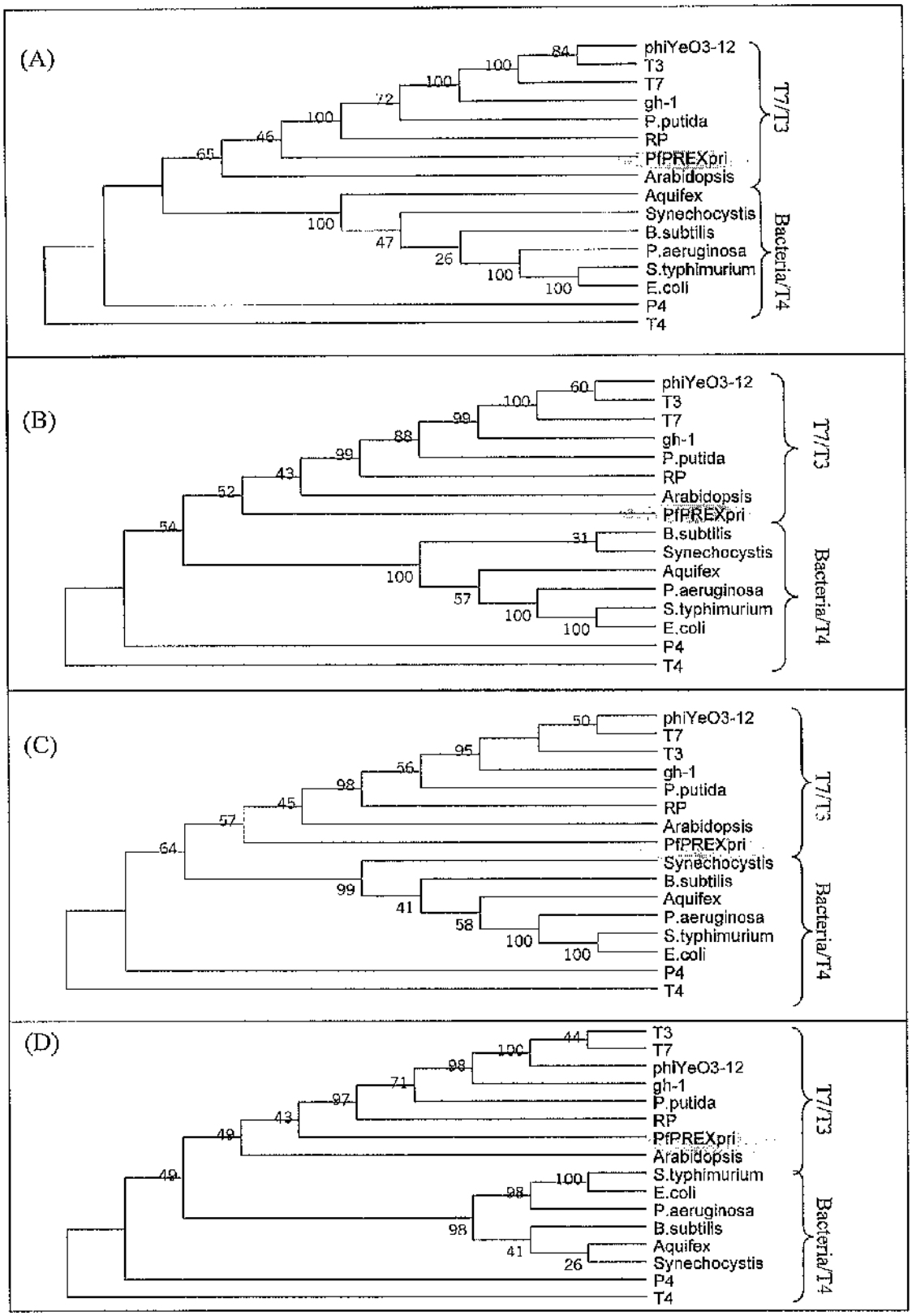

Figure 6.6. Phylogenetic trees generated by MEGA derived from the DNA primase alignment (Figure 6.4). The bootstrap values (100 resamplings) are indicated on the branches. Unrooted trees were generated using the distance method UPGMA (a), the NJ method (b), ME method (c) and MP method (d).

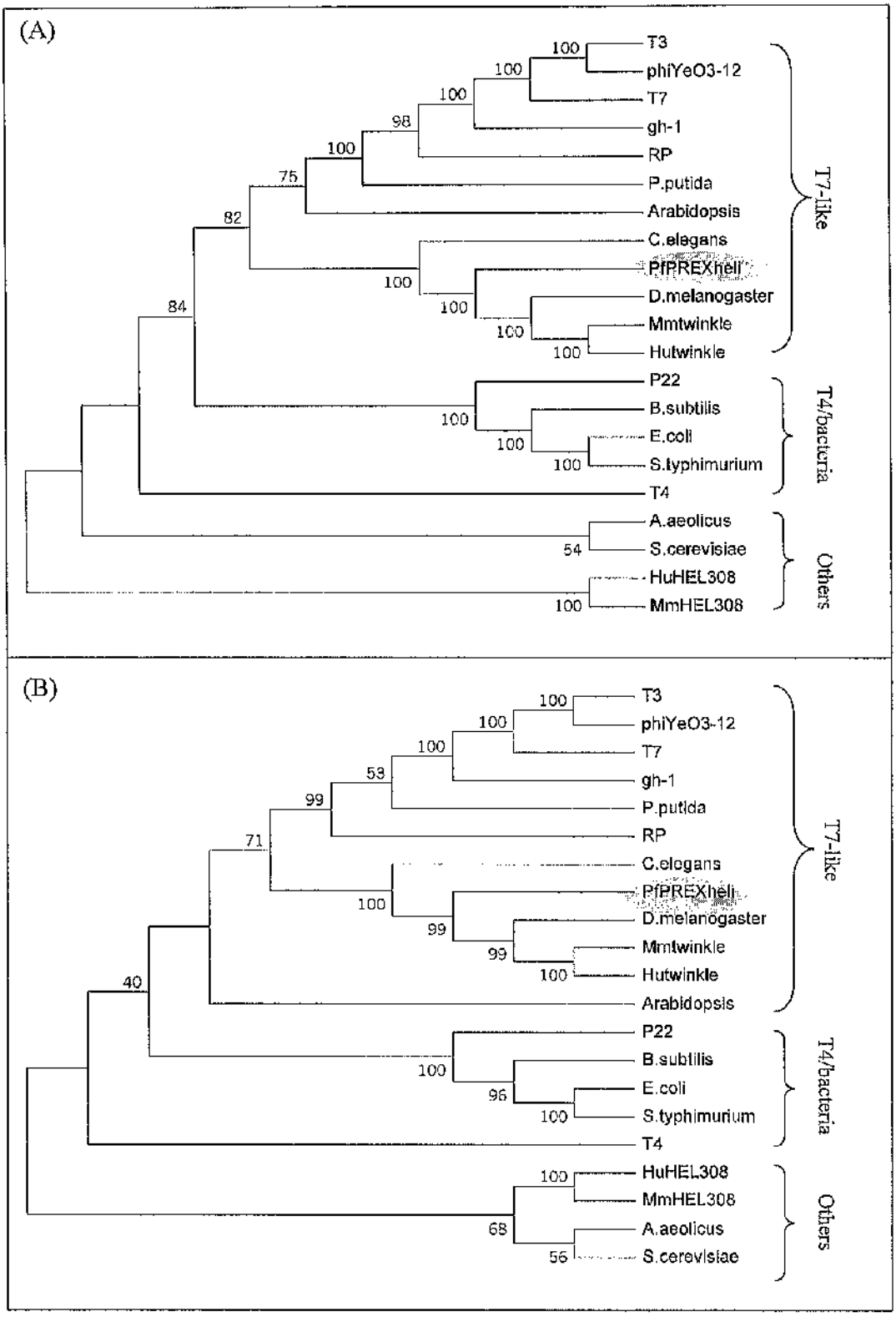
(A)
T3
phiYeO3-12
T7
gh-1
RP
P.putida
Arabidopsis
C.elegans
PfPREXhell
D.melanogaster
Mmtwinkle
Hutwinkle
P22
B.subtilis
E.coli
S.typhimurium
T4
A.aeolicus
S.cerevisiae
HuHEL308
MmHEL308
T7-like
T4/bacteria
Others
100
100
100
98
100
75
82
84
100
100
100
100
100
100
100
54
100
(B)
T3
phiYeO3-12
T7
gh-1
P.putida
RP
C.elegans
PfPREXhell
D.melanogaster
Mmtwinkle
Hutwinkle
Arabidopsis
P22
B.subtilis
E.coli
S.typhimurium
T4
HuHEL308
MmHEL308
A.aeolicus
S.cerevisiae
T7-like
T4/bacteria
Others
100
100
100
53
99
71
100
99
99
100
40
100
96
100
100
68
56

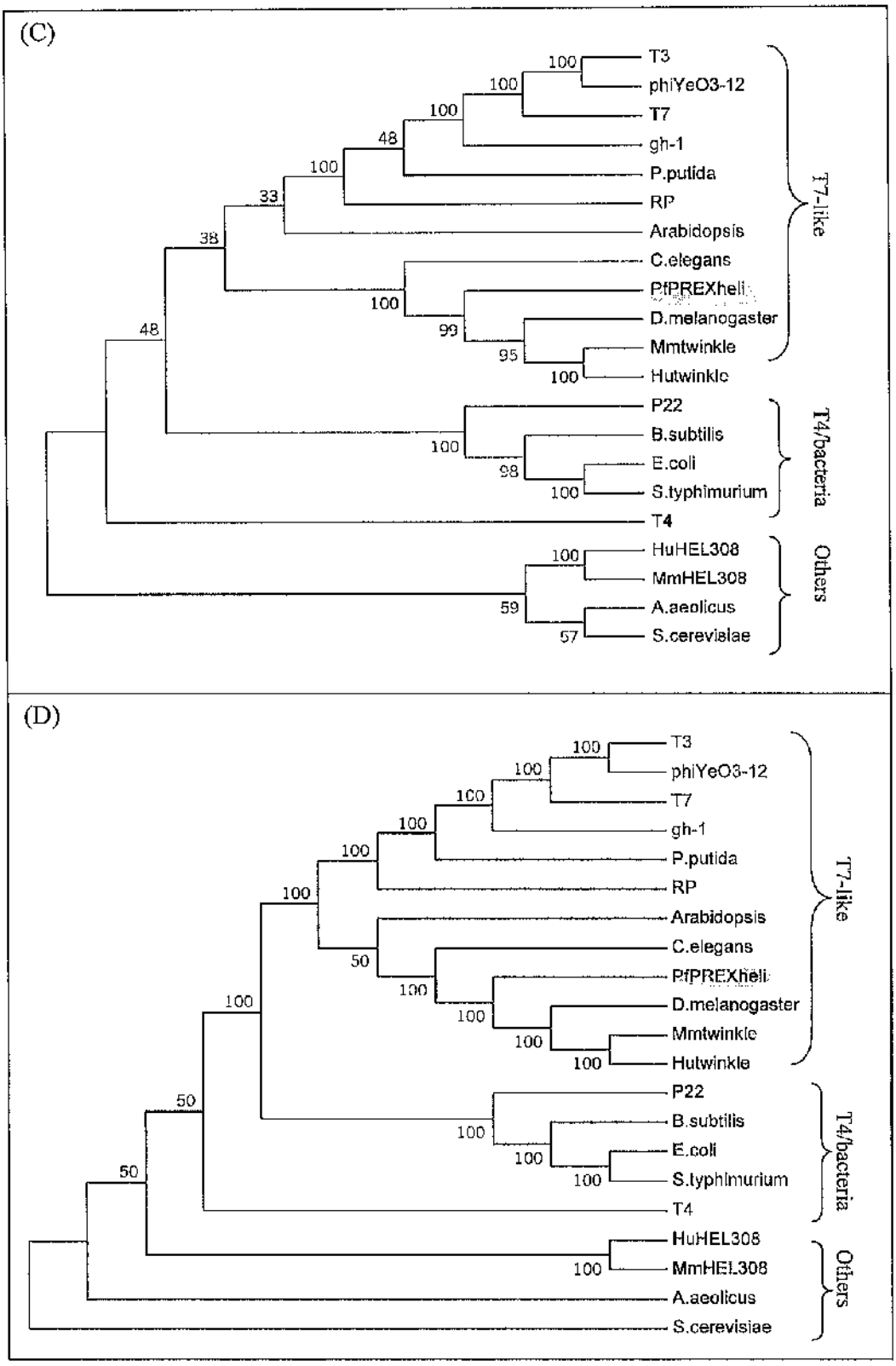

Figure 6.7. Phylogenetic trees generated by MEGA derived from the DNA helicase alignment (Figure 6.5). The bootstrap values (100 resamplings) are indicated on the branches. Unrooted trees were generated using the distance method UPGMA (a), the NJ method (b), ME method (c) and MP method (d).

6.4. Discussion

Work in this chapter aimed to seek the evolutionary origins of *PfPREX* – a gene that encodes several proteins likely to be involved in the replication of plastid DNA. *Plasmodium* has a tendency to fuse genes of related functions (Section 1.4.1) e.g. DHFR-TS, ODC-AdoMetDC, G6PD-6PGL etc. In the case of the DNA primase and DNA helicase domains, there are precedents where these two proteins are fused. This is the case in T-odd bacteriophages which belong to the Podoviridae group. In PfPREX, the phylogenetic analysis points to both the DNA primase and DNA helicase domains branching with similar proteins from this group of T-odd bacteriophages. Therefore, it seems likely that the DNA primase and DNA helicase domains were fused prior to their appearance in PfPREX. Intriguingly, the T7 DNA helicase protein is also found in many eukaryotes – where in some of them, this protein localises to mitochondria (Spelbrink *et al*, 2001). Leipe *et al* (2000) looked in detail at the evolution of the DnaB proteins in Eukaryota. In that study, they observed that the DnaB found in chloroplasts are highly similar to the bacterial ones. Therefore, it was proposed that these DnaB sequences had been vertically inherited via the bacterial endosymbiont – the origin of the plastids. In addition, their phylogenetic analysis found that eukaryotic DnaB homologues grouped with the T-odd bacteriophage proteins. This is the same scenario observed in this chapter (Figure 6.7). However, unlike the results reported by Leipe *et al* (2000), this relationship observed in our phylogenetic trees, obtained strong statistical support (Figure 6 .7). However, the study of Leipe *et al* (2000) was done prior to the discovery of the other T7-like mitochondrial associated eukaryotic sequences. Filée *et al* (2003) carried out a similar study. In their study, it was observed that these T7-like eukaryote DNA helicases form a sister group to the T7/T3 bacteriophage DNA helicases. Incidentally, Filée *et al* (2003) also included the *P. chabaudi* PomI sequence

that corresponds to the PfPREXheli sequence in their phylogenetic analysis and the same branching was observed whereby PfPREXheli sat within the T7-like sequences (Twinkle), forming a sister group with T7/T3 bacteriophage sequences. However, the Twinkle-like sequences are found to be mitochondrial and as mitochondria were derived from a α-proteobacterium, mitochondrial DNA helicase might be expected to more closely related to the bacterial ones if they were derived from the DNA helicase of the endosymbiont. The results obtained indicated that these eukaryote Twinkle sequences originated from a T7/T3 bacteriophage rather than a bacterium. This scenario is similar to that of mitochondrial RNA polymerase which also has a bacteriophage origin (Hedtke *et al*, 1997).

One sequence found in the databases is of particular interest. An *Arabidopsis* sequence that Leipe *et al* (2000) also included in their analysis, has the same domain architecture as with PfPREXpriheli and the phage proteins, whereby the DNA primase and DNA helicase domains are fused together. Leipe *et al* (2000) saw this conservation of architecture and proposed that it was due to a horizontal gene transfer event via a bacteriophage. Like the PfPREXpriheli sequence, the *Arabidopsis* sequence contains an N-terminal target sequence and is predicted by various programmes ranging from ChloroP, MitoProt and Predotar to have potential chloroplast and potential mitochondrial localisation. We were interested to find out if the DNA primase and DNA helicase in both sequences originated from the same source. In the DNA helicase trees (Figure 6.7), the *Arabidoposis* sequence belonged to the T-odd bacteriophage clade whereas, PfPREXheli clustered together with the eukaryotic T7-like DNA helicases. The DNA primase domains of both, on the other hand, clustered together with the T-odd DNA primase sequences, but with weak statistical support (Figure 6.6). These

results seem to suggest that the DNA helicase domain of both *Arabidopsis* and *PfPREX* (and possibly the primase domains) were obtained at different points in evolution. Both sequences appear to have originated from T-odd bacteriophages.

The fact that the Twinkle proteins are associated with the mitochondria in most species in which they are found, indicates that the DNA primase-helicase is ancestrally mitochondrial. The fact that the targeting sequence at the N-terminus of PfPREX directs proteins to the plastid, indicates that a role in plastid DNA replication was acquired secondarily in apicomplexans. Genes originally involved in mitochondrial functions, that later evolved separate functions are common and a T7-like RNA polymerase initially involved in mitochondrial transcription is also known to have taken a secondary role in plastid transcription in plants (Hedtke *et al*, 2000). These data seem to give rise to two possible hypotheses for the presence of such sequences in eukaryotes. The first h is that a horizontal gene transfer occurred between a phage and either the mitochondrion or the nucleus of a eukaryotic cell that was the ancestor of all of those species carrying Twinkle-like helicase today. Given that it appears that T7-like genes have entered eukaryotic cells on more than one occasion (hence the divergence between the *Arabidopsis* helicase/primase and PfPREX), it seems possible that horizontal gene transfer from bacteriophages to eukaryotic cells has occurred more than once. A second hypothesis is that the α-proteobacterium that initially gave rise to the mitochondrion, was itself infected with a bacteriophage whose remnants can now be traced in these fossils. In the case of the apicomplexans these genes secondarily gained plastid-targeting sequences and are now involved in the plastid DNA replication instead.

It seems probable that uniquely in the Apicomplexa, the DNA primase-DNA helicase domains fused into a single gene with a DNA polymerase. Extraordinarily, the DNA polymerase domain is most closely related to bacterial DNA polymerase I, and most closely to thermophilic DNA polymerase I of *Aquifex spp.* The *Plasmodium* DNA polymerase is also rather thermophilic (Section 4.2.3.1) and like the *Aquifex* proteins, lacks 3'-5' exonuclease domain. It seems probable that this gene entered the ancestral apicomplexans by horizontal gene transfer (the same DNA polymerase is found in other apicomplexans e.g. *Toxoplasma* and *Theileria*) – although the point in time and mechanisms of this event remains elusive.

Chapter VII

General Discussion

A gene encoding a plastid DNA replicase, *PfPREX*, from *Plasmodium falciparum* has been cloned and expressed in *E. coli*. The full-length protein is composed of three functional domains, a DNA primase, a DNA helicase and a DNA polymerase. The C-terminal domain encodes a DNA polymerase, with 25-30% identity to prokaryotic DNA polymerases from family A. Homology searches identified the three motifs, A (DFKQIELK), B (AINFGLIYGM) and C (LCVHDE) conserved among these family A DNA polymerases (Delarue *et al*, 1990) in PfPREXpol. In addition, it possesses a 3'-5' exonuclease domain common to this class of enzyme, but no 5'-3' exonuclease domain is found on the same enzyme. The N-terminal domain encodes both a DNA primase and a DNA helicase. The DNA helicase part of PfPREX has the highest similarity to a protein called 'Twinkle', which is a eukaryotic mitochondrial T7-like DNA helicase. This domain contains five key motifs (Ilyina *et al*, 1992), including the Walker A and B motifs, which are found in all DNA helicases and NTP-utilising enzymes. The DNA primase domain revealed less homology to other DNA primases, however all of the key DNA primase motifs identified elsewhere (Ilyina *et al*., 1992) can be located within the PfPREXpri domain.

Since the *PfPREX* gene was over 6 kb in length and possessed a very high A-T content, it was foreseen that attempts to clone the gene in its entirety in *E. coli* would prove difficult, if not impossible. Therefore, the gene was cloned in two separate parts, one containing the DNA helicase and DNA primase domains and the other containing the DNA polymerase domain. Initial attempts to clone the DNA polymerase domain into an *E. coli* expression vector, frequently used in the laboratory, pET-16b (Novagen), failed. Next, the

DNA polymerase domain was cloned into a Strep-tag vector, pASK-IBA (Sigma). The reason for choosing to use this expression system was because of the success of another *Plasmodium* protein (ornithine decarboxylase, s-adenosylmethionine decarboxylase) using this system (Müller *et al*, 1999). Various approaches were taken e.g. introducing the strep-tag as both an N-terminal and a C-terminal extension, in the hope that either would allow the expression of the recombinant protein. This did not work, thus another approach was tested, whereby an additional plasmid was introduced into the *E. coli* expression strain. This plasmid (RIG) (Baca & Hol, 2000) carries the genes that encode three tRNAs (Arg, Ile, Gly) cloned from *E. coli*. These genes direct the constitutive expression of tRNAs that recognise the codons AGA/AGG (Arg), ATA (Ile) and GGA (Gly). Since these codons are used more frequently in *Plasmodium*, the increased levels of the three tRNAs may help *E. coli* to better translate the *Plasmodium* mRNA and thus increase the yield of the recombinant *Plasmodium* protein. However this approach did not increase the yield of the expressed protein. Finally, the Gateway Cloning system (Invitrogen) was used for cloning *PfPREXpol*. The DNA polymerase domain was successfully cloned and expressed to high levels using the pDEST17 vector (Chapter 4). The DNA helicase/DNA primase domain was also functionally expressed using the pDEST17 construct but only a low yield of the recombinant protein was obtained with this system. The construct was moved into pET-DEST42 vector which introduced a C-terminal His-tag as opposed to a N-terminal His-tag, and a pDEST15 vector which had a N-terminal GST-tag. Overall, the pDEST15 construct gave the highest yield of protein and was the final construct used for the production of the recombinant PfPREXpriheli.

PCR experiments using a variety of oligonucleotides from within the sequence of each domain confirmed the identity of each construct. Attempts were also made to sequence each construct. However, with the Gateway vectors, the presence of the *att* recombination sites which contain large inverted repeats, posed a problem for sequencing and the reason being that the inverted repeats tend to form large loops, which prevents sequencing polymerase from progressing. More than ten sequencing attempts on each clone were made to try to sequence the final constructs. The constructs were even shuttled from one vector to another vector (as recommended by Invitrogen) in efforts to eliminate the sequencing problems, but to no avail. Finally, only the pDEST15priheli construct was successfully sequenced and its sequence was shown to be identical to that in the database. The pDESTpol could only be partially sequenced (approximately 2 kb), and the sequence obtained was as predicted. I also tried to re-amplify the DNA polymerase domain from the pDEST17pol construct to eliminate the *att* sites and subclone into pGEM-T vector (Promega) for sequencing. The problem encountered with this construct was the same as the Gateway vectors, whereby only the forward primer gave any sequence reads, while the reverse primer was read back into the vector sequence. Regrettably, we ran out of time to sequence the remaining constructs although PCR amplification consistently indicated that they contained the expected inserts.

The study was able to demonstrate that *PfPREX* does encode for functional DNA polymerase, DNA helicase and DNA primase activities. All of these activities were characterised from the corresponding recombinant proteins. First, the PfPREXpol was shown to possess both DNA polymerase activity and 3'-5' exonuclease activity, while the

PfPREXpriheli recombinant protein was found to possess both DNA primase and helicase activity. The characterisation of all activities was limited and future work should focus on characterising each activity in more detail. Given the probable essential role of each protein in replication of the *Plasmodium* plastid DNA – an ultimate goal would be to seek specific inhibitors of the proteins that could represent lead compounds in chemotherapy of malaria.

All of the *Plasmodium* homologues of *PfPREX* found in other *Plasmodium* species possess putative plastid targeting sequences, which suggests that the PREX protein is targeted to the plastid. Therefore, experiments were designed to confirm this. Unfortunately, the indirect immunofluorescence method could not be optimised to give a clear answer to the localisation of the PREX protein in *Plasmodium*. DAPI was used to stain the nuclear DNA and also the plastid DNA, but due to the close proximity of the nuclear DNA to the plastid DNA, it was impossible to differentiate these two different DNA structures. An *in situ* hybridisation method was used to localise the plastid DNA and to see if the anti-sera that binds to PfPREX protein would give a staining pattern that overlaps the staining pattern of the plastid DNA. Therefore, due to the limitations of both methods, no conclusions could be drawn from the data generated. Hence, a collabration was set up with Dr Shigeharu Sato (NIMR, Mill Hill) who devised a method using GFP technology (Sato, *et al*, 2003) to target both the mitochondrion and the plastid in *Plasmodium*. He used the same method to make GFP constructs containing the plastid-targeting sequence of *PfPREX* (the first 120 amino acids) to see if the sequence does localise GFP to a plastid location. Figure 7.1 shows the results obtained in his experiments.

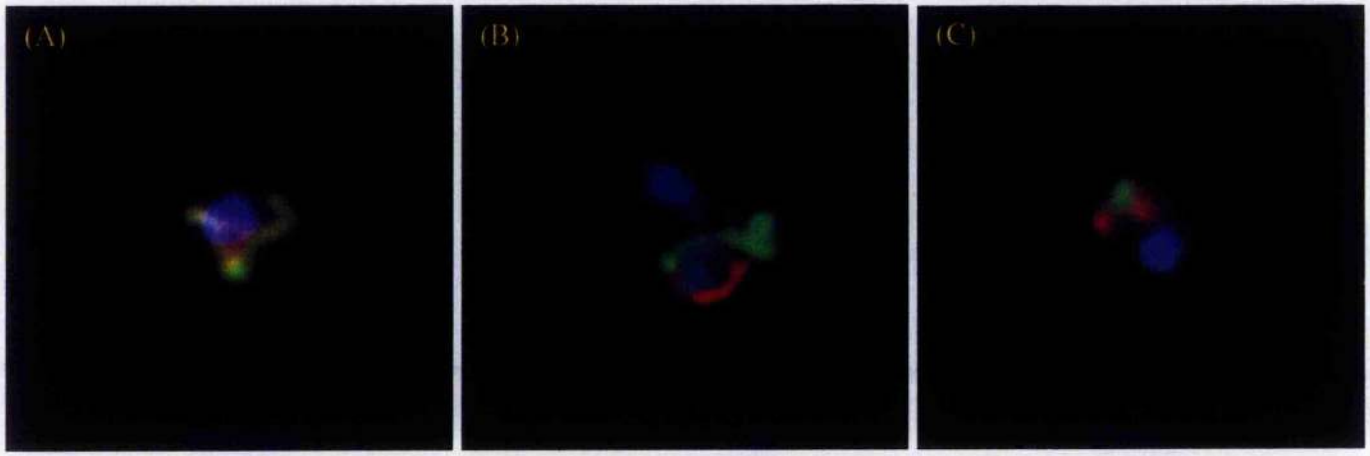

Figure 7.1. GFP containing leader sequences expressed in transfectants in *P. falciparum*. (A) HSP60-leader GFP construct, (B) ACP-leader GFP construct and (C) PfPREX leader-sequence GFP construct. Hoechst 33342 (HT:blue) and Mitotracker Red CM-H_2-Xros (MTR:red) were used to stain the nucleus and mitochondrion respectively. GFP (green). The images were obtained by fluorescence microscopy and the images were superimposed from the three images from the Hoechst, Mitotracker and GFP. Vector used for GFP construct is pSSPF2.

Dr Sato also carried out two sets of control experiments. In the first of these, the leader sequence from the HSP60 protein from *Plasmodium* was cloned into a GFP construct and transfected into *Plasmodium*. Figure 7.1A shows the result of that experiment. One can observe the overlapping of two fluorescence signals, the red belonging to the Mitotracker and the green to the GFP, which merged to yield a yellow hue. This was indicative that the HSP60 leader sequence was directing GFP into the mitochondrion. The second set of transfectants contained the GFP constructs with the ACP leader sequence (Figure 7.2B). This time, the red and green fluorescence were observed as separate entities. In addition, the green fluorescence resembled that of an organellar localisation. Furthermore, ACP has been previously shown to localise to the plastid (Waller *et al*, 1998). The transfectants containing the GFP constructs with PfPREX leader sequence were observed with the same fluorescence pattern as those with the ACP leader sequence. Therefore, the PfPREX leader sequence is concluded to direct GFP into the plastid as with the ACP. In addition, Dr Sato has obtained double transfectants containing GFP with the ACP leader sequence and red fluorescent protein (DsRed) with PfPREX leader sequence, which shows that PfPREX does co-localise with ACP and goes to the plastid (data not shown).

The functional characterisation of the different subunits and the presence of the plastid-targeting sequence at the N-terminus of PfPREX, indicate that *PfPREX* encodes several key components of the replication machinery of the plastid. One might assume that since these replication proteins are associated with the plastid, they could have been derived from the primary endosymbiont from which the plastid is evolved. The primary

endosymbiont is generally accepted to have a eubacterium. Therefore, we would expect the DNA helicase, DNA primase and DNA polymerase of PfPREX to have originated from a eubacterial source. However, the results of the phylogenetic analysis indicate otherwise and have cast an interesting light on an alternative origin of the *PfPREX* gene. Not only was the origin of the DNA polymerase domain different from that of the DNA helicase and DNA primase domains, the results indicated a rather complex origin of the gene, which might have involved more than one gene transfer event. First, the DNA polymerase domain was shown to be most closely related to the *Aquifex* DNA polymerase. *Aquifex* is a thermophilic bacterium belonging to the Archaebacteria group. Not only is the sequence most closely related to the *Aquifex* protein, both also lack the 5'-3' exonuclease domain and the *Plasmodium* protein is optimally active at high temperature (75°C) as is that of the *Aquifex* protein. The likely explanation of this relation is that a horizontal gene transfer (HGT) event had occurred such that the *Aquifex*-like DNA polymerase was introduced into the apicomplexans and replaced the original plastid DNA polymerase by non-orthologous gene displacement. This event must have happened relatively early on in the evolution of the apicomplexan ancestor as the PREX homologues containing this DNA polymerase domain, can be found in several other apicomplexans and among *Plasmodium* species. However, it is not possible to pinpoint where and when exactly the HGT occurred. Also noted is that plants e.g. *Oryza* (rice), appear to possess a plastid DNA polymerase of different origin as shown in Figure 6.2. The *Oryza* plastid DNA polymerase though related to the family A DNA polymerase did not cluster with PfPREXpol.

Even more interesting, the phylogenetic data obtained with the DNA helicase and DNA primase domains of *PfPREX* suggest that these two appear not to be typical eubacterial descendents. Instead, both the DNA primase and DNA helicase were shown not to cluster with the bacterial homologues, but to cluster most closely with the T-odd bacteriophages. This situation is similar to the case of mitochondrial RNA polymerases (Hedtke *et al*, 1997). Therefore, it was proposed that the original mitochondrial RNA polymerase was replaced by the bacteriophage one (Forterre *et al*, 1999). Furthermore, the T-odd bacteriophage-like RNA polymerase was observed to be widespread throughout the eukaryotic lineage (Cermakian *et al*, 1996). Other recent studies have also noted the close relationship between some eukaryotic DNA primases and DNA helicases with these T-odd bacteriophage sequences (Filée *et al*, 2003, Leipe *et al*, 2000), which was also observed in this study. As discussed in Chapter 6, the phylogenetic data obtained support the proposal that along with these eukaryotic sequences, PfPREXpriheli was derived from a T-odd bacteriophage origin. Two hypotheses can be put forward (Section 6.4) to try to explain the presence of such sequences in *Plasmodium*. The first involves a HGT event involving a phage and the eukaryotic ancestor. The second suggests that the original α-proteobacterium that gave rise to the mitochondrion harboured a T-odd bacteriophage, which left behind the DNA primase and DNA helicase as molecular fossils. In this latter case, the T7-like RNA polymerase may have been part of the same phage that infected the mitochondrion. The fact that the DNA helicase domain is also found in many other eukaryotic mitochondria, as with the Twinkle protein, does support an ancient introduction of the phage gene. However, a DNA primase-helicase also related to T7-like primase-helicase but clearly distinct from the PfPREX protein and the Twinkle-like helicases is also present in the *Arabidopsis*

genome and may also play a role in organellar DNA replication. This demonstrates that the T7-like genes have entered eukaryotes on more than one occasion which weakens the second argument that the protomitochondrion carried an infecting phage. Further arguments against this theory include the fact that T-odd phages are known to infect a select group of proteobacteria; but they are not known to infect rickettsial-type α-proteobacteria (Hausmann, 1988). Therefore, it seems unlikely that the protomitochondrion which originated from α-proteobacterium was indeed infected by a T-odd phage. The second argument is T-odd phages are virulent, lytic phages; they infect a host and multiply, which leads to the destruction of the eubacterial host cell. Thus, it is unlikely that a eubacterial endosymbiont harbouring such a phage could have been present in the host long enough to allow it to be integrated into a mitochondrion. Hence, the overall scenario does not support the above theory. However, irrespective of its origin, the PfPREXpriheli had somehow gained a plastid targeting sequence and is now involved in the plastid replication machinery.

Due to the nature of *Plasmodium*'s penchant for combining related genes together, we have here an example, whereby *Plasmodium* has stuck three genes encoding DNA replication proteins altogether. This study has established that due to topological constraint, it is most likely that the PfPREX protein is post-translationally cleaved, in order for each of the replication enzymes to work at its optimum. So far, there are other such multifunctional proteins found in *Plasmodium*, as discussed in Section 1.4.1. Interestingly, Lipps *et al* (2003) recently discovered another such multifunctional DNA replication protein in a thermoacidophile archaeon, *Sulfolobus islandicus*. The ORF904 encodes an

ATPase, DNA primase and a DNA polymerase, functionally similar to PfPREX. They proposed that the ORF904 could be a relict of an evolutionary old but independent DNA replication protein. Another example of a multifunctional DNA replication enzyme is the Mus308 in eukaryotes which possesses both a DNA helicase and a DNA polymerase domain. Given time, one may find more of these types of multifunctional replication proteins spread throughout the various kingdoms of organisms.

Most importantly, the discovery of this gene, *PfPREX* which encodes a plastid DNA replication machinery, has shed some light on the complex evolutionary path that has led to the modern apicomplexan order. The study has also opened the possibility that this protein can be used as a drug target. By disabling the plastid DNA replication machinery, one can kill the parasite and prevent it from continuing its life cycle in the host. It is hoped that this protein will provide a specific target for future drugs used in combating the diseases caused by apicomplexan parasites.

Bibliography

A

Abdel-Monem, M., & Hoffmann-Berling, H. 1976, "Enzymic unwinding of DNA. 1. Purification and characterization of a DNA-dependent ATPase from Escherichia coli", *Eur.J.Biochem*, vol. 65, no. 2, pp. 431-440.

Abdel-Monem, M., Taucher-Scholz, G., & Klinkert, M. Q. 1983, "Identification of *Escherichia coli* DNA helicase I as the traI gene product of the F sex factor", *Proc.Natl.Acad Sci.U.S.A*, vol. 80, no. 15, pp. 4659-4663.

Albà, M. 2001, "Replicative DNA polymerases", *Genome Biol.*, vol. 2, no. 1, p. REVIEWS3002.

Altincicek, B., Hintz, M., Sanderbrand, S., Wiesner, J., Beck, E., & Jomaa, H. 2000, "Tools for discovery of inhibitors of the 1-deoxy-D-xylulose 5-phosphate (DXP) synthase and DXP reductoisomerase: an approach with enzymes from the pathogenic bacterium *Pseudomonas aeruginosa*", *FEMS Microbiol.Lett.*, vol. 190, no. 2, pp. 329-333.

Aravind, L., Leipe, D. D., & Koonin, E. V. 1998, "Toprim--a conserved catalytic domain in type IA and II topoisomerases, DnaG-type primases, OLD family nucleases and RecR proteins", *Nucleic Acids Res.*, vol. 26, no. 18, pp. 420burger5-4213.

Ashburner, M., Ball, C. A., Blake, J. A., Botstein, D., Butler, H., Cherry, J. M., Davis, A. P., Dolinski, K., Dwight, S. S., Eppig, J. T., Harris, M. A., Hill, D. P., Issel-Tarver, L., Kasarskis, A., Lewis, S., Matese, J. C., Richardson, J. E., Ringwald, M., Rubin, G. M., & Sherlock, G. 2000, "Gene ontology: tool for the unification of biology. The Gene Ontology Consortium", *Nat.Genet.*, vol. 25, no. 1, pp. 25-29.

Astatke, M., Grindley, N. D., & Joyce, C. M. 1995, "Deoxynucleoside triphosphate and pyrophosphate binding sites in the catalytically competent ternary complex for the polymerase reaction catalyzed by DNA polymerase I (Klenow fragment)", *J.Biol.Chem.*, vol. 270, no. 4, pp. 1945-1954.

B

Baca, A.M., & Hol, W.G. J. 2000, "Overcoming Codon Bias: A Method for High-Level Overexpression of *Plasmodium* and AT-rich Parasite Genes in *Escherichia coli*", *International Journal for Parasitology*, vol. 30, pp. 113-118.

Bannister, L. H., Hopkins, J. M., Fowler, R. E., Krishna, S., & Mitchell, G. H. 2000, "A brief illustrated guide to the ultrastructure of *Plasmodium falciparum* asexual blood stages", *Parasitol.Today*, vol. 16, no. 10, pp. 427-433.

Basu, A. & Modak, M. J. 1987, "Identification and amino acid sequence of the deoxynucleoside triphosphate binding site in *Escherichia coli* DNA polymerase I", *Biochemistry*, vol. 26, no. 6, pp. 1704-1709.

Basu, S., Basu, A., & Modak, M. J. 1988, "Pyridoxal 5'-phosphate mediated inactivation of *Escherichia coli* DNA polymerase I: identification of lysine-635 as an essential residue for the processive mode of DNA synthesis", *Biochemistry*, vol. 27, no. 18, pp. 6710-6716.

Beese, L. S. & Steitz, T. A. 1991, "Structural basis for the 3'-5' exonuclease activity of *Escherichia coli* DNA polymerase I: a two metal ion mechanism", *EMBO J.*, vol. 10, no. 1, pp. 25-33.

Beese, L. S., Friedman, J. M., & Steitz, T.A. 1993a, "Crystal structures of the Klenow fragment of DNA polymerase I complexed with deoxynucleoside triphosphate and pyrophosphate", *Biochemistry*, vol. 32, no. 51, pp. 14095-14101.

Beese, L. S., Derbyshire, V., & Steitz, T. A. 1993b, "Structure of DNA polymerase I Klenow fragment bound to duplex DNA", *Science*, vol. 260, no. 5106, pp. 352-355.

Bernad, A., Blanco, L., Lazaro, J. M., Martin, G., & Salas, M. 1989, "A conserved 3'----5' exonuclease active site in prokaryotic and eukaryotic DNA polymerases", *Cell*, vol. 59, no. 1, pp. 219-228.

Bernstein, J. A. & Richardson, C. C. 1988, "A 7-kDa region of the bacteriophage T7 gene 4 protein is required for primase but not for helicase activity", *Proc.Natl.Acad.Sci.U.S.A*, vol. 85, no. 2, pp. 396-400.

Blakey, R.L., Benkovic, S.J. 1984, *Folates and Pteridines*, pp. 191-243, Wiley, New York.

Blondal, T., Thorbjarnardottir, S. H., Kieleczawa, J., Hjorleifsdottir, S., Kristjansson, J. K., Einarsson, J. M., & Eggertsson, G. 2001, "Cloning, sequence analysis and functional characterization of DNA polymerase I from the thermophilic eubacterium *Rhodothermus marinus*", *Biotechnol.Appl.Biochem*, vol. 34, no. Pt 1, pp. 37-45.

Boehmer, P. E., & Emmerson, P. T. 1992, "The RecB subunit of the *Escherichia coli* RecBCD enzyme couples ATP hydrolysis to DNA unwinding", *J.Biol.Chem.*, vol. 267, no. 7, pp. 4981-4987.

Bradford, M. 1976, "A Rapid and Sensitive Method for the Quantitation of Microgram Quantities of Protein Utilizing the Principle of Protein-Dye Binding" *Anal. Biochem.* vol. 72, pp. 248-254.

Braithwaite, D. K., & Ito, J. 1993, "Compilation, alignment, and phylogenetic relationships of DNA polymerases", *Nucleic Acids Res.*, vol. 21, no. 4, pp. 787-802.

Bremen, J. 2001, "The ears of the hippopotamus: manifestations, determinants, and estimates of the malaria burden", *Am.J.Trop.Med.Hyg*, vol. 64, no. 1S,2S, pp. 1-11.

Brennan, C. A., & Dombroski, A. J. P. T. 1997, "Transcription termination factor rho is an RNA-DNA helicase", *Cell*, vol. 48, no. 6, pp. 945-952.

Bruce, B. D. 2000, "Chloroplast transit peptides: structure, function and evolution", *Trends Cell Biol.*, vol. 10, no. 10, pp. 440-447.

Burgers, P. M. 1998, "Eukaryotic DNA polymerases in DNA replication and DNA repair", *Chromosoma*, vol. 107, no. 4, pp. 218-227.

Burgers, P. M., Koonin, E. V., Bruford, E., Blanco, L., Burtis, K. C., Christman, M. F., Copeland, W. C., Friedberg, E. C., Hanaoka, F., Hinkle, D. C., Lawrence, C. W., Nakanishi, M., Ohmori, H., Prakash, L., Prakash, S., Reynaud, C. A., Sugino, A., Todo, T., Wang, Z., Weill, J. C., & Woodgate, R. 2001, "Eukaryotic DNA polymerases: proposal for a revised nomenclature", *J.Biol.Chem.*, vol. 276, no. 47, pp. 43487-43490.

Bzik, D. J., Li, W. B., Horii, T., & Inselburg, J. 1987, "Molecular cloning and sequence analysis of the *Plasmodium falciparum* dihydrofolate reductase-thymidylate synthase gene", *Proc.Natl.Acad Sci.U.S.A*, vol. 84, no. 23, pp. 8360-8364.

C

Carlton, J. M., Angiuoli, S. V., Suh, B. B., Kooij, T. W., Pertea, M., Silva, J. C., Ermolaeva, M. D., Allen, J. E., Selengut, J. D., Koo, H. L., Peterson, J. D., Pop, M., Kosack, D. S., Shumway, M. F., Bidwell, S. L., Shallom, S. J., van Aken, S. E., Riedmuller, S. B., Feldblyum, T. V., Cho, J. K., Quackenbush, J., Sedegah, M., Shoaibi, A., Cummings, L. M., Florens, L., Yates, J. R., Raine, J. D., Sinden, R. E., Harris, M. A., Cunningham, D. A., Preiser, P. R., Bergman, L. W., Vaidya, A. B., van Lin, L. H., Janse, C. J., Waters, A. P., Smith, H. O., White, O. R., Salzberg, S. L., Venter, J. C., Fraser, C. M., Hoffman, S. L., Gardner, M. J., & Carucci, D. J. 2002, "Genome sequence and comparative analysis of the model rodent malaria parasite *Plasmodium yoelii yoelii*", *Nature*, vol. 419, no. 6906, pp. 512-519.

Carucci, D.J., Witney, A.A., Muhia, D.K., Warhurst, D.C., Schaap, P., Meima, M., Li, J.L., Taylor, M.C., & Kelly, J.M. 2000, "Guanylyl cyclase activity associated with putative bifunctional integral membrane proteins in *Plasmodium falciparum*", *J.Biol.Chem*, vol. 275, no. 29, pp. 22147-22156.

Caruthers, J.M., Johnson, E.R., & McKay, D.B. 2000, "Crystal structure of the yeast initiation factor 4A, a DEAD-box RNA helicase", *Proc.Natl.Acad Sci.U.S.A*, vol. 97, no.24, pp. 13080-13085.

Caruthers, J.M., & McKay, D.B. 2002, "Helicase structure and mechanism", *Curr.Opin.Struct Biol.*, vol. 12, no.1, pp. 123-133.

Cermakian, N., Ikeda, T. M., Cedergren, R., & Gray, M. W. 1996, "Sequences homologous to yeast mitochondrial and bacteriophage T3 and T7 RNA polymerases are widespread throughout the eukaryotic lineage", *Nucleic Acids Res.*, vol. 24, no. 4, pp. 648-654.

Chang, J. R., Choi, J. J., Kim, H. K., & Kwon, S. T. 2001, "Purification and properties of Aquifex aeolicus DNA polymerase expressed in *Escherichia coli*", *FEMS Microbiol.Lett.*, vol. 201, no. 1, pp. 73-77.

Chavalitshewinkoon, P., de Vries, E., Stam, J. G., Franssen, F. F., van der Vliet, P. C., & Overdulve, J. P. 1993, "Purification and characterization of DNA polymerases from *Plasmodium falciparum*", *Mol.Biochem.Parasitol.*, vol. 61, no. 2, pp. 243-253.

Chen, F., & Lu, J. 2002, "Genomic sequence and evolution of marine cyanophage P60: a new insight on lytic and lysogenic phages", *Appl. Environ. Microbiol.*, vol. 68, no. 5, pp. 2589-2594.

Choi, J. J., Jung, S. E., Kim, H. K., & Kwon, S. T. 1999, "Purification and properties of *Thermus filiformis* DNA polymerase expressed in *Escherichia coli*", *Biotechnol.Appl.Biochem*, vol. 30 (Pt 1), pp. 19-25.

Chomczynski, P. & Sacchi, N. 1987, "Single-step method of RNA isolation by acid guanidinium thiocyanate-phenol-chloroform extraction", *Anal.Biochem*, vol. 162, no. 1, pp. 156-159.

Clarke, J. L., Scopes, D. A., Sodeinde, O., & Mason, P. J. 2001, "Glucose-6-phosphate dehydrogenase-6-phosphogluconolactonase. A novel bifunctional enzyme in malaria parasites", *Eur.J.Biochem.*, vol. 268, no. 7, pp. 2013-2019.

Cloonan, N., Fischer, K., Cheng, Q., & Saul, A. 2001, "Aldolase genes of *Plasmodium* species", *Mol.Biochem.Parasitol*, vol. 113, no. 2, pp. 327-330.

D

De Vries, E., Stam, J. G., Franssen, F. F., van der Vliet, P. C., & Overdulve, J. P. 1991, "Purification and characterization of DNA polymerases from *Plasmodium berghei*", *Mol.Biochem.Parasitol.*, vol. 45, no. 2, pp. 223-232.

Deckert, G., Warren, P.V., Gaasterland, T., Young, W.G., Lenox, A.L., Graham, D.E., Overbeek, R., Snead, M.A., Keller, M., Aujay, M., Huber, R., Feldman, R.A., Short, J.M., Olsen, G.J., & Swanson, R.V. 1998, "The complete genome of the hyperthermophilic bacterium *Aquifex aeolicus*", *Nature* vol. 392, no. 6674, pp. 353-358.

Delarue, M., Poch, O., Tordo, N., Moras, D., & Argos, P. 1990, "An attempt to unify the structure of polymerases", *Protein Eng*, vol. 3, no. 6, pp. 461-467.

Delwiche, C. F., & Palmer, J. D. 1997, "The origin of plastids and their spread via secondary symbiosis", *Plant Syst.Evol.*, vol.11, pp 53-86.

Derbyshire, V., Pinsonneault, J. K., & Joyce, C. M. 1995, "Structure-function analysis of 3'-->5'-exonuclease of DNA polymerases", *Methods Enzymol.*, vol. 262, pp. 363-385.

Dingman, C.W. 1974, "Bidirectional chromosome replication: some toplogical considerations. " *J.Theor.Biol.*, vol. 43, no.1, pp. 187-195.

Dominguez, O., Ruiz, J. F., Lain, d. L., Garcia-Diaz, M., Gonzalez, M. A., Kirchhoff, T., Martinez, A., Bernad, A., & Blanco, L. 2000, "DNA polymerase mu (Pol mu), homologous to TdT, could act as a DNA mutator in eukaryotic cells", *EMBO J.*, vol. 19, no. 7, pp. 1731-1742.

Doublie, S., Tabor, S., Long, A. M., Richardson, C. C., & Ellenberger, T. 1998, "Crystal structure of a bacteriophage T7 DNA replication complex at 2.2 A resolution", *Nature*, vol. 391, no. 6664, pp. 251-258.

Dunn, J.J., & Studier, F.W. 1983, "The nucleotide sequence of bacteriophage T7 DNA and the locations of T7 genetic elements", *J. Mol. Biol.*, vol. 166, no. 4, no. 477-535.

F

Feagin, J. E., Gardner, M. J., Williamson, D. H., & Wilson, R. J. 1991, "The putative mitochondrial genome of *Plasmodium falciparum*", *J.Protozool.*, vol. 38, no. 3, pp. 243-245.

Feagin, J. E. 1992, "The 6-kb element of *Plasmodium falciparum* encodes mitochondrial cytochrome genes", *Mol.Biochem.Parasitol.*, vol. 52, no. 1, pp. 145-148.

Fichera, M. E., & Roos, D. S. 1997, "A plastid organelle as a drug target in apicomplexan parasites", *Nature*, vol. 390, no. 6658, pp. 407-409.

Filée, J., Forterre, P., Sen-Lin, T., & Laurent, J. 2001, "Evolution of DNA polymerase families: evidences for multiple gene exchange between cellular and viral proteins", *J.Mol.Evol.*, vol. 54, no. 6, pp. 763-773.

Filée, J., Forterre, P., & Laurent, J. 2003, "The role played by viruses in the evolution of their hosts: a view based on informational protein phylogenies", *Res.Microbiol.*, vol. 154, no. 4, pp. 237-243.

Forterre, P. 1999, "Displacement of cellular proteins by functional analogues from plasmids or viruses could explain puzzling phylogenies of many DNA informational proteins", *Mol. Microbiol.*, vol. 33, no. 3, pp. 457-465.

Foth, B. J., Ralph, S. A., Tonkin, C. J., Struck, N. S., Fraunholz, M., Roos, D. S., Cowman, A. F., & McFadden, G. I. 2003, "Dissecting apicoplast targeting in the malaria parasite *Plasmodium falciparum*", *Science*, vol. 299, no. 5607, pp. 705-708.

Frick, D.N., & Richardson, C.C. 2001, "DNA primases", *Annu.Rev.Biochem.*, vol. 70, pp. 39-80.

Friedberg, E. C., Feaver, W. J., & Gerlach, V. L. 2000, "The many faces of DNA polymerases: strategies for mutagenesis and for mutational avoidance", *Proc.Natl.Acad Sci.U.S.A*, vol. 97, no. 11, pp. 5681-5683.

Fry, D. C., Kuby, S. A., & Mildvan, A. S. 1986, "ATP-binding site of adenylate kinase: mechanistic implications of its homology with ras-encoded p21, F1-ATPase, and other nucleotide-binding proteins", *Proc.Natl.Acad Sci.U.S.A*, vol. 83, no. 4, pp. 907-911.

Fuks, B. & Schnell, D. J. 1997, "Mechanism of Protein Transport across the Chloroplast Envelope", *Plant Physiol.*, vol. 114, no. 2, pp. 405-410.

Fuller, R. S., & Kornberg, A. 1983, "Purified DnaA protein in initiation of replication at the *Escherichia coli* chromosomal origin of replication", *Proc.Natl.Acad Sci.U.S.A*, vol. 80, no. 19, pp. 5817-5821.

Fuller, C. W., & Richardson, C. C. 1985, "Initiation of DNA replication at the primary origin of bacteriophage T7 by purified proteins. Site and direction of initial DNA synthesis", *J.Biol.Chem.*, vol. 260, no. 5, pp. 3185-3196.

G

Gaikwad, A., Hop, D. V., & Mukherjee, S. K. 2002, "A 70-kDa chloroplast DNA polymerase from pea (*Pisum sativum*) that shows high processivity and displays moderate fidelity", *Mol.Genet.Genomics*, vol. 267, no. 1, pp. 45-56.

Garcia-Diaz, M., Dominguez, O., Lopez-Fernandez, L. A., de Lera, L. T., Saniger, M. L., Ruiz, J. F., Parraga, M., Garcia-Ortiz, M. J., Kirchhoff, T., del Mazo, J., Bernad, A., & Blanco, L. 2000, "DNA polymerase lambda (Pol lambda), a novel eukaryotic DNA polymerase with a potential role in meiosis", *J.Mol.Biol.*, vol. 301, no. 4, pp. 851-867.

Gardner, M. J., Bates, P. A., Ling, I. T., Moore, D. J., McCready, S., Gunasekera, M. B., Wilson, R. J., & Williamson, D. H. 1988, "Mitochondrial DNA of the human malarial parasite *Plasmodium falciparum*", *Mol.Biochem.Parasitol.*, vol. 31, no. 1, pp. 11-17.

Gardner, M. J., Williamson, D. H., & Wilson, R. J. 1991a, "A circular DNA in malaria parasites encodes an RNA polymerase like that of prokaryotes and chloroplasts", *Mol.Biochem.Parasitol.*, vol. 44, no. 1, pp. 115-123.

Gardner, M. J., Feagin, J. E., Moore, D. J., Spencer, D. F., Gray, M. W., Williamson, D. H., & Wilson, R. J. 1991b, "Organisation and expression of small subunit ribosomal RNA genes encoded by a 35-kilobase circular DNA in *Plasmodium falciparum*", *Mol.Biochem.Parasitol.*, vol. 48, no. 1, pp. 77-88.

Gardner, M. J., Feagin, J. E., Moore, D. J., Rangachari, K., Williamson, D. H., & Wilson, R. J. 1993, "Sequence and organization of large subunit rRNA genes from the extrachromosomal 35 kb circular DNA of the malaria parasite *Plasmodium falciparum*", *Nucleic Acids Res.*, vol. 21, no. 5, pp. 1067-1071.

Gardner, M. J., Preiser, P., Rangachari, K., Moore, D., Feagin, J. E., Williamson, D. H., & Wilson, R. J. 1994, "Nine duplicated tRNA genes on the plastid-like DNA of the malaria parasite *Plasmodium falciparum*", *Gene*, vol. 144, no. 2, pp. 307-308.

Gardner, M. J. 1999, "The genome of the malaria parasite", *Curr.Opin.Genet.Dev.*, vol. 9, no. 6, pp. 704-708.

Gardner, M. J., Hall, N., Fung, E., White, O., Berriman, M., Hyman, R. W., Carlton, J. M., Pain, A., Nelson, K. E., Bowman, S., Paulsen, I. T., James, K., Eisen, J. A., Rutherford, K., Salzberg, S. L., Craig, A., Kyes, S., Chan, M. S., Nene, V., Shallom, S. J., Suh, B., Peterson, J., Angiuoli, S., Pertea, M., Allen, J., Selengut, J., Haft, D., Mather, M. W., Vaidya, A. B., Martin, D. M., Fairlamb, A. H., Fraunholz, M. J., Roos, D. S., Ralph, S. A., McFadden, G. I., Cummings, L. M., Subramanian, G. M., Mungall, C., Venter, J. C., Carucci, D. J., Hoffman, S. L., Newbold, C., Davis, R. W., Fraser, C. M., & Barrell, B. 2002, "Genome sequence of the human malaria parasite *Plasmodium falciparum*", *Nature*, vol. 419, no. 6906, pp. 498-511.

Gibbs, P.E., McGregor, W. G., Maher,V. M., Nisson, P., & Lawrence, C. W. 1998, "A human homolog of the *Saccharomyces cerevisiae REV3* gene, which encodes the catalytic subunit of DNA polymerase zeta", *Proc.Natl.Acad.Sci.U.S.A.*, vol. 95, no. 12, pp. 6876-6880.

Gorbalenya, A. E., Koonin, E. V., Donchenko, A. P., & Blinov, V. M. 1989, "Two related superfamilies of putative helicases involved in replication, recombination, repair and expression of DNA and RNA genomes", *Nucleic Acids Res.*, vol. 17, no. 12, pp. 4713-4730.

Gorbalenya, A. E., Koonin, E. V., & Wolf, Y. I. 1990, "A new superfamily of putative NTP-binding domains encoded by genomes of small DNA and RNA viruses", *FEBS Lett.*, vol. 262, no. 1, pp. 145-148.

Gorbalenya, A. E., & Koonin, E. V. 1993, "Helicases: amino acid sequence comparisons and structure-function relationships", *Curr.Opin.Struct.Biol.*, vol. 3, pp. 419-429.

Gray, M. W. 1993, "Origin and evolution of organelle genomes", *Curr.Opin.Genet.Dev.*, vol. 3, no. 6, pp. 884-890.

Gray, M. W. & Lang, B. F. 1998, "Transcription in chloroplasts and mitochondria: a tale of two polymerases", *Trends Microbiol.*, vol. 6, no. 1, pp. 1-3.

Guex, N. & Peitsch, M. C. 1997, "SWISS-MODEL and the Swiss-PdbViewer: an environment for comparative protein modeling", *Electrophoresis*, vol. 18, no. 15, pp. 2714-2723.

H

Hall, M. C., & Matson, S. W. 1999, "Helicase motifs: the engine that powers DNA unwinding", *Mol.Microbiol.*, vol. 34, no. 5, pp. 867-877.

Harris, P. V., Mazina, O. M., Leonhardt, E. A., Case, R. B., Boyd, J. B., & Burtis, K. C. 1996, "Molecular cloning of *Drosophila* mus308, a gene involved in DNA cross-link repair with homology to prokaryotic DNA polymerase I genes", *Mol.Cell Biol.*, vol. 16, no. 10, pp. 5764-5771.

Harwood, J. L. 1996, "Recent advances in the biosynthesis of plant fatty acids", *Biochim.Biophys.Acta*, vol. 1301, no. 1-2, pp. 7-56.

He, C. Y., Shaw, M. K., Pletcher, C. H., Striepen, B., Tilney, L. G., & Roos, D. S. 2001, "A plastid segregation defect in the protozoan parasite *Toxoplasma gondii*", *EMBO J.*, vol. 20, no. 3, pp. 330-339.

Hedtke, B., Borner, T., & Weihe, A. 1997, "Mitchondrial and chloroplast phage-type RNA polymerases in *Arabidopsis*", *Science*, vol. 277, no. 5327, pp. 809-811.

Hedtke, B., Borner, T., & Weihe, A. 2000, "One RNA polymerase serving two genomes", *EMBO Rep.*, vol. 1, no. 5, pp. 435-440.

Hellgren, U., Berggreb-Palme, I., Bergqvist, Y. and Jerling, M. 1997, "Enantioselective pharmacokinetics of mefloquine during long-term intake of the prophylactic dose", *Br.J. Clin.Pharmacol.*, vol. 44, pp. 119 -124.

Hien, T. T., & White, N. J. 1993, "Qinghaosu", *Lancet*, vol, 341, no. 8845, pp. 603-608.

Horrocks, P., Jackson, M., Cheesman, S., White, J. H., & Kilbey, B.J. 1996, "Stage specific expression of proliferating cell nuclear antigen and DNA polymerase delta from *Plasmodium falciparum*", *Mol.Biochem.Parasitol.*, vol. 79, no. 2, pp.177-182.

Hopkins, J., Fowler, R., Krishna, S., Wilson, I., Mitchell, G., & Bannister, L. 1999, "The plastid in *Plasmodium falciparum* asexual blood stages: a three- dimensional ultrastructural analysis", *Protist.*, vol. 150, no. 3, pp. 283-295.

Howe, C. J. 1992, "Plastid origin of an extrachromosomal DNA molecule from *Plasmodium*, the causative agent of malaria", *J.Theor.Biol.*, vol. 158, no. 2, pp. 199-205.

Huang, Y.P., Downie, J.A., & Ito, J. 1999, "Primary structure of the DNA polymerase I gene of an alpha-proteobacterium, *Rhizobium leguminosarum*, and comparison with other family A DNA polymerases", *Curr.Microbiol.*, vol. 38, no. 6, pp. 355-359.

Huang, J. & Levin, D. B. 2001, "Expression, purification and characterization of the *Spodoptera littoralis* nucleopolyhedrovirus (SpliNPV) DNA polymerase and interaction with the SpliNPV non-hr origin of DNA replication", *J.Gen.Virol.*, vol. 82, no. 7, pp. 1767-1776.

Huberts,P., & Mizrahi,V. 1995, "Cloning and sequence analysis of the gene encoding the DNA polymerase I from *Mycobacterium tuberculosis*", *Gene*, vol. 164, no. 1, pp. 133-136.

Hubscher, U., Nasheuer, H. P., & Syvaoja, J. E. 2000, "Eukaryotic DNA polymerases, a growing family", *Trends Biochem.Sci.*, vol. 25, no. 3, pp. 143-147.

I

Ilyina, T. V., Gorbalenya, A. E., & Koonin, E. V. 1992, "Organization and evolution of bacterial and bacteriophage primase- helicase systems", *J.Mol.Evol.*, vol. 34, no. 4, pp. 351-357.

Inselburg, J. & Banyal, H. S. 1984, "*Plasmodium falciparum*: synchronization of asexual development with aphidicolin, a DNA synthesis inhibitor", *Exp.Parasitol.*, vol. 57, no. 1, pp. 48-54.

Ito, J. & Braithwaite, D. K. 1991, "Compilation and alignment of DNA polymerase sequences", *Nucleic Acids Res.*, vol. 19, no. 15, pp. 4045-4057.

Ivanetich, K. M., & Santi, D.V. 1990, "Bifunctional thymidylate synthase-dihydrofolate reductase in protozoa", *FASEB J.*, vol. 4, no. 6, pp. 1591-1597.

J

Jeanmougin,F., Thompson,J.D., Gouy,M., Higgins,D.G., & Gibson,T.J. 1998, "Multiple sequence alignment with Clustal X". *Trends Biochem.Sci.*, vol 23, no. 10, pp. 403-5.

Jelenska, J., Crawford, M. J., Harb, O. S., Zuther, E., Haselkorn, R., Roos, D. S., & Gornicki, P. 2001, "Subcellular localization of acetyl-CoA carboxylase in the apicomplexan parasite *Toxoplasma gondii*", *Proc.Natl.Acad.Sci U.S.A*, vol. 98, no. 5, pp. 2723-2728.

Jensen, J.B., & Trager, W. 1978, "Some recent advances in the cultivation of *Plasmodium falciparum*", *Isr.J.Med.Sci.*, vol. 14, no. 5, pp. 563-70.

Jomaa, H., Wiesner, J., Sanderbrand, S., Altincicek, B., Weidemeyer, C., Hintz, M., Turbachova, I., Eberl, M., Zeidler, J., Lichtenthaler, H. K., Soldati, D., & Beck, E. 1999, "Inhibitors of the nonmevalonate pathway of isoprenoid biosynthesis as antimalarial drugs", *Science*, vol. 285, no. 5433, pp. 1573-1576.

Joseph, J. T., Aldritt, S. M., Unnasch, T., Puijalon, O., & Wirth, D. F. 1989, "Characterization of a conserved extrachromosomal element isolated from the avian malarial parasite *Plasmodium gallinaceum*", *Mol.Cell Biol.*, vol. 9, no. 9, pp. 3621-3629.

Joyce, C. M., & Grindley, N. D. 1984, "Method for determining whether a gene of *Escherichia coli* is essential: application to the polA gene", *J.Bacteriol.*, vol. 158, no. 2, pp. 636-643.

Joyce, C.M., Kelley, W.S., Grindley, N.D. 1982, "Nucleotide sequence of the *Escherichia coli polA* gene and primary structure of DNA polymerase I", *J.Biol.Chem.*, vol. 257, no. 4, pp. 1958-1964.

Joyce, C. M. & Steitz, T. A. 1994, "Function and structure relationships in DNA polymerases", *Annu.Rev.Biochem*, vol. 63, pp. 777-822.

Joyce, C. M. & Steitz, T. A. 1995, "Polymerase structures and function: variations on a theme?", *J.Bacteriol.*, vol. 177, no. 22, pp. 6321-6329.

Joyce, C. M. 1997, "Choosing the right sugar: how polymerases select a nucleotide substrate", *Proc.Natl.Acad Sci.U.S.A*, vol. 94, no. 5, pp. 1619-1622.

K

Kaneko, T., Tanaka, A., Sato, S., Kotani, H., Sazuka, T., Miyajima, N., Sugiura, M. & Tabata, S. 1995, "Sequence analysis of the genome of the unicellular cyanobacterium *Synechocystis* sp. strain PCC6803. I. Sequence features in the 1 Mb region from map positions 64% to 92% of the genome", *DNA Res.*, vol. 2, no. 4, pp. 153-166.

Karam, J. D., & Konigsberg, W. H. 2000, "DNA polymerase of the T4-related bacteriophages", *Prog.Nucleic Acid Res.Mol.Biol.*, vol. 64, pp. 65-96.

Kedzierski, L., Escalante, A. A., Isea, R., Black, C. G., Barnwell, J. W., & Coppel, R. L. 2002, "Phylogenetic analysis of the genus *Plasmodium* based on the gene encoding adenylosuccinate lyase", *Infect.Genet.Evol.*, vol. 1, no. 4, pp. 297-301.

Kelman, Z. & O'Donnell, M. 1995, "DNA polymerase III holoenzyme: structure and function of a chromosomal replicating machine", *Annu.Rev.Biochem*, vol. 64, pp. 171-200.

Kilbey, B. J., Fraser, I., McAleese, S., Goman, M., & Ridley, R.G. 1993, "Molecular characterisation and stage-specific expression of proliferating cell nuclear antigen (PCNA) from the malarial parasite, *Plasmodium falciparum*", *Nucleic Acids Res.* vol. 21, no. 2, pp.239-243.

Killick-Kendrick, R. 1978, "Taxonomy, zoogeography and evolution," in *Rodent Malaria*, R. P. W. Killick-Kendrick, ed., Academic Press, London, pp. 1-53.

Kimura, S., Uchiyama, Y., Kasai, N., Saotome, A., Ueda, T., Ando, T., Ishibashi, T., Namekawa, S., Oshige, M., Furukawa, T., Yamamoto,T., Hashimoto, J., & Sakaguchi, K. 2002, "A novel DNA polymerase homologous to *Escherichia coli* DNA polymerase I from a higher plant, rice (*Oryza sativa L.*) ", *Nucleic Acids Res.*, vol. 30, no. 7, pp. 1585-1592.

Klenow, H. & Overgaard-Hansen, K. 1970, "Proteolytic cleavage of DNA polymerase from *Escherichia coli* B into an exonuclease unit and a polymerase unit", *FEBS Lett.*, vol. 6, no. 1, pp. 25-27.

Kohler, S., Delwiche, C. F., Denny, P. W., Tilney, L. G., Webster, P., Wilson, R. J., Palmer, J. D., & Roos, D. S. 1997, "A plastid of probable green algal origin in Apicomplexan parasites", *Science*, vol. 275, no. 5305, pp. 1485-1489.

Kornberg, A. 1960, "Biological synthesis of deoxyribonucleic acid", *Science*, vol. 131, pp. 1503-1508.

Kornberg, A., & Baker, T. 1992, "*DNA replication*", 2nd edn. New York. W.H. Freeman and Company.

Kornberg, A. 1984, "Enzyme studies of replication of the Escherichia coli chromosome", *Adv.Exp.Med.Biol.*, vol. 179, pp. 3-16.

Korolev, S., Nayal, M., Barnes, W. M., Di Cera, E., & Waksman, G. 1995, "Crystal structure of the large fragment of *Thermus aquaticus* DNA polymerase I at 2.5-A resolution: structural basis for thermostability", *Proc.Natl.Acad Sci.U.S.A*, vol. 92, no. 20, pp. 9264-9268.

Korolev, S., Hsieh, J., Gauss, G. H., Lohman, T. M., & Waksman, G. 1997, "Major domain swiveling revealed by the crystal structures of complexes of *Escheichia coli* Rep helicase bound to single-stranded DNA and ADP", *Cell*, vol. 90, no. 4, pp. 635-647.

Kowalski, D., & Eddy, M. J. 1989, "The DNA unwinding element: a novel, cis-acting component that facilitates opening of the *Escherichia coli* replication origin", *EMBO J.*, vol. 8, no. 13, pp. 4335-4344.

Krause, T., Luersen, K., Wrenger, C., Gilberger, T. W., Muller, S., & Walter, R. D. 2000, "The ornithine decarboxylase domain of the bifunctional ornithine decarboxylase/S-adenosylmethionine decarboxylase of *Plasmodium falciparum*: recombinant expression and catalytic properties of two different constructs", *Biochem.J.*, vol. 352 Pt 2, pp. 287-292.

Kumar, S., Tamura, K., Jakobsen, I. B., & Nei, M. 2001, "MEGA2: molecular evolutionary genetics analysis software", *Bioinformatics.*, vol. 17, no. 12, pp. 1244-1245.

Kunst, F., Ogasawara, N., Moszer, I., Albertini, A.M., Alloni, G., Azevedo, V., Bertero, M.G., Bessieres, P., Bolotin, A., Borchert, S., Borriss, R., Boursier, L., Brans, A., Braun, M., Brignell, S.C., Bron, S., Brouillet, S., Bruschi, C.V., Caldwell, B., Capuano, V., Carter, N.M., Choi, S.K., Codani, J.J., Connerton, I.F., Cummings, N.J., Daniel, R.A., Denizot, F., Devine, K.M., Dusterhoft, A., Ehrlich, S.D., Emmerson, P.T., Entian, K.D., Errington, J., Fabret,C., Ferrari, E., Foulger, D., Fritz, C., Fujita, M., Fujita, Y., Fuma, S., Galizzi, A., Galleron, N., Ghim, S.Y., Glaser, P., Goffeau, A., Golightly, E.J., Grandi, G., Guiseppi, G., Guy, B.J., Haga, K., Haiech, J., Harwood, C.R., Henaut, A., Hilbert, H., Holsappel, S., Hosono, S., Hullo, M.F., Itaya, M., Jones, L., Joris, B., Karamata, D., Kasahara, Y., Klaerr-Blanchard, M., Klein, C., Kobayashi, Y., Koetter, P., Koningstein, G., Krogh, S., Kumano, M., Kurita, K., Lapidus, A., Lardinois, S., Lauber, J., Lazarevic, V., Lee, S.M., Levine, A., Liu, H., Masuda, S., Mauel, C., Medigue, C., Medina, N., Mellado, R.P., Mizuno, M., Moestl, D., Nakai, S., Noback, M., Noone, D., O'Reilly, M., Ogawa, K., Ogiwara, A., Oudega, B., Park, S.H., Parro, V., Pohl, T.M., Portetelle, D., Porwollik, S., Prescott, A.M., Presecan, E., Pujic, P., Purnelle, B., Rapoport, G., Rey, M., Reynolds, S., Rieger, M., Rivolta, C., Rocha, E., Roche, B., Rose, M., Sadaie, Y., Sato, T., Scanlan, E., Schleich, S., Schroeter, R., Scoffone, F., Sekiguchi, J., Sekowska, A., Seror, S.J., Serror, P., Shin, B.S., Soldo, B., Sorokin, A., Tacconi, E., Takagi,T., Takahashi, H., Takemaru, K., Takeuchi , M., Tamakoshi, A., Tanaka, T., Terpstra, P., Tognoni, A., Tosato, V., Uchiyama, S., Vandenbol, M., Vannier, F., Vassarotti, A., Viari, A., Wambutt, R., Wedler, E., Wedler, H., Weitzenegger, T., Winters, P., Wipat, A., Yamamoto, H., Yamane, K., Yasumoto, K., Yata, K., Yoshida, K., Yoshikawa, H.F., Zumstein, E., Yoshikawa, H., & Danchin, A. 1997, "The complete genome sequence of the gram-positive bacterium *Bacillus subtilis*", *Nature*, vol. 390, no. 6657, pp. 249-256.

Kusakabe, T. & Richardson, C. C. 1996, "The role of the zinc motif in sequence recognition by DNA primases", *J.Biol.Chem.*, vol. 271, no. 32, pp. 19563-19570.

L

Laemmli, U. K. 1970, "Cleavage of structural proteins during the assembly of the head of bacteriophage T4", *Nature*, vol. 227, pp. 680-685.

Law, A. E., Mullineaux, C. W., Hirst, E. M., Saldanha, J., & Wilson, R. J. 2000, "Bacterial orthologues indicate the malarial plastid gene ycf24 is essential", *Protist.*, vol. 151, no. 4, pp. 317-327.

Lawyer, F.C., Stoffel, S., Saiki, R.K., Myambo, K., Drummond, R., & Gelfand, D.H. 1989, "Isolation, characterization, and expression in *Escherichia coli* of the DNA polymerase gene from *Thermus aquaticus*", *J.Biol.Chem.*, vol. 264, no. 11, pp. 6427-6437.

Leipe, D. D., Aravind, L., Grishin, N. V., & Koonin, E. V. 2000, "The bacterial replicative helicase DnaB evolved from a RecA duplication", *Genome Res.*, vol. 10, pp. 5-16.

Lell, B., & Kremsner, P. G. 2002, "Clindamycin as an antimalarial drug: review of clinical trials", *Antimicrob. Agents Chemother.*, vol. 46, no. 8, pp.2315-2320.

Lemon, K. P., & Grossman, A. D. 1998, "Localisation of bacterial DNA polymerase: evidence for a factory model of replication", *Science*, vol. 282, no.5393, pp. 1516-1519.

Le Roch, K.G., Zhou, Y., Blair, P. L., Grainger, M., Moch, J. K., Haynes, J. D., De La Vega, P., Holder, A. A., Batalov, S., Carucci, D. J., & Winzeler, E. A. 2003, "Discovery of gene function by expression profiling of the malaria parasite life cycle", *Science*, vol.301, no. 5639, pp. 1503-1508.

Lewis, D. L., Farr, C. L., Wang, Y., Lagina, A.T. 3rd., & Kaguni, L. S. 1996, "Catalytic subunit of mitochondrial DNA polymerase from *Drosophila* embryos. Cloning, bacterial overexpression, and biochemical characterization", *J.Biol.Chem.*, vol 271, no. 38 pp 23389-23394.

Lipps, G., Rother, S., Hart, C., & Krauss, G. 2003, "A novel type of replicative enzyme harbouring ATPase, primase and DNA polymerase activity", *EMBO J.*, vol. 22, no. 10, pp. 2516-2525.

M

Marians, K. J. 2000, "Crawling and wiggling on DNA: structural insights to the mechanism of DNA unwinding by helicases", *Structure.Fold.Des*, vol. 8, no. 12, p. R227-R235.

Marini, F. & Wood, R. D. 2002, "A human DNA helicase homologous to the DNA cross-link sensitivity protein Mus308", *J.Biol.Chem.* , vol. 277, no. 10, pp. 8716-8723.

Martin, W. & Herrmann, R. G. 1998, "Gene transfer from organelles to the nucleus: how much, what happens, and Why?", *Plant Physiol.*, vol. 118, no. 1, pp. 9-17.

Masutani, C., Araki, M., Yamada, A., Kusumoto, R., Nogimori, T., Maekawa, T., Iwai, S., & Hanaoka, F. 1999, "*Xeroderma pigmentosum* variant (XP-V) correcting protein from HeLa cells has a thymine dimer bypass DNA polymerase activity", *EMBO J.*, vol. 18, no. 12, pp. 3491-3501.

Matesanz, F., Duran-Chica, I., & Alcina, A. 1999, "The cloning and expression of Pfacs1, a *Plasmodium falciparum* fatty acyl coenzyme A synthetase-1 targeted to the host erythrocyte cytoplasm", *J.Mol.Biol*, vol. 291, no. 1, pp. 59-70.

Matson, S. W., & Kaiser-Rogers, K. A. 1990, "DNA helicases", *Annu.Rev.Biochem.*, vol. 59, pp. 289-329.

Matson, S. W. 1991, "DNA helicases of *Escherichia coli*", *Prog.Nucleic Acid Res.Mol.Biol.*, vol. 40, pp. 289-326.

Matsui, M., Oka, A., Takanami, M., Yasuda, S., & Hirota, Y. 1985, "Sites of dnaA protein-binding in the replication origin of the *Escherichia coli* K-12 chromosome", *J.Mol.Biol.*, vol. 184, no. 3, pp. 529-533.

McClelland, M., Sanderson, K.E., Spieth, J., Clifton, S.W., Latreille, P., Courtney, L., Porwollik, S., Ali, J., Dante, M., Du, F., Hou, S., Layman, D., Leonard, S., Nguyen, C., Scott, K., Holmes, A., Grewal, N., Mulvaney, E., Ryan, E., Sun, H., Florea, L., Miller, W., Stoneking, T., Nhan, M., Waterston, & R., Wilson, R.K. 2001, "Complete genome sequence of *Salmonella enterica serovar Typhimurium* LT2", *Nature*, vol. 413, no. 6858, pp. 852-856.

McConkey, G. A., Rogers, M. J., & McCutchan, T. F. 1997, "Inhibition of *Plasmodium falciparum* protein synthesis. Targeting the plastid-like organelle with thiostrepton", *J.Biol. Chem.*, vol. 272, no. 4, pp. 2046-2049.

McFadden, G. I. & Waller, R. F. 1997, "Plastids in parasites of humans", *Bioessays*, vol. 19, no. 11, pp. 1033-1040.

McFadden, G. I. & Roos, D. S. 1999, "Apicomplexan plastids as drug targets", *Trends Microbiol.*, vol. 7, no. 8, pp. 328-333.

Mendelman, L. V., Beauchamp, B. B., & Richardson, C. C. 1994, "Requirement for a zinc motif for template recognition by the bacteriophage T7 primase", *EMBO J.*, vol. 13, no. 16, pp. 3909-3916.

Meshnik, E. 2002, "Artemisinin: mechanisms of action, resistance and toxicity", *Int.J.Parasitol.*, vol. 32, no. 13, pp. 1655-1660.

Morgenstern, B., Dress, A., & Werner, T. 1996, "Multiple DNA and protein sequence alignment based on segment-to-segment comparison", *Proc.Natl.Acad Sci.U.S.A*, vol. 93, no. 22, pp. 12098-12103.

Moriya, S., Ogasawara, N., & Yoshikawa, H. 1985, "Structure and function of the region of the replication origin of the *Bacillus subtilis* chromosome. III. Nucleotide sequence of some 10,000 base pairs in the origin region", *Nucleic Acids Res.*, vol. 13, no. 7, pp. 2251-2265.

Morrison, A., Bell, J. B., Kunkel, T. A., & Sugino, A. 1991, "Eukaryotic DNA polymerase amino acid sequence required for 3'----5' exonuclease activity", *Proc.Natl.Acad Sci.U.S.A*, vol. 88, no. 21, pp. 9473-9477.

Müller, S., Da'dara, A., Luersen, K., Wrenger, C., Das, G. R., Madhubala, R., & Walter, R. D. 2000, "In the human malaria parasite *Plasmodium falciparum*, polyamines are synthesized by a bifunctional ornithine decarboxylase, S- adenosylmethionine decarboxylase", *J.Biol.Chem.*, vol. 275, no. 11, pp. 8097-8102.

N

Nagasawa, K., Kitamura, K., Yasui, A., Nimura, Y., Ikeda, K., Hirai, M., Matsukage, A., & Nakanishi, M. 2000, "Identification and characterization of human DNA polymerase beta 2, a DNA polymerase beta -related enzyme", *J.Biol.Chem.*, vol. 275, no. 40, pp. 31233-31238.

Nakayama, N., Arai, N., Bond, M.W., Kaziro,Y., & Arai, K. 1984, "Nucleotide sequence of dnaB and the primary structure of the dnaB protein from *Escherichia coli*", *J.Biol. Chem.*, vol. 259, no. 1, pp. 97-101.

Nelson, J. R., Lawrence, C. W., & Hinkle, D. C. 1996, "Thymine-thymine dimer bypass by yeast DNA polymerase zeta", *Science*, vol. 272, no. 5268, pp. 1646-1649.

Nelson, K.E., Clayton, R.A., Gill, S.R., Gwinn, M.L., Dodson, R.J., Haft, D.H., Hickey, E.K., Peterson, J.D., Nelson, W.C., Ketchum, K.A., McDonald, L., Utterback, T.R., Malek, J.A., Linher, K.D., Garrett, M.M., Stewart, A.M., Cotton, M.D., Pratt, M.S., Phillips, C.A., Richardson, D., Heidelberg, J., Sutton, G.G., Fleischmann, R.D., Eisen, J.A., & Fraser, C.M. 1999, "Evidence for lateral gene transfer between Archaea and bacteria from genome sequence of *Thermotoga maritima*", *Nature* vol. 399, no. 6734, pp. 323-329.

Nelson, K., Paulsen, I., Weinel, C., Dodson, R., Hilbert, H., Fouts, D.,Gill, S., Pop, M., Martins Dos Santos, V., Holmes, M., Brinkac, L., Beanan, M., DeBoy, R., Daugherty, S., Kolonay, J., Madupu, R., Nelson, W., White, O., Peterson, J., Khouri, H., Hance, I., Lee, P., Holtzapple, E., Scanlan, D., Tran, K., Moazzez, A., Utterback, T., Rizzo, M., Lee, K., Kosack, D., Moestl, D., Wedler, H., Lauber, J., Hoheisel, J., Straetz, M., Heim, S., Kiewitz, C., Eisen, J., Timmis, K., Duesterhoft, A., Tummler, B., & Fraser, C. 2002, "Complete genome sequence and comparative analysis of the metabolically versatile *Pseudomonas putida* KT2440", *Environ. Microbiol.*, vol. 4, no. 12, pp. 799-808.

Nielsen, H., Engelbrecht, J., Brunak, S., & von Heijne, G. 1997, "Identification of prokaryotic and eukaryotic signal peptides and prediction of their cleavage sites", *Protein Eng.*, vol. 10, no. 1, pp. 1-6.

O

Ohashi, E., Bebenek, K., Matsuda, T., Feaver, W. J., Gerlach, V. L., Friedberg, E. C., Ohmori, H., & Kunkel, T. A. 2000, "Fidelity and processivity of DNA synthesis by DNA polymerase kappa, the product of the human DINB1 gene", *J.Biol.Chem.*, vol. 275, no. 50, pp. 39678-39684.

Ohmori, H., Friedberg, E. C., Fuchs, R. P., Goodman, M. F., Hanaoka, F., Hinkle, D., Kunkel, T. A., Lawrence, C. W., Livneh, Z., Nohmi, T., Prakash, L., Prakash, S., Todo, T., Walker, G. C., Wang, Z., & Woodgate, R. 2001, "The Y-family of DNA polymerases", *Mol.Cell*, vol. 8, no. 1, pp. 7-8.

Ollis, D. L., Brick, P., Hamlin, R., Xuong, N. G., & Steitz, T. A. 1985, "Structure of large fragment of *Escherichia coli* DNA polymerase I complexed with dTMP", *Nature*, vol. 313, no. 6005, pp. 762-766.

Olsen, G. J. 1988, "Phylogenetic analysis using ribosomal RNA", *Methods Enzymol.*, vol. 164, pp. 793-812.

P

Pajunen, M.I., Kiljunen, S.J., Soderholm, M.E., & Skurnik, M. 2001, "Complete genomic sequence of the lytic bacteriophage phiYeO3-12 of *Yersinia enterocolitica* serotype O:3", *J. Bacteriol.*, vol. 183, no. 6, pp. 1928-1937.

Pajunen, M.I., Elizondo, M.R., Skurnik, M., Kieleczawa, J., & Molineux, I.J. 2002, "Complete nucleotide sequence and likely recombinatorial origin of bacteriophage T3", *J. Mol.Biol.*, vol. 319, no. 5, pp. 1115-1132.

Pandey, V. N., Williams, K. R., Stone, K. L., & Modak, M. J. 1987, "Photoaffinity labeling of the thymidine triphosphate binding domain in *Escherichia coli* DNA polymerase I: identification of histidine-881 as the site of cross-linking", *Biochemistry*, vol. 26, no. 24, pp. 7744-7748.

Pandey, V. N. & Modak, M. J. 1988, "Affinity labeling of *Escherichia coli* DNA polymerase I by 5'-fluorosulfonylbenzoyladenosine. Identification of the domain essential for polymerization and Arg-682 as the site of reactivity", *J.Biol.Chem.*, vol. 263, no. 13, pp. 6068-6073.

Pandey, V. N., Kaushik, N. A., Pradhan, D. S., & Modak, M. J. 1990, "Template primer-dependent binding of 5'-fluorosulfonyl-benzoyldeoxyadenosine by *Escherichia coli* DNA polymerase I. Identification of arginine 682 as the binding site and its implication in catalysis", *J.Biol.Chem.*, vol. 265, no. 7, pp. 3679-3684.

Pardoll, D.M., Vogelstein, B., & Coffey, D.S. 1980, "A fixed site of DNA replication in eukaryotic cells", *Cell*, vol 19, no.2, pp. 527-536.

Parkhill, J., Dougan, G., James, K.D., Thomson, N.R., Pickard, D., Wain, J., Churcher, C., Mungall, K.L., Bentley, S.D., Holden, M.T.G., Sebaihia, M., Baker, S., Basham, D., Brooks, K., Chillingworth, T., Connerton, P., Cronin, A., Davis, P., Davies, R.M., Dowd, L., White, N., Farrar, J., Feltwell, T., Hamlin, N., Haque, A., Hien, T.T., Holroyd, S., Jagels, K., Krogh, A., Larsen, T.S., Leather, S., Moule, S., O'Gaora, P., Parry, C., Quail, M., Rutherford, K., Simmonds, M., Skelton, J., Stevens, K., Whitehead, S., & Barrell, B.G. 2001, "Complete genome sequence of a multiple drug resistant *Salmonella enterica* serovar Typhi CT18", *Nature*, vol. 413, no. 6858, pp. 848-852.

Peitsch, M.C. 1996, "ProMod and Swiss-Model: Internet-based tools for automated comparative protein modelling", *Biochem.Soc.Trans.*, vol. 24, no. 1, pp. 274-279.

Podobnik, M., McInerney, P., O'Donnell, M., & Kuriyan, J. 2000, "A TOPRIM domain in the crystal structure of the catalytic core of *Escherichia coli* primase confirms a structural link to DNA topoisomerases", *J.Mol.Biol.*, vol. 300, no. 2, pp. 353-362.

Polesky, A. H., Steitz, T. A., Grindley, N. D., & Joyce, C. M. 1990, "Identification of residues critical for the polymerase activity of the Klenow fragment of DNA polymerase I from *Escherichia coli*", *J.Biol.Chem.*, vol. 265, no. 24, pp. 14579-14591.

Polesky, A. H., Dahlberg, M. E., Benkovic, S. J., Grindley, N. D., & Joyce, C. M. 1992, "Side chains involved in catalysis of the polymerase reaction of DNA polymerase I from *Escherichia coli*", *J.Biol.Chem.*, vol. 267, no. 12, pp. 8417-8428.

Pons, M. E., Diaz, A., Lacks, S. A., & Lopez, P. 1991, "The polymerase domain of *Streptococcus pneumoniae* DNA polymerase I. High expression, purification and characterization", *Eur.J.Biochem.*, vol. 201, no. 1, pp. 147-155.

Preiser, P. R., Wilson, R. J., Moore, P. W., McCready, S., Hajibagheri, M. A., Blight, K. J., Strath, M., & Williamson, D. H. 1996, "Recombination associated with replication of malarial mitochondrial DNA", *EMBO J.*, vol. 15, no. 3, pp. 684-693.

R

Ridley, R. G., White, J. H., McAleese, S. M., Goman, M., Alano, P., de Vries, E., & Kilbey, B. J. 1991, "DNA polymerase delta: gene sequences from *Plasmodium falciparum* indicate that this enzyme is more highly conserved than DNA polymerase alpha", *Nucleic Acids Res.*, vol. 19, no. 24, pp. 6731-6736.

Rimchala, P., Karbwang, J., Sukontason, K., Banmairuroi, V., Molunto, P and Na-Bangchang, K.1996. "Pharmacokinetics of quinine in patients with chronic renal failure", *Eur. J. Clin. Pharmacol.*, vol. 49, pp. 497-501.

Roos, D.S., Crawford, M. J., Donald, R, G, K., Kissinger, J.C., Klimczak, L, J., & Striepen, B. 1999, "Origin, targeting and function of the apicomplexan plastid", *Curr.Opin.Microbiol.*, vol. 2, pp. 426-432.

Rosenthal, P. J. 1996, "Conservation of key amino acids among the cysteine proteinases of multiple malarial species", *Mol.Biochem.Parasitol.*, vol. 75, no. 2, pp. 255-260.

S

Salas, M. 1991, "Protein-priming of DNA replication", *Annu.Rev.Biochem.*, vol. 60, pp. 39-71.

Salcedo, E., Cortese, J.F., Plowe, C.V., Sims, P.F.G., & Hyde, J.E. 2001, "A bifunctional dihydrofolate synthetase--folylpolyglutamate synthetase in *Plasmodium falciparum* identified by functional complementation in yeast and bacteria", *Mol.Biochem.Parasitol.*, vol. 112, no. 2, pp. 239-52.

Sambrook, J., Fristsch, E. F., & Maniatis, T. 1989, *Molecular cloning: A laboratory manual*, 2nd edn, Cold Spring Habour NY.

Sancar, A. 1996, "DNA excision repair", *Annu.Rev.Biochem.*, vol. 65, pp. 43-81.

Sato, S., Tews, I., & Wilson, R. J. 2000, "Impact of a plastid-bearing endocytobiont on apicomplexan genomes", *Int.J.Parasitol.*, vol. 30, no. 4, pp. 427-439.

Sato, S. & Wilson, R. J. 2002, "The genome of *Plasmodium falciparum* encodes an active delta-aminolevulinic acid dehydratase", *Curr.Genet.*, vol. 40, no. 6, pp. 391-398.

Sato, S., Rangachari, K., & Wilson, R. J. 2003, "Targeting GFP to the malarial mitochondrion", *Mol.Biochem.Parasitol.*, vol. 130, pp. 155-158.

Saul, A., & Battistutta, D. 1988, "Codon usage in *Plasmodium falciparum*", *Mol.Biochem. Parasitol.*, vol. 27, no. 1, pp. 35-42.

Sawaya, M. R., Guo, S., Tabor, S., Richardson, C. C., & Ellenberger, T. 1999, "Crystal structure of the helicase domain from the replicative helicase-primase of bacteriophage T7", *Cell*, vol. 99, no. 2, pp. 167-177.

Schwede, T., Kopp, J., Guex, N., & Peitsch, M. C. 2003, "SWISS-MODEL: An automated protein homology-modeling server", *Nucleic Acids Res.*, vol. 31, no. 13, pp. 3381-3385.

Seto, H., Hatanaka, M., Kimura, S., Oshige, M., Tsuya, Y., Mizushina, Y., Sawado, T., Aoyagi, N., Matsumoto, T., Hashimoto, J., & Sakaguchi, K. 1998, "Purification and characterization of a 100 kDa DNA polymerase from cauliflower inflorescence", *Biochem. J.*, vol. 332 (Pt 2), pp. 557-563.

Sharief, F. S., Vojta, P. J., Ropp, P. A., & Copeland, W. C. 1999, "Cloning and chromosomal mapping of the human DNA polymerase theta (POLQ), the eighth human DNA polymerase", *Genomics*, vol. 59, no. 1, pp. 90-96.

Sibley, C. H., Hyde, J. E., Sims, P. F., Plowe, C.V., Kublin, J. G., Mberu, E. K., Cowman, A. F., Winstanley, P. A., Watkins, W. M., & Nzila, A. M. 2001, "Pyrimethamine-sulfadoxine resistance in Plasmodium falciparum: what next? ", *Trends Parasitol.*, vol. 17, no. 12, pp. 582-588.

Singh, D., Chaubey, S., & Habib, S. 2003, "Replication of the Plasmodium falciparum apicoplast DNA initiates within the inverted repeat region", *Mol.Biochem.Parasitol.*, vol. 126, no. 1, pp. 9-14.

Smiley, B.L., Lupski, J.R., Svec, P.S., McMacken, R., & Godson, G.N.1982, "Sequences of the *Escherichia coli* dnaG primase gene and regulation of its expression", *Proc. Natl. Acad. Sci. U.S.A.*, vol. 79, no. 15, pp. 4550-4554.

Soll, J., & Tien, R. 1998, "Protein translocation into and across the chloroplastic envelope membranes", *Plant Mol.Biol.*, vol. 38, no. 1-2, pp. 191-207.

Soultanas, P., Dillingham, M. S., Velankar, S. S., & Wigley, D. B. 1999, "DNA binding mediates conformational changes and metal ion coordination in the active site of PcrA helicase", *J.Mol.Biol.*, vol. 290, no. 1, pp. 137-148.

Sousa, R. 1996, "Structural and mechanistic relationships between nucleic acid polymerases", *Trends Biochem.Sci.*, vol. 20, no. 5, pp. 186-190.

Spadari, S., Sala, F., & Pedrali-Noy, G. 1984, "Aphidicolin and eukaryotic DNA synthesis", *Adv.Exp.Med.Biol.*, vol. 179, pp. 169-181.

Spadari, S., Pedrali-Noy, G., Falaschi, M. C., & Ciarrocchi, G. 1984, "Control of DNA replication and cell proliferation in eukaryotes by aphidicolin", *Toxicol.Pathol.*, vol. 12, no. 2, pp. 143-148.

Spelbrink, J.N., Li, F.Y., Tiranti, V., Nikali, K., Yuan, Q.P.,Tariq, M., Wanrooij, S., Garrido, N., Comi, G., Morandi, L., Santoro, L., Toscano, A., Fabrizi, G.M., Somer, H., Croxen, R., Beeson, D., Poulton, J., Suomalainen, A., Jacobs, H.T., Zeviani, M., & Larsson, C. 2001, "Human mitochondrial DNA deletions associated with mutations in the gene encoding Twinkle, a phage T7 gene 4-like protein localized in mitochondria", *Nat. Genet.*, vol. 28, no. 3, pp. 223-231.

Steitz, T. A. 1998, "A mechanism for all polymerases", *Nature*, vol. 391, no. 6664, pp. 231-232.

Steitz, T. A. 1999, "DNA polymerases: structural diversity and common mechanisms", *J.Biol.Chem.*, vol. 274, no. 25, pp. 17395-17398.

Strack, B., Lessl, M., Calendar, R., & Lanka, E. 1992, "A common sequence motif, -E-G-Y-A-T-A-, identified within the primase domains of plasmid-encoded I- and P-type DNA primases and the alpha protein of the *Escherichia coli* satellite phage P4", *J.Biol.Chem.*, vol. 267, no. 18, pp. 13062-13072.

Surolia, N. & Padmanaban, G. 1991, "Chloroquine inhibits heme-dependent protein synthesis in *Plasmodium falciparum*", *Proc.Natl.Acad Sci.U.S.A*, vol. 88, no. 11, pp. 4786-4790.

Surolia, N. & Padmanaban, G. 1992, "de novo biosynthesis of heme offers a new chemotherapeutic target in the human malarial parasite", *Biochem.Biophys.Res.Commun.*, vol. 187, no. 2, pp. 744-750.

Surolia, N. & Surolia, A. 2001, "Triclosan offers protection against blood stages of malaria by inhibiting enoyl-ACP reductase of *Plasmodium falciparum*", *Nat.Med.*, vol. 7, no. 2, pp. 167-173.

Szafranski, P., Smith, C. L., & Cantor, C. R. 1997, "Cloning and analysis of the dnaG gene encoding *Pseudomonas putida* DNA primase", *Biochim.Biophys.Acta*, vol. 1352, no. 3, pp. 243-248.

T

Taylor, A. F. & Smith, G. R. 1985, "Substrate specificity of the DNA unwinding activity of the RecBC enzyme of *Escherichia coli*", *J.Mol.Biol.*, vol. 185, no. 2, pp. 431-443.

Thommes, P. & Hubscher, U. 1992, "Eukaryotic DNA helicases: essential enzymes for DNA transactions", *Chromosoma*, vol. 101, no. 8, pp. 467-473.

Thompson, J. D., Higgins, D. G., & Gibson, T. J. 1994, "CLUSTAL W: improving the sensitivity of progressive multiple sequence alignment through sequence weighting, position-specific gap penalties and weight matrix choice", *Nucleic Acids Res.*, vol. 22, no. 22, pp. 4673-4680.

Tissier, A., McDonald, J. P., Frank, E. G., & Woodgate, R. 2000, "Polymerase iota, a remarkably error-prone human DNA polymerase", *Genes Dev.*, vol. 14, no. 13, pp. 1642-1650.

Toh, H. 1986, "T7 and *Escherichia coli* share homology for replication-related gene products", *FEBS Lett.*, vol. 194, no. 2, pp. 245-248.

Tougu, K., Peng, H., & Marians, K. J. 1994, "Identification of a domain of *Escherichia coli* primase required for functional interaction with the DnaB helicase at the replication fork", *J.Biol.Chem.*, vol. 269, no. 6, pp. 4675-4682.

Triglia, T., & Cowman, A.F. 1994, "Primary structure and expression of the dihydropteroate synthetase gene of *Plasmodium falciparum*", *Proc.Natl.Acad/.Sci.U.S.A.*, vol. 91, no. 15, pp. 7149-7153.

Tseng, T. Y., Frick, D. N., & Richardson, C. C. 2000, "Characterization of a novel DNA primase from the *Salmonella typhimurium* bacteriophage SP6", *Biochemistry*, vol. 39, no. 7, pp. 1643-1654.

U

Umek, R. M., & Kowalski, D. 1990, "The DNA unwinding element in a yeast replication origin functions independently of easily unwound sequences present elsewhere on a plasmid", *Nucleic Acids Res.*, vol. 18, no. 22, pp. 6601-6605.

V

Vaidya, A. B., & Arasu, P. 1987, "Tandemly arranged gene clusters of malarial parasites that are highly conserved and transcribed", *Mol.Biochem.Parasitol.*, vol. 22, no. 2-3, pp. 249-257.

Vaidya, A. B., Akella, R., & Suplick, K. 1989, "Sequences similar to genes for two mitochondrial proteins and portions of ribosomal RNA in tandemly arrayed 6-kilobase-pair DNA of a malarial parasite", *Mol.Biochem.Parasitol.*, vol. 35, no. 2, pp. 97-107.

van Dooren, G. G., Waller, R. F., Joiner, K. A., Roos, D. S., & McFadden, G. I. 2000, "Traffic jams: protein transport in *Plasmodium falciparum*", *Parasitol.Today*, vol. 16, no. 10, pp. 421-427.

van Dooren, G. G., Su, V., D'Ombrain, M. C., & McFadden, G. I. 2002, "Processing of an apicoplast leader sequence in *Plasmodium falciparum* and the identification of a putative leader cleavage enzyme", *J.Biol.Chem.*, vol. 277, no. 26, pp. 23612-23619.

Velankar, S. S., Soultanas, P., Dillingham, M. S., Subramanya, H. S., & Wigley, D. B. 1999, "Crystal structures of complexes of PcrA DNA helicase with a DNA substrate indicate an inchworm mechanism", *Cell*, vol. 97, no. 1, pp. 75-84.

Versalovic, J., & Lupski, J. R. 1993, "The *Haemophilus influenzae* dnaG sequence and conserved bacterial primase motifs", *Gene*, vol. 136, no. 1-2, pp. 281-286.

W

Walker, J. E., Saraste, M., Runswick, M. J., & Gay, N. J. 1982, "Distantly related sequences in the alpha- and beta-subunits of ATP synthase, myosin, kinases and other ATP-requiring enzymes and a common nucleotide binding fold", *EMBO J.*, vol. 1, no. 8, pp. 945-951.

Waller, R. F., Keeling, P. J., Donald, R. G., Striepen, B., Handman, E., Lang-Unnasch, N., Cowman, A. F., Besra, G. S., Roos, D. S., & McFadden, G. I. 1998, "Nuclear-encoded proteins target to the plastid in *Toxoplasma gondii* and *Plasmodium falciparum*", *Proc.Natl.Acad Sci.U.S.A*, vol. 95, no. 21, pp. 12352-12357.

Waller, R. F., Reed, M. B., Cowman, A. F., & McFadden, G. I. 2000, "Protein trafficking to the plastid of *Plasmodium falciparum* is via the secretory pathway", *EMBO J.*, vol. 19, no. 8, pp. 1794-1802.

Warhust, D. C. 2001, "New developments: chloroquine-resistance in *Plasmodium falciparum*", *Drug Resist.Updat.*, vol. 4, no. 3, pp. 141-144.

Warhust, D. C. 2002, "Resistance to antifolates in Plasmodium falciparum, the causative agent of tropical malaria", *Sci. Prog.*, vol. 85, no. 1, pp. 89-111.

Warrell, D. A. 1992, "Pathophysiology of severe falciparum malaria", *P.N.G.Med.J.*, vol. 35, no. 4, pp. 229-232.

Washington, M. T., Rosenberg, A. H., Griffin, K., Studier, F. W., & Patel, S. S. 1996, "Biochemical analysis of mutant T7 primase/helicase proteins defective in DNA binding, nucleotide hydrolysis, and the coupling of hydrolysis with DNA unwinding", *J.Biol.Chem.*, vol. 271, no. 43, pp. 26825-26834.

Weber, J. L. 1987, "Analysis of sequences from the extremely A + T-rich genome of *Plasmodium falciparum*", *Gene*, vol. 52, no. 1, pp. 103-109.

Weissig, V., Vetro-Widenhouse, T. S., & Rowe, T. C. 1997, "Topoisomerase II inhibitors induce cleavage of nuclear and 35-kb plastid DNAs in the malarial parasite *Plasmodium falciparum*", *DNA Cell Biol.*, vol. 16, no. 12, pp. 1483-1492.

West, S.C. 1996, "DNA helicases: new breeds of translocating motors and molecular pumps", *Cell*, vol. 96, pp. 177-180.

White, N, J. 1997, "Assessment of the pharmacodynamic properties of antimalarial drugs *in vivo*", *Antimicrob.Agents Chemother.* vol. 41, no. 7, pp. 1413-1422.

White, J. H., Kilbey, B. J., de Vries, E., Goman, M., Alano, P., Cheesman, S., McAleese, S., & Ridley, R.G. 1993, "The gene encoding DNA polymerase alpha from *Plasmodium falciparum*", *Nucleic Acids Res.*, vol. 21, no. 16, pp. 3643-3646.

White, J. H. & Kilbey, B. J. 1996, "DNA replication in the malaria parasite", *Parasitol.Today*, vol. 12, pp. 151-155.

WHO 1998, *World Health Organization. Factsheet No. 94 (World Health Organization, Geneva, 1998).*

Wiesner, J., Hintz, M., Altincicek, B., Sanderbrand, S., Weidemeyer, C., Beck, E., & Jomaa, H. 2000, "*Plasmodium falciparum*: detection of the deoxyxylulose 5-phosphate reductoisomerase activity", *Exp.Parasitol.*, vol. 96, no. 3, pp. 182-186.

Williamson, D. H., Gardner, M. J., Preiser, P., Moore, D. J., Rangachari, K., & Wilson, R. J. 1994, "The evolutionary origin of the 35 kb circular DNA of *Plasmodium falciparum*: new evidence supports a possible rhodophyte ancestry", *Mol.Gen.Genet.*, vol. 243, no. 2, pp. 249-252.

Williamson, D. H., Preiser, P. R., & Wilson, R. 1996, "Organelle DNAs: the bit players in malaria parasite DNA replication", *Parasitol.Today*, vol. 12, pp. 357-362.

Williamson, D. H., Preiser, P. R., Moore, P. W., McCready, S., Strath, M., & Wilson, R. J. 2002, "The plastid DNA of the malaria parasite *Plasmodium falciparum* is replicated by two mechanisms", *Mol.Microbiol.*, vol. 45, no. 2, pp. 533-542.

Wilson, I. 1993, "Plastids better red than dead", *Nature*, vol. 366, no. 6456, p. 638.

Wilson, R. J., Denny, P. W., Preiser, P. R., Rangachari, K., Roberts, K., Roy, A., Whyte, A., Strath, M., Moore, D. J., Moore, P. W., & Williamson, D. H. 1996, "Complete gene map of the plastid-like DNA of the malaria parasite *Plasmodium falciparum*", *J.Mol.Biol.*, vol. 261, no. 2, pp. 155-172.

Wilson, R. J. & Williamson, D. H. 1997, "Extrachromosomal DNA in the Apicomplexa", *Microbiol.Mol.Biol.Rev.*, vol. 61, no. 1, pp. 1-16.

Wilson, R. J. 2002, "Progress with parasite plastids", *J.Mol.Biol.*, vol. 319, no. 2, pp. 257-274.

Wittmann, H. G. 1983, "Architecture of prokaryotic ribosomes", *Annu.Rev.Biochem.*, vol. 52, pp. 35-65.

Z

Zeidler, J., Schwender, J., Mueller, C., & Lichtenthaler, H. K. 2000, "The non-mevalonate isoprenoid biosynthesis of plants as a test system for drugs against malaria and pathogenic bacteria", *Biochem.Soc.Trans.*, vol. 28, no. 6, pp. 796-798.

Zhang, Z., Green, B. R., & Cavalier-Smith, T. 2000, "Phylogeny of ultra-rapidly evolving dinoflagellate chloroplast genes: a possible common origin for sporozoan and dinoflagellate plastids", *J.Mol.Evol.*, vol. 51, no. 1, pp. 26-40.

Zhang, Z., Green, B. R., & Cavalier-Smith, T. 2000, "Phylogeny of ultra-rapidly evolving dinoflagellate chloroplast genes: a possible common origin for sporozoan and dinoflagellate plastids", *J.Mol.Evol.*, vol. 51, no. 1, pp. 26-40.

Ziegelin, G., Linderoth, N. A., Calendar, R., & Lanka, E. 1995, "Domain structure of phage P4 alpha protein deduced by mutational analysis", *J.Bacteriol.*, vol. 177, no. 15, pp. 4333-4341.

Zuegge, J., Ralph, S., Schmuker, M., McFadden, G. I., & Schneider, G. 2001, "Deciphering apicoplast targeting signals--feature extraction from nuclear-encoded precursors of *Plasmodium falciparum* apicoplast proteins", *Gene*, vol. 280, no. 1-2, pp. 19-26.

Zyskind, J. W., Cleary, J. M., Brusilow, W. S., Harding, N. E., & Smith, D. W. 1983, "Chromosomal replication origin from the marine bacterium *Vibrio harveyi* functions in *Escherichia coli*: oriC consensus sequence", *Proc.Natl.Acad Sci.U.S.A*, vol. 80, no. 5, pp. 1164-1168.

Appendices

APPENDIX A

1. Media

Luria-Bertani Broth

10 g NaCl

10 g Tryptone

5 g Yeast Extract

Make up to 1 litre with distilled water with pH adjusted to 7.0 with 5M NaOH before autoclaving.

SOB

20 g Bacto-Tryptone

24 g Yeast Extract

0.5 g NaCl

2.5 ml 1M KCl

900 ml H_2O

Adjust pH to 7.0 with 10M NaOH and add H_2O to 990 ml. Sterilise by autoclaving and store at room temperature. Before use, add 10 ml sterile 1M $MgCl_2$.

SOC

Identical to SOB medium, except it contains 20 ml sterile 1M glucose.

2. Buffers

PBS

10X

80 g NaCl

2g KCl

26.8 g Na_2HPO_4-7 H_2O

2.4 g KH_2PO_4

800 ml H_2O

Adjust pH to 7.4 with HCl and sterilise by autoclaving.

Denhardt's Solution

250X

50 g Ficoll 400

50 g polyvinylpyroolidone

50 g BSA

600 ml H_2O

Adjust volume to 1 litre with H_2O. Divide in aliquots and store at –20°C.

DTT

1M

3.085 g DTT

20 ml 10 mM Sodium acetate (pH 5.2)

Divide into 1 ml aliquots and sterilise by filtration. Store at –20°C.

0.5M EDTA (pH 8.0)

186.12 g Na_2EDTA-2 H_2O

Adjust pH to 8.0 with NaOH and adjust volume to 1 litre with H_2O. Sterilise by autoclaving.

$MgCl_2$

1M

203.31g $MgCl_2$

800 ml H_2O

Adjust volume to 1 litre with H_2O. Sterilise by autoclaving.

MOPS

10X

41.85 g MOPS

6.8 g sodium acetate

800 ml DEPC-treated H_2O

Add 20 ml of a DEPC-treated 0.5M EDTA and adjust pH to 7.0 with 10M NaOH. Adjust volume to 1 litre with DEPC-treated H_2O. Protect from light and store at 4°C. Sterilise by autoclaving.

NaOAc

3M

408.24 g sodium acetate

800 ml H_2O

Adjust to pH 5.2 with glacial acetic acid and adjust volume to 1 litre with H_2O. Sterilise by autoclaving.

NaCl

5M

292.2 g sodium chloride

800 ml H_2O

Adjust volume to 1 litre and sterilise by autoclaving.

SDS

10%

100 g SDS

900 ml H_2O

Heat to 68°C to dissolve crystals and adjust pH to 7.2 with HCl. Adjust volume to 1 litre.

TCA

100%

500 g trichloroacetic acid

227 ml H_2O

TRIS

1M

121.14 g TRIS
800 ml H_2O
Adjust pH to desired value by adding concentrated HCl. Adjust volume to 1 litre with H_2O and sterilise by autoclaving.

SSC

20X

175.3 g NaCl

88.2 g sodium citrate

800 ml H_2O

Adjust pH to 7.0 with HCl and make up to 1 litre with H_2O. Sterilise by autoclaving.

TE

1X

10 ml 1M TRIS

2ml 0.5M EDTA (pH 8.0)

Mix and adjust volume to 1 litre with H_2O. Sterilise by autoclaving.

3. Buffers for electrophoresis of DNA

6X Loading buffer

0.25 % bromophenol blue

40 % (w/v) sucrose

50 X TAE buffer

242 g TRIS

57.1 ml Glacial acetic acid

Make up to 1 litre with H_2O. Dilute to 1X prior to use.

4. Buffers for electrophoresis of RNA

20X Northern gel buffer

96.5 g Na_2HPO_4

5.5 g NaH_2PO_4

Make up to 1 litre with DEPC-treated H_2O.

1X Northern gel buffer

50 ml 20X northern gel buffer

88 ml formaldehyde

860 ml DEPC-treated H_2O

Make up to 1 litre with DEPC-treated H_2O.

RNA sample buffer

50 % glycerol

1 mM EDTA

0.4 % bromophenol blue

DEPC-treatment (per 100 ml)

0.01% DEPC or 0.1 ml DEPC to 1000 ml of a solution (e.g. H_2O)

Shake and incubate overnight in a fume hood. Autoclave the solution to inactivate the remaining DEPC.

5. Buffers for the electrophoresis of proteins

10% Ammonium persulphate (APS)

1g APS

8 ml H_2O

Adjust volume to 10 ml with H_2O. Store at 4°C.

10X Running Buffer

10 g SDS

30.3 g TRIS

144.1 g Glycine

800 ml H_2O

Make up to 1 litre and dilute to 1x prior to use.

2X SDS PAGE sample buffer

10 ml 1.5M Tris (pH 6.8)

6 ml 20% SDS

30 ml Glycerol

15 ml β-mercaptoethanol

1.8 mg Bromophenol blue

Adjust volume to 100 ml with H_2O. Aliquot in 10 ml stock solution.

10% Resolving gel (10 ml volume)

4 ml H_2O

3.3 ml 30% acyl-bisacrylamide mix

2.5 ml 1.5M TRIS (pH 8.8)

0.1 ml 10% SDS

0.1 ml 10% APS

10 µl TEMED

5% Stacking gel (5 ml volume)

3.4 ml H_2O

0.83 ml 30 % acryl-bisacrylamide mix

0.63 ml 0.5 M TRIS (pH 6.8)

50 µl 10% SDS

50 µl 10% APS

5 µl TEMED

Coomassie Blue staining solution

2.5 g Coomassie Brilliant Blue R-250

450 ml Methanol

100 ml Acetic acid

400 ml H_2O

Adjust volume to 1 litre with H_2O.

Coomassie Blue destaining solution

450 ml Methanol

100 ml Acetic acid

400 ml H_2O

Adjust volume to 1 litre with H_2O.

6. Buffers for Western blotting

10X Transfer buffer

24.22 g TRIS

112.5 g Glycine

Make up to 1 litre with H_2O.

Use at 1 X - 100 ml 10X stock, 200 ml methanol and 700 ml H_2O. Prechill at 4°C.

10X TBS

24.22g TRIS

80 g NaCl

Adjust pH to 7.6 and make up to 1 litre with H_2O. Store at 4°C.

Ponceau S solution

0.5 % Ponceau S

1% Acetic acid

7. Buffers for indirect immunofluorescence

Blocking buffer

0.01% Tween 20

0.05% Sodium azide

1% BSA

Make up in PBS.

Immunobuffer

0.1 M TRIS, pH 7.4

2.3 M NaCl

0.01% Tween 20

1% BSA

0.05% Sodium azide

8. Buffers for *In situ* hybridisation

Hybridisation buffer

37.5 % formamide

2X SSC

1 mM TRIS, pH 7.2

0.1 mM EDTA

10% Dextran sulphate

1 µg Herring sperm DNA

Detection buffer

4X SSC

0.2% Tween 20

APPENDIX B

Le Roch *et al* (2003) transcriptome analysis data for *PfPREX* from Plasmodb website

Expression data for chr14.glm_129

Home | Downloads | Tools | Queries | BLAST | History | CDs&Links | Browse | Data Sources | SRT | Help

DeRisi *Plasmodium falciparum* HB3 time course microarray data
Averaged and normalized data for array element(s): N150_19
(see below for raw data)

PlasmoDB gene chr14.glm_129 / Array element(s): N150_19
DeRisi Plasmodium falciparum HB3 lifecycle Study

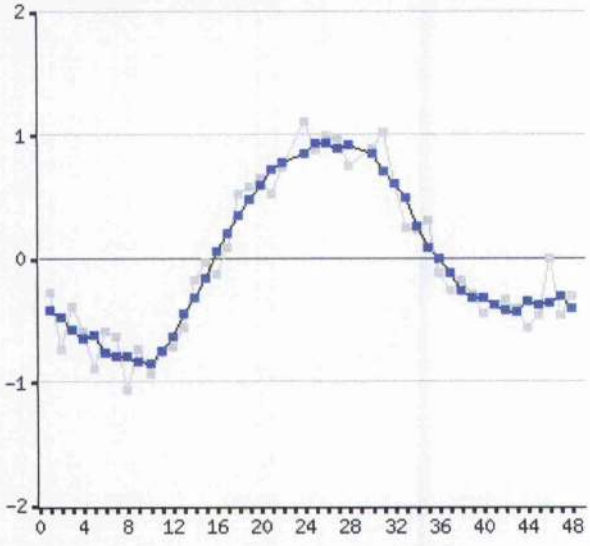

x-axis:

Time in hours after adding synchronized culture of HB3 parasites to fresh blood

y-axis:

log base(2) of Cy5/Cy3 ratio

blue plot:

smoothed normalized log base(2) of Cy5/Cy3 for chr14.glm_129

grey plot:

normalized log base(2) of Cy5/Cy3 for chr14.glm_129

DeRisi Lab. Malaria Transcriptome Database: chr14.glm_129

PlasmoDB gene: chr14.glm_129

Raw expression data for array element N150_19
(some time points are averaged values from multiple replicates)

Array element(s): N150_19
DeRisi Plasmodium falciparum HB3 lifecycle Study

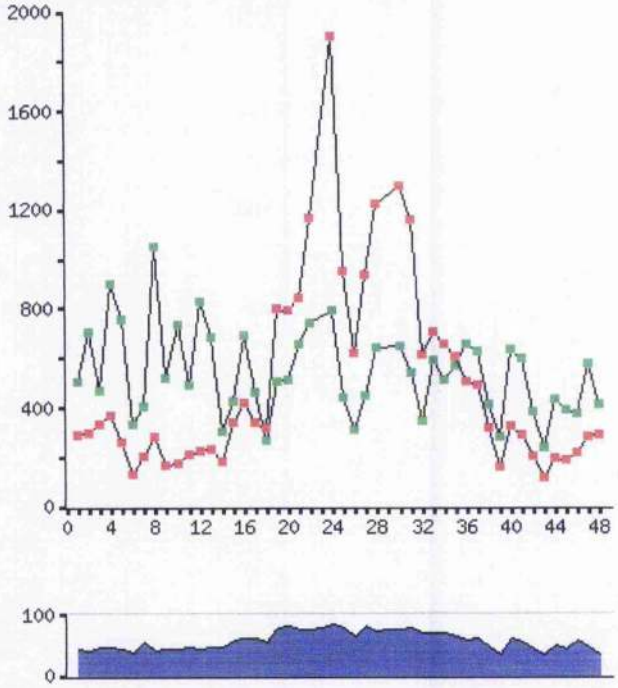

x-axis:

Time in hours after adding synchronized culture of HB3 parasites to fresh blood

y-axis:

raw expression value (65535 = saturation)

red plot:

raw expression values for Cy5 (experimental) channel for N150_19

green plot:

raw expression values for Cy3 (control) channel for N150_19

▸Download raw data for N150_19
(in tab-delimited format)

Percentile graph for N150_19
▸Download tab-delimited percentile data

DeRisi Lab. Malaria Transcriptome Database: N150_19

PlasmoDB Version: 4.1
PlasmoDB Date: 2003/08/01

Plasmodium Sequence Release Date: 202/10/03

To cntact PlasmoDB,
send email to help@plasmodb.org

P. falciparum chr14.glm_129

Plasmodium falciparum / CHR 14 / chr14.glm_129 / Expression

40% identity to 99% of (U23502) POM1 [Plasmodium chabaudi chabaudi] protein coding gene predicted by GlimmerM

THIS PAGE:	Microarrays▾ Ben Mamoun time series▾ Scripps/GNF Lifecycle▾ DeRisi HB3 study▾ Mass spec. data▾ Features(G)▾
LINKS TO OTHER DATA:	Summary▸ Gene model▸ DNA/RNA features▸ Protein features▸ NRDB▸ Motifs▸ Sequences▸ Expression GO assignments▸ Pathways▸ Orthologs/Paralogs▸ 3-D structures▸ MR4 reagents▸ Links▸
USER COMMENTS:	View/Add comments

Microarray elements linked to this gene

back to top▲<>

element_id	array description	array size
N150_19	DeRisi *P. falciparum* 70-mer oligo array, version 1	7392
N150_19	DeRisi *P. falciparum* 70-mer oligo array, version 2	7744
N150_19	MRA-452, 23K (MR4 *P. falciparum* long oligo)	23232

Ben Mamoun *Plasmodium falciparum* developmental time series study

back to top▲<>

*** *None* ***

2003 Lifecycle Study using the Scripps/GNF Malaria Array

back to top▲<>

*** *None* ***

DeRisi *Plasmodium falciparum* HB3 intraerythrocytic cycle study

back to top▲<>

PlasmoDB gene chr14.glm_129 / Array element(s): N150_19
DeRisi Plasmodium falciparum HB3 lifecycle Study

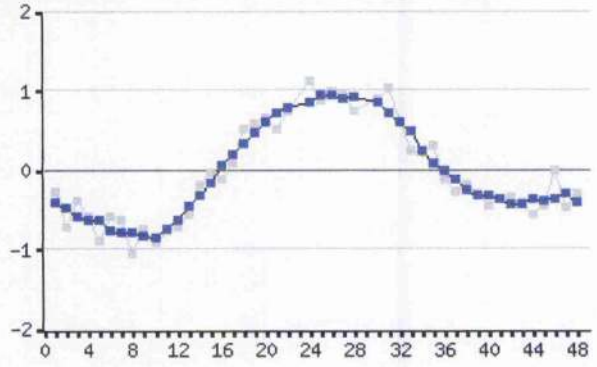

x-axis

Time in hours after adding synchronized culture of HB3 parasites to fresh blood

blue plot:

averaged smoothed normalized log base(2) of Cy5/Cy3 for chr14.glm_129

grey plot:

averaged normalized log base(2) of Cy5/Cy3 for chr14.glm_129

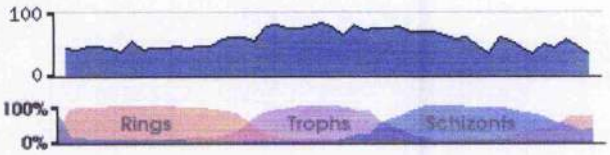

▸View/download raw data

Averaged percentile graph

P. falciparum HB3 stages

DeRisi Lab. Malaria Transcriptome Database: chr14.glm_129 N150_19

Query for genes whose minimum and/or maximum expression occurs at (approximately) the same time as this one:

Timing of maximal expression: 26 hours post-invasion

Maximum expression time plus or minus: 3 hours

Timing of minimum expression: 10 hours post-invasion

Minimum expression time plus or minus: 3 hours

Query parameters: Timing of both max and min expression

Induction ratio cut-off: >= 2-fold induction

Maximum percentile cut-off: >= 80th percentile

Run query: Run query

Query for array elements whose expression profiles are similar to this one:

Query profile: this profile only (takes ~3 seconds)

Minimum shift amount: +0 hours *(shifted queries only)*

Maximum shift amount: +47 hours *(shifted queries only)*

Distance method: Pearson correlation

Search goal: show most similar profiles

Target data: smoothed data

Display expression graphs: yes - show graphs

Maximum hits to return: 10

Run query: Run query

Or click here to modify the query profile using a Java applet:

Load applet: Load applet

back to top

Predicted protein features

back to top

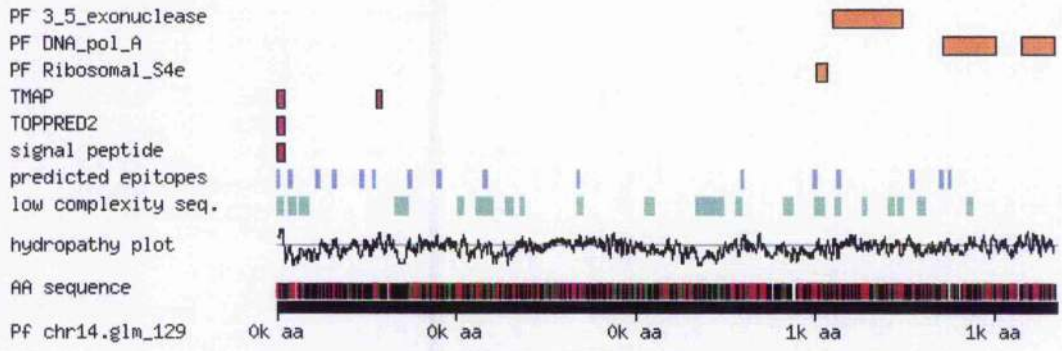

Description: Place the mouse over a feature to see its details.

Location: ID: Score:

AA residue color code P MC DE ILVA RKH STG FYW NQ

APPENDIX C

Figure C.1. Nucleotide sequence of *PfPREX*. (Accession no:- AAN36724.1)

ATGAAGTAAGAAAAATAATATATACTATATATATTTGTTATACAATGATTTCTATGATAT
ACTACCATGCTTTTGTATAAGTTTTATTTTTTATACTTTTTGCTCGTACATTTGTCGTTA
TGCATACGTTATAGAAATCAAAATAAAACTGATTCTTATTTAAAAACAAATTATAAATTA
TTAAAAAAGAGGAAAAAATATGAAAACCGTAGATATAAATTTCCAAAAAACAGAAAAGGA
AATAATAACAATATATATGATGCTATAAATAATATATTAACTAATAATATATATAATAAT
GACACATATAAAAACCGAATATTTTTTAGCAATGAGAAAAATGATGAGAATTTTATCAAG
ACCAATAAATATTCTTATTATGAAAAAAGAAATAAGATCAAATTAAATAGTGCTACTAGC
ACTTTTGTTTCAAAGTATTATAAAATAAATATTAATGATGTATATAATTATTTACATAGA
AAAAAATATGAATTTATAGAAACAGATATTAAGATAACGTTAAAGTATTGTCCACTTTGT
CCTCCACATAAATATAAATATGATAATATGTATAAACATGAAATATTTAAAAACACAGGA
AATAGTTACTGTCATAGATGTGGATATAAAGGAAGTTCTATGATTTCAAATTGAAAATG
GGGGATCTAATAACTAGTAATTTTGAAAGTACTGTAGTACATAATAATAATTTTTATGAA
GAAGAAGAAGAAAAAATAACACTAAATGATGTAAAGGTTTATAATATGAATTTATTATAT
TCAAAAGAAGCTGAAAACCCAAGGAATTATTTAATGAATGTAAGGAAGTTAAGCATTGAT
ACTTTAAAAAAGTTTTTAACAGGTTTTTCTGTTATGGAATTTCAATCTTTTGAAAGTTCT
GGTAAATTTGAAAAACACGAACGTATTATATTTCCATTCATAAAAAAAGTAGATGAAATA
AATATGATAGAAACGAATGGAATCAACAGTAACATGAACAAAATGAACAACAACAACAAC
AACAACAACAACAACAACAACAATAATAATAATAATAATAATATAAATGATAACTAT
GAACTGGTACCAATAAAAATTAGAAGTTTAAAGGATAAAGGTTATATGAGATTATATCCT
AAAAATGTTAGAAATGAAATGAAATTATTTTTTTTGGTGATCATTTAATTAAAAATTCA
GAAGAAATAGTTTTGACAGAAGGAGAAATTGATGCCATGACAATAAGTCAAGAAACAAAA
TATCCAGCTATATCTTTACCAAATGGATCAAAATCTTTACCTATATATTTATTACCATAT
TTAGAAAGGTTTAAAAAAATACATTTATGGCTAGATTTTGATAAAGCTGGAAAATCAAGC
GTCTTCAATTTCGTTAATAAAATCGGATTAGGAAGAACCAACGTAATTACGGATGCCAAT
GTTCACTATTTAAATCCAGATGTTTTTAAGACAAGACAAAAGTCCAGGTTAACCAAAAAG
AGTCTTCTCCTTACATCAATCCCTTCTAATGCTATGGAGATTCTTCAAAAAGATAAAGAA
GAAAATATGCATAATATATATGATACTACTAATAATGACTATATGGATAATAAAATACTG
AGTAATAATTTAAAAAGTATAAGTAGTGACAAAATAAAGAAAAAAGAAGAAATTGATCTA
TTTAATGGACAGAAAATTTCTAGCAATAATATAAATGTAAATATACTAAAAAACAAAAAA
AACGAAACAGATAATATTAACAAATAAGGAAAATAAAAGTGATAATAACTTGAAAGAAGGA
ATGGAAAAAAAAAGAGATACAAAATGAAATAAGTGCAATTGAAGATAATAATAATAATAAA
AATAATATAATAGAAAATAATAATGATGATATGTCAGAAAAAATAAAAGTAGAAAAATCG
ATTGAAGATAATATTTCTTATTTTGTTGATAATAATATTATGTATATACCAAATAATATA
ATTATAAAAGATGCGAATGATTGTTTGAAACATAATATTGATATAAGATTCTTTATAGAA
ACTAGTGAAAACGTAAAACATAGTCAAATATTGAATTTTAATGATTTAAGGCAACGTATA
TTAGAAGAATTAAAATATCCTGATCGAATTAATGGTGTAAAAAGTAAAACCATTCCATCA
TCAAATAAATATTCATATGGATTAAGAATGGGACAATTATCTATATGGACTGCTTCTACA
GGTGTAGCAAAAACTACCTTATTGTCTCAACTCTCTTTAGATTATTCTATCCAAGGAGTA
TCAACATTATGGGGATCATTTGAAATAAATAATGTAAAATTAGGAAAAGTCATGTTAAAT
CAATTTTGTGGAAAAAACCTTCAAAAAAATATAGAATTATTTGATATATATGCTGATAAA
TTTGAACTGTTACCTCTTAAATTTTTAAAGTTCCATGGTAGTACAAATATTGATCAGGTT
ATAGATGCTATGGATTATGCTGTGTATGCATATGATGTAAAACATATAATTATTGATAAT
TTACAATTTATGTTAAATATAAATAAATTTTCTGATATATATGAATTACAAAATATTGCT
ATAGATAAACTTAGATCCTTTACTACAAACAAAAATGTTCACACAACTTTAGTTGTTCAT
CCAAGGAAAGAGGATAACAATTTATTATCTATTTCATCCGTTTTTGGTAGTGTAAAATCA
ACTCAAGAAGCAGATAATGTGTTTATTATACAAAGACATGTATCAAAAACAAATGAAACT
GTTTTCTTTACAGATATTAAAAAAAATAGATTTAAAGGAAGTTTAGGGAAAATACCTTAT
TTATATAATAAAGAAAATATGACAATAAAAGAAATATCAATAAATAACTTTAATGAGCAT
GTAGTTTCAAATACTTATTTACCATCAAATAAATTTTCTTCTTCATCATTACAAAATAAT
ACTACTAATAATAATTTTATACAAAATGATAATTTAAATTTCACCTTATGTGATGAATAT
GATTATATGAAACAGCTAGCTGATGAATATGAATCAAAACATGCTTTTAAAAAAGGTTAT
AGGTCTAAATTAGATCCTAATTTAAGGGTGAATAATATAGATATGATAAAAACAGAAATA
ATTGACAATACCGATATGAATAACAATAAAAATGTTACTCTTTATGTGGATAGTTTACAG
AATATAAAAACTATATCGACTGATGATAAAACTAATGATGATAAAAGAGATGTAAATGAA
ATAAAAAGCATTAAAAACAATGAACGTAAAAATACATTAAAGATTGATGGAAACAAATCA
TTAGGTTCTACACAAAATTTAAATTACGAAATGAAAATAAAAACAATAATAATAATAAC
AATAATAATAAGAGTAATCAAGAAATGGAAAAGAATAACATAGATGATAAATCATCAACA
GGAAATAATAAAAATATAAATGGCAACTCAAAAGGTAATAATAATATTAATAATAATAAC
AAGAATAAGAACAGTAGTAGTAGTAGTAGTAGTAATTATAATAATAATGAGGGG

ATTAAAAATATATTAAACACATCGGCACAAAATAACATTCCTTTTAAAGATACAATATGG
TCATATACACTAACTAATGAAGGATTAATAAAATTGTGTGAAGAACTAAAAGATGAAGAA
CCAGAAAAACTTAAAAATCGAGTTGTCGTTCTTTCGATGAGAAATTGTATAATTGATAAT
AATTCTTCTATAAAAGATATAAGAACATTTATAAAAACAAATAAATTAAACATAAAAACT
GCAGGAAAAAATTTAAAAAAAAATGGATATATTTATTAGTATTTACAAAATATACCAAAG
GAATATATTACAATTAAAAGTGGACAGAAATATGGACCAAATAAAGGACTACCAAATGAC
AAATCAAAAAACAAAATAAAGGAACCACATAATAATAATATGTTGGAATATAATAAAGTT
GGATCTAACATCGGTGATGGACAAAATACATCATCATCATGTATGAATATTAATAAAATA
CATAGTGAAGAAGAAAACAATATATACATAAATAATAATAATAATAATATGAATAAGGAA
CCCCAAACATTATTACCAAATGATAGAAATGATTCAAACTCTCATAGTTATAATAATATT
AATTATACAATGGTTAAAAATGGTAACGAAGGAAATATAAATGATTATCTAAATAGAAAT
TATGAAAATAATGTAGATAACCATCATAATGATGAAATTACAAAGAAATACATAAAGGAT
AATATTATAAATGTAGATGATAATATAATTAAAAAGAAAGATATATTTAAATTAAAAAAT
GAAAATAATGAAATTACAGAGTGCGCATTTGAATATTTTGAGTCTAAAAAAAAATTTGAT
GATGATATAGAATCTACATTCTTTATTATAAATGATAATAATTATAATGAAAATATAAAT
TTAATATATAAAGATATAAAATATTGTGGATTAGATATTGAAACAACAGGTTTAGAAGTG
TTCGATGAAAATATAAGATTAATTCAAATAGCTGTAGAAAATTATCCAGTAATTATTTAT
GATATGTTTAATATAAACAAAAAAGATATATTAGATGGATTAAGAAAAGTATTAGAAAAT
AAAAATATAATAAAAATAATACAAAATGGAAAATTTGATGCAAAATTTTTGCTTCATAAT
AATTTCAAAATTGAAAATATTTTTGATACATATATAGCTAGTAAATTATTAGATAAAAAT
AAGAATATGTATGGATTTAAATTAAATAATATAGTTGAGAAATATTTAAATGTAATATTG
GACAAACAACAACAAAATAGTGTATGGAATAATTCCTTGTTAAATAATAATCAACTATTT
TATGCTGCTCGTGATTCTAGTTGTTTATTAAAATTATATAAAAAGTTAAAAGAAGAAATA
AAAAAGAAAATTTACATATAGTAAATGATATTGAAAATAAATGTATCCTACCTATATGT
GATATGGAATTAAATGGTATTAAAGTAGATTTAGAAAATTTACAAAAAAGTACAAATGAA
ATATTAAATGAATTAAATATTGAGAAAGATAATTTAAAAAAAAAATTAAAAGACGAAAAT
ATAAATGTAAATTCTCAACAACAAGTATTGAAAGCTTTGCAAAAAAATAATGTTCGTGAT
ATTTCTAATAAACTAACAGAAAATACATCTGATTCCAACTTAAAAAATTTTCTAAATCAT
GAAGAAATTATAAGTTTACGTAATCATAGAAGATTATATAAATTGTATTCAGCTTTTTAT
TTAAAATTACCATTACATATTAATACAAAAACAAATAAAATACATACTACCTTTAATCAA
TTAAAAACATTCTCAGGAAGATTTAGTAGTGAAAAACCAAATTCACAACAAATACCTAGA
CAAAAAAATATAAGAGAAATATTTATACCAAACGATAATAATACTTCATTATAGCTGAC
TTTAAACAAACCGAGCCTAAAATTGCAGCAGAAATTACAAATGATGAAATTATGCTTAAA
GCATATAATAATAATAATAGATTTACATACATTAACAGCTAGTATTATAACTAAAAAAAAT
ATACCAGATATTAATAAAGAAGATAGACATATAGCAAAAGCTATCAATTTGGTCTTATA
TATGGTATGAATTATGTCAACTTAAAAAATTATGCAAATACGTATTATGGTTTAAATATG
TCTTTAGATCAATGTCTATATTTTTATAATTCTTTTTTTGAACACTACAAAGGAATATAT
AAATGGCATAATCAAGTAAAACAAAAAAGAGCTTTACAGTATTCTACACTTTCAAATAGA
AAAGTTATATTCCCATACTTCTCTTTCACAAAAGCTCTTAATTATCCTGTACAAGGTACA
TGTGCTGATATTTTAAAATTAGCTCTAGTAGATTTATATGACAACTTAAAGGATATTAAT
GGTAAAATTATCCTATGTGTGCATGATGAAACTATAATCGAAGTAAATAAAAAATTTCAG
GAACAAGCTCTTAAAATTTTAGTACAATCTATGGAAAATTCGGCTTCTTACTTTTTGAAA
AAAGTTAAATGTGAGGTTTCTGTAAAAATAGCTGAAAATTGGGGATCAAAGGATTAACAT
GAAGATATCGAAAAAATAATATATATATATATATATAACATATATATGATATAAAATAAA
ATAAATGTTCCCATGGAATGATATATATATATATATACACGTCATTATATTTTCTTC
AAATTTATAGATATT

Figure C.2. Amino acid sequence of *PfPREX*.

MLLYKFYFLYFLLVIILSLCIRYRNQNKTDSYLKTNYKLLKKRKKYFNRRY
KFFKNRKGNNNNIYDAINNNNTNNIYNNDTYKNRIFFRNEKNDENFIKTN
KYSYYEKRNKIKLNSATSTFVSKYYKININDVYNYLHRKKYEFIETDIKI
TLKYCPFCPPHKYKYDNMYKHEIFKNTGNSYCHRCGYKGSFYDFKLKMGD
LITSNFESTVVHNNNFYEEEEEKITLNDVKVYNMNLLYSKEAENARNYLM
NVRKLSIDTLKKFLIGFSVMEFQSFESSGKFFKHECIIFPFIKKVDEINM
IETNGINSNMNKMNKNNNNNNNNNNNNNNNNNNNNINDNYEVVRIKIRSLKD
KGYMRLYFKNVRNEMKLFFFGDHLIKNSEEIVLTEGEIDAMTISQETKYP
AISLPNGSKSLPIYLLPYLERFKKIHLWLDFDKAGKSSVFNFVNKIGLGR
TNVITDANVHYLNPDVFKRRQKSRLTKKSLLLTSMASNAMEILQKDKFFN
MHNIYDTTNNDYMDNKILSNNLKSISSDKIKKKEEIDLFNGQKISSNNIN
VNILKNKKNETDNITNKENKSDNNLKFGMFKKFIQNEISVIEDNNNNKNN
IIENNNDDMSEKIKVEKSIEDNISYFVDNNIMYIFNNIIIKDANDCLKHN
IDIRFFIETSEKVKHSQILNFNDLRQRILEELKYPDRINGVKSKTIPSLN
KYLYGLRMGELSIWTGSTGVGKTTLLSQLSLDYCIQGVSTLWGSFEINNV

KLGKVMLNQFCGKNLEKNIELFDIYADKFELLPLKFLKFHGSTNIDQVID
AMDYAVYAYDVKEIIIDNLQFMLNINKFSDIYELQNIAIDKFRSFSTNKN
VHITLVVHPRKEDNNLLSISSVFGSVKSTQEADNVFIIQREVSKTNETVF
FIDIKKNRFKGSLGKIPYLYNKENMTIKEISINNFNEHVVSNTYLPSNKF
SSSSLQNNTTNNNFIQNDNLNFTLCDEYDYMKQLADEYESKHAFKKGYRS
KLDPNLRVNNIDMIKTEIIDNSDMNNNKNVTLYVDSLENIKTISTDDKTN
DDKRDVNEIKSIKNNERKNTLKIDGNKSLGSTQNLNYENENKNNNNNNNN
NKSNQEMEKNNIDDKSSTGNNKNINGNSKGNNNINNNNKNKNSSSSSSSS
SNYNNNEGIKNILNTSAQNNIPFKDTIWSYTLTNEGLTKLCEELKDEEAE
KLKNRVVVLSMRNCIIDNNSSIKDIRTFIKINKLNIKTAGKNLKKMDIFI
SILQNIPKEYITIKSGQKYGPNKGLPNDKSKNKIKEPHNNNMLEYNKVGS
NIGDGQNTSSSCMNINKIYSEEENNIYINNNNNNMNKEPQTLLPNDRNDS
NSHSYNNINYTMVKNGNEGNINDYLNRNYENNVDNIIINDEITKKYIKDNI
INVDDNIIKKKDIFKLKNENNEITECAFEYFESKKKFDDDIESRFFIIND
NNYNENINLIYKDIKYCGLDIETTGLEVFDENIRLIQIAVENYPVIIYDM
FNINKKDILDGLRKVLENKNIIKIIQNGKFDAKFLLHNNFKIENIFDTYI
ASKLLDKNKNMYGFKLNNIVEKYLNVILDKQQQNSVWNNSLLNNNQLFYA
ARDSSCLLKLYKKLKEEIKKENLHIVNDIENKCILPICDMELNGIKVDLE
NLQKSTNEILNELNIEKDNLKKKLKDENINVNSQQQVLKALQKNNVRDIS
NKLIENTSDSNLKNFLNHEEIISLRNYRRLYKLYSAFYLKLPLHTNTKTN
KIHTTFNQLKTFSGRFSSEKPNLQQIPRQKNIREIFIPNDNNIFIIADFK
QIELKIAAEITNDEIMLKAYNNNIDLHTLTASIITKKNIPDINKEDRHIA
KAINFGLIYGMNYVNLKNYANTYYGLNMSLDQCLYFYNSFFEHYKGIYKW
HNQVKQKRALQYSTLSNRKVIFPYFSFTKALNYPVQGTCADILKLALVDL
YDNLKDINGKIILCVHDEIIIEVNKKFQEEALKILVQSMENSASYFLKKV
KCEVSVKIAENWGSKD

Figure C.3. Amino acid sequence of *P. chabaudi Pomt* sequence (Accession no:- AAA84746.1).

NSFKIKRERKRKNKVINLLNPNSASLSSSEESNADASSNSNAEASQQENLDQSDTEKEKENDVYFIDNGI
MYIWNKIFVKDANDCLKNNIDVQFFIKNSEKVKHSQILNFNDLRQHILEELKYPDRINGVRSKTIPSLNK
FLYGLRMGELSIWTGSTGVGKTTLLSQLSLDYCIQGVSTLWGSFEINNIKLAKVMLNQFCGKNLEKNIDL
FDLYADKFELLPLKFLKFHGSTNIDQVLDAMDYAVYAYDVKHIIIDNLQFMLNINKFSDIYELQNIAIDK
FRSFSTNKNVHITLVVHPRKEDNNLLSISSVFGSVKSTQEADNVFIIQRQISKNNEAVFFIDIKKNRFKG
SLGRIPYLYNKENMTIKEMPINYLNDFLSNNGSIGGSSSNNYLNKNGSYSNVLQNISSASNNNMDFTLCD
EYDYMKQLSDEYESKHAFRRYNNKTCKCVADSGGLSLLKSSTLGSGTRRGDIFSEIKGNGKNAENEDIEK
EKEKCNSKISELLKQNDEKVAHTKTTNNSVTAQSLGSNEIRSKEKNTKKKSVTENVGLQNNDSTNLKGGN
KNSEINTDTMNNKNVTKGKYSSYLLSNEGLEKLCKEF

Figure C.4. Amino acid sequence of *PyPREX*.

MPWYLFYFFYIFFLNLALGIRRRKNRLKNEYYIKINYKLLKKKKNDLKKKFGIINGFVSKPNEKLLKKQF
RAYYKRNNDIEWGSNEKNCYNNLNKIKNKLNAMSTFVSKYYKININDVYNYLNRKKYEYIETDVKITLKY
CPFCPPHKYKYDNMYKHEIFKNTGNSYCHRCGYKGSFYDFKLKMGDLVTSNFESPIVNDTYEEEKITFND
VKVYNMNLLYSKEAENARNYLINERKINFETLKKYYIGFSVMEFQSLENSGKFEKHECLVFPFIRKISNT
NENENNCKSIYKGIGKTEDEGDIYEVVRIKVRSLKDKGYMRLYPKNVRSDMKLFFFGDHLITNSDEVVLT
EGEIDAMTIFQETNYFALSLPNGSKSLPIYLLPHLEKFKKIHLWLDFDKAGKSSVFNFVNKIGLGRTNVI
TDANVHYLNENAFKIKRERKKKNKIINLLNPNSASLLPNEDSNVDVSTDSNCKSDYQEELGQSNSEKEKE
KNSENDVYFIDNGIMYIWNKISIKDANDCLKNDIDIQFFIKNSEKVKHSQILNFNDLRQHILEELKYPDR
INGVKSKTIPSLNKFLYGLRMGELSIWTGSTGVGKTTLLSQLSLDYCIQGVSTLWGSFEINNIKLGKVML
NQFCGKNLEKNIDLFDLYADKFELLPLKFLKFHGSTNIDQVLDAMDYAVYAYDVKHIIIDNLQFMLNINK
FSDIYELQNIAIDKFRSFSTNKNVHITLVVHPRKEDNNLLSISSVFGSVKSTQEADNVFIIQRQISKNNE
AVFFIDIKKNRFKGSLGRIPYLYNKENMTIKEMPINYLNDFLSNNSSIGSNNSNNYLNKNGSYSNVLQNV
SSVSNNNMDFTLCDEYDYMKQLSDEYESKHAVRKYNNKIGKCVADSGGLSLLKSSTLRSETRRGDIFSEI
KEYEKNTENEDIEKEKEKYNSKISELLKKSDEKLTNTKTTNDNTTAQSLSSNEIRSKEKNTKKKSVTENV
GFQNNDSINLKSGNKNSDIDADKMDDKNLITRKFSSYLLSNEGLEKLCKELKDDEKGKFQNVVISISMRK
CVINNNSPIKDIRNFIKVNKLNIKTSGNNLKKKDVFINVLQSIPKEYISIITEGDREKYENKNGGDTSGN

NDIIKSTQKETFIESQRQGNINTNNNKGDEYNNVRNMDEEGDNNVIKNNMNNEMYNNQVDPRLDDKIIKK
YMDDNIINVDGNIVKKCGRFKLENDKDKVKIEENLYYYEPEKNFNDNIETRFFIINDKNYNEKINYIYNG
IKYCGLDMETTGLEVFGEKIRLIQIAVENYPVIIYDMFNITNNNILDGLRKILNDENIVKIIQNGKFDTK
FLIYNNFNITNIFDTYIASKLLDKNKNMYGFKLNNIVEKYLSVYLDKQQQNSVWNNSLLNNNQLFYAARD
SSCLIKLYKKLSEQITAENMQIVNDIENKCILPICDMELNGIKVDLESLNKSTDQILNELNVERDKLKKE
LKNDDINVNSQQQILKALQDNNVRDLSNKLIDNTSDANLKNFINHNAVILLRNYRKLYKLYSAFYLKLPL
HINKKTNKIHTTFNQLKTFSGRFSSEKPNLQQIPRQKNIREIFIPTENNIFIIADFKQIELKIAAEITND
EIMLKAYNNNIDLHTLTASIITKKGINEINKEDRHVAKAINFGLLYGMNYVNLRTYANTYYNVKMNLDQC
LYFYNSFFEHYKGLSRWHNSVKQTKALEYSTLSNRKVVFPYFSFTKALNYPVQGTCADILKLALVELYKN
LRHINGKIILCVHDEIIIEVDKKHQEEALKILVESMENSASFFLKKVKCEVSVKIAENWGRKD

Figure C.5. Amino acid sequence of *PbPREX*.

MPKFKTAIRQRKNRLKKAYYIKINYKLLKKKKNDLKKKFGIINGFVSKPNEKLLKKQFRA
YYKANNDIEWGSNEKNSCNNLNKIKNKLNAMSTFVSKYYKININDVYNYLNRKKYEYIET
DVKITLKYCPFCPPHKYKYDNMYKHEIFKNTGNSYCHRCGYKGSFYDFKLKMGDLITSNF
ESPIVNDTYEEEKITFNDVKVYNMNLLYSKEAENARNYLINERKINFETLKKYYIGFSVM
EFQSLENSGKFEKHECLVFPFIRKISNTNENENNCKSIYKGIGNTNDEEDIYEVVRIKVR
SLKDKGYMRLYPKNVRSDMKLFFFGDHLITNSDEVVLTEGEIDAMTIFQETNYPAISLPN
GSKSLPIYLLPQLEKFKKIHLWLDFDKAGKSSVFNFVNKIGLGRTNVTTDANVHYLNENT
FKIKRERKKKNKIINLLNSNNASFLPSEDSNVEVSTNSNCKGGHQEELDQSNTEKEKEKI
SENDVYFIDNGIMYIWNKISIKDANDCLKNDIDIQFFIKNSEKVKHSQILNFNDLRQHIL
EELKYPDRINGVRSKTIPSLNKFLYGLRMGELSIWTGSTGVGKTTLLSQLSLDYCIQGVS
TLWGSFEINNIKLGKVMLNQFCGKNLEKNIDLFDLYADKFELLPLKFLKFHGSTNIDQVL
DAMDYAVYAYDVKHIIIDNLQFMLNINKFSDIYELQNIAIDKFRSFSTNKNVHITLVVHP
RKEDNNLLSISSVFGSVKSTQEADNVFIIQRQISKNNEMTIKEMPINYLNDFLSNNSSIG
NNNSNNYLNKNGSYSNVLQNVSSVSNNNMDFTLCDEYDYMKQLSDEYESKHAVRKYNNNI
GKCVADSGGLSLLKSSTLGSGTRRGNIFNENKEYGKNTENEDIEKDKERYNSKIIELLKQ
NNEKVTNTKTTNDSTTVQCLSSNEIQSKEKNTKKKSVTENVGLHNNDSTNFKSGNKNSDI
DVDKMDNTNLITGNFSSYLLSNEGLEKLCKELKDDEKGKFQNIVISISMRKCVINNNSPI
KDIRNFIKVNKLNIKTSGNNLKKKDVFINVLQSIPKEYISITEGGREKNGGNTSDINDI
IKATQKEIFFESQRQGNINTNNNKGDEYNNVRNMDEGGENNAIKNNTNNEMYNNQVDPRL
DDKIIKKYIDDNIINVDGNIVKRCGLFKLINDKDKVKIEENLYYYEPEKNFNDNIETRFF
IINDKNYNEKINYIYNGIKYCGLDMETTGLEVFGEKIRLIQISVENYPVIIYDMFNITNN
NILDGLRKILNDENIVKIIQNGKFDTKFLLYNNFNITNIFDTYIASKLLDKNKNMYGFKL
NNIVEKYLSVYLDKQQQNSVWNNSLLNNNQLFYAARDSSCLIKLYKKLSEQIKAENMQIV
NDIENKCILPICDMELNGIKVDLENLNKSTDQIINELNVERDKLKKELKNEDINVNSQQQ
ILKALQDNNVRDLSNKLIDNTSDANLKNFINHNAVILLRNYRKLYKLYSAFYLKLPLHIN
KKTNKIHTTFNQLKTFSGRFSSEKPNLQQIPRQKNIREIFIPTENNIFIIADFKQIELKI
AAEITNDEIMLKAYNNNIDLHTLTASIITKKGINEINKEDRHVAKAINFGLLYGMNYVNL
RTYANTYYNVKMNLDQCLYFYNSFFEHYKGLSRWHNIVKQTKALEYSTLSNRKVVFPYFS
FTKALNYPVQGTCADILKLALVELYKNLRHINGKIILCVHDEIIIEVDKKHQEEALRILV
ESMENSASFFLKKVKCEVSIKIAQNWGTKD

Figure C.6. Partial amino acid sequence of *PcPREX*.

MGLIKLGIQRRKNRLKKANYIKINYKLLKKKKDLKKNIGIINELVSKPNEELLKKQFRAY
YKRNNNIEWSKNENNSYNNLNKTKNKLNAMSTFVSKYYKININDVYNYLNRKKYEYIETD
VKITLKYCPFCPPHKYKYDNMYKHEIFKNTGNSYCHRCGYKGSFYDFKLKMGDLVTSNFE
SPIVNDTYEEEKITFNDVKVYNMNLLYSKEAENARNYLMNERKINFETLKKYYIGFSVME
FQSLENSGKFEKHECLVFPFIRKITTTDENENNCKSIYKGAGKTEDEGDTYEVVRIKVRS
LKDKAYMRLYPKNVRSDMKLFFFGDHLITDSDEVVLTEGEIDAMTIFQETNYPAISLPNG
SKSLPIYLLPHLEKYKKIHLWLDFDKAGKSSVFNFVNKIGLGRTNVITDANVHYLNENSF
KIKRERKRKNKVINLLNPNSASLSSSEESNADASSNSNAFASQQENLDQSDTEKEKENDV
YFIDNGIMYIWNKIFVKDANDCLKNNIDVQFFIKNSEKVKHSQILNFNDLRQHILEELKY
PDRINGVRSKTIPSLNKFLYGLRMGELSIWTGSTGVGKTTLLSQLSLDYCIQGVSTLWGS
FEINNIKLAKVMLNQFCGKNLEKNIDLFDLYADKFELLPLKFLKFHGSTNIDQVLDAMDY
AVYAYDVKHIIIDNLQFMLNINKFSDIYELQNIAIDKFRSFSTNKNVHITLVVHPRKEDI
IYFLFHQFLVVMTIKEMPINYLNDFLSNNGSIGGSSSNNYLNKNGSYSNVLQNISSASNN
NMDFTLCDEYDYMKQLSDEYESKHAFRRYNNKTGKCVADSGGLSLLKSSTLGSGTRRGDI
FSEIKGNGKNAENEDIEKEKEKCNSKISELLKQNDEKVAFTKTTNNSVTAQSLGSNFIRS
KEKNTKKKSVTENVGLQNNDSTNLKGGNKNSEINTDTMNNKNVTKGKYSSYLLSNEGLEK
LCKELKEDDQEKFKNVIISMSMRNCVINNNSPIKDIRNFIKVNKLNIKTSGNNLKKKDVF
INVLQSIPKEYISITEGDTSGSNDSINCTQKETFSGSQRQGNMSTNKNTGGEYSNMGSMD

EEGDNNGIKNDMNNEMYDNQIEARLDDEITKKYMDDNIINVDGNIVKKCAREKLINDKDN
TEIEENLYYYERKKTLMIILRLDELMETTGLEVFGEKIRLIQIAVENYPVIIYDMFNITN
NNILDGLRKILNDENIVKIIQNGKFDTKFLLYNNFNITNIFDTYIASKLLDKNKNMYGFK
LNNIVEKYLSVYLDKQQQNSVWNNSLLNNNQLFYAARDSSCLLKLYKKLSEQIVAENMQI
VNDIENKCILPICDMELNGITVDLE

Figure C.7. Amino acid sequence of *PkPREX*.

MVRCQLFLFYLILIHYVLAVRNKSRPKADFYLKTNCELVKRRKNGSKAYFKRKVRDEDLGLRSFYDQLRG
GRSNCSSAGNHDNHVDRRNSGALRATSTFVSKYYKINTNDVYSYLNRKKYEYIETDVKITLKYCPFCPPH
KYKYDNMYKHEIFKNTGNSYCHRCGYKGSFYDFKLKMGDLVTSNFESTVVNNTTYEEEKITFNDVKVYNM
NLLYSKFAEGARKYLVEERKLNLETLKKYYIGFSIMEFQSLENSGKFEKHECLIFPFIKKANDMNSIGLN
GNRNNTNEKDSYEIVRIKVRSLRDKGYMRLYPKNVKDEMKLFFFGDHLVSNSEEIVLTEGEIDAMTVNQE
TNYAAISLPNGSKSLPIYLLPYLERFKKIHLWLDFDKAGKSSVFNFVNKIGLGRTNVINDTNVQYLDEQV
FERKRKNMLTKGGLLLPLMIGDNAIGVAEQKQDAIKENTQSGEKNGNTECIAGGNEPNTAVDFISGTKKS
DLQITEKAKSEGDGKNNSICGDTGNKQEEAQKKVNEESKVRAFHFVQNNIMYIPNNIVVKDANDCLRHNI
DIRFFIENSEKVKHSQILNFNDLRQNILEELKYPDRINGIKSKTIPSLNKFLYGLRMGELSIWTGPTGVG
KTTLLSQLSLDYCIQGVSTLWGSFEINNIKLGKVMLNQFCGKNLEKNIELFDLYADKFELLPLKFLKFIG
STNIDQVLDAMDYAVYAYDVKHIIIDNLQFMLNINKFSDIYELQNIAIDKFRSFSTNKNVHITLVVHPRK
EDNNLLSIASVFGSVKSTQEADNVFIIQRQVSKTNETVFFIDIKKNRFKGCLGRIPYLYNKENMTIKEMS
IGYLNDAIPSSGYGTKVTTPPSNFVPNVGPLRGGLDFTLCDEYDYMKQLSEEYESKHAMRKYRVGADGRV
SGVGSASTNNPNASSSVHRAPNECRNDSGATDSLRNNQNNDNKSVNQVCDAEDDPTSNNRVVNTNDKSEE
CRIKKNMLKGDDQGRTTTPVGKTTKSDKPSGDIIHVQNSPNTKREKQEAAPDVPKQNVSSYRLSSEGITK
LCEEIKDNKNEMLKDREITISMRNCVINKDSTIKDIRNFIKTNKLNIKTAGKNLKKVDVFIAILQSIPKE
YITIKYGGGDVEKDNPDKNSVGNRTGENVKRTKVHSTLAENNNGVITGGNPSGALPVGGPTKNNFNIVSS
VKESSASGHNIGHSLRGYVSHFGKEDALSGEKQYSEEIKSIYGEEVTKRYIQDNIINVDDNIVKRSGMFK
LEGDNKMVSNEKLEYYEPVKKFDDDIESRFFLINDNNYNEKINNIYKNVTHCGLDIETTGLEVFDEKIRL
IQIAVENYPVIIYDMFNITKESILTGLREILKNEKVVKIIQNGKFDAKFLMHNNFQVDNIFDTYIASKLL
DKNKNMYGFKLNNIVEKYLNVTLDKQQQNSVWNNSLLNNNQLFYAARDSSCLLKLYKKLKSEICKENNMET
VNDIENKCILPICDMELNGITVDLESLKKSTNEILSELNIETSKLKAELKDEEININSQQQVLKALQNNN
VRDISNKLIENTSDSNLKNFLNHKEVVLLRNYRRLYKLYSAFYLKLPQHINKKTNKIRTTFNQLKTFSGR
FSSEKPNLQQIPRQKNIREIFIPQKDNIFIIADFKQIELKIAAEITNDDIMLKAYNNNIDLHTLTASIIT
KKPIADVNKEDRHIAKAINFGLIYGMNYVNLKNYANTYYNLNMNLDQCLYFYNSFFEHYKGIYRWHNQIK
QIRGLEYSTLSNRKVIFPYFSFTKALNYFVQGTCADILKLSLVELYKNLKPIHGKIILCVHDEIIIEVDK
KYQEDALKILVESMENSASFFLKKVKCEVSVKIAQNWGSKE

Figure C.8. Amino acid sequence of *PvPREX*.

MVRCRFFLFYLILIHYALAVRNKSRPKADFYLKTNCELVKRRKNGSKAYFKRKARGEDLG
SRARYDDSQLWGRRNRCSGGNRVNRSNRERGALRATSTFVSKYYKINKINDVYSYLNRKKY
EFIETDVKITLKYCPFCPPHKYKYDNMYKHEIFKNTGNSYCHRCGYKGSFYDFKLKMGDL
ITSNFENTVVDRTYEEEKITFNDVKVYSMNLLYSKEAEAARKYLTEERKLNLETLKKYYV
GFSIMEFQSLENSGKFEKHECLIFPFIRKANGASSLGLMGSKHSTNEIDAQENASYEVVR
IKVRSLRDKGYMRLYPKNVKDEVKLFFFGDHLVGSSEEVVLTEGEIDAMTVSQETNYAAI
SLPNGSKSLPIYLLPYLERFKKIHLWLDFDKAGKSSVFNFVNKIGLGRTNVITDANVHYL
DEQLFERKEKNLLTKGGLLVPLTVGDSPIGVAEQKQGGIKENTQRGEENGHSENTLDGRS
PNTAADPTSGTNKADLKTAEKEGDRRKNPICGETGSTQEGEQKKASENCKAKTLHFVQNN
IMYLPNSIVVKDANDCLKHNIDVRFFIQNSEKVKHSQILNFNDLRQNILEELKYPDRING
VKSKTIPSLNKFLYGLRMGELSIWTGPTGVGKTTLLSQLSLDYCIQGVSTLWGSFEIKNI
KLGKVMLNQFCGKNLEKNIDLFDLYADKFELLPLKFLKFIGSTNIDQVLDAMDYAVYAYD
VKHIIIDNLQFMLNINKFSDIYELQNIAIDKFRSFSTNKNVHITLVVHPRKEDNNLLSIA
SVFGSVKSTQEADNVFIIQRHVSKTNETVFFIDIKKNRFKGSLGRIPYLYNKENMTIKEM
SIGYLNDSISSSGYGANGTPPSSNFLPSVNPPRDGLDFTLCDEYDYMKQLADEYESKHAV
RRYRLGADGKANGVGSGSTNRPNASSLKCSQNVNSTDGGLVDSSRNNQNRDNKPVNQVGG
VEDDPTRSNHVGSANGRGEKGGIKNILKGTDRGDTAPPVGGTPTSDKPSGGSSHVCTPAK
PTGEKQELTADMSKQSVPSYRLSSEGIIKLCEEIKDNKGETLKDREITISMRSCVINKDS
TIKDLRNFIKTNKLNIKTAGKNLKKVDVFIAILQSIPKEYITVKYVGGDVGKGNPTNNNV
RMGGGENVKGGRLNGALAGNHNSVNGGGSPSRAIPIGGPTKNDLNIVTTARESPVNSHNL
GHISSGHGSAPLTGDGQVGEKHYSEEIKSLYGEEVTKRYIQDNIINVDDNIVKRSGIFKL
EGDDKMVGSEKLEYYEPVKKFDDDIESRFFLIHDSNYNERINHIYKNVTHCGLDIETTGL
EVFDEKIRLIQIAVEDYPVIIYDMFNITKESILTGLREVLKNEKVVKIIQNGKFDAKFLM
HNKFEVANIFDTYIASKLLDKNKNMYGFKLNNIVEKYLNVTLDKQQQNSVWNNSLLNNNQ
LFYAARDSSCLLKLYKKLKSEICRENNMGTVNDIENKCILPICDMELNGITVDLESLSKST
NEILSELNEETSKLKAELKDEEINVNSQQQVLKALQNKNVRDVSNKLIENTSDSNLKNFL

NHREVVLLRNYRRLYKLYSAFYLKLPQHINKKTNKIHTTSNQLKTFSGRFSSEKPNLQQI
PRQKNIREIFIPQKDNIFIIADFRQIELKIAAEITNDDIMLKAYNNNIDLHTLTASIITK
KAIADVNKEDRHIAKAINFGLIYGMNYVNLKNYANTYYNLNMNLDQCLYFYNSFFEHYKG
IYRWHNQIKQMRALEYSTLSNRKVIFPYFSFTKALNYPVQGTCADILKLSLVELYKNLRP
INGKIILCVHDEIIIEVDKKYQEDALKILVESMENSASFFLKKVKCEVSVKIAQNWGSKE

Figure C.9. Amino acid sequence of *TaPREX*.

MEPTYYTNQNLNETTLRIPKKRLIGRSKVAFLFFLTRLILISSLLQFSESVKTDLSQGSF
SISKRGRKTPRPEIPCNIFEKLNTIHKLNAVDKFSMISMKSLKQLSNLRNLIRFKYNKGS
RNYKNRNFYKCLFVKNLNEPQIDGGNIIYGSQFYAYSPSSYENVPSYNGSYGLDESNTFV
SNHYRNMGEDIVEYLNRKKIEYNESPVKYTLKFCPFCPPHRFKSDNLYKHEIFKNSGNSY
CHRCGYKGSLFDFKAHMGDLPGAFDIASDPITNPFGAKKVQKDPDVTITDVNKFEDNLYN
NPEYACVLEYLTKTRGLKTHVLKKYHVGAGTFKFKSVTGKLEPEKCVVFPWLSTPHKPYA
DMGDDVEIRDESEGFDYNREYTTDKLNVNRIKIRSIYDKSKIKILPRGGTWGMFGGHLIQ
EALEKDSIVLSEGELDAMSIFQETGRITISLPNGANSLPLALLPKLEKFNEIYLWMDFDA
PGQSSISHFANKLGIQRVKIVHPLNTPSTTGTTTTGTTTTGAGTTTKGTKSTTTATPTSK
SKMMKDANEVLLSGGVDMNNYFKNATVMTHSQILTFNDIKQLVYNELSDPVTTCGIKSIT
MPGLSNLLKGHRRGELTVWTGSTGSGKTTLLSQLSLDYCLQGVSTLWGSFEINNVRLAKT
MLRQFSGRNLENSLNEFDYYANKFNELPLRFLKFHGSTNIDIVLDAMDYAVYVYDVQHII
IDNIQFMLSNYSCPSQNSSYGGYSSTKDVYELQNRTIEKFRRFVTNKNIHLSLVVHPRKE
ADGIQLGLSSVFGSVKSTQEADNVIILQNILNESRCIDVKKNRFAGLLGRVYFKFDPVSL
TAQEFKVTEYLNEYTTNNFTKAKVKKDQTESFTVPSGAFPINGGSEVKSKVSLSNFKINL
PQVNSTNLSTEPMNIPITTSTMMTEDYQSRAVPASTTTNYRERERNNLGLTGIDLLNLKP
VSQYVNKIIQQNYSTTSNGNQESGDSSTKQDSTESSGVDLTKSNMTGTGDNSNSSGKCRK
KSSKSDPVEEEYLSMRGLKISKSSTIKEMRDFVKKNGLGELVKTAGKGIKKEAIYENIRS
TIPQSAVVNTKQTEKLDASGESETVETIKVEDEGSPKSEVHSFGVSTSKSLLKLERINVV
PNNDIDEFKLKYLSKLPKSLYKGESQPPSQPEKVASNDQPPIPVDVYYSVNYDPLLIDGI
IYVDSYEKLESLKPLFKDPKAVGVDIETTGLDHNTNQIRLVQLSVPNQPSVIIDLFKLNT
KNPESDNVVPGRNELIKCEWLKNLFKSKDTVKVFHNGKFDINFLRVYGFEFEGPIFDTMV
ASKLLVASRYISCKLTHIVSERYLNIVLDKTQQYSDWSTLQLFEEQLLYSARDSFVLLPLY
VILEHLLKINNLADIASVENKCILATSDMELNGIKVDEDKLRILQDELKQEHQEISNDLY
SQLNHSEINLNSQKQVLEKLQELKIMDRSKKKIISDTSESTLIRNMSNPIISSLREYRKA
NKALTAFTQKLPNHINPITSRIYPNYNQLGAESGRFSCDGPNLQQVPRDKKFRECFVAPK
GSKFVIADFSQIELRIAAEIANDPKMIQAYQQNVDLHSLTASILKNKSINEVNKEERQLA
KAVNFGLIFGMSINGLRMYAETGYNLKLTQTEAKEIYTSFFNNFKGILNWHNSVKNSRPT
MVRTLGNRLSVFESFSFTRSLNYPVQGTSADITKETMARLVDSVKPLNAKIIICVHDEII
LEVPEDNAEKALKMLIDTMVKSGEKYLKKVPVEAMGSIGDSWADKS

Figure C.10. Amino acid sequence of *TpPREX*.

MEPTYYTNQALNEPTLRISKKRYYKVAFLFFLTRLILISCLFPFSECVKTDLSQGSF
SISKRGRQFPPPRTLCNIFKTFNTIHKFSPVDKLNMISVKSLKDISNLRNLIRFRYN
KRDRNYRNRSFYKCLFVSNLNKPQMESGKIIDGGSFYSYPPTSYPNMPSYNGSYGLD
ESNTFVSNHYRNMGEDIVEYLNRKKIEYNESPIKYTLKFCPFCPPHRFKSDNLFKHE
IFKNSGNSYCHRCGYKGSLFDFKAHMGDLPGAFDIASDPITSPFGAKKVQKDPDVTI
EDVNKFEDNLYNNPEYACVLDYLTKTRGLKPHVLKKYHVGAGSFKFKSVTGKLEQEK
CVVFPWLSTPNKLYPNDEVETQTDDSEGFDYNREFTTDKLNVNRIKIRSIYDKSKIK
ILPRGGAWGMFGGHLIQEAQEKDSIVLSEGELDAMSIYQETGRLTISLPNGANSLPL
ALLPKLEKFNEIYLWMDFDAPGQSSISHFANKLGIQRVKVVHPLNTPTTTATTTKGT
TTSTKGAGTTTKGSKSTTATTQKTTSKMLKDANEVLLSGGVDMNNYFKNATVMTHSQ
ILTFSDIRQLVYNELSDPVTTCGIKSITMPGLSNLLKGHRRGELTVWTGSTGSGKTT
LLSQLSLDYCLQGVSTLWGSFEINNVRLAKTMLRQFSGRNLENNLNEFDYYANKFNE
LPLRFLKFHGSTNIDIVLDAMDYAVYVYDVQHIIIDNLQFMLSNYSGPSQNSSFGGY
SSSKDIYELQNRTIEKFRRFVTNKNIHLSLVVHPRKEADGIQLGLSSVFGSVKSTQE
ADNVIILQNILNESRCIDVKKNRFAGLLGRVYFKFDPVSLTAQEFKVTEYLNEYTTN
FTKPKVKKDQPDTPTVPSGGFPINGTPETKPKVSLSNFKLNLPQVNGSNVSNEPIGI
PNVGTMTSEDLQSRPTPATSTNYKDKERNNVGLIGIDLLNLKPITQQINKIIQQNYT
TSSNSNSDSSDSSGKPEGEDTSGDDNTNSNLVGTNDKSNSSGKGGKLKTKSELVEEE
YLSMRGLKITKNSSIKEMRDFVKKNGLGELVKTAGKGIKKDAIYENIRSIIPQSAII
TTKPTEEEVESVKEDSSVDTTKVEDESSARSDVHSFGVSTSKSLLKLERVNVTPNND
ITEFKLKYLSKLPKSLYKGEPPSSSKPTPVTTGDQVSIPVDVYYSVNFDPLIIDGII
YVDSYDKLQSLEPLFKDPKAVGVDIETTGLDHNTNQIRLVQLSVPNQPSLIIDLFKL
STNNPDAESVVPGRNELIKCEWLKKLFKSKETVKVFHNGKFDINFLRVYGFEFEGPI

FDTMVASKLLVASRYISCKLTHVSERYLNIVLDKTQQYSDWSTLQLFEEQLLYSARD
SFVLLPLYVILEHLLKINNLSDIASVENKCILATSDMELNGIQVDEDKLKFLQDELK
QEHQEISNTLYSQLNQSEINLNSQKQVLEKLQELKIMDKSKKKIISDTSESTLIRNM
SNPIISSLREYRKANKALTAFTQKLPNHINPITSRIYPNYNQLGAESGRFSCDGPNL
QQVPRDKKFRECFVAPKGSKFVIADFSQIELRIAAEIANDPKMIQAYQQKVDLHSLT
ASILKNKNINDVNKEERQLAKAVNFGLIFGMSINGLRMYAETGYNLKLTQNEAKEIY
TSFFNNFKGILNWHNSVKNSRPTMVRTLGNRLSVFESFSFTRSLNYPVQGTSADITK
ETMARLVDLVKPLNAKIIICVHDEIILEVPEDNAEKALKMLIDTMVKSGEKYLKKVP
VEAMGSIGDSWADKS

Figure C.11. Multiple alignment of amino acid sequences of *Plasmodium* PREX homologues

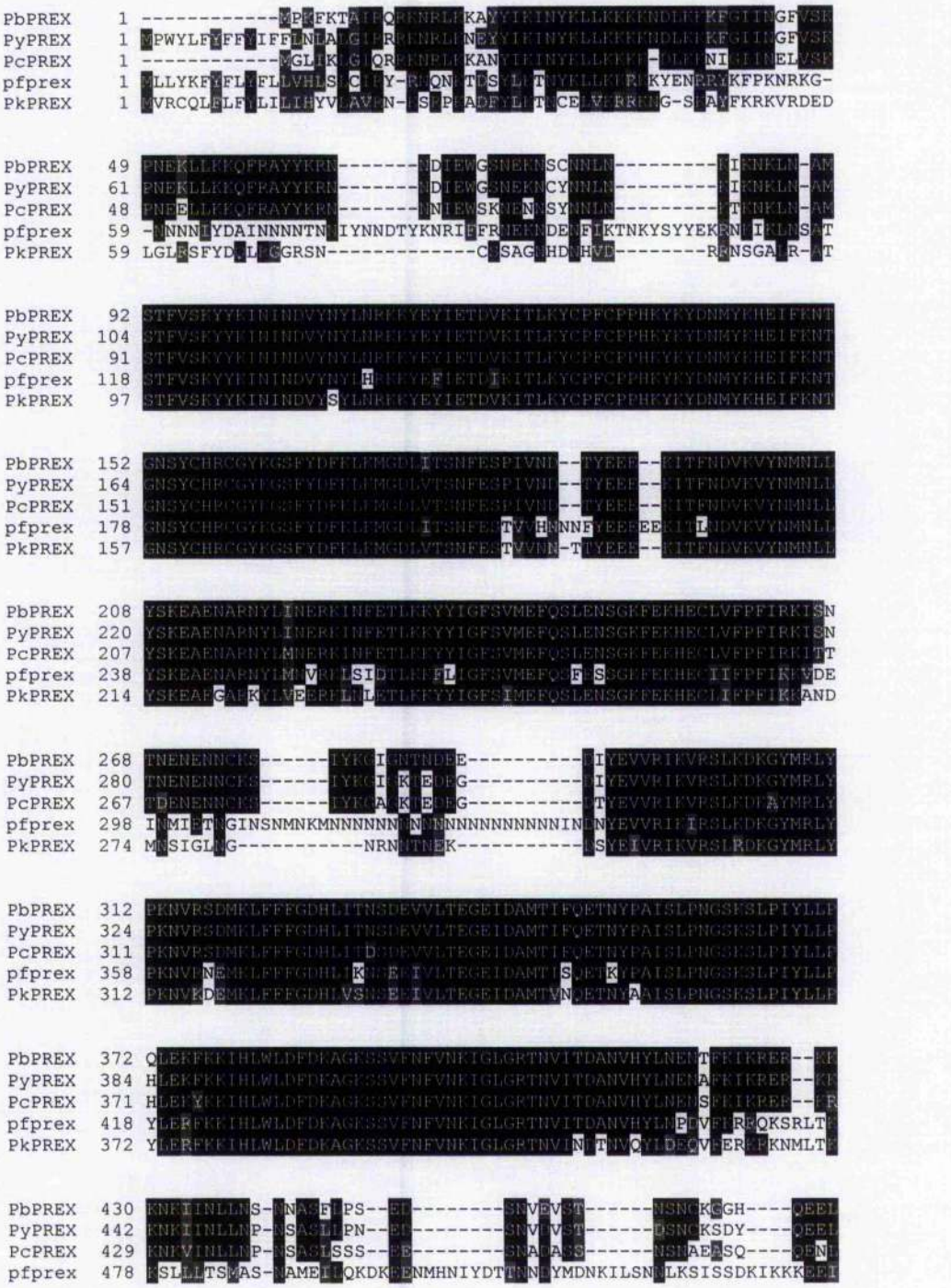

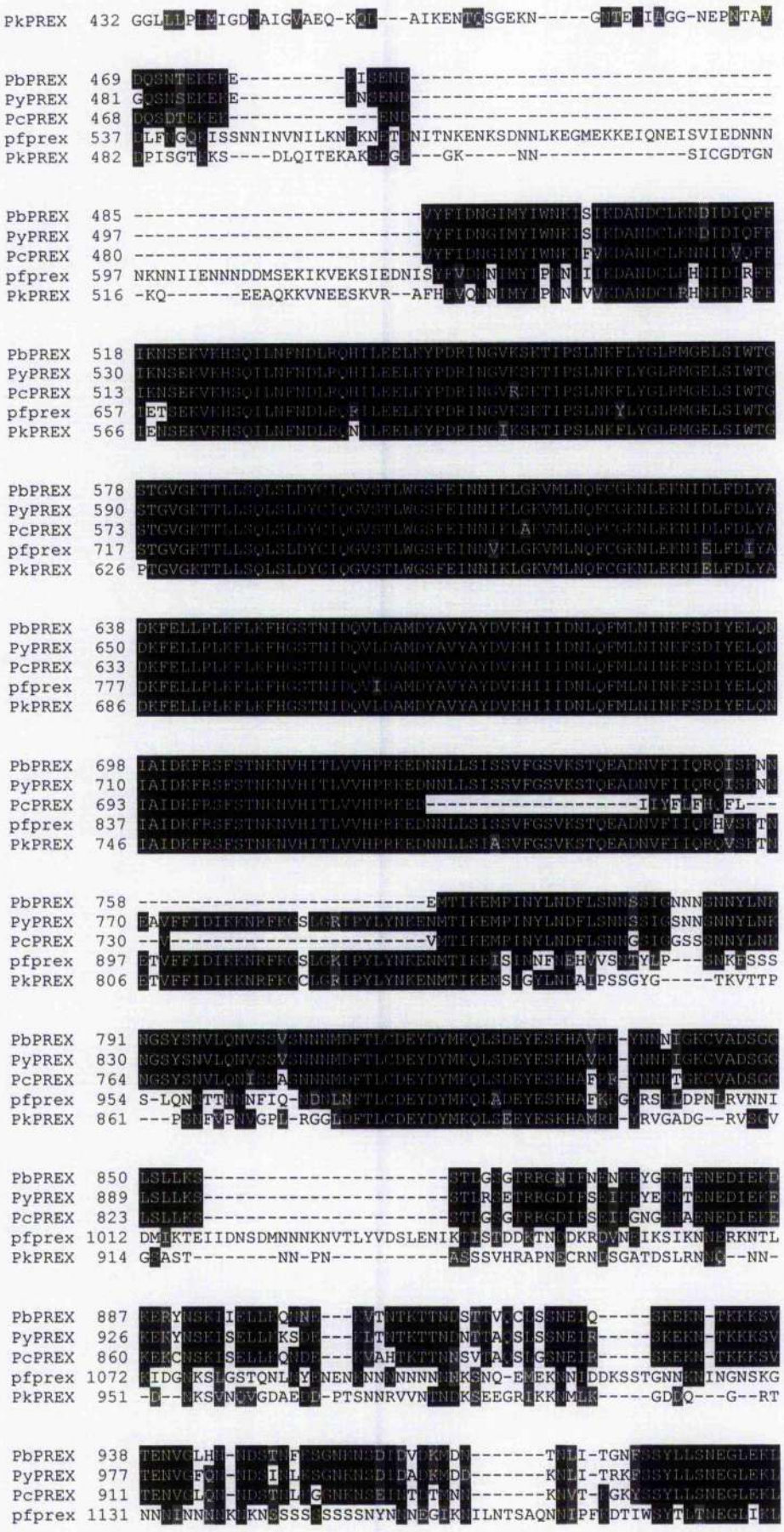

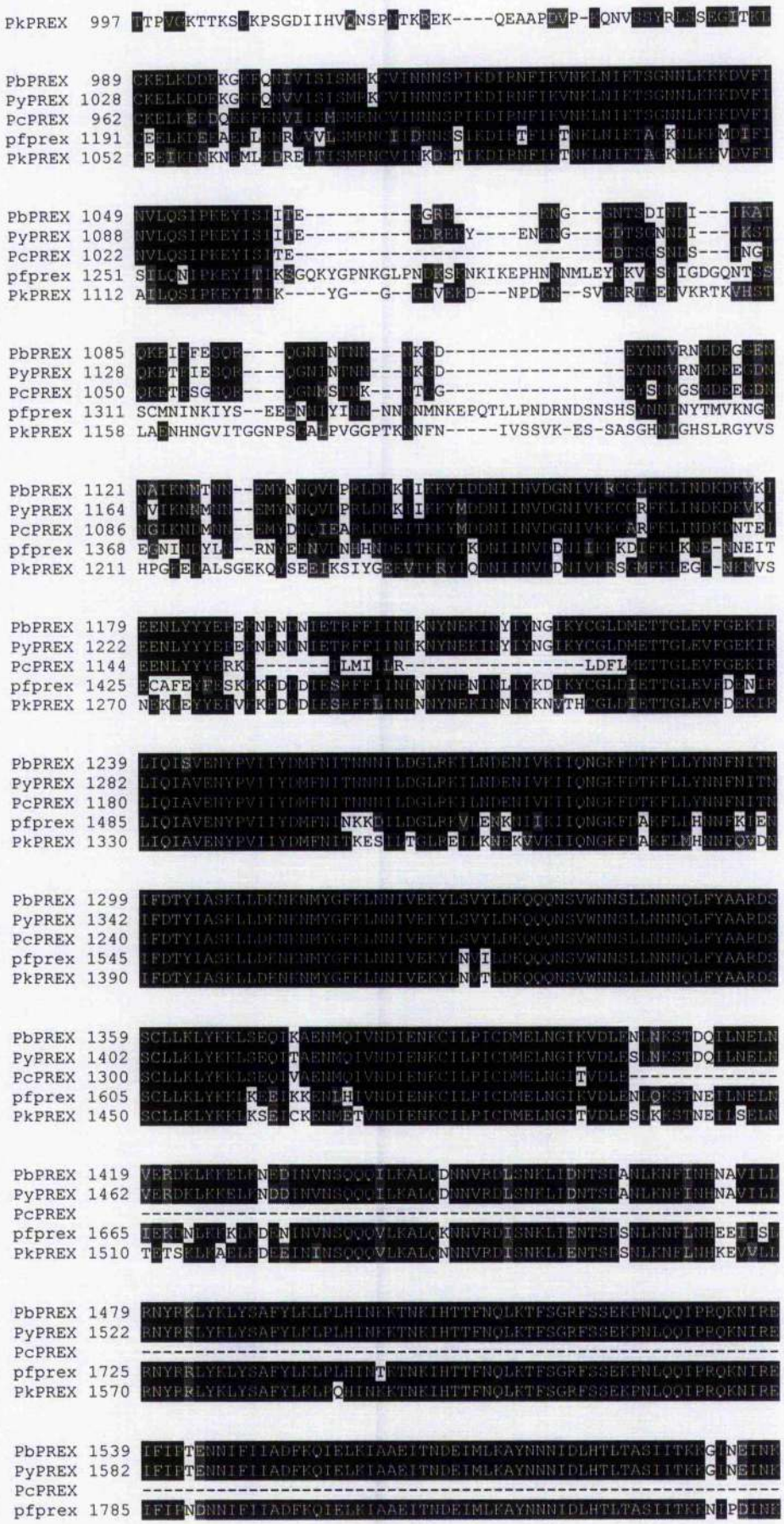

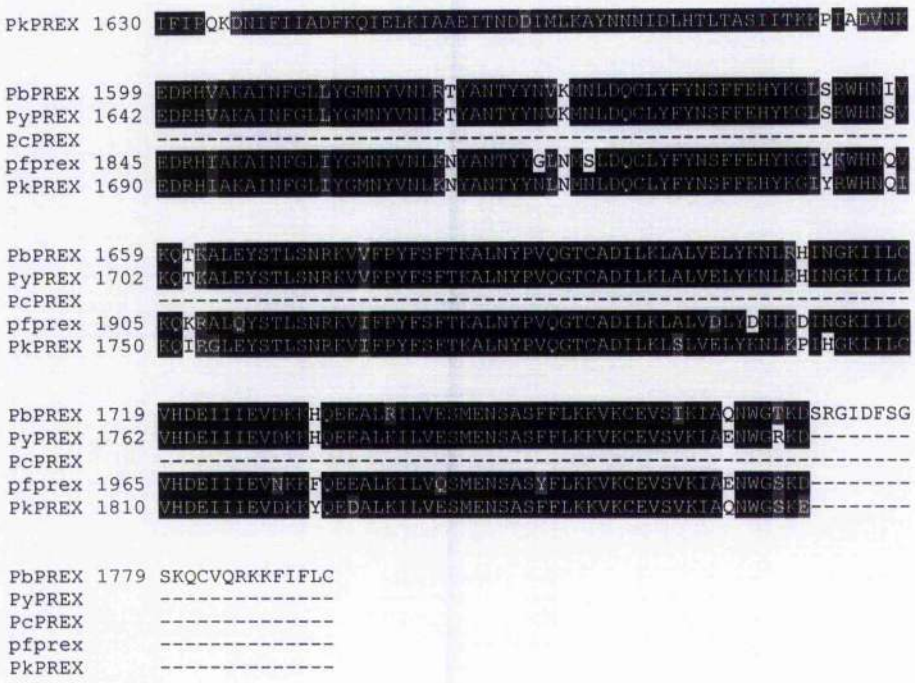

Figure C.11. Multiple alignment of amino acid sequences of *Plasmodium* PREX homologues. Sequences were aligned using ClustalX 1.81. Black shading indicates identical amino acids; grey shading indicates conserved amino acid substitutions. The numberings on the left hand side shows the relative position of the amino acid in the respective sequences. Abbreviations: *P. falciparum* (Pf), *P. berghei* (Pb), *P. chabaudi* (Pc), *P. knowlesi* (Pk), *P. vivax* (Pv) and *P. yoelii* (Py). Introns boundaries were determined using ORF finder at http://www.ncbi.nlm.nih.gov/gorf/gorf.html.

APPENDIX D

Figure D.1. Full alignment of deduced amino acid sequences of DNA polymerase domains of DNA polymerases from family A

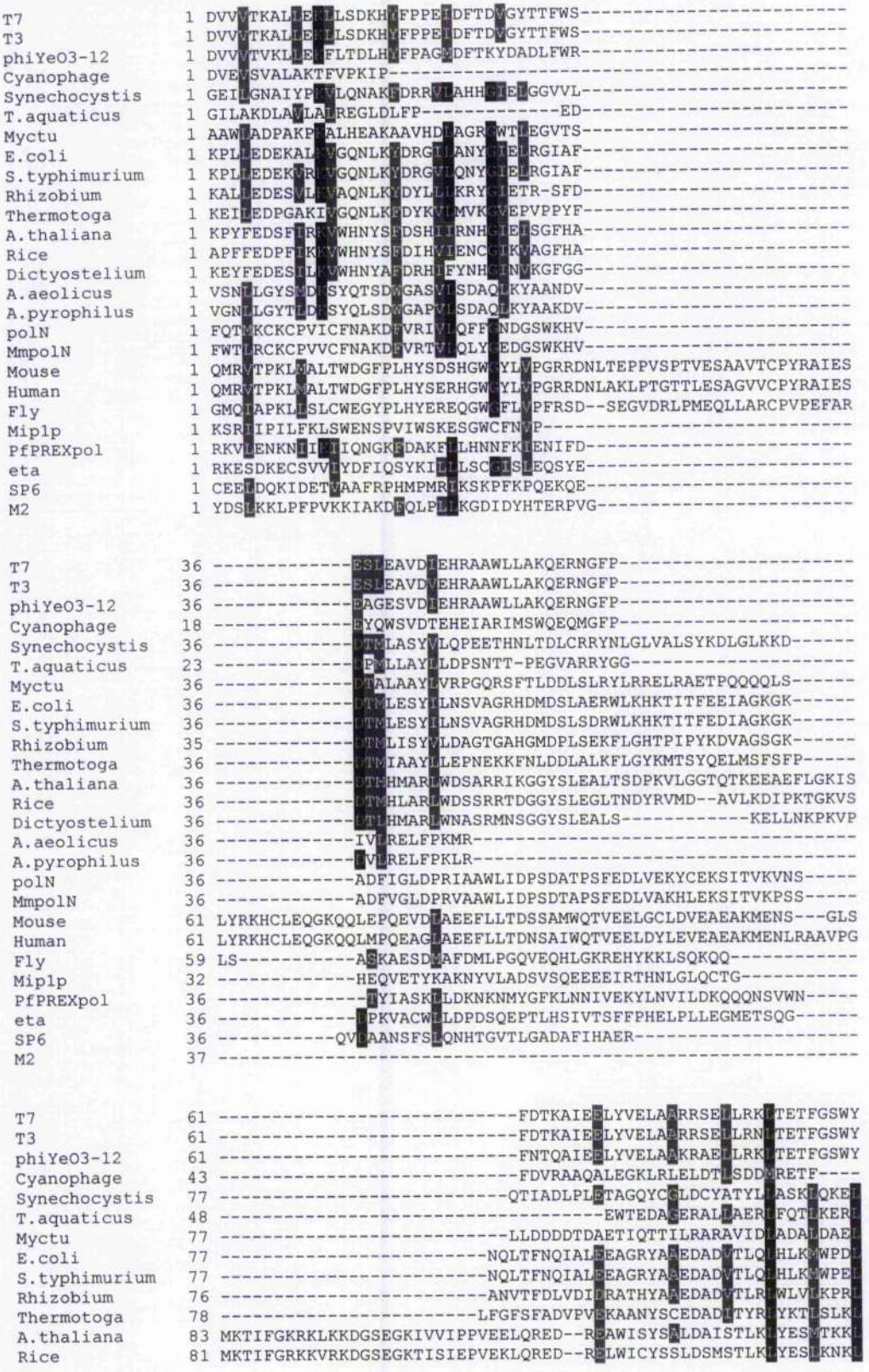

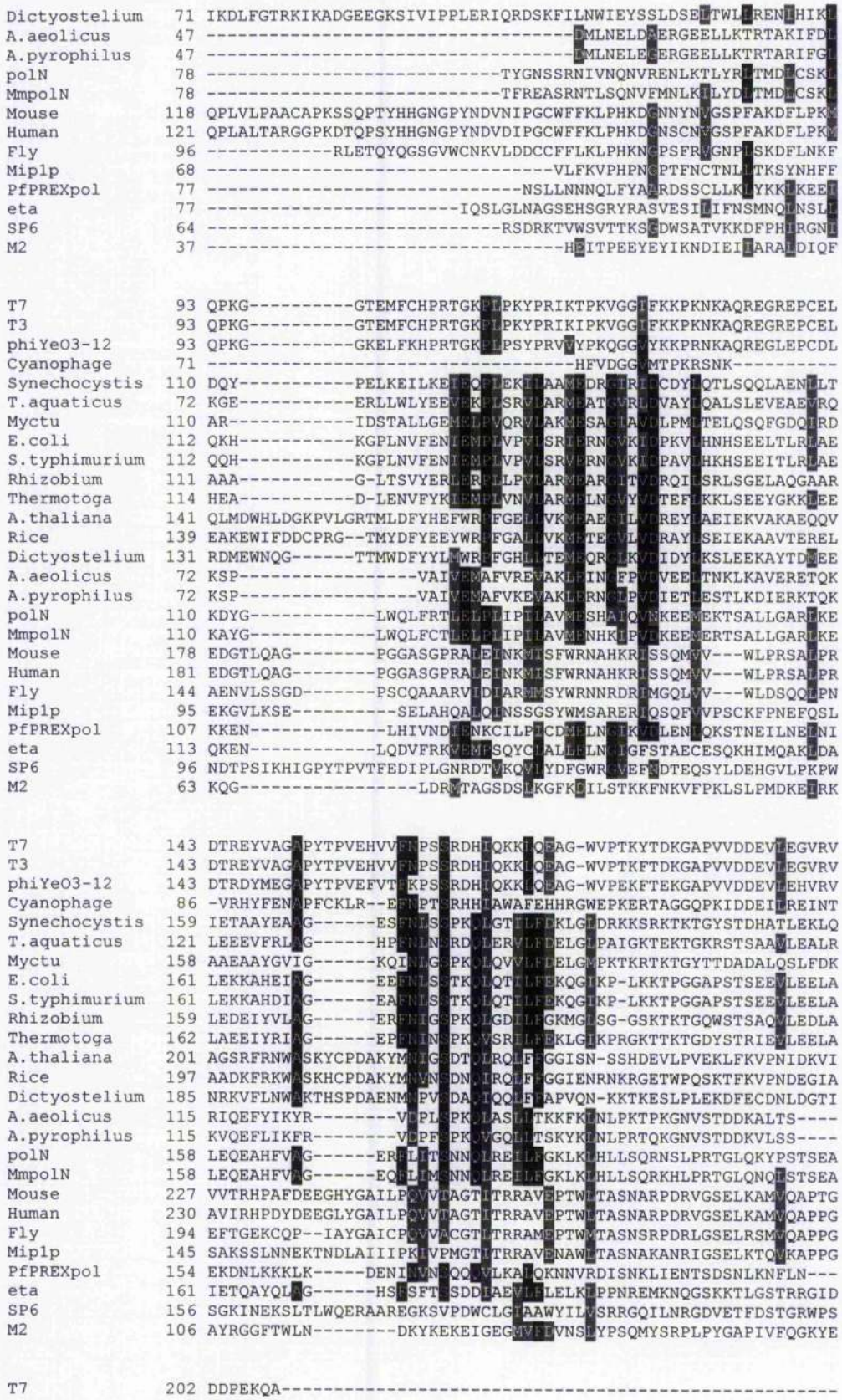

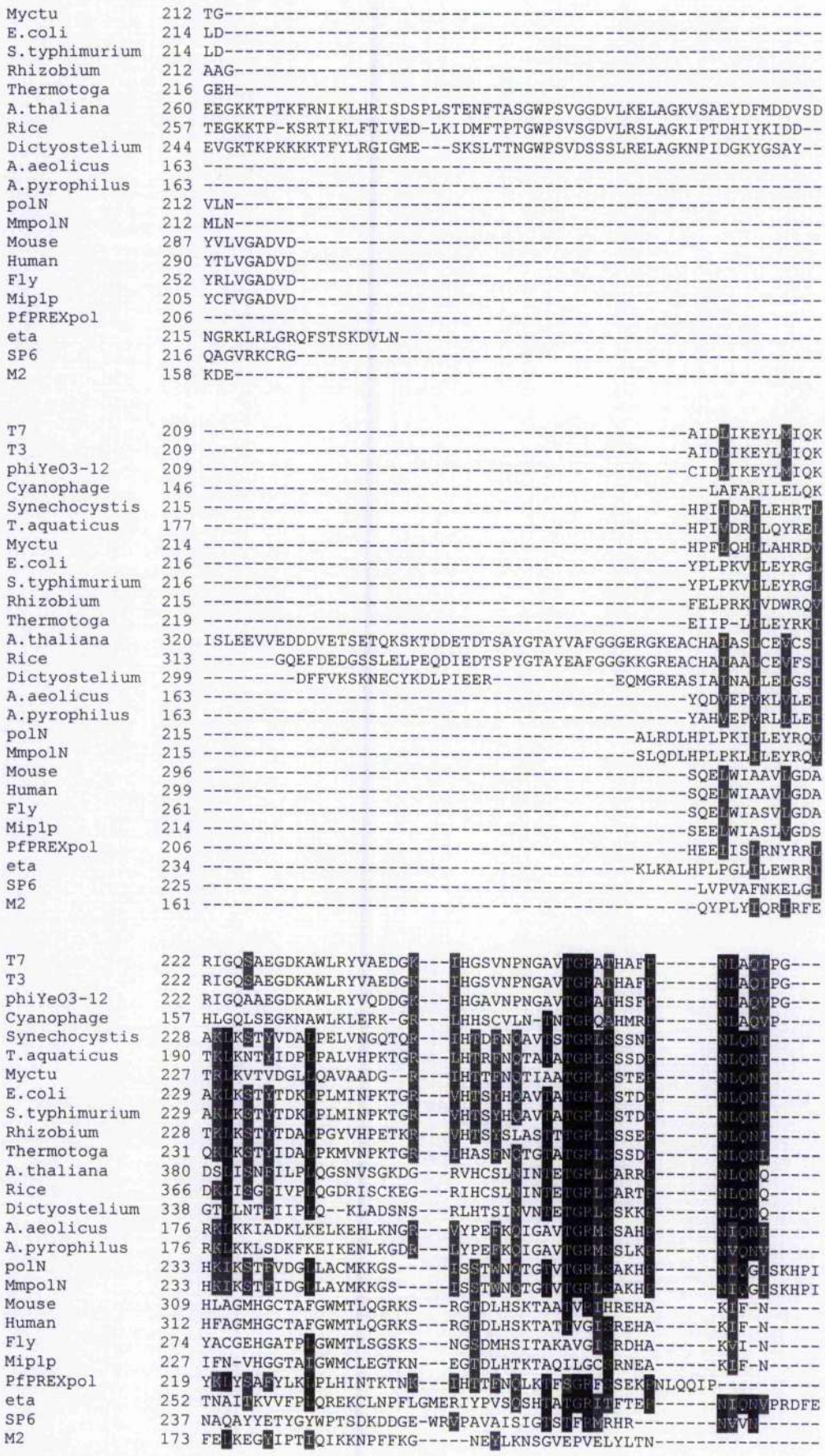
Myctu 212 TG
E.coli 214 LD
S.typhimurium 214 LD
Rhizobium 212 AAG
Thermotoga 216 GEH
A.thaliana 260 EEGKKTPTKFRNIKLHRISDSPLSTENFTASGWPSVGGDVLKELAGKVSAEYDFMDDVSD
Rice 257 TEGKKTP-KSRTIKLFTIVED-LKIDMFTPTGWPSVSGDVLRSLAGKIPTDHIYKIDD--
Dictyostelium 244 EVGKTKPKKKKTFYLRGIGME---SKSLTTNGWPSVDSSSLRELAGKNPIDGKYGSAY--
A.aeolicus 163
A.pyrophilus 163
polN 212 VLN
MmpolN 212 MLN
Mouse 287 YVLVGADVD
Human 290 YTLVGADVD
Fly 252 YRLVGADVD
Mip1p 205 YCFVGADVD
PfPREXpol 206
eta 215 NGRKLRLGRQFSTSKDVLN
SP6 216 QAGVRKCRG
M2 158 KDE
T7 209 AIDEIKEYLMIQK
T3 209 AIDEIKEYLMIQK
phiYeO3-12 209 CIDEIKEYLMIQK
Cyanophage 146 LAFARILELQK
Synechocystis 215 HPIEDALLEHRTL
T.aquaticus 177 HPIVDRILQYREL
Myctu 214 HPFEQHLLAHRDV
E.coli 216 YPLPKVLLEYRGL
S.typhimurium 216 YPLPKVLLEYRGL
Rhizobium 215 FELPRKIVDWRQV
Thermotoga 219 EIIP-LILEYRKI
A.thaliana 320 ISLEEVVEDDDVETSETQKSKTDDETDTSAYGTAYVAFGGGERGKEACHAIASLCEVCSI
Rice 313 -------GQEFDEDGSSLELPEQDIEDTSPYGTAYEAFGGGKKGREACHAIAALCEVFSI
Dictyostelium 299 ---------DFFVKSKNECYKDLPIEER----------EQMGREASIAHNALLELGSI
A.aeolicus 163 YQDVEPVKLVLEI
A.pyrophilus 163 YAHVEPVRLLLEI
polN 215 ALRDLHPLPKIILEYRQV
MmpolN 215 SLQDLHPLPKLILEYRQV
Mouse 296 SQEIWIAAVLGDA
Human 299 SQEIWIAAVLGDA
Fly 261 SQEIWIASVLGDA
Mip1p 214 SEEIWIASLVGDS
PfPREXpol 206 HEEIISIRNYRRL
eta 234 KLKALHPLPGLILEWRRI
SP6 225 LVPVAFNKELGI
M2 161 QYPLYIQRIRFE
T7 222 RIGQSAEGDKAWLRYVAEDGR---IHGSVNPNGAVTGEAIHAFP------NLAQIPG---
T3 222 RIGQSAEGDKAWLRYVAEDGR---IHGSVNPNGAVTGEAIHAFP------NLAQIPG---
phiYeO3-12 222 RIGQAAEGDKAWLRYVQDDGK---IHGAVNPNGAVTGEAIHSFP------NLAQVPG---
Cyanophage 157 HLGQLSEGKNAWLKLERK-GR---LHHSCVLN-INTGEQEHMRI------NLAQVP----
Synechocystis 228 AKIKSTYVDAIPELVNGQTQR---IHTDFNGAVTSTGRLSSNP------NLQNI-----
T.aquaticus 190 TKIKNTYIDPIPALVHPKTGR---LHTRFNQTATATGRLSSDP------NLQNI-----
Myctu 227 TRIKVTVDGLIQAVAADG--R---IHTTFNQTIAATGRLSTEP------NLQNI-----
E.coli 229 AKIKSTYTDKIPLMINPKTGR---VHTSYHQAVTATGRLSTDP------NLQNI-----
S.typhimurium 229 AKIKSTYTDKIPLMINPKTGR---VHTSYHQAVTATGRLSTDP------NLQNI-----
Rhizobium 228 TKIKSTYTDAIPGYVHPETKR---VHTSYSLASTTTGRLSSEP------NLQNI-----
Thermotoga 231 QKIKSTYIDAIPKMVNPKTGR---IHASFNQTGTATGRLSSDP------NLQNL-----
A.thaliana 380 DSIISNFILPIQGSNVSGKDG---RVHCSLNINTETGRLSARP------NLQNQ-----
Rice 366 DKIISGFIVPIQGDRISCKEG---RIHCSLQINTETGRLSARTP------NLQNQ-----
Dictyostelium 338 GTILNTFIIPIQ--KLADSNS---RLHTSINVNTETGRLSKKP------NLQNQ-----
A.aeolicus 176 RKIKKIADKLKELKEHLKNGR---VYPEFKQIGAVTGRMSAHP------NIQNI-----
A.pyrophilus 176 RKIKKLSDKFKEIKENLKGDR---LYPEFKQIGAVTGRMSSLKP------NVQNV-----
polN 233 HKIKSTFVDGILACMKKGS-----ISSTWNQTGVTGRLSAKHP------NIQGISKHPI
MmpolN 233 HKIKSTFIDGILAYMKKGS-----ISSTWNQTGVTGRLSAKHP------NIQGISKHPI
Mouse 309 HLAGMHGCTAFGWMTLQGRKS---RGTDLHSKTAATVPIHREHA------KIF-N-----
Human 312 HFAGMHGCTAFGWMTLQGRKS---RGTDLHSKTATTVGLSREHA------KIF-N-----
Fly 274 YACGEHGATPIGWMTLSGSKS---NGSDMHSITAKAVGISRDHA------KVI-N-----
Mip1p 227 IFN-VHGGTAIGWMCLEGTKN---EGTDLHTKTAQILGCSRNEA------KIF-N-----
PfPREXpol 219 YKIYSAFYLKIPLHINTKTNK---IHTTFNKLKTFSGPFSEKFNLQQIP----------
eta 252 TNAITKVVFPIQREKCLNPFLGMERIYPVSQSHTATGRITFTEP------NIQNVPRDFE
SP6 237 NAQAYYETYGYWPTSDKDDGE-WRVPAVAISIGTSTFFMRHR-------NVVI------
M2 173 FEIKEGYIPTIQIKKNPFFKG-----NEYLKNSGVEPVELYLTN----------

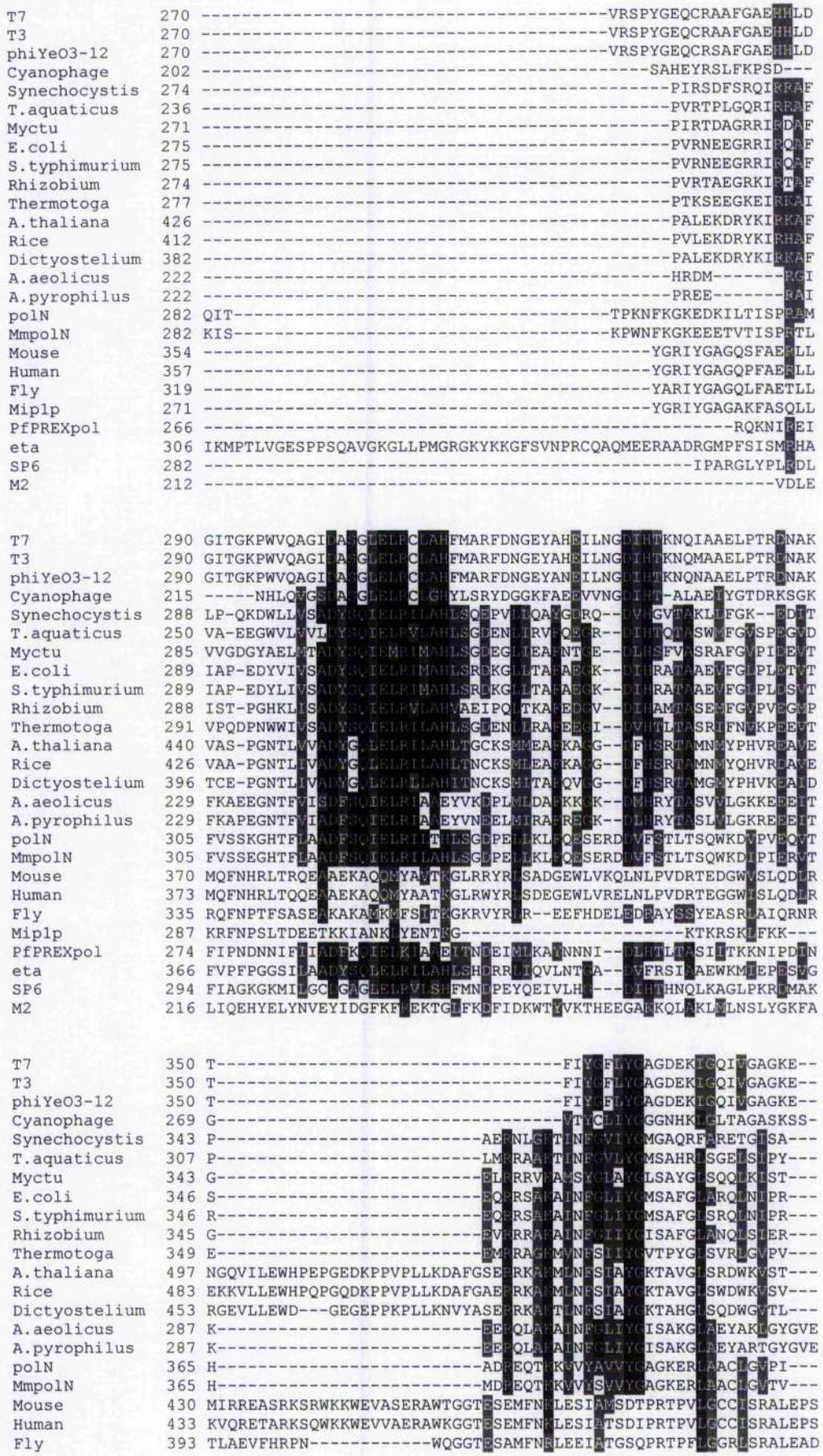
T7 270 VRSPYGEQCRAAFGAEHHLD
T3 270 VRSPYGEQCRAAFGAEHHLD
phiYeO3-12 270 VRSPYGEQCRSAFGAEHHLD
Cyanophage 202 SAHEYRSLFKPSD
Synechocystis 274 PIRSDFSRQIRRAF
T.aquaticus 236 PVRTPLGQRIRRAF
Myctu 271 PIRTDAGRRIRDAF
E.coli 275 PVRNEEGRRIRQAF
S.typhimurium 275 PVRNEEGRRIRQAF
Rhizobium 274 PVRTAEGRKIPTAF
Thermotoga 277 PTKSEEGKEIRKAI
A.thaliana 426 PALEKDRYKIRKAF
Rice 412 PVLEKDRYKIRHAF
Dictyostelium 382 PALEKDRYKIRKAF
A.aeolicus 222 HRDM RGI
A.pyrophilus 222 PREE RAI
polN 282 QIT TPKNFKGKEDKILTISPPAM
MmpolN 282 KIS KPWNFKGKEEETVTISPPTL
Mouse 354 YGRIYGAGQSFAEPLL
Human 357 YGRIYGAGQPFAEPLL
Fly 319 YARIYGAGQLFAETLL
Mip1p 271 YGRIYGAGAKFASQLL
PfPREXpol 266 RQKNIKEI
eta 306 IKMPTLVGESPPSQAVGKGLLPMGRGKYKKGFSVNPRCQAQMEERAADRGMPFSISMPHA
SP6 282 IPARGLYPLRDL
M2 212 VDLE
T7 290 GITGKPWVQAGIDASGLELPCLAHFMARFDNGEYAHPILNGDIHTKNQIAAELPTRPNAK
T3 290 GITGKPWVQAGIDASGLELPCLAHFMARFDNGEYAHPILNGDIHTKNQMAAELPTRPNAK
phiYeO3-12 290 GITGKPWVQAGIDASGLELPCLAHFMARFDNGEYANPILNGDIHTKNQNAAELPTRPNAK
Cyanophage 215 NHLQWGSDASGLELPCLGHYLSRYDGGKFAEPVVNGDIHT-ALAEIYGTDRKSGK
Synechocystis 288 LP-QKDWLLWSADYSQIELRILAHLSQEPVLLQAFGRQ--DVHGVTAKLLFGK--EDIT
T.aquaticus 250 VA-EEGWVLWVLDYSQIELRVLAHLSGDENLIRVFQEGR--DIHTQTASWMFGVSPEGVD
Myctu 285 VVGDGYAELRTADYSQIEMRIMAHLSGEEGLIEAFNTGE--DLHSFVASRAFGVPIEEVT
E.coli 289 IAP-EDYVIVSADYSQIELRIMAHLSRDKGLLTAFAEGK--DIFRAIAAEVFGLPLDTVT
S.typhimurium 289 IAP-EDYLIVSADYSQIELRIMAHLSRDKGLLTAFAEGK--DIFRAIAAEVFGIPLDSVT
Rhizobium 288 IST-PGHKLISADYSQIELRVLAHVAEIPQLTKAFEDGV--DIHAMTASEMFGVPVDGVP
Thermotoga 291 VPQDPNWWIVSADYSQIELRILAHLSGDENLIRAFEEGI--DVHTLTASRIFNVKPEEVT
A.thaliana 440 VAS-PGNTLWVADYGQLELRILAHLTGCKSMMEAFKAGG--DFHSRTAMNMYPHVREAVE
Rice 426 VAA-PGNTLIVADYGQLELRILAHLTNCKSMLEAFKAGG--DFHSRTAMNMYQHVREAVE
Dictyostelium 396 TCE-PGNTLIVADYGQLELRLLAHITNCKSMITAFQVGG--DFHSRTAMGMYPHVKEAID
A.aeolicus 229 FKAEEGNTFWISDFSQIELRIAAEYVKGPLMLDAFKKGK--DMHRYTASVVLGKKEEEIT
A.pyrophilus 229 FKAPEGNTFWIADFSQIELRIAAEYVNGELMIRAFREGK--DLHRYTASLVLGKREEEIT
polN 305 FVSSKGHTFLAADFSQIELRILTHLSGDPELLKLFQESERDLVFSTLTSQWKDVPVEQVT
MmpolN 305 FVSSEGHTFLAADFSQIELRILAHLSGDPELLKLFQESERDLVFSTLTSQWKDIPIERVT
Mouse 370 MQFNHRLTRQEAAEKAQGMYAVTKGLRRYRLSADGEWLVKQLNLPVDRTEDGWVSLQDLR
Human 373 MQFNHRLTQQEAAEKAQGMYAATKGLRWYRLSDEGEWLVRELNLPVDRTEGGGWISLQDLR
Fly 335 RQFNPTFSASEAKAKAMKGFSLTKGKRVYRLR--EEFHDELEDPAYSSYEASRLAIQRNR
Mip1p 287 KRFNPSLTDEETKKIANKLYENTKG KTKRSKLFKK
PfPREXpol 274 FIPNDNNIFIIADFKSIELKIAAEITNGEIMLKAFNNNI--DLHTLTASIITKKNIPDIN
eta 366 FVPFPGGSIPAADYSQLELRILAHLSHDRRLIQVLNTGA--DVFRSIAAEWKMIEPEEVG
SP6 294 FIAGKGKMILGCLGAGLELPVLSHFMNLPEYQEIVLHT---DIHTHNQLKAGLPKRLMAK
M2 216 LIQEHYELYNVEYIDGFKFTEKTGLFKDFIDKWTYVKTHEEGAFKQLAKLMLNSLYGKFA
T7 350 T FIKGFLYGAGDEKIGQIVGAGKE
T3 350 T FIKGFLYGAGDEKIGQIVGAGKE
phiYeO3-12 350 T FIKGFLYGAGDEKIGQIVGAGKE
Cyanophage 269 G VTYGLIYGGGNHKLGLTAGASKSS
Synechocystis 343 P AENNLGFTINFGVIYGMGAQRFARETGISA
T.aquaticus 307 P LMSRAAHTINRGVLYGMSAHRLSGELSIPY
Myctu 343 G ELERRVPAMSKGLAYGLSAYGLSQQLKISST
E.coli 346 S EQERSAPAINFGLIYGMSAFGLARQLNIPR
S.typhimurium 346 R EQERSAPAINFGLIYGMSAFGLSRQLNIPR
Rhizobium 345 G EVERRAPAINFGIIYGISAFGLANQLSIER
Thermotoga 349 E EMERAGRMVNFSIIYGVTPYGLSVRLGVPV
A.thaliana 497 NGQVILEWHPEPGEDKPPVPLLKDAFGSEGRKAPMNFSIAYGKTAVGLSRDWKVST
Rice 483 EKKVLLEWHPQPGQDKPPVPLLKDAFGAEGRKAPMNFSIAYGKTAVGLSWDWKVSV
Dictyostelium 453 RGEVLLEWD GEGEPPKPLLKNVYASEGRKAPTNFSIAYGKTAHGLSQDWGVTL
A.aeolicus 287 K EEQLAPAINFGLIYGISAKGLAEYAKLGYGVE
A.pyrophilus 287 K EEQLAPAINFGLIYGISAKGLAEYARTGYGVE
polN 365 H ADEEQTKKVVYAVVYGAGKERLAACLGVPI
MmpolN 365 H MDEEQTKKVVESVVYGAGKERLAACLGVTV
Mouse 430 MIRREASRKSRWKKWEVASERAWTGGTESEMFNKLESIAMSDTPRTPVLCCCISRALEPS
Human 433 KVQRETARKSQWKKWEVVAERAWKGGTESEMFNKLESIATSDIPRTPVLCCCISRALEPS
Fly 393 TLAEVFHRPN WQGGTESAMFNRLEEIATGSQPRTPFLGGRLSRALEAD

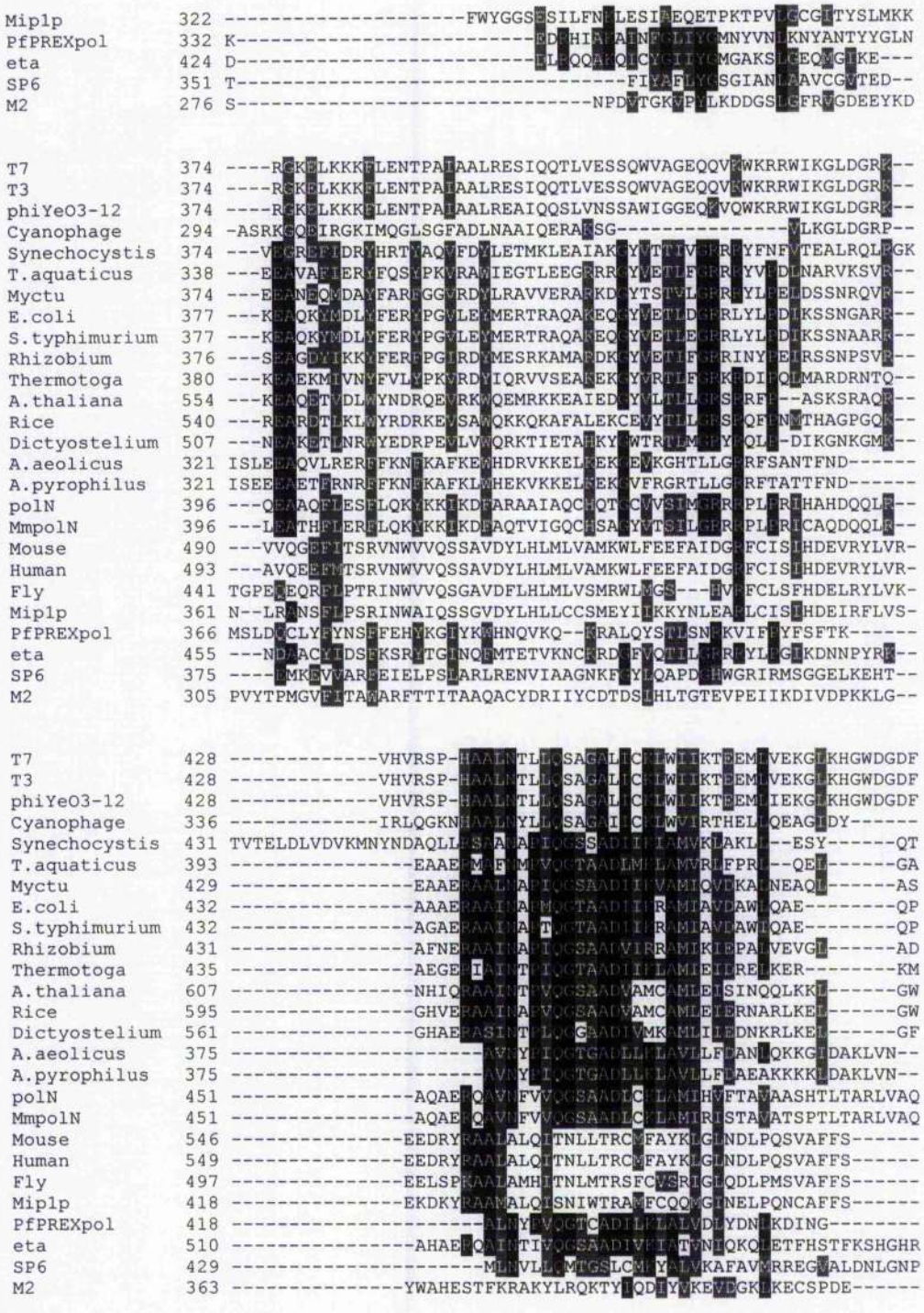

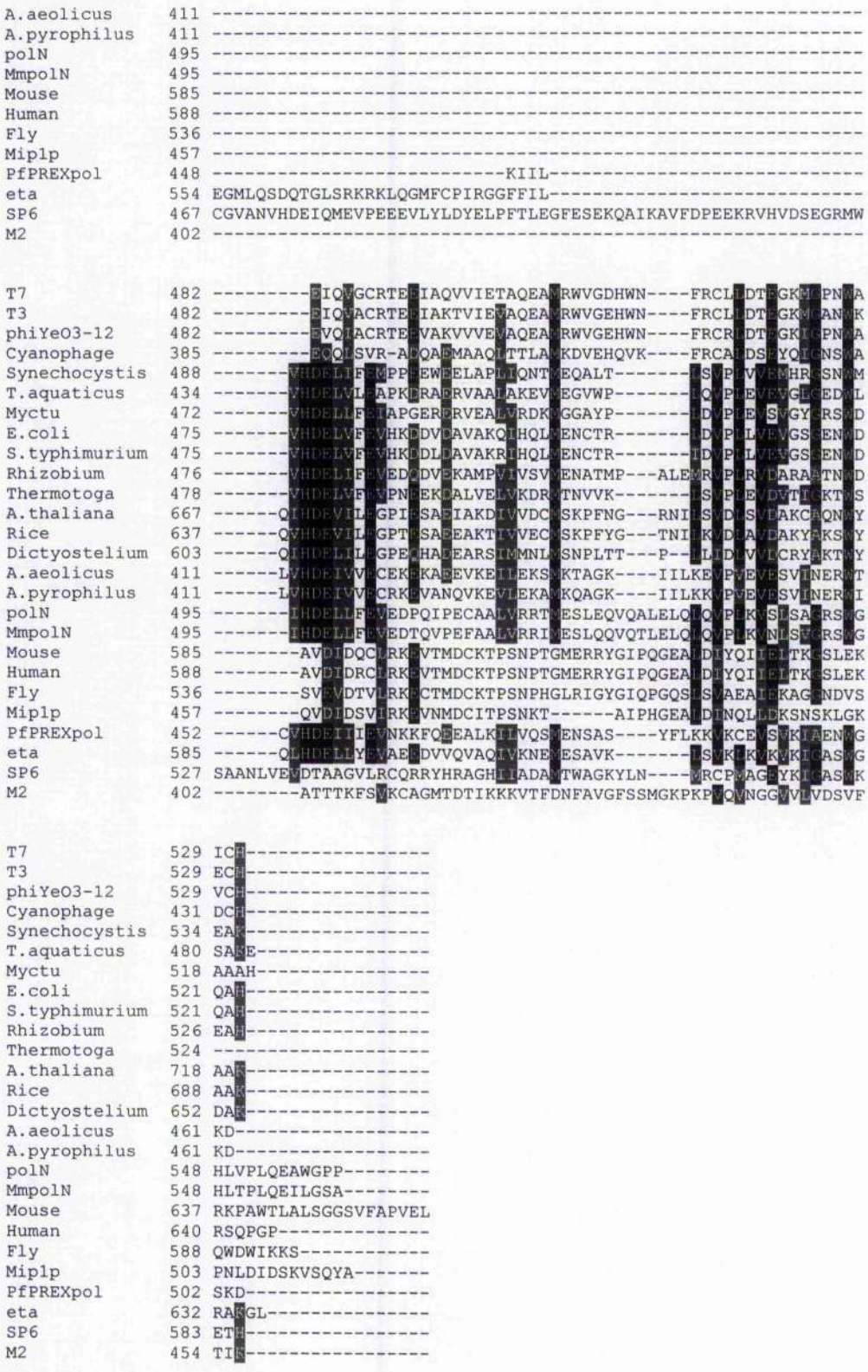

Figure D.1. Full alignment of deduced amino acid sequences of DNA polymerase domains of DNA polymerases from family A. Details of sequences used are shown in Table 6.1, alongside PfPREXpol. These sequences were aligned using DIALIGN. Black shading indicates identical amino acids; grey shading indicates conserved amino acid substitutions. The numberings on the left hand side is the relative position of the amino acid in the respective sequences.

Figure D.2. Full alignment of deduced amino acid sequence of DNA primases

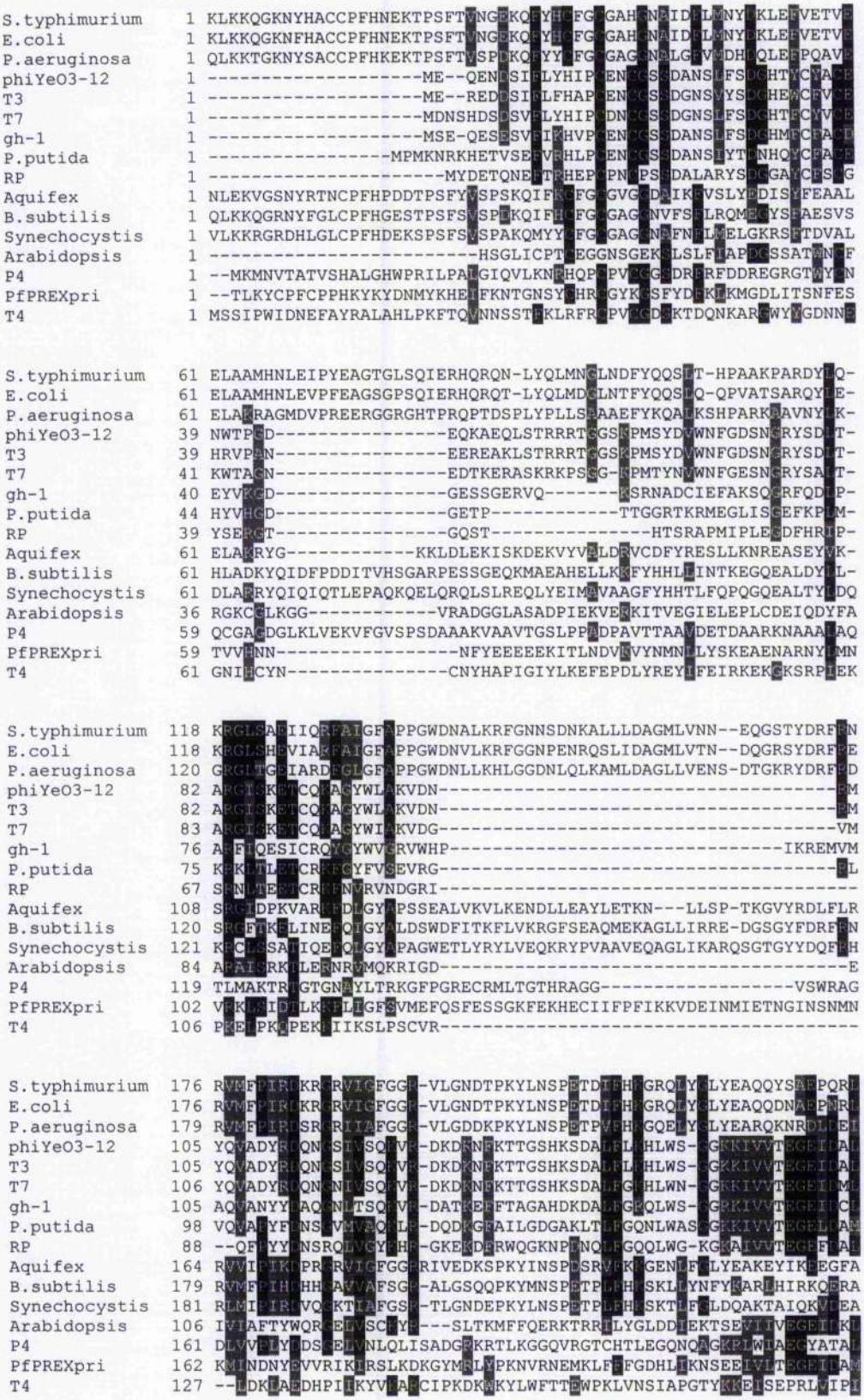

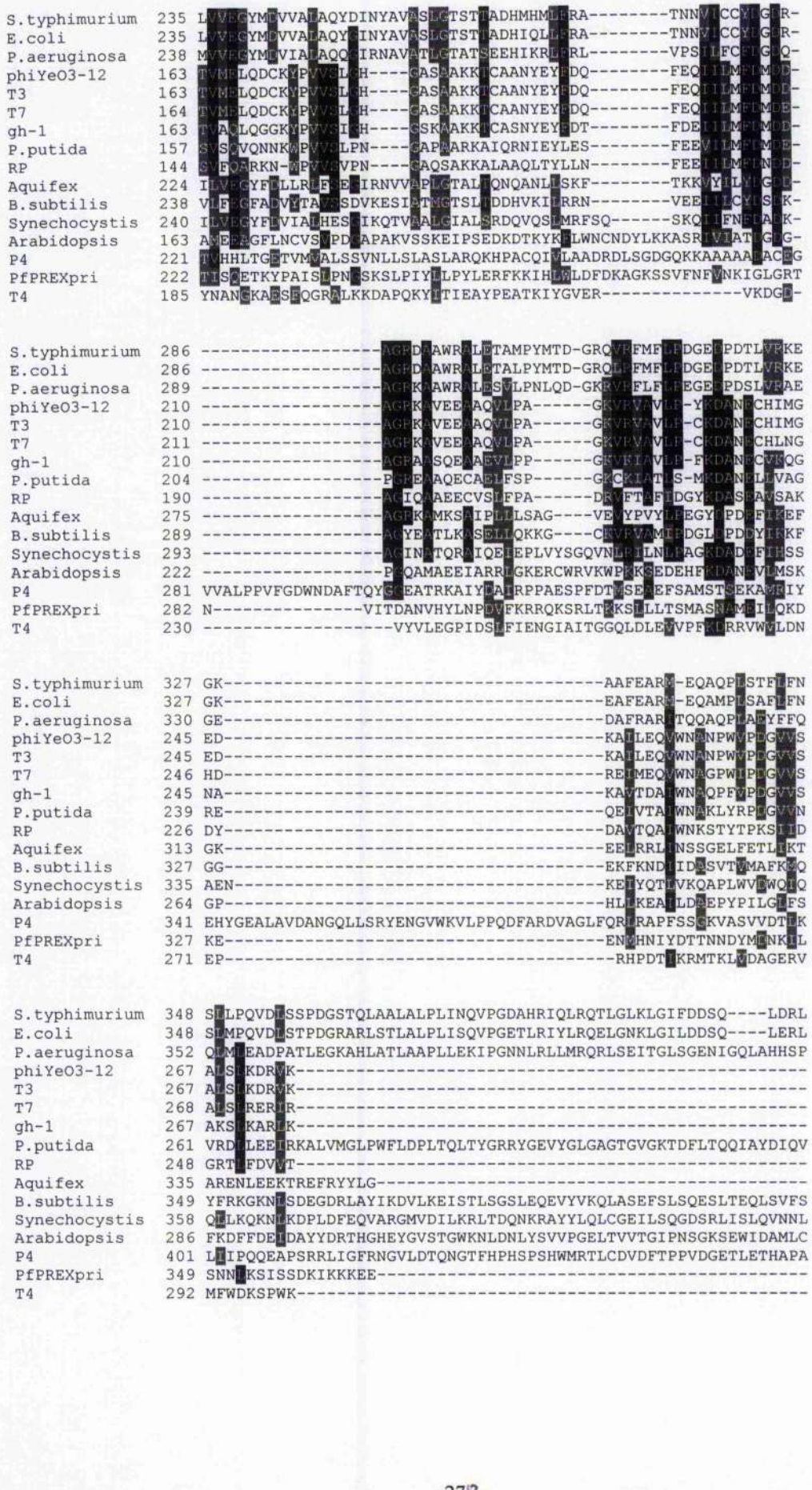

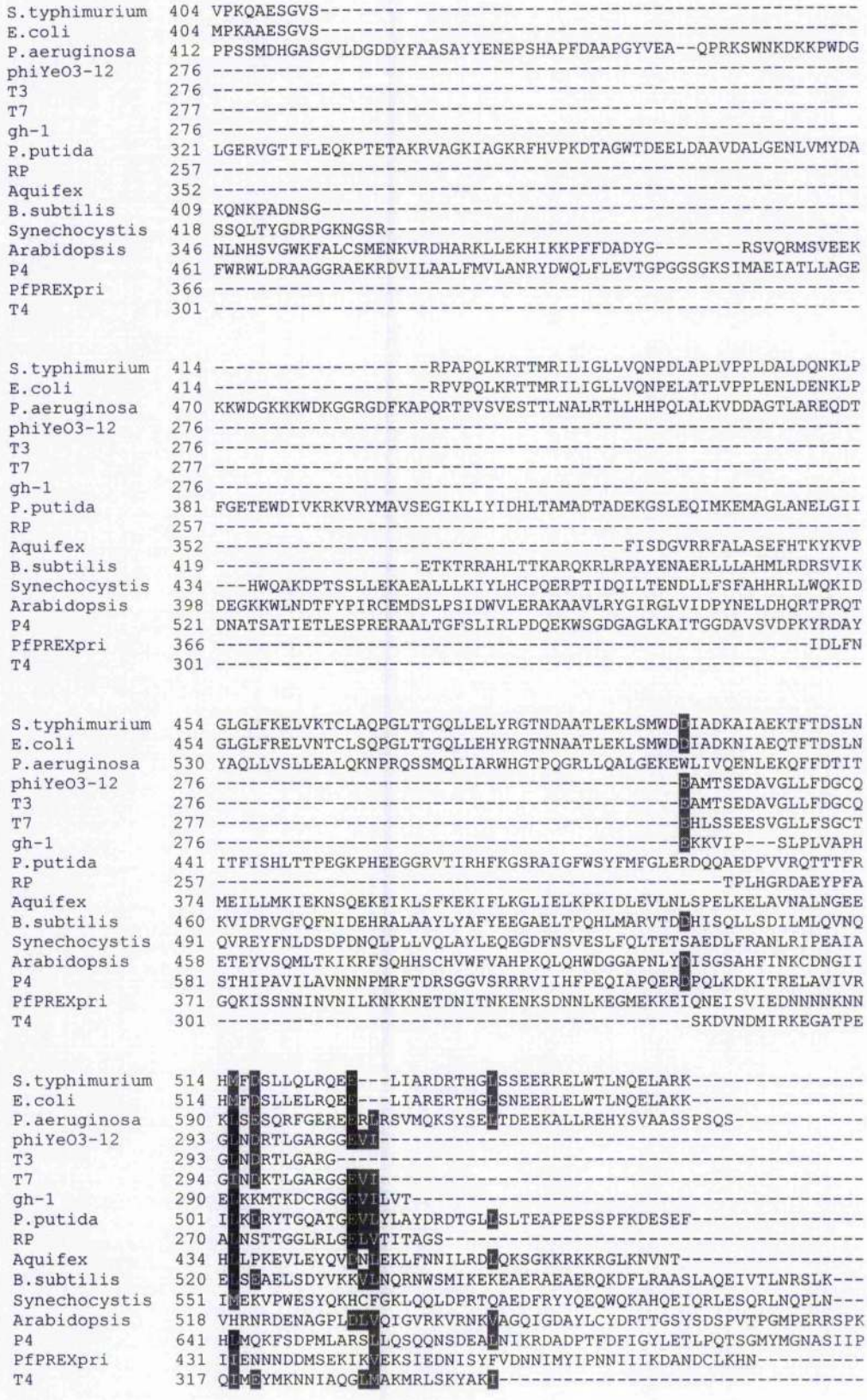
S.typhimurium 404 VPKQAESGVS
E.coli 404 MPKAAESGVS
P.aeruginosa 412 PPSSMDHGASGVLDGDDYFAASAYYENEPSHAPFDAAPGYVEA--QPRKSWNKDKKPWDG
phiYeO3-12 276
T3 276
T7 277
gh-1 276
P.putida 321 LGERVGTIFLEQKPTETAKRVAGKIAGKRFHVPKDTAGWTDEELDAAVDALGENLVMYDA
RP 257
Aquifex 352
B.subtilis 409 KQNKPADNSG
Synechocystis 418 SSQLTYGDRPGKNGSR
Arabidopsis 346 NLNHSVGWKFALCSMENKVRDHARKLLEKHIKKPFFDADYG--------RSVQRMSVEEK
P4 461 FWRWLDRAAGGRAEKRDVILAALFMVLANRYDWQLFLEVTGPGGSGKSIMAEIATLLAGE
PfPREXpri 366
T4 301
S.typhimurium 414 ----------RPAPQLKRTTMRILIGLLVQNPDLAPLVPPLDALDQNKLP
E.coli 414 ----------RPVPQLKRTTMRILIGLLVQNPELATLVPPLENLDENKLP
P.aeruginosa 470 KKWDGKKKWDKGGRGDFKAPQRTPVSVESTTLNALRTLLHHPQLALKVDDAGTLAREQDT
phiYeO3-12 276
T3 276
T7 277
gh-1 276
P.putida 381 FGETEWDIVKRKVRYMAVSEGIKLIYIDHLTAMADTADEKGSLEQIMKEMAGLANELGII
RP 257
Aquifex 352 ----------FISDGVRRFALASEFHTKYKVP
B.subtilis 419 ----------ETKTRRAHLTTKARQKRLRPAYENAERLLLAHMLRDRSVIK
Synechocystis 434 ---HWQAKDPTSSLLEKAEALLLKIYLHCPQERPTIDQILTENDLLFSFAHHRLLWQKID
Arabidopsis 398 DEGKKWLNDTFYPIRCEMDSLPSIDWVLERAKAAVLRYGIRGLVIDPYNELDHQRTPRQT
P4 521 DNATSATIETLESPRERAALTGFSLIRLPDQEKWSGDGAGLKAITGGDAVSVDPKYRDAY
PfPREXpri 366 ----------IDLFN
T4 301
S.typhimurium 454 GLGLFKELVKTCLAQPGLTTGQLLELYRGTNDAATLEKLSMWDFIADKAIAEKTFTDSLN
E.coli 454 GLGLFRELVNTCLSQPGLTTGQLLEHYRGTNNAATLEKLSMWDCIADKNIAEQTFTDSLN
P.aeruginosa 530 YAQLLVSLLEALQKNPRQSSMQLIARWHGTPQGRLLQALGEKEWLIVQENLEKQFFDTIT
phiYeO3-12 276 ----------FAMTSEDAVGLLFDGCQ
T3 276 ----------FAMTSEDAVGLLFDGCQ
T7 277 ----------FHLSSEESVGLLFSGCT
gh-1 276 ----------FKKVIP---SLPLVAPH
P.putida 441 ITFISHLTTPEGKPHEEGGRVTIRHFKGSRAIGFWSYFMFGLERDQQAEDPVVRQTTTFR
RP 257 ----------TPLHGRDAEYPFA
Aquifex 374 MEILLMKIEKNSQEKEIKLSFKEKIFLKGLIELKPKIDLEVLNLSPELKELAVNALNGEE
B.subtilis 460 KVIDRVGFQFNIDEHRALAAYLYAFYEEGAELTPQHLMARVTDCHISQLLSDILMLQVNQ
Synechocystis 491 QVREYFNLDSDPDNQLPLLVQLAYLEQEGDFNSVESLFQLTETSAEDLFRANLRIPEAIA
Arabidopsis 458 ETEYVSQMLTKIKRFSQHHSCHVWFVAHPKQLQHWDGGAPNLYDISGSAHFINKCDNGII
P4 581 STHIPAVILAVNNNPMRFTDRSGGVSRRRVIIHFPEQIAPQERDPQLKDKITRELAVIVR
PfPREXpri 371 GQKISSNNINVNILKNKKNETDNITNKENKSDNNLKEGMEKKEIQNEISVIEDNNNNKNN
T4 301 ----------SKDVNDMIRKEGATPE
S.typhimurium 514 HMFDSLLQLRQE---LIARDRTHGLSSEERRELWTLNQELARK----------
E.coli 514 HMFDSLLELRQE---LIARERTHGLSNEERLELWTLNQELAKK----------
P.aeruginosa 590 KLSESQRFGEREERLRSVMQKSYSELTDEEKALLREHYSVAASSPSQS----------
phiYeO3-12 293 GLNDRTLGARGGEVI----------
T3 293 GLNDRTLGARG----------
T7 294 GLNDKTLGARGGEVI----------
gh-1 290 EKKMTKDCRGGEVILVT----------
P.putida 501 ILKERYTGQATGEVLYLAYDRDTGLESLTEAPEPSSPFKDESEF----------
RP 270 ANNSTTGGLRLGELVTITAGS----------
Aquifex 434 HELPKEVLEYQVLNLEKLFNNILRDLQKSGKKRKKRGLKNVNT----------
B.subtilis 520 ELSEAELSDYVKKVLNQRNWSMIKEKEAERAEAERQKDFLRAASLAQEIVTLNRSLK---
Synechocystis 551 IMEKVPWESYQKHCFGKLQQLDPRTQAEDFRYYQEQWQKAHQEIQRLESQRLNQPLN---
Arabidopsis 518 VHRNRDENAGPLDLVQIGVRKVRNKVAGQIGDAYLCYDRTTGSYSDSPVTPGMPERRSPK
P4 641 HLMQKFSDPMLARSLLQSQQNSDEALNIKRDADPTFDFIGYLETLPQTSGMYMGNASIIP
PfPREXpri 431 IIENNNDDMSEKIKVEKSIEDNISYFVDNNIMYIPNNIIIKDANDCLKHN----------
T4 317 QIMDYMKNNIAQGLMAKMRLSKYAKI----------

Figure D.2. Full alignment of deduced amino acid sequence of DNA primases. Details of sequences used are shown in Table 6.3 alongside PfPREXpri. These sequences were aligned using DIALIGN. Black shading indicates identical amino acids; grey shading indicates conserved amino acid substitutions. The numberings on the left hand side are the relative positions of the amino acid in the respective sequences.

Figure D.3. Full alignment of deduced amino acid sequence of DNA helicases

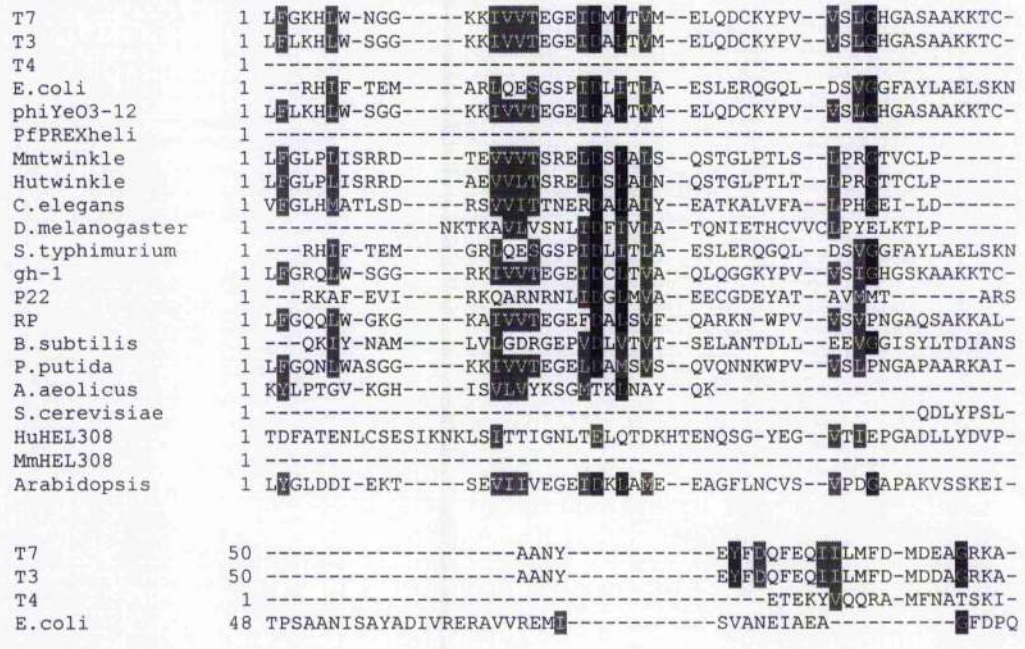

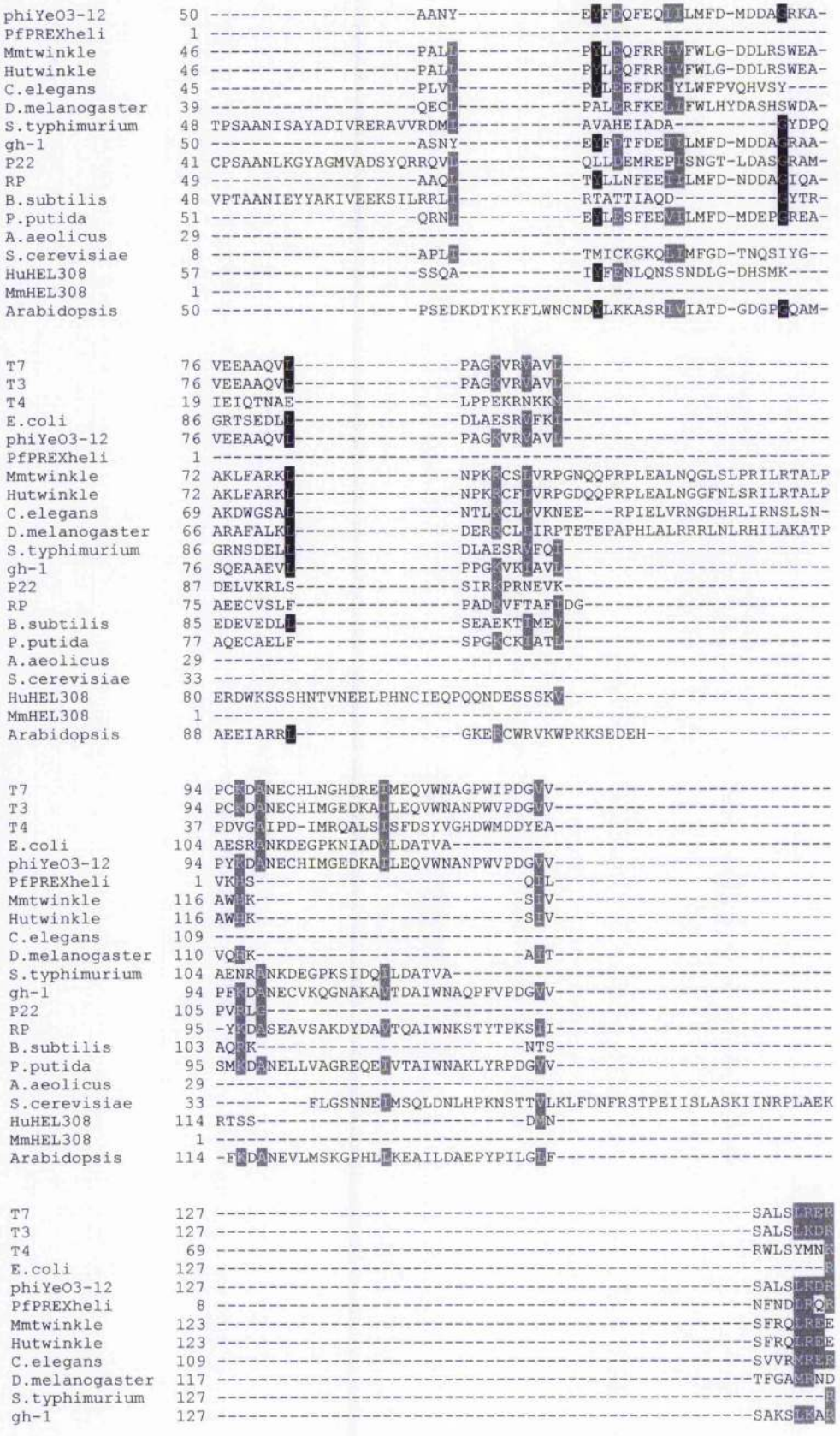

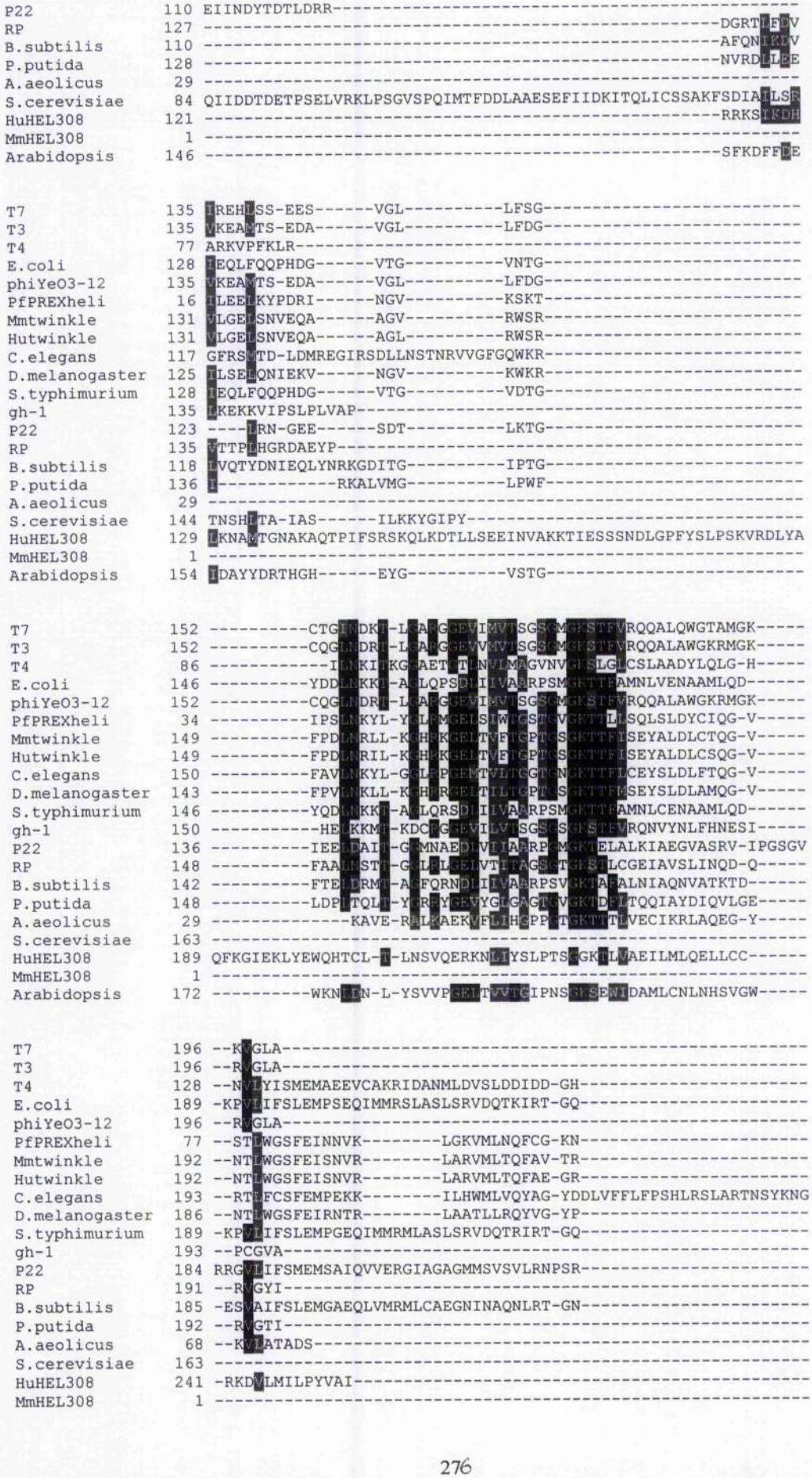
P22 110 EIINDYTDTLDRR
RP 127
B.subtilis 110
P.putida 128
A.aeolicus 29
S.cerevisiae 84 QIIDDTDETPSELVRKLPSGVSPQIMTFDDLAAESEFIIDKITQLICSSAKFSDIAFLSR
HuHEL308 121
MmHEL308 1
Arabidopsis 146
T7 135
T3 135
T4 77 ARKVPFKLR
E.coli 128
phiYeO3-12 135
PfPREXheli 16
Mmtwinkle 131
Hutwinkle 131
C.elegans 117 GFRSMTD-LDMREGIRSDLLNSTNRVVGFGQWKR
D.melanogaster 125
S.typhimurium 128
gh-1 135
P22 123
RP 135
B.subtilis 118
P.putida 136
A.aeolicus 29
S.cerevisiae 144 TNSHLTA-IAS
HuHEL308 129 LKNAMTGNAKAQTPIFSRSKQLKDTLLSEEINVAKKTIESSSNDLGPFYSLPSKVRDLYA
MmHEL308 1
Arabidopsis 154
T7 152
T3 152
T4 86
E.coli 146
phiYeO3-12 152
PfPREXheli 34
Mmtwinkle 149
Hutwinkle 149
C.elegans 150
D.melanogaster 143
S.typhimurium 146
gh-1 150
P22 136
RP 148
B.subtilis 142
P.putida 148
A.aeolicus 29
S.cerevisiae 163
HuHEL308 189 QFKGIEKLYEWQHTCL-T-LNSVQERKNLIYSLPTSGGKTLVAEILMLQELLCC
MmHEL308 1
Arabidopsis 172
T7 196 --KVGLA
T3 196 --RVGLA
T4 128 --NVIYISMEMAEEVCAKRIDANMLDVSLDDIDD-GH
E.coli 189 -KPVIIFSLEMPSEQIMMRSLASLSRVDQTKIRT-GQ
phiYeO3-12 196 --RVGLA
PfPREXheli 77 --STLWGSFEINNVK
Mmtwinkle 192 --NTLWGSFEISNVR
Hutwinkle 192 --NTLWGSFEISNVR
C.elegans 193 --RTIFCSFEMPEKK
D.melanogaster 186 --NTLWGSFEIRNTR
S.typhimurium 189 -KPVIIFSLEMPGEQIMMRMLASLSRVDQTRIRT-GQ
gh-1 193 --PCGVA
P22 184 RRGVIIFSMEMSAIQVVERGIAGAGMMSVSVLRNPSR
RP 191 --RVGYI
B.subtilis 185 -ESMAIFSLEMGAEQLVMRMLCAEGNINAQNLRT-GN
P.putida 192 --RVGTI
A.aeolicus 68 --KVIATADS
S.cerevisiae 163
HuHEL308 241 -RKDVLMILPYVAI
MmHEL308 1

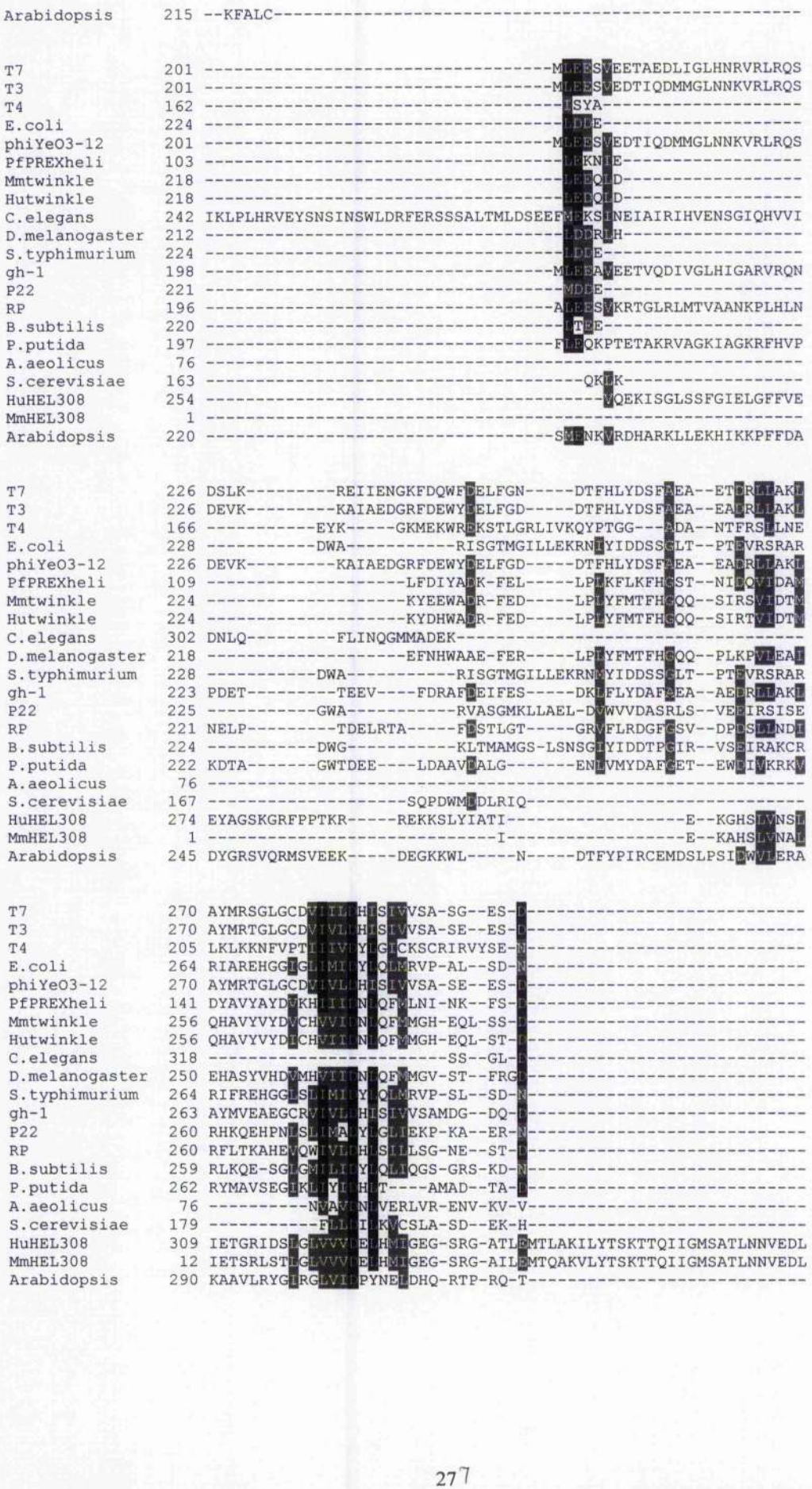

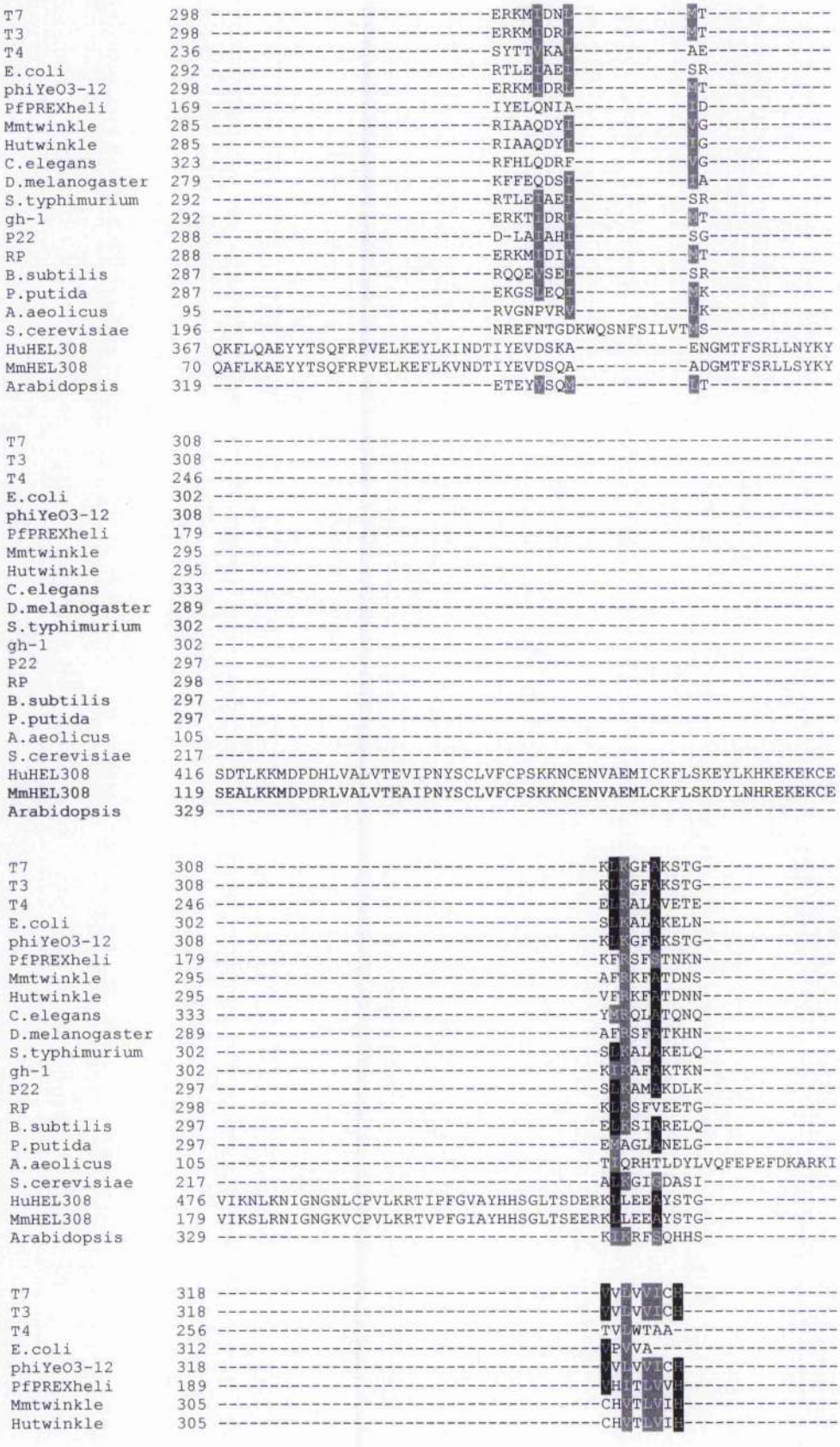

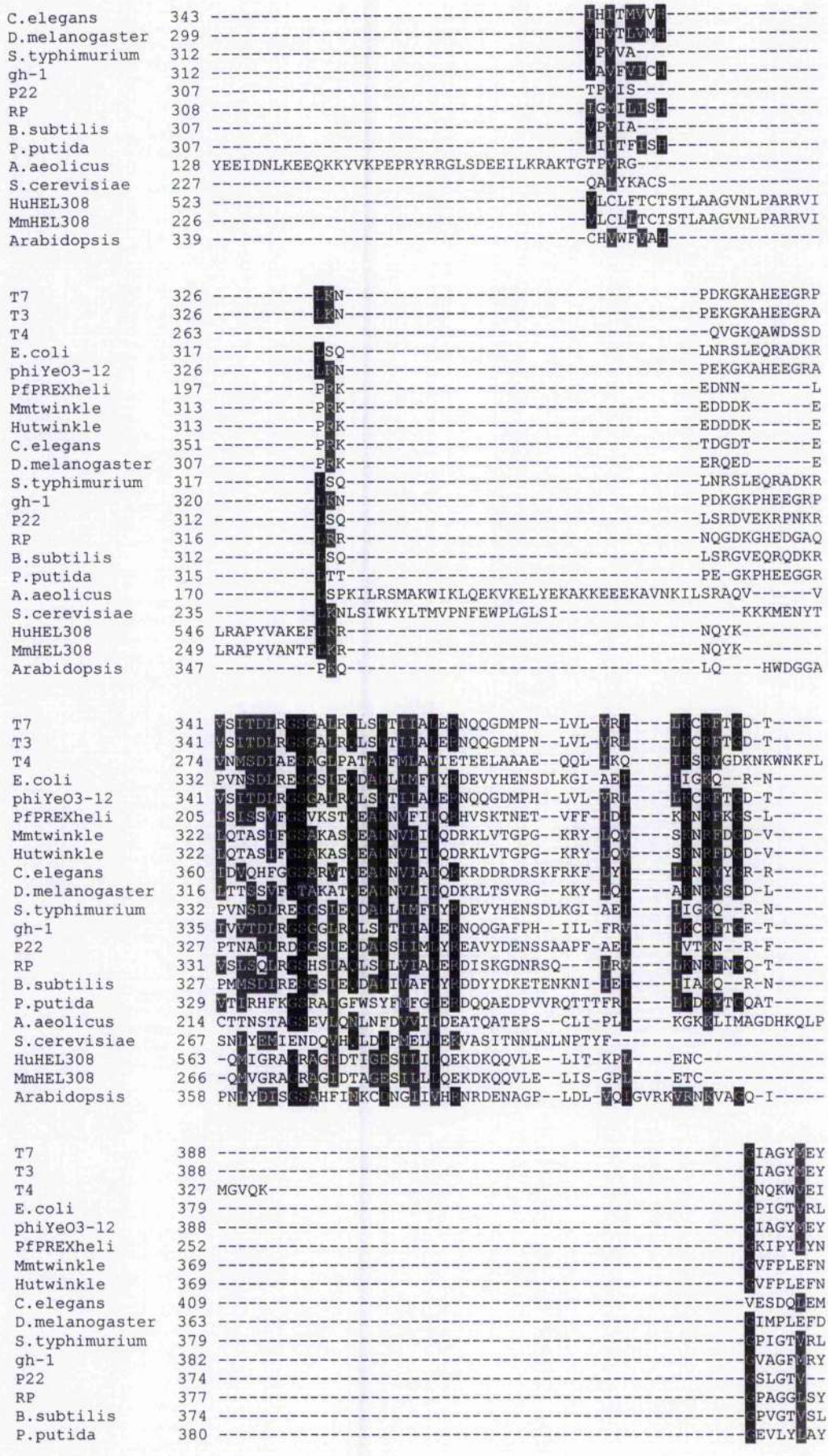
C.elegans 343
D.melanogaster 299
S.typhimurium 312
gh-1 312
P22 307
RP 308
B.subtilis 307
P.putida 307
A.aeolicus 128
S.cerevisiae 227
HuHEL308 523
MmHEL308 226
Arabidopsis 339
T7 326
T3 326
T4 263
E.coli 317
phiYeO3-12 326
PfPREXheli 197
Mmtwinkle 313
Hutwinkle 313
C.elegans 351
D.melanogaster 307
S.typhimurium 317
gh-1 320
P22 312
RP 316
B.subtilis 312
P.putida 315
A.aeolicus 170
S.cerevisiae 235
HuHEL308 546
MmHEL308 249
Arabidopsis 347
T7 341
T3 341
T4 274
E.coli 332
phiYeO3-12 341
PfPREXheli 205
Mmtwinkle 322
Hutwinkle 322
C.elegans 360
D.melanogaster 316
S.typhimurium 332
gh-1 335
P22 327
RP 331
B.subtilis 327
P.putida 329
A.aeolicus 214
S.cerevisiae 267
HuHEL308 563
MmHEL308 266
Arabidopsis 358
T7 388
T3 388
T4 327
E.coli 379
phiYeO3-12 388
PfPREXheli 252
Mmtwinkle 369
Hutwinkle 369
C.elegans 409
D.melanogaster 363
S.typhimurium 379
gh-1 382
P22 374
RP 377
B.subtilis 374
P.putida 380

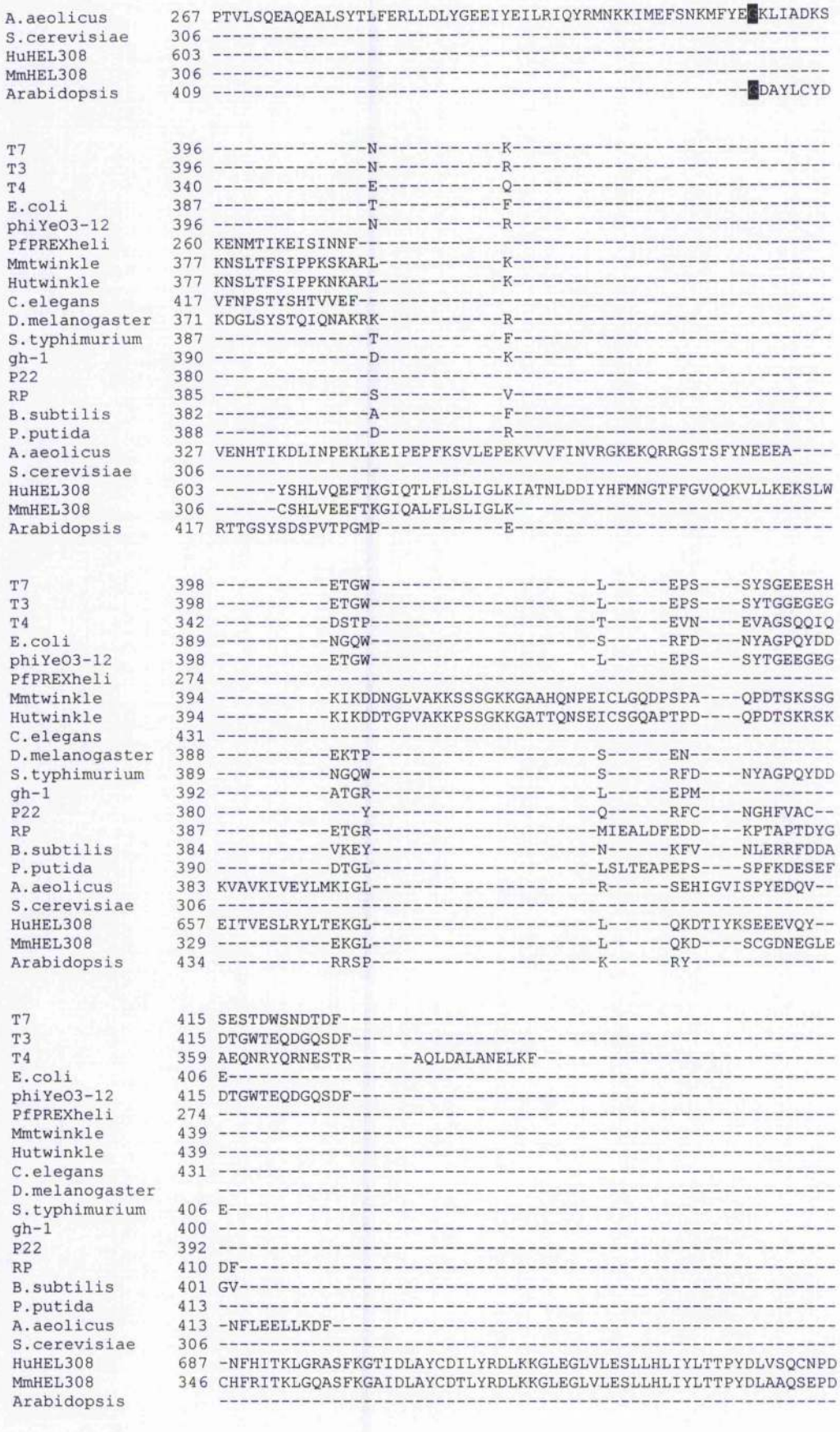
A.aeolicus 267 PTVLSQEAQEALSYTLFERLLDLYGEEIYEILRIQYRMNKKIMEFSNKMFYEKLIADKS
S.cerevisiae 306
HuHEL308 603
MmHEL308 306
Arabidopsis 409 DAYLCYD
T7 396 N K
T3 396 N R
T4 340 E Q
E.coli 387 T F
phiYeO3-12 396 N R
PfPREXheli 260 KENMTIKEISINNF
Mmtwinkle 377 KNSLTFSIPPKSKARL K
Hutwinkle 377 KNSLTFSIPPKNKARL K
C.elegans 417 VFNPSTYSHTVVEF
D.melanogaster 371 KDGLSYSTQIQNAKRK R
S.typhimurium 387 T F
gh-1 390 D K
P22 380
RP 385 S V
B.subtilis 382 A F
P.putida 388 D R
A.aeolicus 327 VENHTIKDLINPEKLKEIPEPFKSVLEPEKVVVFINVRGKEKQRRGSTSFYNEEEA
S.cerevisiae 306
HuHEL308 603 YSHLVQEFTKGIQTLFLSLIGLKIATNLDDIYHFMNGTFFGVQQKVLLKEKSLW
MmHEL308 306 CSHLVEEFTKGIQALFLSLIGLK
Arabidopsis 417 RTTGSYSDSPVTPGMP E
T7 398 ETGW L EPS SYSGEEESH
T3 398 ETGW L EPS SYTGGEGEG
T4 342 DSTP T EVN EVAGSQQIQ
E.coli 389 NGQW S RFD NYAGPQYDD
phiYeO3-12 398 ETGW L EPS SYTGEEGEG
PfPREXheli 274
Mmtwinkle 394 KIKDDNGLVAKKSSSGKKGAAHQNPEICLGQDPSPA QPDTSKSSG
Hutwinkle 394 KIKDDTGPVAKKPSSGKKGATTQNSEICSGQAPTPD QPDTSKRSK
C.elegans 431
D.melanogaster 388 EKTP S EN
S.typhimurium 389 NGQW S RFD NYAGPQYDD
gh-1 392 ATGR L EPM
P22 380 Y Q RFC NGHFVAC
RP 387 ETGR MIEALDFEDD KPTAPTDYG
B.subtilis 384 VKEY N KFV NLERRFDDA
P.putida 390 DTGL LSLTEAPEPS SPFKDESEF
A.aeolicus 383 KVAVKIVEYLMKIGL R SEHIGVISPYEDQV
S.cerevisiae 306
HuHEL308 657 EITVESLRYLTEKGL L QKDTIYKSEEEVQY
MmHEL308 329 EKGL L QKD SCGDNEGLE
Arabidopsis 434 RRSP K RY
T7 415 SESTDWSNDTDF
T3 415 DTGWTEQDGQSDF
T4 359 AEQNRYQRNESTR AQLDALANELKF
E.coli 406 E
phiYeO3-12 415 DTGWTEQDGQSDF
PfPREXheli 274
Mmtwinkle 439
Hutwinkle 439
C.elegans 431
D.melanogaster
S.typhimurium 406 E
gh-1 400
P22 392
RP 410 DF
B.subtilis 401 GV
P.putida 413
A.aeolicus 413 NFLEELLKDF
S.cerevisiae 306
HuHEL308 687 NFHITKLGRASFKGTIDLAYCDILYRDLKKGLEGLVLESLLHLIYLTTPYDLVSQCNPD
MmHEL308 346 CHFRITKLGQASFKGAIDLAYCDTLYRDLKKGLEGLVLESLLHLIYLTTPYDLAAQSEPD
Arabidopsis

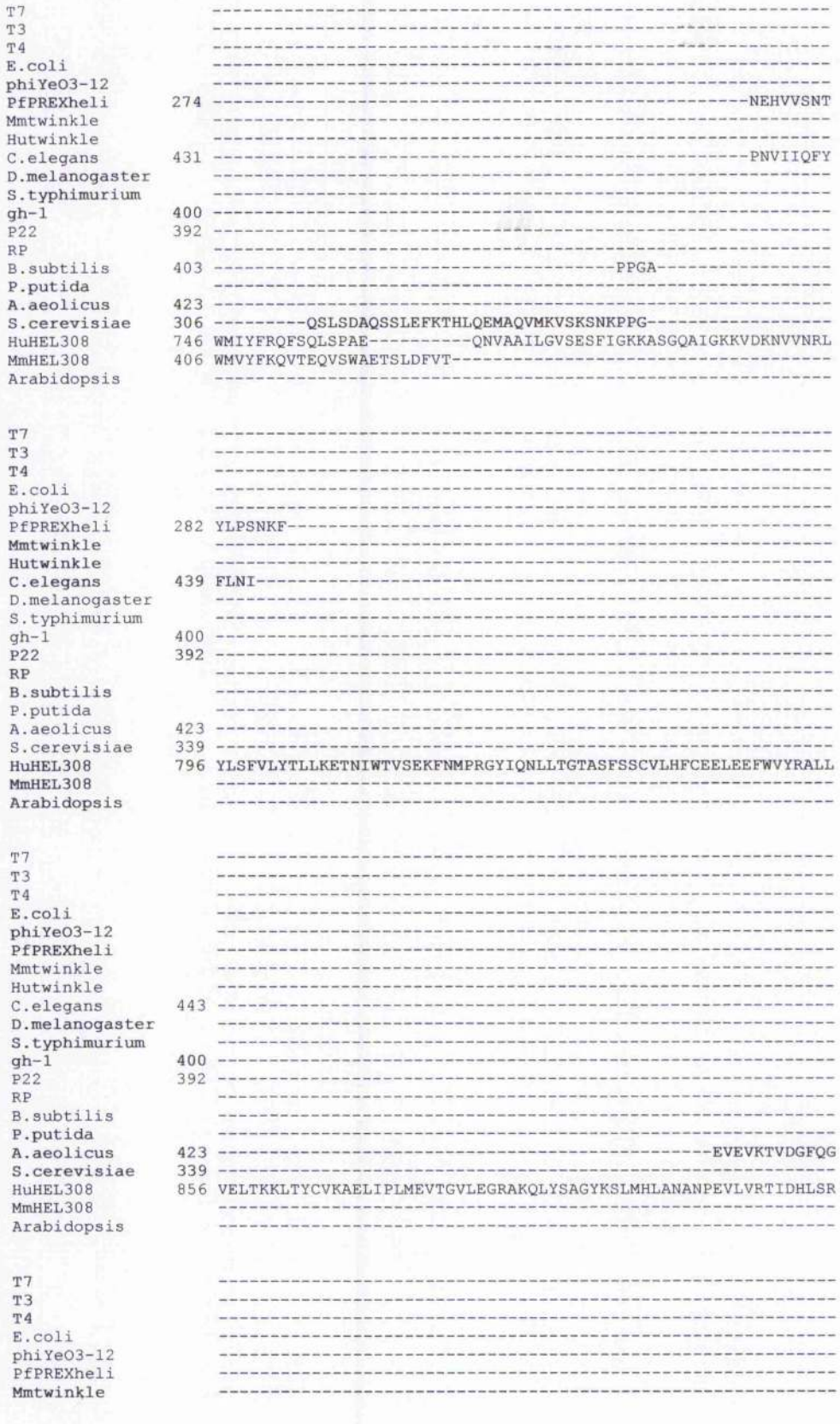
T7
T3
T4
E.coli
phiYeO3-12
PfPREXheli 274 ----------NEHVVSNT
Mmtwinkle
Hutwinkle
C.elegans 431 ----------PNVIIQFY
D.melanogaster
S.typhimurium
gh-1 400
P22 392
RP
B.subtilis 403 ----------PPGA----------
P.putida
A.aeolicus 423
S.cerevisiae 306 ---------QSLSDAQSSLEFKTHLQEMAQVMKVSKSNKPPG----------
HuHEL308 746 WMIYFRQFSQLSPAE----------QNVAAILGVSESFIGKKASGQAIGKKVDKNVVNRL
MmHEL308 406 WMVYFKQVTEQVSWAETSLDFVT----------
Arabidopsis
T7
T3
T4
E.coli
phiYeO3-12
PfPREXheli 282 YLPSNKF----------
Mmtwinkle
Hutwinkle
C.elegans 439 FLNI----------
D.melanogaster
S.typhimurium
gh-1 400
P22 392
RP
B.subtilis
P.putida
A.aeolicus 423
S.cerevisiae 339
HuHEL308 796 YLSFVLYTLLKETNIWTVSEKFNMPRGYIQNLLTGTASFSSCVLHFCEELEEFWVYRALL
MmHEL308
Arabidopsis
T7
T3
T4
E.coli
phiYeO3-12
PfPREXheli
Mmtwinkle
Hutwinkle
C.elegans 443
D.melanogaster
S.typhimurium
gh-1 400
P22 392
RP
B.subtilis
P.putida
A.aeolicus 423 ----------EVEVKTVDGFQG
S.cerevisiae 339
HuHEL308 856 VELTKKLTYCVKAELIPLMEVTGVLEGRAKQLYSAGYKSLMHLANANPEVLVRTIDHLSR
MmHEL308
Arabidopsis
T7
T3
T4
E.coli
phiYeO3-12
PfPREXheli
Mmtwinkle

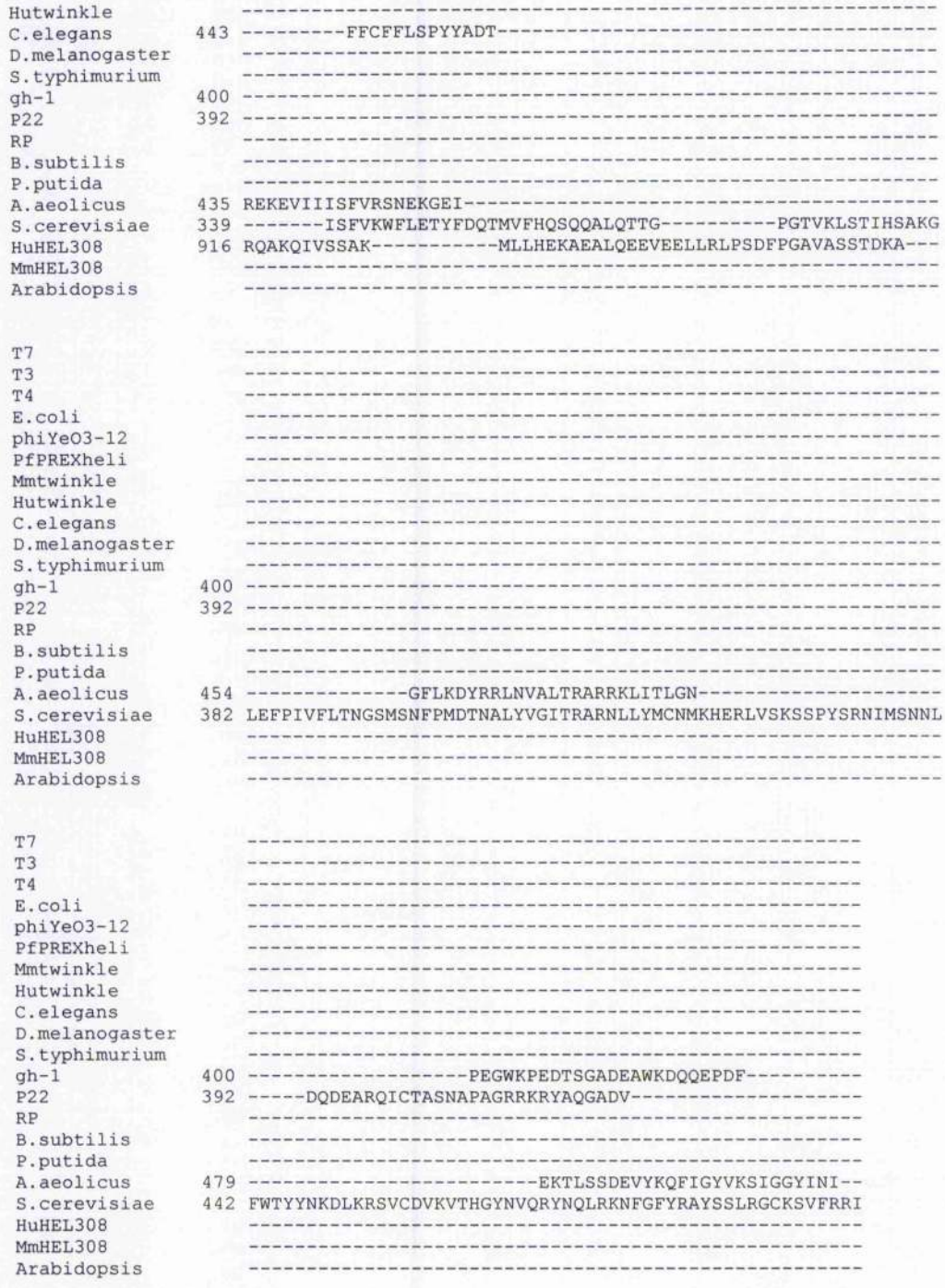

Figure D.3. Full alignment of deduced amino acid sequence of DNA helicases. Details of sequences used are shown in Table 6.4 alongside PfPREXheli. These sequences were aligned using DIALIGN. Black shading indicates identical amino acids; grey shading indicates conserved amino acid substitutions. The numberings on the left hand side are the relative positions of the amino acid in the respective sequences.